

CLINICAL ELECTROCARDIOGRAPHY
Interpretation on a Physiologic Basis

A Hoeber-Harper Book



CLINICAL ELECTROCARDIOGRAPHY

Interpretation on a Physiologic Basis

MANUEL GARDBERG, M.D.

Clinical Associate Professor of Medicine, Louisiana State
University School of Medicine; Senior Attending Physician
and Director of the Cardiac Research Laboratory of the
Touro Infirmary, New Orleans

With chapters by

RICHARD ASHMAN, Ph.D. IRVING L. ROSEN, M.D.

LOUIS LEVY, II, M.D.

CLINICAL ELECTROCARDIOGRAPHY

Interpretation On A Physiologic Basis

Copyright © 1957, by Paul B. Hoeber, Inc.,
Medical Book Department of Harper & Brothers

All rights reserved.

For information address Paul B. Hoeber, Inc.,
Medical Book Department of Harper & Brothers,
49 East 33rd Street, N.Y.C. 16.

Printed in the United States of America

Library of Congress catalog card number: 56-12075

*This book is dedicated to
Dr. Richard Ashman,
Scientist, Philosopher, and Teacher, to whom the
author is grateful for thirty years
of guidance and encouragement*

Contents

Preface	ix
Deflections of the Electrocardiogram	1
1. Electrical Phenomena of the Heart	3
2. Depolarization of the Ventricles: The QRS Complex	17
3. The Precordial Leads	30
4. T Wave: An Introduction to QRS-T Relationship	38
5. Quantitative Analysis of QRS-T Relationship	50
6. Injury	69
7. Ischemia	80
8. Left Ventricular Hypertrophy	87
9. Right Bundle Branch Block	92
10. Left Bundle Branch Block	104
11. Coronary Disease	112
12. Right Ventricular Hypertrophy <i>In Collaboration with Louis Levy, II, M.D.</i>	215
13. Disturbances of the Cardiac Mechanism <i>Richard Ashman, Ph.D.</i>	239
14. Drugs, Electrolyte and Metabolic Disturbances <i>Irving L. Rosen, M.D.</i>	266
15. Heart Disease of Various Etiologic Types	282
16. Vectorcardiography and Spatial Vector Electrocardiography	286
Appendix	303
Index	309

Preface

The teaching of electrocardiography is a notably difficult task. Frequently the student is not offered an opportunity to visualize the mechanism of production of the deflections of the electrocardiogram and the changes which are produced in them by various influences and lesions. It is the ambitious purpose of this book to attempt to fill the need for a visual method that is based on a knowledge of physiologic principles. It is hoped that it will aid the medical student and the practicing physician in interpretation of the electrocardiogram with greater accuracy and security.

The visual presentation of the formation of the QRS complex of the electrocardiogram requires some notion of the order in which the various parts of the ventricles become excited. Direct human investigation being impossible, the writer, with Ashman, undertook to formulate a hypothesis. All of the evidence available from animal experimentation and the observed anatomic characteristics of the human heart were employed to modify Lewis' original hypothesis and to develop it into three dimensions. Bayley's thinking and teaching played no small part in inspiring this effort.

There is no direct evidence derived from work on the human heart that the wave of excitation follows the path which has been hypothesized. However, when a problem does not lend itself to direct attack one must be content to speculate on it within the framework of the known facts; the hypothesis thus formed is then tested against the observed phenomena. Extending this further, one attempts to make predictions on the basis of the hypothesis. The manner in which the hypothesis is found to fit the observed facts

and the accuracy of the predictions are the only "proofs" which can be obtained.

Nature performs with distressingly great frequency a series of human experiments for us. Infarction occurs spontaneously in a great variety of myocardial locations. Autopsies furnish opportunities to test the hypothesis, particularly when tracings before and after infarction are available. It is doubtful that the value of the evidence would be enhanced if the location of the infarct were chosen deliberately and the infarction accomplished by ligature so that the data might be regarded as resulting from experimentation. No experiment devised by man could be as free from extraneous technical influences. No experimental finding recorded since establishment of our hypothesis is at variance with it. Prinzmetal's findings that the endocardial layers of the ventricle seem to produce little electrical effect do not deprive the remainder of the ventricular wall of the ability to be excited from within outward, even if we assume that dog and man are alike. Durrer's recent findings on dogs are confirmatory, as are those of Scher. The more recent finding that polarity of the membrane is reversed during activation does not materially affect the presentations or analyses contained in this book.

For thirteen years this visualization of the path of the wave of excitation has been an important part of our basis of thought in electrocardiography. We have found it to fit most of the observed electrocardiographic data, and it has been an important visual aid in the teaching of electrocardiography.

The presentation in this book follows conventional electrocardiographic theory as originated by Lewis, Wilson, Ashman, and Bayley. Conventional standard limb leads,

and unipolar limb leads, are presented as projection of the derived spatial QRS loops. Precordial leads are derived by the solid angle method.

If and when an accurate method of spatial vector recording is found, we believe that the spatial analyses as developed here will be found to hold very well.

The author has included in this book only that documentation considered to be essential in a volume of a clinical nature. For complete references the reader is referred to the monumental work by Lepeschkin.

M. G.

New Orleans

Acknowledgments

The facilities of the Cardiac Research Laboratory of Touro Infirmary, which is supported by the J. Aron Research Fund of that institution and by the John A. Hartford Foundation of New York City, were employed in the development of part of the material presented in this book.

The author wishes to acknowledge the help of Dr. Richard Ashman, Director of the Heart Station, Charity Hospital, New Orleans, in the preparation of every chapter in the book. In addition, Dr. Ashman wrote the chapter Disturbances of the Cardiac Mechanism.

The chapter Drugs, Electrolyte and Metabolic Disturbances was written by Dr. Irving L. Rosen, Instructor in Medicine at Louisiana State University School of Medicine, New Orleans, who has also given invaluable aid in many other ways.

The chapter Right Ventricular Hypertrophy and the section Myocardial Infarction in the chapter Coronary Disease were written with the collaboration of Dr. Louis Levy, II, Heart Station of Charity Hospital, New Orleans.

The encouragement and support of Dr. Edgard Hull, Assistant Dean, and of Dr.

W. R. Akenhead, Head of the Department of Medicine, both of the Louisiana State University School of Medicine, are deeply appreciated, as is the encouragement of Dr. John S. LaDue of New York.

The entire manuscript was typed three times by Mrs. William Kingsmill, a Herculean task when one considers that this feat was performed without interruption of her duties as office assistant and secretary to the author in his private practice.

The author wishes also to acknowledge the help of the staff of the Touro Infirmary, especially Drs. Robert Haspel, I. L. Robbins, John Dyer, Horner Dupuy, B. A. Goldman, Willard Wirth, and others who permitted the use of tracings from their own records.

Mrs. Kate Rittenberg and Mrs. Kay Greene, volunteer workers in the Cardiac Research Laboratory at Touro Infirmary, also lent aid in an important manner, as did Mr. Carol Goldberg, a medical student at the Louisiana State School of Medicine.

Mr. Felix Schillesci photographed the illustrations, and the author is grateful to him for his cooperation and the fine quality of his work.

CLINICAL ELECTROCARDIOGRAPHY
Interpretation on a Physiologic Basis

Deflections of the Electrocardiogram

The electrocardiogram is a record of the differences of potential produced between various points on the surface of the body by the electrical phenomena accompanying the heart beat. With each cardiac cycle a distinctive series of deflections or waves appears on the record. The ordinates represent the magnitude of the potential at every instant during the heart beat and the abscissae represent time. Upward deflections of the trace (above the base line) are positive while downward deflections are negative. Figure 1 illustrates the

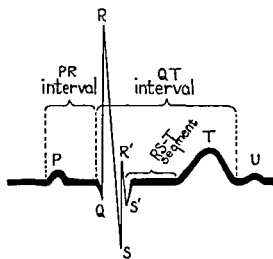


FIG. 1. Deflections and intervals of the electrocardiogram. Conventionally the ordinates represent the potential at such standardization that 10 mm. = 1 millivolt. The abscissae represent time; 1 mm. = .04 second.

designations assigned to the various "waves" and other characteristics of the electrocardiogram that are commonly measured in clinical electrocardiography (though rarely does a single lead show all of these waves).

The first deflection of the trace results from auricular activity and is known as the P wave. Following this is the frequently depressed

P-Q segment which extends from the end of the P to the next deflection, Q. The time from the beginning of the P wave to the end of the P-Q interval is known as the P-R interval. Following this there is a series of more rapid deflections: An initial downward (negative) deflection is called a Q wave. The first upward (positive) deflection—whether or not preceded by a Q—is known as an R wave. The downward deflection which follows an R wave is called an S wave. If a second positive deflection follows an S wave it is called R' and if a negative deflection follows an R' it is called an S'. The entire rapid series of deflections which follows the PR interval is known as the QRS complex. The QRS complex is related to ventricular activation.

Following the QRS complex there is usually an isoelectric or nearly isoelectric interval known as the RST segment which ends at the point at which the broad T wave begins. The T wave is due to electrical effects associated with the latter part of ventricular systole. Following the T wave there is occasionally seen a U wave of unknown significance.

The Q-T interval is measured from the beginning of the QRS complex to the end of the T wave.

The clinical analysis of electrocardiograms employs, among other methods, careful measurement of the magnitude and duration of the various waves and the duration of the intervals. Tables of the normal values of the magnitude and duration of these characteristics of the electrocardiogram are furnished in the appendix. The detailed analysis of the various deflections of the electrocardiograms and of their relation to one another constitutes the greater part of the subject of this book.

1. Electrical Phenomena of the Heart

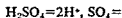
When a compound such as sodium chloride is dissolved in water there is a dissociation of the molecules into the component atoms according to the formula:



The plus and minus signs in the formula indicate that the sodium atom in dissociation carries a positive charge of electricity (lacks one electron) and that the chloride atom in dissociation carries a negative charge of electricity (carries one extra electron). Such electrically charged atoms are called *ions*. Compounds capable of such dissociation are called *electrolytes*.

Since the body fluids, both intra- and extra-cellular, contain quantities of electrolytes and these take part in many biologic processes, it should not be surprising to learn that some of these biologic processes are accompanied by measurable electrical phenomena.

As a matter of fact, the first electrical phenomena studied by man were derived from solutions of electrolytes. The poles of the voltaic cell (the first "wet cell" battery) derived their electrical charges from the ions of a strong electrolyte, sulfuric acid.



Through chemical action the positive pole (copper) of the cell derives its positive charges from the H^+ ions and the negative pole (zinc) derives its negative charges from the SO_4^- ions.

Potential and Difference of Potential

If the positive pole of a voltaic cell is connected to the negative pole by means of a conductor a *current* of electricity will flow between them. Conventionally the current is

regarded as flowing *from* the positive pole *to* the negative pole.* This flow of current from the positive pole to the negative pole is regarded as the result of a greater electrical "pressure" or potential at the positive pole. The force which propels the current and which derives from the difference in the electrical pressure which exists between the two poles is known as the *electromotive force* (E.M.F.). It is measured by the *difference in potential* (P.D.) between the two poles.

The instrument employed in the measurement of potential differences and potentials is the *galvanometer*. The unit of measurement of potential difference is the *volt*. The electrocardiograph is a specialized recording galvanometer. The galvanometer not only measures the magnitude of the potential difference between the two objects to which it is connected but also indicates which object possesses the higher potential. The needle or stylus accomplishes this by swinging above the zero mark (base line on EKG's) if the flow of current is in the one direction and below the zero mark if the flow of current is in the opposite direction.

Thus, if we connect the positive pole of a battery to the negative pole through a galvanometer the indicator will show a difference of potential of +6 volts. If we reverse the connections the reading will be -6 volts. It is therefore necessary for the terminals of the galvanometer to be labeled + and - respectively so that we will know in what direction the current is flowing through the instrument. Usually commercial instruments are labeled in such a manner that when the "posi-

* This convention persists though it is now held that *electrons* flow from the negative to the positive pole.

“positive” terminal of the galvanometer is connected to the positive pole of a battery the reading is positive. When the positive terminal is connected to the negative pole of the battery the current flows in the opposite direction and the reading is negative. In making Lead I of the electrocardiogram, if the right and left arm electrodes are reversed the tracing will show all the deflections accurately but “upside down.”

It is important to remember that if the terminals of a galvanometer are connected to the two poles of a battery and the difference of potential recorded is, say, 6 volts nothing has been learned of the actual potential at either pole: for $6-0=+6$, $12-6=+6$, $3-(-3)=+6$ and, $-6-(-12)=+6$. A current will flow from a point of higher positive potential to a point of lower positive potential and likewise from a point of less negative to a point of greater negative potential, in the latter case just as air will flow from a jar containing a partial vacuum to another jar containing a more nearly complete vacuum if the two are connected by means of a tube.

It is possible to record the actual potential at a point on the body if one connects the other terminal of the galvanometer to a point on the body of zero potential. We employ the “central terminal” in clinical electrocardiography as a supposedly zero potential. This will be described later.

In electrocardiography records of the potential at a point on the body made by connecting that point through a galvanometer to the central terminal are called *unipolar leads*, and records of the difference of potential between any two points on the body made by connecting these two points through a galvanometer are called *bipolar leads*.

Potentials Produced by a Dipole in a Volume Conductor

If the tips of two insulated wires leading from the poles of a battery are placed in a very dilute solution of an electrolyte the solution will act as a conductor of the current, which will flow from the positive pole to the negative

pole. The lines of flow that the current follows in the solution are indicated in Fig. 2. Their general distribution is similar to that of the lines of magnetic flow produced in air by a bar magnet. The potentials existing at various distances and in various directions from the dipole are of interest to us in electrocardiography because the potentials that result from the dipoles in the myocardium

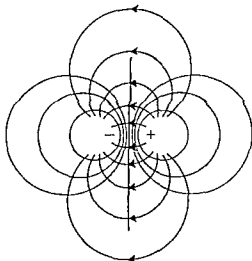


FIG. 2. Lines of current flow for a dipole immersed in a volume conductor. The equipotential lines are perpendicular to the lines of current flow.

must be studied by placing electrodes on the body at some distance from the heart (for obvious reasons). The body is commonly regarded as behaving in this regard as if it were a volume of a solution of electrolytes.

In discussing the potentials that are found in the solution at various points it will be advisable to employ a device that serves to simplify the representation of the forces under discussion. For centuries it has been found convenient to represent forces by means of the arrow symbol. The direction in which the arrow points indicates the *direction* of the forces and the length of the arrow is employed to indicate the *magnitude* of the forces. Such arrow symbols are called *vectors*. Conventionally electromotive forces or differences of potential are represented by

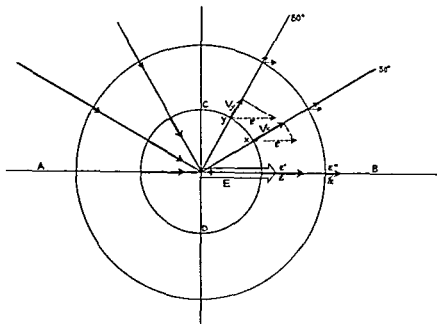


FIG. 3. Electrical field about a dipole immersed in an infinite volume conductor. The solid arrow E' , of magnitude 2 units, represents the potential at a point which lies on the axis of the dipole (AB) and is one unit distant from the midpoint of the dipole. The dashed arrows labeled E' are translations of E' to points x and y which lie on the lines drawn at 30° and 60° angles respectively to the axis (AB) of the dipole and which are one unit distant from the midpoint of the dipole. The potentials at the points x and y are indicated by the length of the arrows V_x and V_y , obtained by dropping perpendiculars from E' to the lines joining the points x and y to the midpoint of the dipole.

The solid arrow E'' of magnitude one half unit represents the potential at a point on the axis, AB , of the dipole which is 2 units distant from the midpoint of the dipole. Its magnitude is one quarter that of E' because the potential varies inversely with the square of the distance. The potential at points that lie upon the lines 30° and 60° and which are at 2 units distance from the dipole may be constructed just as was done for the points which are at 1 unit distance.

vectors pointing from the point of lower potential to the point of higher potential.

When we study the potential at all points in the solution about the dipole described above we find that a plane placed perpendicular to the line joining the two charges and bisecting that line divides the solution into a positive and a negative field. Thus, in Figs. 2 and 3 all points to the right of this plane (shown in Fig. 3 as a line CD) are found to have a positive potential and all points to the left are found to have a negative potential. If we measure the magnitude of the potential in both the positive and the negative fields at points along the line AB drawn through the

two poles of the dipole we find that the magnitude of the potential, whether positive or negative, diminishes rapidly as we move away from the center of the dipole and beyond either pole. The magnitude of the potential is inversely proportional to the square of the distance from the midpoint of the dipole. In other words, if the potential at one unit distance from the dipole is 2 volts, at two units

$$\text{distance it is } 2 \times \frac{1}{2 \times 2} = \frac{1}{2} \text{ volts.}$$

If we measure the potentials at points along a line drawn through the center at an angle to the line AB (the axis of the dipole) we find

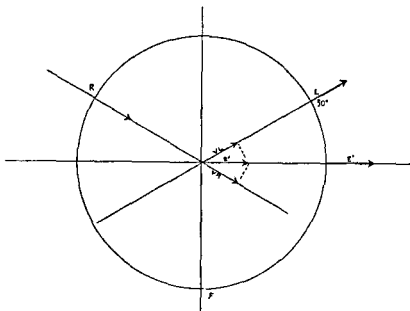


FIG. 4. Construction of the direction and relative magnitude of the E.M.F. of a dipole, given the potential at two points in the field at equal distance from the dipole.

The magnitude (VL) of the potential measured at L is laid off on the line joining the dipole midpoint to L and the magnitude of the potential at R is laid off on the line joining R to the dipole midpoint. Perpendiculars are erected at the ends of each of these projected magnitudes. The intersection of the perpendiculars locates the arrow tip, and the midpoint of the dipole represents the origin of the vector that represents the direction and magnitude of the E.M.F. that produced the potentials recorded at R and L .

It is important to point out that when the potential at an electrode is negative (as at R above) it is laid off on the lead line so that it points away from the electrode. If the potential is positive (as at L above) it is laid off on the lead line so that it points toward the electrode.

that the potentials along this line also diminish with the square of the distance from the center of the dipole but that they are uniformly smaller in magnitude than the potentials found at points on the line AB at corresponding distances. The relationship between the potentials at corresponding distances on the two lines is the cosine of the intervening angle. Thus, to determine the potential at a point (say, x , Fig. 3) lying on a line which makes an angle of 30 degrees with the axis AB of the dipole we need only to multiply the potential at a point which is on the line AB and at the same distance from the center of the dipole by the cosine of the intervening angle. This is accomplished geometrically by dropping perpendiculars

from the ends of the vector representing the potential at that distance on the line AB to the line (30 degrees) upon which the point in question (x) lies (see Fig. 3, dotted E'). This is called *projecting* the vector.

It is readily seen that the greater the angle between AB and the line upon which the point lies the smaller will be the potential at that point; at a point C , on the line CD at 90 degrees to the axis of the dipole the potential is zero.

This knowledge of the electrical field about a dipole immersed in a conducting solution permits us to plot in a very simple manner the potential differences which will be recorded between any two points in the field produced by that dipole.

Vector Analysis

Figure 4 shows the system represented in Fig. 3 with E' transferred to the center of the dipole and with perpendiculars dropped to the lines connecting the midpoint of the dipole to points R and L . This practice of using E' at the center of the figure as if it were E (of figure 3) is necessitated by the fact that clinically we can only measure E in terms of its effect at a distance from the heart (E').

In Figs. 3 and 4 measurement of the potential at point L (or R) involves measuring the difference in potential between the point L (or R) and the midpoint of the dipole, for this latter point is at 0 potential. It is for this reason that in the geometric representation the lines for the unipolar leads VR and VL are drawn from the center of the figure to the point at which the potential is measured.

In clinical electrocardiography, by reversing this maneuver, we can deduce the direction and relative magnitude of the electromotive force of the heart (E' , Fig. 3) by recording the potential at the points R and L , laying off these values on the lines connecting the center zero point to R and L respectively, and giving them the same point of origin (the center). Perpendiculars are then constructed at the extremities of these transferred projections (dotted lines of Fig. 4). The point of intersection of these perpendiculars defines the vector E' , which represents the direction and relative magnitude of the E.M.F. that produced the potentials measured at R and L . This will be accurate only if the points R and L are equidistant from the dipole under investigation.

Usually in clinical electrocardiography we measure the potential at a third point F in addition (Fig. 4), so that we have three leads. Since these leads are measured between a point of zero potential and the points R , L , and F they are *unipolar leads*. R is the right arm, L is the left arm, and F is the left leg. The zero potential is theoretically achieved by employing the *central terminal*.

It was Frank N. Wilson who first connected lead wires to each of the extremities (R , L , and F) and joined them to form the central terminal (Fig. 7). Originally each of these three extremities was connected to the common or central terminal through 5000-ohm resistances. Today 100,000-ohm resistances are generally employed. Theoretically the potential of the central terminal is always zero under the idealized conditions which have been assumed in this presentation up to this point.

The Standard Limb Leads of the electrocardiogram are derived by measuring the difference of potential between (1) the points L and R (Lead I), (2) the points F and R (Lead II), and (3) the points F and L (Lead III) (Fig. 5).

In recording Lead I, the right arm and left arm are connected to the galvanometer in such a manner that a higher potential at the left arm produces a positive deflection. In recording Leads II and III the connections are made in such a manner that a higher potential at the left leg gives a positive deflection. The beginner should label his triangles as shown in the figure so as not to become confused. If we connect the three points R , L , and F by means of straight lines we have an equilateral triangle each side of which is one of the lead lines, as shown in the figure. This is the *Einthoven triangle*. If a dipole is situated at the center (in the heart) which produces an E.M.F. of the direction and relative magnitude represented by the vector E , the differences of potential recorded on Leads I, II, and III can be derived very simply by dropping perpendiculars from the ends of the vector E to the three sides of the triangle (see Fig. 5). It is seen that for the three standard leads perpendiculars from the midpoint of the dipole fall upon the centers of the lead lines, LR , FR , and FL .

Conversely, if we record the difference of potential on any two of the leads, say Leads I and III, and lay these off on the corresponding sides of the triangle we can then erect perpendiculars at the extremities of the projected

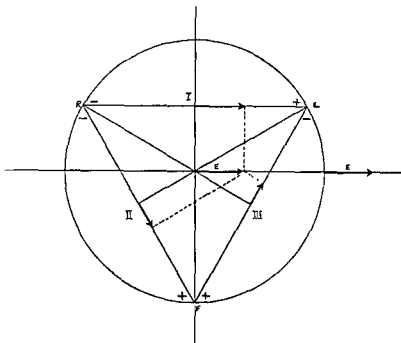


FIG 5. Construction of the direction and relative magnitude of the E.M.F. produced by a dipole given the potentials of Lead I and Lead III.

The potential recorded on the bipolar Lead I is laid off on the line of Lead I (LR). The center point of the line is zero. If the potential on Lead I is positive it is laid off on LR so that it points to L ; if negative it is laid off on LR so that it points to R . The potential on Lead III is laid off on the line of Lead III (FL) and, given a negative deflection for this lead, it must be laid off so that it points toward L . Perpendiculars are dropped at the ends of the projected magnitudes and their intersection defines the direction and relative magnitude of the E.M.F. which produced the deflections.

vectors thus constructed and employ the intersection of the perpendiculars to define the vector E of the E.M.F. produced by the heart (Fig 5).

If the direction of the electromotive force produced by the cardiac dipoles is not in the plane of the triangle formed by the three points on the body which we have chosen (the frontal plane) but is directed partly forward or backward, the vector representing it must be projected upon the frontal plane by dropping perpendiculars from it to the frontal plane (Fig. 6). The projected frontal plane vector can then be re-projected upon the three sides of the triangle and upon the three unipolar lead lines which are in the frontal plane. Actually it is erroneous to say that this double projection is necessary. One might

simply drop perpendiculars from the ends of the vector to the line of each lead. However the method described above is much more easily visualized by most persons. Furthermore, much of our analysis of cardiac vectors in clinical electrocardiography can only deal with the frontal plane projections of the vector.

If, in a problem involving vector analysis it becomes necessary to employ both unipolar and standard limb leads a mathematical correction is necessary to bring the two types of leads to the same standardization by multiplying the unipolar lead deflection by $\sqrt{3}$ (1.732).^{*} The Goldberger unipolar lead aV_L is made by disconnecting the electrode

^{*} See Appendix I.

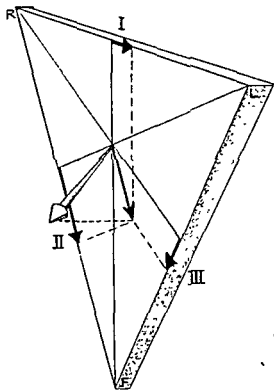


FIG. 6. Representation of projection of spatial vector upon the plane (frontal plane) of the Einthoven triangle and reprojection of the frontal plane vector upon the lines of the standard limb leads.

on the left arm from the central terminal when the right arm unipolar lead is made (Fig. 7). Leads aV_R and aV_F are made in a corresponding manner. This increases the deflections by 50 percent. While this is some 23 percent less than the $\sqrt{3}$ correction the aV leads are defined here because they have been incorporated into most commercially available apparatus.

Certain relationships of the deflections of the limb leads are of importance. For the standard limb leads the formula $I + III = II$ (Einthoven's Law), is of especial importance in checking the technic.

The sum of the potentials (at any instant) of the three unipolar limb leads must always equal zero.

These relationships do not depend upon the equilateral triangle nor upon the assumption that the central terminal is at zero potential.

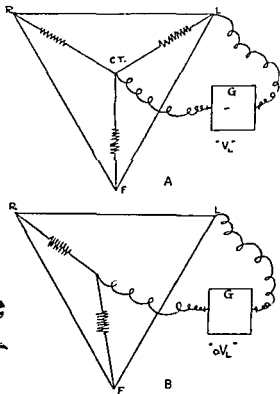


FIG. 7. *A* is the Wilson central terminal. Wires from the right arm, left arm, and left leg are connected through 5000-ohm resistances to form a terminal which may then be employed as an indifferent or "zero" terminal. In the figure the galvanometer is recording the potential at the left shoulder (Lead V_L).

B is the corresponding Goldberger Lead, aV_L . The central terminal is disconnected from the left shoulder, increasing the deflection in the Lead (aV_L) by 50 per cent over that obtained in *A* (V_L).

Origin of Electromotive Forces in Heart Muscle

The tissue cell, containing electrolytes and immersed in extracellular fluid also containing electrolytes, is represented diagrammatically by most workers to behave as shown in Fig. 8. The resting cell is regarded as having a layer of negative ions accumulated adjacent to the inner surface of its limiting membrane and a corresponding number of positive ions adjacent to the outer surface of the cell membrane. The explanation of this phenomenon is extremely complex but seems to be related to the differences in the concentration of the several ions in the intracellular and

extracellular fluids. The pairs of oppositely charged ions are, of course, dipoles. Each dipole is potentially a source of current flow (Fig. 8a). In the resting cell the integrity of the cell membrane furnishes sufficient electrical resistance to prevent any current flow between the poles of the dipoles, and no difference of potential is recorded by the galvanometer.

If we stimulate the end of the cell near *A* (Fig. 8b) the effect is to decrease the electrical resistance of the cell membrane in this area, to increase its permeability, and to depolarize (remove the dipoles from) it. The diminution of the electrical resistance of the stimulated portion of the cell membrane permits an electrical current to flow from the positive charges to the negative charges, for the intracellular and extracellular fluids are good conductors. The lines of current flow are as indicated in Fig. 8c. The similarity between the pattern of the lines of current flow in this figure and that of a dipole oriented as in Fig. 2 is readily seen. The cell now behaves electrically as if a layer of dipoles (dotted) were situated at the margin between the depolarized and the polarized portions of the cell membrane (Fig. 8b). This layer of dipoles is of the same density as that on the membrane itself.

The stimulus or excitation, once begun, proceeds across the cell at uniform speed, causing the dipoles to disappear, as explained above, in the new areas of the cell membrane which it invades (Fig. 8c). The electrical effect of the wave of excitation (represented by the dotted line) is the same as that which would be produced by a layer of dipoles moving across the cell (see dotted dipoles, Fig. 8b and c).

When the excitatory process reaches the end of the cell near *B* the entire cell membrane has become depolarized (Fig. 8d). There are now no electrical charges, therefore no difference of potential exists between *B* and *A* and the galvanometer needle drops back to zero. It is seen that in recording these phenomena we have used a galvanometer

which records continuously the difference between the potential at *B* and the potential at *A*. The paper is moved at a constant speed by a driving mechanism while the needle of the galvanometer writes upon it the deflections produced by the differences of potential that occur between *B* and *A* during the process described above. The electrocardiographic apparatus is just such a galvanometer.

It is important to state that the type of curves shown in the figure will be obtained only if the electrodes are at a distance from the cell. More of this later.

Depolarization of a Syncytium

Figure 9 is a diagrammatic representation of the resting myocardial syncytium. This very much simplified diagram serves to give us some visualization of what we believe happens when heart muscle is stimulated.

If we cause excitation along the edge of the syncytium near *A* the membrane here becomes depolarized and the situation becomes that depicted in Fig. 9b. The dipoles which are now unopposed by the ones that were wiped out now produce a difference in potential between *B* and *A*, in much the same manner as was shown for the single cell except that here there is more nearly an actual layer of dipoles situated at the site of the wave of excitation.

As the wave of excitation passes over the syncytium toward *B* a succession of depolarizations takes place. Figure 9c shows another stage. Actually, of course, we are dealing with a solid mass of syncytial muscle and the wave of excitation, which appears as a line in Fig. 9b and c is really a surface and the row of dipoles which precedes it is a layer of dipoles (Fig. 9d).

From this point on we shall think of the wave of excitation as a surface passing through the muscle carrying positive charges on its front and negative charges behind. As it moves through the muscle it is always progressing in the direction toward which the positive charges point.

The vector representing the electromotive

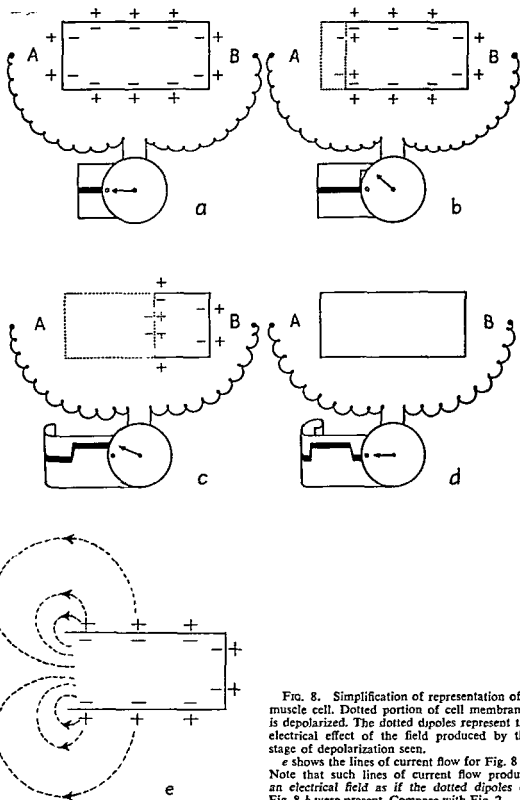


FIG. 8. Simplification of representation of a muscle cell. Dotted portion of cell membrane is depolarized. The dotted dipoles represent the electrical effect of the field produced by the stage of depolarization seen.

e shows the lines of current flow for Fig. 8 b. Note that such lines of current flow produce an electrical field as if the dotted dipoles of Fig. 8 b were present. Compare with Fig. 2.

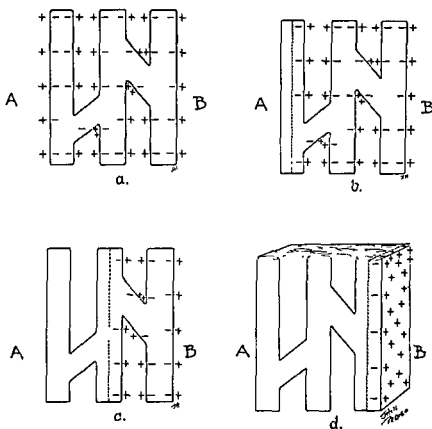


FIG. 9. Depolarization of a Syncytium. The simplified diagram shows that depolarization (beginning all along left margin) produces an effect as if a layer of dipoles were moving through the muscle mass.

force produced by a dipole is conventionally drawn from the negative toward the positive pole. It follows that the direction of the electromotive force produced by a flat wave of excitation is perpendicular to the surface of the wave and points in the direction of the positive charges.

Depolarization of a Spherical Mass of Muscle

If we have a sphere of muscle immersed in a solution of electrolytes (Fig. 10) and we cause excitation at the point *P*, the wave of excitation will spread out in all directions from the point *P* and will progress across the sphere toward *B*. The surfaces *x*, *y*, *z*, and *h*, which are saucer-shaped, represent the wave of excitation in four of the successive positions that it occupies as it moves toward *B*.

It is seen that the wave of excitation be-

comes larger as it approaches the middle of the sphere and then becomes smaller again as it approaches the outer surface of the sphere near *B*.

This figure affords us an opportunity to discuss a few important things about the wave of excitation and the electromotive force produced by it. It is generally assumed that electrolytes are homogeneously distributed throughout healthy cardiac muscle and, therefore, that a wave of excitation passing through a mass of such muscle will have its dipoles uniformly spread over its surface. Any wave of excitation passing through such muscle, therefore, must carry on its surface the same number of dipoles per unit area of that surface. Since the magnitude of the electromotive force produced must depend upon the total number of dipoles on the wave of

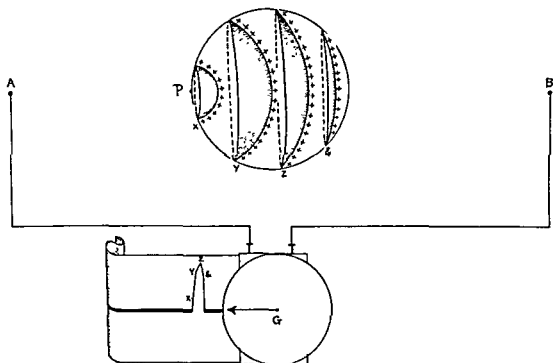


FIG. 10. Depolarization of a sphere of muscle. Depolarization, starting at a point on the left, proceeds in all directions at uniform speed. The wave of excitation assumes the successive forms X, Y, Z, and & and produces the corresponding deflections on the galvanometer.

excitation it is clear that *the magnitude of the electromotive force produced by a flat wave of excitation is proportional to the area of the wave of excitation*. This holds at any electrode distance that is applicable in clinical electrocardiography.

Only injured muscle contains fewer dipoles in some areas than others. There is no justification for the assumption that hypertrophied muscle contains a greater concentration of dipoles than does normal muscle.

Depolarization of a Bowl-shaped Mass of Muscle

We are now ready to proceed to more complicated forms. Figure 11 represents a mass of cardiac muscle in the shape of a bowl whose walls are of *uniform thickness throughout*. If we cause excitation of the entire inner (endocardial) surface of the bowl *at the same time*, the wave of excitation will immediately assume the shape of the inner surface and will be bowl-shaped also. As the wave of excitation moves at uniform

speed through the thickness of the walls of the muscular bowl it retains its bowl shape; it simply expands in size (Fig. 11b). Because he has found it extremely useful in helping students to visualize the subject the author will now introduce the device shown in Fig. 11c. It consists of cutting away half of the muscular bowl in the figure so that the wave of excitation and its relation to the muscular walls can be seen more clearly. Figure 11c and d shows how the wave of excitation in the shape of an expanding bowl approaches the outer surface of the muscular bowl. Since the walls of the bowl are of uniform thickness the wave of excitation reaches the outer surface at all points at the same time and disappears.

Here the wave of excitation is not a flat or near-flat surface and we need, therefore, to consider the direction and the magnitude of the electromotive force which it produces in a manner different from that which has been employed heretofore. Let us first consider a simplified diagram derived from the

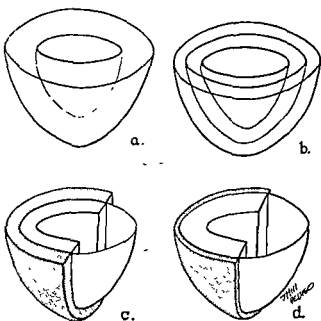


FIG. 11. *a* is a bowl-shaped mass of muscle the entire inner surface of which is excited simultaneously, producing a bowl-shaped wave of excitation as shown in *b*. *c* shows the same state of affairs represented in *b* employing the device of cutting away one half of the bowl but leaving the wave of excitation intact. This device and stippling of the undepolarized portion of the muscle makes visualization of the process clear. *d* is a later stage of depolarization.

cut surface of Fig. 11 presenting it as Fig. 12*a*. In this figure the dipoles *a* and *a'*, *b* and *b'*, *c* and *c'*, and *d* and *d'* will be considered in pairs. The first pair, *a* and *a'* are readily seen almost to neutralize one another. The potentials produced by each of the succeeding pairs of dipoles are determined by the parallelogram of forces. The vectors representing the dipoles *b* and *b'* are drawn with the proper angle between them and the parallelogram is completed using these two vectors as sides as shown in Fig. 12*b*. The diagonal *R* then indicates the direction and the magnitude of the resultant force.

If we repeat this process with the pairs of dipoles *c* and *c'* and *d* and *d'* we find that as we approach the apex of the figure (12*a*) the resultant for each successive pair of dipoles is larger but that it retains the same direction. Thus, the sum of the resultants of

all of the dipoles of Fig. 12*a* must have a direction perpendicular to the line *xy* (Fig. 12*c*).

It can further be shown that the *magnitude* of the resultant force of Fig. 12*a* will be the same as that derived from a distribution of dipoles along the line *xy* of the same density as that along the curved wave of excitation which it bridges.

Similarly, it is true that in the case of a solid, as represented by Fig. 12*d* the resultant electromotive force is of a direction and magnitude identical to those that would be derived from a flat wavefront situated in the plane drawn through the free edge of the bowl-shaped wave of excitation and limited in extent by that edge. Its extent and form, as shown in Fig. 12*d*, is best represented by fitting a lid to the free edge of the wave of excitation of Fig. 11 (*a*, *b*, *c*, and *d*). In the drawing 12*d* a section is cut out of this lid to clarify its relations to the wave of excitation and to the muscle wall.

It can be seen that when the wave of excitation moves toward the outer surface of the structure represented, this lid becomes larger and larger. Therefore, the electromotive force represented by the vector in Fig. 11 becomes correspondingly greater and greater until the wave reaches the outer surface. At this time the wave and the electromotive force suddenly disappear.

Thus, from this point on we shall follow the rule that *the magnitude of the electromotive force produced by a wave of excitation of any shape is proportional to the area cut off by its free margins on a plane passed through its free margins, and its direction is perpendicular to this plane.*

Figure 13 represents a bowl-shaped muscular structure with one wall (the one nearer the reader) thinner than the others. If excitation of the entire inner surface occurs it is clear that the wave of excitation will reach the surface first where the wall is thinnest, for we have assumed that the wave of excitation moves with uniform speed in healthy muscle. Thus, when the wave of excitation

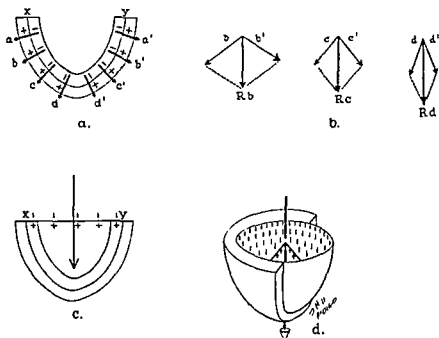


FIG. 12. Vector analysis of depolarization of the bowl-shaped mass of muscle of Fig. 11.

has progressed about halfway through the rest of the walls of the structure of Fig. 13 it will have arrived at the surface and begun to disappear in the thin wall nearest the reader. The effect of this is to produce a "defect" in the bowl-shaped wave of excitation (Fig. 13c). The wave of excitation now has free margins in two planes instead of one.

The effect of this "defect" in the bowl-shaped wave of excitation is determined in the same manner as was done for the upper margin in Fig. 12c and in Fig. 11a, b, c, and d. A vector N is constructed perpendicular to the plane of the defect. Its length or magnitude is proportional to the area in that plane enclosed by the margins of the defect. The origin of this electrical force can possibly be best explained by pointing out the fact that the disappearance of the wave in the area of the defect leaves a corresponding area of dipoles opposite this area unneutralized.

We now have two vectors, M and N , representing the electromotive force produced by the wave front of Fig. 13c. The resultant of these two electromotive forces, rep-

resented by vector R , is determined by applying the principle of the parallelogram of forces. It should be noted that an important effect of the "defect" which appears in the wave of excitation in Fig. 13c is that it caused a change in *direction* of the electromotive force. Thus, in Fig. 13a and b the electromotive force represented by the vector M , is becoming greater but it remains in the vertical direction downward. However, when the wave of excitation reaches the surface of the thin near wall, the electromotive force, represented by the vector R , swings to a partly backward direction, and some time later (Fig. 13d) its direction becomes even more backward (away from the reader). As the wave of excitation progresses outward it reaches the surface of the surrounding slightly thicker muscular wall and the defect becomes larger, and the vector N must also become larger. The larger the vector N becomes the more backward will be the direction of R .

Thus, depolarization of such a muscular structure as shown in Fig. 13 produces an electromotive force which varies both in mag-

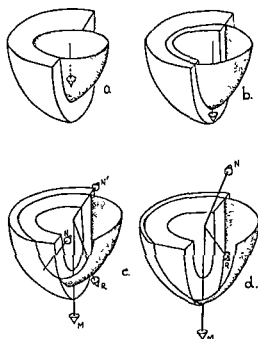


FIG. 13. Depolarization of bowl-shaped mass of muscle with one thin wall (wall nearest reader). The wave of excitation is stipple shaded. The vector representing the E.M.F. produced during depolarization of this structure changes first in magnitude and then in direction during the process. In *a* and *b* the wave of excitation is bowl-shaped and the vector is constructed as for Fig. 11. In *c* the thin wall nearest the reader has been penetrated and a defect appears in the bowl-shaped wave. *M* is the vector constructed for the area cut off on a plane passed through the free margin of the top rim of the bowl. *N* is the vector representing the area cut off on a plane passed through the free margin of the defect. *R* is obtained by adding *N* and *M* vectorially, employing the parallelogram of forces. *d* is a later stage. For such a structure the vector representing the E.M.F. produced by depolarization is seen to change first in magnitude only, then in direction.

nitude and direction. This is so directly applicable to the human heart that the reader is urged to study it carefully. The similarity between Fig. 13*c* and Fig. 15, which represents the wave of excitation in the left ven-

tricle 0.04 second after the beginning of ventricular activation, should serve to indicate that Fig. 13 is designed to show something of what we shall find when we come to consider depolarization of the ventricles.

2. Depolarization of the Ventricles: The QRS Complex

Our next step is to consider depolarization of the ventricles of the human heart. In so doing we must remember that the right ventricle is very much thinner than the left ventricle, that the interventricular septum is at least as thick as the thickest portion of the free wall of the left ventricle and that both the interventricular septum and the free wall of the left ventricle tend to taper in thickness from base to apex so that the apex of the left ventricle is commonly no more than half as thick as the basal portion. It is also important to realize that the right ventricle is shorter than the left.

We assume that the exciting stimulus reaches the muscle of the ventricles through the bundle of His and its branches. The right and left main branches of the bundle of His traverse the corresponding surfaces of the interventricular septum giving but a few twigs to these surfaces during their course. The left bundle gives off more twigs to the left side of the septum than the right bundle does to the right side of the septum. When the two main branches of the bundle of His reach almost to the apices of the ventricles each breaks up into a fine network of fibers which lines the rest of the endocardial surface of the corresponding ventricle (the Purkinje network).

Thus when an impulse passes down the bundle of His the first area to be excited to an extent sufficient to produce any measurable electrical effect will be the left side of the interventricular septum (Bayley). This effect results from a scant and patchy wave of excitation as shown in Figs. 14 and 15

(0.005 second). It is quickly opposed but not neutralized by an even more scant and more patchy excitation on the right side of the septum. The electrical effect at this stage of the process of depolarization of the ventricles may be represented by a small vector pointing from left to right in Figs. 14 and 15 (0.005 second).

About 0.01 second later the impulse has reached the apices of the two ventricles and the network of distributing fibers, and confluent waves of excitation are quickly formed on the endocardial surface of the ventricular apices as shown in Figs. 14 and 15 (0.015 second). The waves of excitation on the two surfaces of the interventricular septum are more complete but are still not confluent. The apparently greater extent of the right wave on the endocardial surface of the right ventricle is due to the fact that the impulse traverses less distance to reach a point on the lateral wall of the right ventricle than to reach a similar point on the lateral wall of the left ventricle. The electrical effects of the two waves of excitation on the opposite sides of the septum tend to balance one another and we will, therefore, construct a vector which represents largely the two waves of excitation on the endocardial surface of the apices. Actually, the wave of excitation is probably still more confluent on the left side of the septum than on the right side at this stage and the rightward component of the direction of the vector representing this stage of activation is contributed to by this effect. This vector, drawn according to the principles laid down in Chapter 1, will be, as shown

in Figs. 14 and 15 (0.015 second), almost perpendicular to the free margins of the waves of excitation which it represents and not of great magnitude because the waves are not very large.

About 0.005 second later (0.02 second after the beginning of ventricular activation) the impulse has spread to produce waves of excitation that extend a considerable distance up the walls of the two ventricles. The portion of the wave of excitation in the apex of the right ventricle has already penetrated to the epicardial surface for it has little thickness to traverse and this has produced a hole

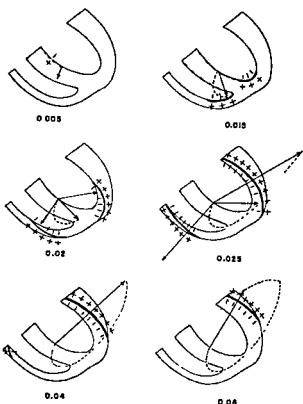


FIG. 14. The waves of excitation are shown in two-dimensional diagrams representing longitudinal sections through the heart. The waves of excitation in the interventricular septum at 0.02 and 0.025 seconds are omitted for purposes of analysis because their electrical effects are assumed to cancel one another.

The construction of vectors for each wave of excitation when two such waves are present at the same time is demonstrated, as well as the resultant vector. The dotted line is the spatial QRS loop.

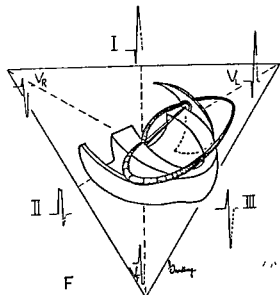
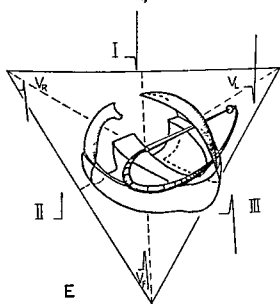
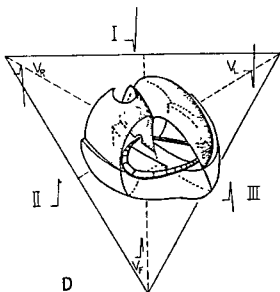
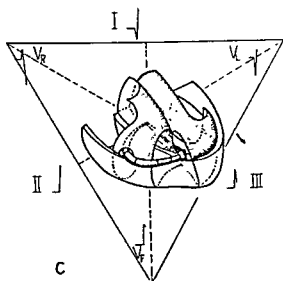
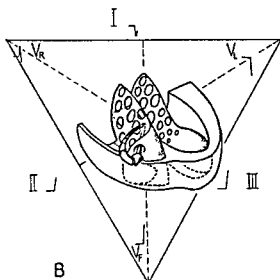
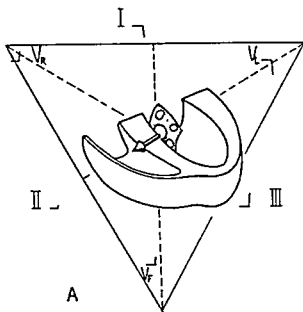
in the wave of excitation in the right ventricle. The two waves of excitation in the interventricular septum have become confluent in the neighborhood of the apex and have advanced sufficient distance through the thickness to have met at the apex of the septum where this structure is thinnest. At the same time the contiguous portion of the wave of excitation in the apical portion of the left ventricle has penetrated almost to the epicardial surface, the extent at any point depending upon the time of arrival of the impulse and upon the thickness of the ventricle at that point. The hole in the left ventricular wave of excitation as it appears in Figs. 14 and 15 (0.020 second), is actually the result of the meeting of the two waves of excitation in the septum. We may again regard the waves in the two sides of the septum as having little electrical effect because they balance one another. The electrical effect

FIG. 15. The drawings show the lower half of the ventricular portion of a heart in semi-transverse position and counterclockwise rotation about its longitudinal axis as viewed from the apex. Six stages of the process of depolarization of the ventricles are represented much as they were published by Gardberg and Ashman in 1943. The wave of excitation at each stage is represented by the shell-like structure shaded by stippling. The spatial vector representing the electrical effect of the wave of excitation present at each stage of depolarization is shown as a cone-tipped arrow. A, .005 second after beginning of activation; B, .015 second after beginning of activation; C, .020 second after beginning of activation; D, .025 second after beginning of activation; E, .040 second after beginning of activation; F, .060 second after beginning of activation.

The deflections of the limb leads of the electrocardiogram are also shown as they are developed by the succession of cardiac vectors.

At those stages of activation in which two waves of excitation occur (0.025 second) the spatial vector shown is the resultant of two vectors, each representing one of these waves of excitation (Fig. 14).

The earthworm-like structure represents the path described by the tip of the spatial vector as the process of depolarization proceeds and is, therefore, the spatial QRS loop. The most common normal variations in the spatial QRS loop occur in the first and last portions. It is not rare for these portions of the loop to be bent away from the general plane of the loop.



at this stage, then, may be regarded as being produced by two not very large waves of excitation, one in the left ventricle facing toward the left of the long axis of the heart, the other in the right ventricle facing toward the right of the long axis of the heart. The resultant force may be represented by a vector in the long axis of the heart as shown in Figs. 14 and 15 (0.020 second).

At 0.025 second after the beginning of the activation of the ventricles the situation is as represented in Figs. 14 and 15 (0.025 second). The impulse has reached the entirety of the endocardial surface of the two ventricles. The holes in the two waves of excitation are larger, due to (1) meeting of the portions in the septum in a wider area, and (2) penetration of the waves of excitation to the epicardial surface in wider area, specifically, in the areas where the wave of excitation was first formed and where the ventricular wall is thinnest. The electrical effects of the two waves in the septum canceling one another leaves us to consider the two large waves of excitation in the free walls of the two ventricles. In Fig. 14 and 15 (0.025 second) a vector is constructed for each of these almost oppositely directed waves and by employing the parallelogram of forces we find that the resultant may be represented by a rather small vector pointing a bit to the left of the long axis of the heart. The vector for the wave of excitation in the free wall of the left ventricle is made larger than that for the right because, as the figure shows, the wave of excitation is larger in the left ventricle than in the right.

In the succeeding few hundredths of a second the wave of excitation in the right ventricle becomes smaller more rapidly than does the wave in the left ventricle for the reason that the wall of the right ventricle is so much thinner than that of the left. Both waves are reaching the epicardial surface first in those regions where the waves appeared first. The effect thus produced is that the anterior edge of each wave is "retreating" toward the base more rapidly on the right

than on the left. Because the wave in the right ventricle is becoming progressively smaller in relation to the wave in the left the resultant vector becomes longer and longer and shifts progressively to a more leftward direction through these stages.

At 0.04 second there remains only a basal narrow rim of wave of excitation in the right ventricle (if any) while a rather large wave remains in the left ventricle. Of the stages of excitation that we have considered this is the first in which there is a large wave in one ventricle unopposed by a large or moderately large wave in the other. It is at this stage, then, that the largest electrical effect occurs. The vector which represents the electrical effect at this stage (Figs. 14 and 15 [0.04 second]) is the longest that occurs during the depolarization of the ventricles, and its direction, as shown in the figures, is necessarily approximately at right angles to the long axis of the heart.

After 0.04 second the wave of excitation in the left ventricle becomes progressively smaller and points in a progressively more backward direction. At the same time only small waves are present in the right ventricle near the base and in the conus. Because the conus is a less purely muscular structure than is the right ventricle the conduction of the impulse is probably slower in this area and a wave might persist here longer than would otherwise be expected.* At 0.06 second the situation is as depicted in Figs. 14 and 15 (0.06 second) and following this the vector simply becomes smaller and smaller and points very slightly more and more backward until it finally fades away.

It should not be necessary to point out that the margins of the waves of excitation are not smooth lines as depicted in the drawings but are irregular and that they are fringed by a zone of spotty or nonconfluent activation. The use of the sharply demarcated

* There is probably a great deal of variation in the electrical effects (in both magnitude and direction) produced in this region. The author believes that at times the electrical effects produced in this region may be practically nil.

line in the drawings is justified by the simplification of the technics of drawing and the clarity that it lends to the presentation.

Inscription of the Limb Leads of the Electrocardiogram

If we project, in succession, all the vectors described in the preceding paragraphs upon the three sides of the Einthoven triangle in the manner described in Chapter 1 we can derive the three standard limb leads of the clinical electrocardiogram (Fig. 16, 0.005 second through 0.06 second). It is to be remembered that each vector must first be projected upon the frontal plane before it can be projected upon the three sides of the triangle (see Chapter 1). In the figures the projection upon the frontal plane is accomplished by the perspective employed in drawing the vectors (note foreshortening). It should be obvious that even a very long vector pointing straight backward or straight forward—that is, perpendicular to the frontal plane—will have a zero projection upon that plane and will have no effect on the limb leads.

In Fig. 16 (0.005 second) we note that the earlier activation of the left side of the septum is responsible for the beginning of the Q wave in Lead I and at the same time for the beginning of the R wave in Lead III. The Q in Lead I and the R in Lead III are continued by the activation of the apices of the two ventricles as seen in Fig. 16 (0.015 second). The author believes that the apices of the two ventricles may at times be responsible for most of the Q in Lead I (and R in Lead III). The ascent of R in Lead I and the descent of S in Lead III are produced by the combined effects of the waves of excitation in the lateral walls of the two ventricles. At 0.04 second the apex of R in Lead I and of S in Lead III are simultaneously produced by electrical effects largely attributable to the lateral wall of the left ventricle. The same applies to most of the descent of R in Lead I and the ascending limb of S in Lead III (see Fig. 16, 0.06 second). The relationship in time of the peak

of R_I and the depth of S_{III} is dependent upon the orientation of the heart. It will be seen later that they are not always simultaneous.

If we project, in succession, the same series of vectors upon the lines of Leads V_R , V_L and V_F (see Chapter 1), we derive the QRS complexes of the three *unipolar limb leads* of the electrocardiogram.

The normal variations in the appearance of the limb leads are accounted for by variations in the orientation (position) of the heart with respect to the body. This subject will be discussed in terms of the spatial QRS loop.

The Spatial QRS Loop and Frontal Plane Loop; Rotations

During activation of the ventricles the cardiac vector is constantly changing in magnitude and direction. We have represented only a few of the stages in the process of depolarization and thus only a few of the vectors that occur. Although these may be sufficient to serve as a representation of the entire process it is obvious that an infinite number of stages occurs between any two stages that we have shown and, therefore, there is also an infinite number of vectors. These may be represented as in Fig. 17 if we give all of the vectors a common point of origin. The pathway described by the tip of the vector in its successive positions from the beginning of the activation to the end of that process is called the *spatial QRS loop*. It is represented as the earthworm-like structure on the drawings of Fig. 15. It is seen that the long axis of this loop is approximately perpendicular to the anatomic axis of the heart.

The *frontal plane loop* is the projection of the spatial loop upon the frontal plane. In the drawings the frontal plane loop is the spatial loop as drawn in the plane of the paper. Actually, for the *spatial* dimensions and directions of the loop we depend upon the optical illusion created by perspective, shading, and relation of the various parts of the loop to the drawing of the half-model of the heart.

The reader may clarify the difference be-

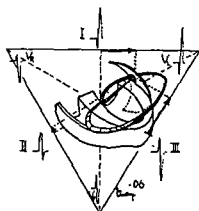
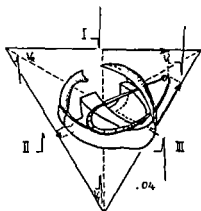
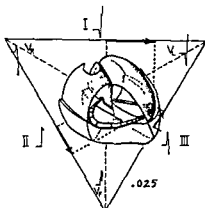
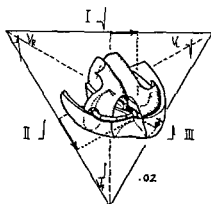
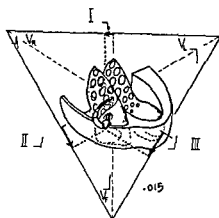
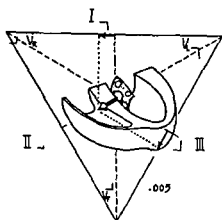


FIG. 16. Reduction of Fig. 15. Each vector is projected upon the sides of the Einthoven triangle, developing the standard limb leads. The unipolar limb leads are developed by projecting the same vectors onto the medians of the triangle.

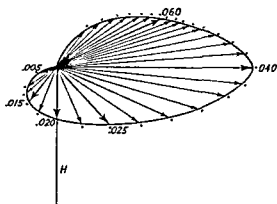


FIG. 17. The idealized spatial QRS loop, drawn by the tips of the vectors as they occur in succession. The timing of the loop is indicated in seconds.

H is the anatomic axis of the heart.

tween the spatial vectors and loop and the frontal plane vectors and loop by placing a piece of thin white paper over the drawing of the process of depolarization at 0.06 second (Fig. 15) and tracing the triangle, the vector, and the loop with a pencil. If we now compare this tracing, which is the projection of the loop and the vector on the frontal plane, with the drawing from which it was traced (and which retains the illusion of the third dimension) (Fig. 15, 0.06 second) he may see more clearly the distinction between the *spatial* and the *frontal plane* vectors and loops.

It has thus been shown how the QRS complex of the electrocardiogram is produced. It has also been shown what the spatial QRS loop (vectorcardiogram) is, as well as the frontal plane loop or vectorcardiogram. The relationship between these should now be clear.

The shape of the spatial QRS loop is not exactly the same for every normal heart but we have reason to believe that it is remarkably constant in its general form and proportions. There are variations especially at the beginning and at the ends of the loops, where, instead of remaining in one plane as shown in the drawings, the vectors may deviate to one or the other side of that plane. Minor wiggles in and out of this plane are common in any part of the loop. Of course,

the general form of the loop probably varies to the extent that it may be a bit wider or narrower in some persons than the form which is shown here.

The anatomic relation of the spatial QRS loop to the long axis of the heart is an important one. The long axis of the loop is at about a 90° angle to the anatomic axis. It must be clear to the reader that if the position of the heart is changed the spatial orientation of the QRS loop will be changed with it. Change in the spatial orientation of the QRS loop alters the frontal plane projection of the loop and therefore the form of the QRS complexes of the limb leads. In Fig. 18 the spatial loop is represented by the border of the plastic ellipse and the plastic rod which supports it is the anatomic axis of the heart. The small model of the ventricles will serve to clarify the orientation of the heart in space. Changes in the position of the heart are generally referred to as rotations. Three varieties of rotations are usually described: (1) rotation about a vertical axis, (2) rotation about an anteroposterior axis, and (3) rotation about the long axis of the heart.

Rotation about the *vertical* axis refers to changes of the position of the heart which move the apex back or forward (posteriorly or anteriorly) with relation to the base. Long ago Pardee pointed out that some hearts are so oriented that the apex points a good deal more anteriorly than is the case in others. Rotation about the anteroposterior axis simply makes the heart more transverse or more vertical. Rotation about the *long axis* of the heart involves turning the heart about its long or anatomic axis. If we do this while looking at the apex of the heart from a point on an extension of the long axis below the heart we will see that we can term these rotations clockwise and counterclockwise depending upon whether we turn the heart in the same or in the opposite direction in which the hands of a clock move. With the heart in the sthenic or semitransverse position strong counterclockwise rotation (Fig. 18a) produces a

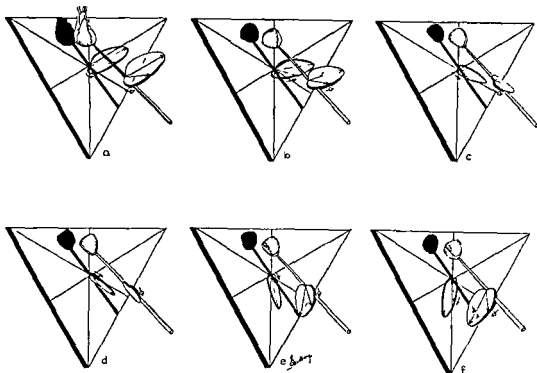


FIG. 18. The QRS loop shown in Fig. 17 was cut out of $\frac{1}{8}$ "-thick plastic and fastened to a rod representing the anatomic or long axis, H , of Fig. 17. The rod extends upward past the loop so that a small model of the heart could be fastened to the end of the rod. If the lower end of H is held by a ring stand and clamp, a projector may be used to throw a shadow of the loop upon a triangle fastened to a wall or held upright in a stand. If the center of the lens of the projector, the zero point of the spatial loop, and the center of the triangle are arranged in a straight line perpendicular to the surface of the triangle the shadow of the loop which appears on the triangle is the frontal plane loop. If the vectors of the frontal plane loop are projected upon the three sides of the triangle (as was done in Fig. 16) the standard limb leads of the electrocardiogram are developed. If these vectors are projected upon the medians of the triangle the unipolar limb leads are developed.

b , c , d , e , and f show the effects upon the frontal plane loop and therefore upon the limb leads of rotation of the heart about the anatomic axis H in a clockwise direction. Between c and d there is an intermediate position (or rotation) in which the shadows (or projection) of the edges of the spatial loop on the triangle are superimposed. a , b , and c are called counterclockwise rotations because if we begin with this intermediate position (between c and d) the heart must be rotated counterclockwise to attain them. Conversely d , e , and f are called clockwise rotations.

The small curved arrows (solid tipped for the spatial loop) indicate the order of development of the successive vectors that make up the loop.

QRS pattern characterized by a Q wave in Lead I, a fairly high R wave in Lead I, and a small R and a deep S in Lead III. In the less strongly rotated hearts which are still counterclockwise (Fig. 18b and c) S_{III} becomes smaller, R_{III} becomes more prominent and of longer duration, R_I becomes larger and Q_I becomes smaller as we approach the

intermediate rotation ("no rotation"). As we continue the rotation in the same direction we note that even in the slightly clockwise rotated heart (Figs. 18d, 19b) a Q appears in Lead III while only a tiny or no Q is present in Lead I. R in III becomes higher, while R in Lead I becomes smaller and soon an S appears in Lead I (Figs. 18e, 19b). In the strong clock-

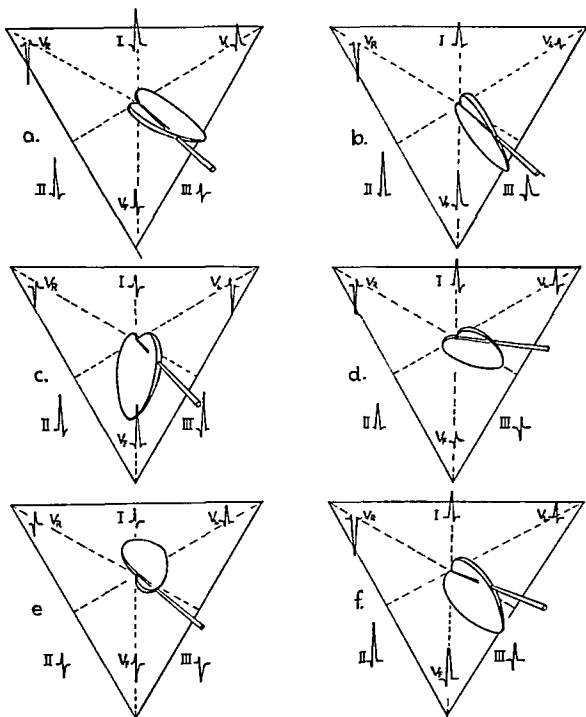


FIG. 19. The spatial QRS model held at eye level against a background upon which the triangle is drawn so that frontal plane projection can be visualized. *a*, *b*, and *c* correspond to Figs. 18*c*, *d*, and *f* respectively. *d* represents the spatial loop when anatomic axis is held as for transverse heart with apex back and rotated slightly clockwise about the anatomic axis. *e* represents the loop model orientation for a semi-transverse heart, slightly counterclockwise, with apex back. *f* is the orientation of the spatial loop when the heart is transverse, rotated clockwise about the anatomic axis and with the apex forward.

wise rotation R_I is quite small, R_{III} is very large and S_I is prominent. It is obvious in such cases that the peak of R_I and the peak of R_{III} are not simultaneous. It is for this reason that it is generally said that clockwise rotation is characterized by a Q in Lead III and an S in Lead I. If the reader will fashion a loop of cardboard and attach it to an applicator or small dowel rod ($\frac{1}{8}$ " in the manner shown in Fig. 18, he can, by holding it at eye-level against a background upon which he has drawn an equilateral triangle, study the effect of an infinite number of positions and rotations of the heart.

Figure 19*d* shows the loop of a slightly clockwise, apex-back transverse heart. This position of the heart is common in stocky persons and in pregnant women. Figure 19*e* shows the loop of a counterclockwise apex-back semitransverse heart. It is characteristic of the counterclockwise apex-back hearts that a pronounced S wave appears in all three standard limb leads. Figure 19*f* is an apex-forward clockwise-rotated heart with a more transverse anatomic axis than is seen in Fig. 19*c*.

The "rotations" of the heart represent not only variations in the positions of the heart from individual to individual but also variations which may occur in the same individual under different circumstances. The position of the heart changes with changes in the position of the body, and during ordinary respiration. Ordinarily electrocardiograms are made with the patient in the supine position. If the patient is lying just a little less than flat—either to the one side or the other or propped up a little—sufficient change in the position of the heart relative to the body may occur to cause a "change" from a previous electrocardiogram to appear. Many errors in interpretation have been made on this basis. The change in the position of the heart thus produced is complex, being combinations of rotation about two or more axes. If the reader learns to use a model loop properly he can easily establish that such changes in the QRS complex in

serial tracings are not of pathologic significance. The technic is described below. With regard to single electrocardiograms it is fairly safe to say that if one cannot find by trial and error a position of the loop such that projection on the frontal plane will account for the QRS complexes of the three limb leads, then that electrocardiogram is probably in some way abnormal. Slight inconsistencies must be disregarded. The reader should first practice with a group of known normals. If it is necessary to place the long axis of the heart in an impossible position e.g. pointing to the right or much more transverse than 0 degrees (horizon) to account for the QRS pattern then the electrocardiogram is abnormal unless a definite displacement of the heart can be demonstrated. It is necessary to permit considerable rotation about the anatomic axis to include most normal tracings. This is because the electrical rotation as reflected on the limb leads is exaggerated.

Technic of Analysis of Limb Leads by Means of the Model Loop

Given the three standard limb leads of an electrocardiogram one should first construct the idealized frontal plane loop. This is accomplished by measuring the various deflections of each lead and laying them off as projections on the appropriate sides of the Einthoven triangle as shown in Fig. 20. The polarity of the various leads must not be confused (see Chapter 1). A perpendicular is then dropped at the end of each projection into the interior of the triangle. These perpendiculars form the limiting extents of the loop in a number of directions. One begins to draw the loop at the center (zero) of the triangle. Since R_I , Q_{II} , and Q_{III} are the first deflections of the tracings shown the beginning of the loop must be a curved line which first touches (*but does not cross*) the lines drawn perpendicular to the ends of these projections. It is seen therefore that the loop must start to the right touching the line perpendicular to the pro-

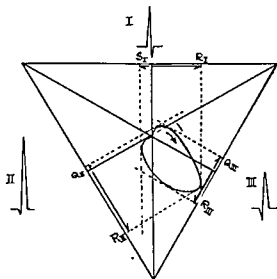


FIG. 20. Constructing the frontal plane loop from the limb leads. The peak values of all deflections of each lead are laid off on the appropriate sides of the Einthoven triangle. Perpendiculars are dropped and the loop is drawn within the limits formed by these perpendiculars (see text). The model spatial loop can now be held at eye level and by trial and error the orientation is found which produces a projection on the frontal plane like that of the constructed loop. If the model loop is held in a mechanical stand parallel light can be used to throw a shadow on the triangle drawn on the wall. Projection by this method is especially valuable in teaching.

jection Q_{II} , and then the line drawn perpendicular to the projection Q_{III} . Alternately, it may be drawn to the point at which the two perpendiculars intersect. It must then curve downward to remain within the limitations of Q_{III} and reach the perpendicular to the projection of R_I , possibly at the point at which it is intersected by the perpendicular to the projection R_{II} ; then upward so as to remain within the limitation of R_{III} . Finally it reaches the perpendicular to the projection S_I from whence it turns back to the center.

Of course the loop is frequently a wavy line. However, it is to be remembered that we are drawing an idealized loop. With some practice and attention to details idealized loops can be drawn which are satisfactory for clinical analysis. It is not to be denied that there are at times alternate forms but these are not frequently troublesome.

After the frontal plane loop has been drawn one holds the model of the spatial QRS loop (grasping it by the anatomic axis) at eye level and finds, by trial and error, the orientation of the spatial loop whose projection upon the frontal plane produces the constructed loop. A fairly close approximation of the anatomic axis of the heart results from this procedure.

If one has two tracings on the same individual which look different one constructs the frontal plane loop for each tracing and then finds whether the change from one frontal plane loop to the other can be produced by changing the rotation of the loop about the anatomic axis (Fig. 19a-b) by making the anatomic axis more vertical or more transverse (Fig. 19c-f, or f-c), by making the anatomic axis more (or less) parallel to the frontal plane (apex back or forward, Fig. 19a-e), or by various combinations of these changes. If this can be done the change from one tracing to the other may be nonpathologic.

All six limb leads may be used in the same way but it must be remembered that the deflections of V_R , V_L , and V_F must be multiplied by $\sqrt{3}$ before they are employed as projections upon the lead lines.

Electrical Axis: Axis "Deviation"

It has long been customary in describing electrocardiograms to note the general direction of the electrical effects as projected upon the frontal plane. Originally this was accomplished by laying off the peak values of the QRS potentials on any two leads on the appropriate sides of the Einthoven triangle and dropping perpendiculars whose intersection defines a vector as described for Fig. 5. The direction of this vector is called the electrical axis of the QRS. In Fig. 21 the peak value of R_I (12 mm.) is measured off on the line of Lead I (the horizontal side of the triangle) and the depth of S is measured off on the line of Lead III. Perpendiculars are dropped at the ends of these measured projec-

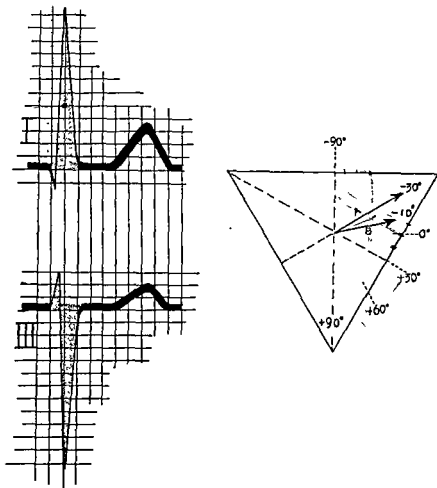


FIG. 21. Electrical axis of QRS plotted on the Einthoven triangle (A) by plotting the peak potentials of Leads I and III and (B) by plotting the mean potentials (area) of the QRS complexes of the same leads.

tions and their intersection defines the vector A which is seen to have a direction of -30° .

Later Wilson popularized the practice of measuring the *mean* QRS axis. To accomplish this one must first measure the *areas* of the various QRS deflections in each lead giving each its proper algebraic sign and then add them. In Lead I of Fig. 21 the area of R (shaded) calculated according to the formula for the area of a triangle ($\frac{1}{2} \times \text{base} \times \text{altitude}$) = $\frac{1}{2} \times 12 \times 1.6 = +9.6$ units. The unit is one small rectangle of the EKG paper. The Q wave has an area of about -0.6 unit (minus because it is a negative deflection).

The addition of AQ^* and $AR = +9$ units. The $AQRS_I$, then is 9 units. If we measure the area of S_{III} we find that $AS_{III} = \frac{1}{2} \times 1.3 \times -12 = -7.8$. $AR_{III} = \frac{1}{2} \times 1 \times 3 = +1.5$. $AQRS_{III} = AS_{III} + AR_{III} = -6.3$ units.

If we plot these values for $AQRS_I$ and $AQRS_{III}$ on the appropriate sides of the Einthoven triangle and drop perpendiculars we define the vector B as the mean axis of QRS ($AQRS$) on the frontal plane. The direction of this vector is -10° .

The figure shows the difference between

* Bayley originated this designation for mean values; A=area.

plotting the peak values and plotting the mean values of the QRS complexes. The most immediately apparent superiority of Wilson's method is that it avoids the error which occurs in the peak method when the latter is applied to tracings in which the peak values in any two leads are not reached at the same time. Obviously the plotting of instantaneous values which do not occur at the same time is unrealistic.

If a QRS axis plotted as described above lies between -0° and -90° it is said to be

deviated to the left. If a QRS axis lies between $+90^\circ$ and 180° it is said to be deviated to the right.

The same type of measurements and axis determination is applied to the T wave or any other deflection of the electrocardiogram.

The mean spatial QRS vector is generally at right angles to the anatomic axis and its direction may be represented on the model of the loop by the 0.04 second vector of Fig. 15 because this vector is also perpendicular to the anatomic axis.

Suggested Reading

- Cohn, A. E., and Raisbeck, M. J. An investigation of the relations of the position of the heart to the electrocardiogram. *Heart* 9:311, 1921-22.
- Durrer, D., and van der Tweel, L. H. Spread of activation in the left ventricular wall of the dog. I. *Am. Heart J.* 46:683, 1953.
- Durrer, D., and van der Tweel, L. H. Spread of activation in the left ventricular wall of the dog. II. *Am. Heart J.* 47:192, 1954.
- Durrer, D., van der Tweel, L. H., and Blickman, J. R. The spread of the activation in the left ventricular wall of the dog. *Koninklijke Akademie van Wetenschappen, Proceedings, Series C.56.* 2:288, 1953.
- Durrer, D., van der Tweel, L. H., and Blickman, J. R. Spread of the activation in the left ventricular wall of the dog. III. *Am. Heart J.* 48:13, 1954.
- Durrer, D., van der Tweel, L. H., Berreklouw, S., and van der Wey, L. P. Spread of activation in the left ventricular wall of the dog. IV. *Am. Heart J.* 50:860, 1955.
- Gardberg, M., and Ashman R. The QRS complex of the electrocardiogram. *Arch. Int. Med.* 72:210, 1943.
- Harris, A. S. The spread of excitation in turtle, dog, cat and monkey ventricles. *Am. J. Physiol.* 134:319, 1941.
- Lewis, T. *The Mechanism and Graphic Registration of the Heart Beat.* London, Shaw and Sons, (ed. 3) 1925.
- Mann, H. A method of analyzing the electrocardiogram. *Arch. Int. Med.* 25:283, 1920.
- Meek, W. J., and Wilson, A. The effect of changes in position of the heart on the QRS complex of the electrocardiogram. *Arch. Int. Med.* 36:614, 1925.
- Wilson, F. N., Macloed, A. G., and Barker, P. S. The potential variations produced by the heart at the apices of Einthoven's triangle. *Am. Heart J.* 7:207, 1931.

3. The Precordial Leads

Originally the precordial leads were made by placing an electrode connected to one pole of the galvanometer upon the chest wall near the heart while an electrode connected to the other pole of the galvanometer was placed upon a "distant" portion of the body. The latter electrode was called the "indifferent" electrode, for the magnitude of the potential changes at the distant point is relatively small as compared to the magnitude of the potentials at the point close to the heart. The electrode placed on the chest wall near the heart was known as the exploring electrode. Originally the "indifferent" electrode was placed upon the left leg and the exploring electrode was placed in the fifth interspace near the apex of the heart. The lead was designated Lead IV. In recording this lead it was customary to attach the left arm lead wire to the electrode on the left leg and the right arm lead wire to the precordial electrode. The complexes were recorded with the polarity reversed and all normal leads showed deep Q waves and inverted T waves. When the polarity of these leads was reversed and multiple chest leads had been recommended by Wilson the left leg was still the most popular "indifferent" electrode. Such leads were designated CF. Some employed the right arm for the "indifferent" electrode position. Leads made with the indifferent electrode on the right arm were designated CR.

Wilson first suggested the connection of all three extremity electrodes (each through a relatively large resistance) to a common point, and the employment of this *central terminal* as the indifferent electrode. Its potential was regarded as being about zero. While this assumption is now known to be

erroneous it still remains the best indifferent electrode known. Leads made with the central terminal as an indifferent electrode are called V leads or unipolar leads. Conventionally six precordial leads are made, the exploring electrode being placed at the following positions:

V_1 in the 4th interspace at the right sternal margin

V_2 in the 4th interspace at the left sternal margin

V_3 midway between V_2 and V_4

V_4 in the 5th interspace in the midclavicular line

V_5 in the anterior axillary line at the same level as V_4

V_6 in the midaxillary line at the same level as V_4

In addition to these V_7 , in the posterior axillary line, and V_8 , in the scapular line at the same horizontal level as V_6 , are occasionally used.

In representing the limb leads, which are assumed to be recorded by equidistant electrodes that are not too close to the heart, vector analysis seems to be satisfactory. However, when we place an electrode upon the anterior chest wall 2-3 cm. from the heart it becomes impossible to employ vector analysis, at least without making correction for the distance. Furthermore, when there are two waves of excitation (one in the right ventricle and one in the left, e.g., at 0.025 second) it is possible to make errors resulting from the general assumption of single dipole representation (implied by setting up a single vector) which we have employed in analysis and synthesis of the limb leads.

It has been assumed that the potential at

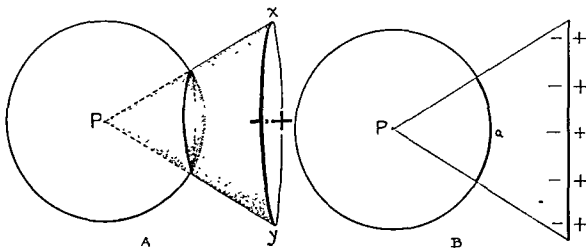


FIG. 22. In *A*, *xy* is a disc-shaped wave of excitation. *P* is an electrode.

If lines are drawn from *P* to the margins of *xy* a cone is constructed. This cone is a solid angle. If a unit sphere is constructed about *P* as a center the previously described cone cuts off an area of the surface of this sphere; this area is a measure of the solid angle.

B is a two-dimensional simplification of *A*.

any point in a homogeneous medium is proportionate to the solid angle subtended at that point by the free margins of the wave of excitation. In Figure 22*A*, *xy* is a circular, flat wave of excitation. The potential at *P* is proportionate to the area on the unit sphere (inscribed about *P*) which is cut off by the cone which has *xy* as a base and *P* as an apex. Since solid figures of this kind are extremely difficult to produce for waves of excitation which have the shapes described for those in the heart it is common practice to employ the simple representation shown in Fig. 22*B*. Here the solid angle is measured by the arc *a*. This simplification is itself unsatisfactory unless the third dimension of the wave of excitation is kept in mind.

Figure 23 represents the waves of excitation postulated for the human heart at 0.005–0.015 second, 0.020 second, 0.025 second, and 0.040 second, respectively. The waves of excitation at 0.005 second, and 0.015 second are placed on the same diagram. The first horizontal row of diagrams of the figure represents the effects of the waves of excitation upon the electrode placed at the position, *V*₁.^{*} The solid angle drawn to the small area of activation on the left side of the septum at 0.005 second produces a small positive

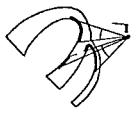
deflection in Lead *V*₁. At 0.015 second two solid angles are drawn, one to each of the waves of excitation present at this time (one in the apex of the right ventricle, the other in the apex of the left ventricle). These solid angles are both small. One (left ventricular) is positive and the other (right ventricular) is negative. The net effect of the two solid angles is represented as zero. Obviously, however, a slight change in the position of the heart may cause the net effect to become negative and a change in position of the heart in the opposite direction may cause it to become positive. The same effect would result from a slight change in the placement of the electrode. It is not surprising, therefore, that there is variation in the duration of the R wave in Lead *V*₁ of the electrocardiogram. Furthermore, it is apparent that, if as activation proceeds there is a wavering of the balance between the effects of the two apical waves of excitation, the potential at the electrode may be first positive, then negative, and then positive again producing a small notch in the R wave of the lead. Such notches are not uncommon in the R waves in Leads *V*₁, *V*₂, and at times in *V*₃.

^{*} At this point the reader should review Fig. 14 which shows the orientation of the dipoles on each wave of excitation of Fig. 23.

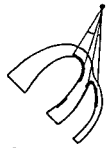
V_1



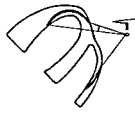
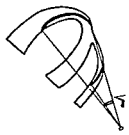
V_3



V_5



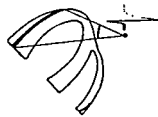
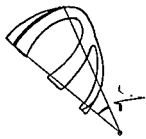
.005 - .015



.020



.025



.04



(13)

Fig. 23. A longitudinal transverse section through the ventricles is seen from above. For each diagram the back of the body is above and the anterior surface of the body, where the precordial electrodes are placed, is below. The heart is in an apex forward position. The solid angles marked with the heavy arcs are negative; those marked with the thinner arcs are positive.

The first horizontal row of diagrams depicts the development of the potentials at V_1 . The second horizontal row of diagrams shows the development of the potentials at V_4 and the third horizontal row of diagrams represents the development of the potentials at V_6 . The waves of excitation (heavy lines) are depicted at 0.005-0.015, 0.02, 0.025, and 0.04 seconds as shown in Fig. 14. The potentials are estimated on the basis of the solid angle method. The solid angle subtended at the electrode is negative when the electrode faces the negative surface of the wave of excitation and positive when the electrode faces the positive surface of the wave of excitation (see Fig. 14 for polarity). Thus single dipole representation is not employed for the precordial leads. When two waves of excitation are present and the solid angles are of opposite sign (V_1 at 0.02 second) the solid angles are added algebraically (by estimation). The complexes are drawn as solid lines to the extent to which they are completed in the representative diagrams. The dotted completions of the diagrams are obvious derivations from diagrams (not shown) representing the last stages of activation.

The solid angle is not drawn for the small wave of excitation on the left side of the septum at 0.005-second, because it would complicate the diagram. Its effect, which seems fairly obvious, is, however, drawn into the complex (see small Q in V_2).

At 0.020 second the solid angle to the wave in the right ventricle is smaller than the solid angle to the wave in the left ventricle. The former is positive and the latter is negative. The net effect is *slight* negativity at V_1 . However, there is not a great difference in the sizes of the solid angles and here, again, a small difference in the position of the electrode (or of the heart) may easily change the net effect. In the figures representing the waves of excitation at 0.015 second and 0.020 second the waves of excitation in the septum are omitted because they are assumed to neutralize one another and because including them would thus, unnecessarily complicate the diagrams. At 0.025 second the positive solid angle to the wave in the right ventricle appears to be almost as large as the negative solid angle to the wave in the left ventricle. However, the difference would be greater if the figure had been represented in three dimensions, and the net effect, therefore, is represented as definitely negative. At 0.04 second there is virtually only one solid angle (the right ventricle is almost completely depolarized at this time), and it is large and negative. Thus the largest deflection in Lead V_1 is usually a deep S wave.

The second row of diagrams of Fig. 23 represents the potentials recorded at V_3 at the same times as those chosen for the analysis of Lead V_1 . They are developed in the same manner as has been described above. The only special comment which is required is that although the solid angles at 0.015 second appear large it is to be remembered that the waves of excitation at this time are rather small in all of their dimensions. A large three-dimensional solid angle, therefore, will occur only if the electrode is quite close to the heart. Since this electrode (V_3) is quite close to the apex of the interventricular groove and since in some patients the heart is quite close to the chest wall rather high R waves in V_3 are not unusual. Finally, since the position of the heart determines the relationship of the electrode to the waves of excitation, variation in the position of the

heart determines the potential at the electrode.

The third row of diagrams of Fig. 23 represents the manner in which the deflections in the electrocardiogram recorded at V_5 are developed.

Thus, the most commonly encountered pattern of normal precordial leads shows the following characteristics: V_1 is characterized by a small R wave of variable duration and a deeper S wave. The R wave becomes progressively larger from V_1 to V_5 . The R wave in V_6 is generally but not always smaller than in V_5 , due to the greater distance from the heart. The peak of the R wave tends to occur at a later time as we move the electrode from V_1 to V_6 . The S wave is usually deeper in V_5 than in V_1 and commonly becomes less deep as we move the electrode to the left. Usually it finally disappears or is small in V_6 . Much variation occurs. S is sometimes absent in V_3 , is more frequently absent in V_4 , and still more frequently absent in V_5 , and most frequently absent in V_6 .

Some of the variations in the normal pattern of precordial leads are due to variation in the position and rotation of the heart. Figure 24 represents the effect upon the precordial potentials of an apex-back position of the heart. The most pronounced effect is the appearance of well-marked S waves in all of the precordial leads. R in V_1 may also be of very short duration. Correlation between the frontal plane loop which indicates the apex-back position and the precordial leads (with deep S waves in all leads) is seen. Commonly, too, with the heart in this position the R waves are of almost equal height from V_3 through V_5 .

In many normal persons the S in V_1 is quite small. This is presumably due to a combination of distance effect and rotation of the heart. It is often associated with clockwise rotation in vertical hearts. At times a normal Q in V_4 , V_5 , and V_6 may be as large as 5 or 6 mm.

In still other cases, especially in thin young adults and in children, the R waves in V_4 and V_5 are very high; 25 mv. is not rare. This

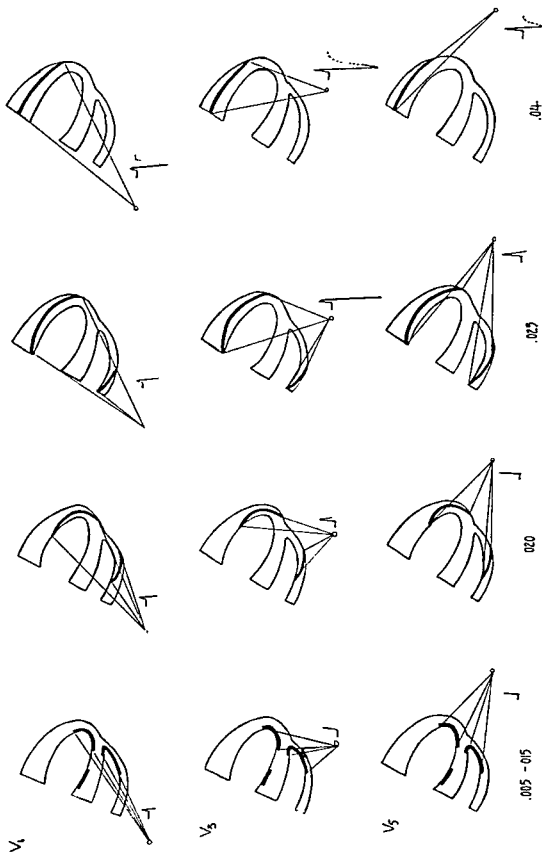


FIG. 24. The precordial leads when the apex is back. The pronounced S waves in all of the precordial leads are characteristic of the apex back heart. Compare with Fig. 23.

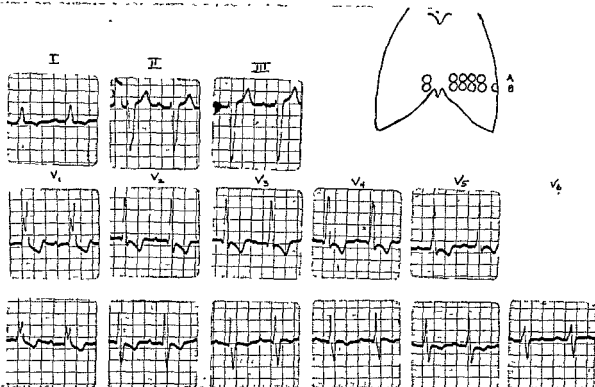


FIG. 25. A, The precordial electrode positions arranged along a horizontal line at the level of the xiphisternal junction.

B, The effect of slight change in electrode position upon the precordial leads.

is probably due to the proximity of the heart to the chest wall in an *apex-forward* position. At times the S in V₂ and V₃ is very deep.

Finally, in some cases the precordial leads, while in every other respect quite normal, are rather small. The explanation of this phenomenon is not immediately available. Some light may be thrown upon it by continued study of contour-eccentricity effects. Abnormally small deflections in the precordial leads will be taken up under the proper headings.

The T waves in the precordial leads are usually highest in Leads V₃ and V₄. In V₁ the T wave is positive in about 60 per cent of adult normals and negative in 40 per cent (Ashman). In children and many young adults, especially females, the T may be negative in V₂ and V₃. It is rare for it to be negative even in V₄ in young women.

The repeated emphasis of the critical importance of the relationship between the posi-

tion of the electrode and the position of the heart should not be forgotten. The impossibility of placing the electrode in precisely the same relationship to the heart in two successive examinations of the patient makes it extremely important to realize that changes which appear in the deflections upon repeated examinations may be due to this factor rather than to changes in the heart. Changes in the limb leads due to changes in position of the heart resulting from unremarked changes in body position, to flatulence, etc., have been referred to in a previous chapter. The changes in the precordial leads due to the same factors and to the additional difficulty in placing the electrodes in the same relationship to the heart are more marked. A great many errors have been made because of failure to realize that this is true. In general it is to be remembered that interpretation of serial precordial leads is full of pitfalls. Figure 25

illustrates the extent of the effect which may result from placing the electrodes only one electrode's width higher or lower than on the previous examination.

For these reasons the author began several years ago to place the precordial electrodes along a horizontal line across the chest at the level of the xiphisternal junction. V_1 is made to the right of the sternum at its margin. V_2 is made at the left sternal margin. From V_2 through V_5 the electrode positions are adjacent to one another as shown in Fig. 25. V_6 is made in the left midaxillary line.

Successive examinations on the same patient seem to yield more constant results with these electrode positions but the method does not obviate the difficulties outlined above in a very important degree.

The foregoing description of the normal precordial leads has been limited to the conventional precordial leads. Obviously an unlimited number of precordial leads can be made. However, it is found expedient to delay discussion of the normal precordial findings over other portions of the chest until those problems upon which they bear are described.

Suggested Reading

American Heart Association. Standardization of precordial leads. *Am. Heart J.*, 15:107, 1938.

Johnston, F. D., Rosenbaum, F. F., and Wilson, F. N. The ventricular complex in multiple precordial leads. *Mod. Concepts of Cardiovascular Disease*, 12, No. 6, June, 1943.

Kossmann, C. E., and Johnston, F. D. The precordial electrocardiogram. I. The potential variations of the precordium and of the extremities in normal subjects. *Am. Heart J.*, 10:925, 1935.

Wilson, F. N., Johnston, F. D., Macloed, A. G., and Barker, P. S. Electrocardiograms

that represent the potential variations of a single electrode. *Am. Heart J.*, 9:477, 1934.

Wilson, F. N., Johnston, F. D., Rosenbaum, F. F., and Barker, P. S. On Einthoven's triangle, the theory of unipolar electrocardiographic leads and the interpretation of the precordial electrocardiogram. *Am. Heart J.*, 32:277, 1946.

Wilson, F. N., Johnston, F. D., Rosenbaum, F. F., Erlanger, H., Kossmann, C. E., Hecht, H., Cotrim, N., deOliveira, R., and Barker, P. S. The precordial electrocardiogram. *Am. Heart J.*, 27:19, 1944.

4. T Wave: An Introduction to QRS-T Relationship

Origin and Shape of T Wave

We have seen that the QRS complex is produced by the electrical effects of depolarization of the ventricular myocardium. Following depolarization the muscle is returned to the resting state by metabolic processes that cause the dipoles to reaccumulate across the cell membranes. These metabolic processes are much slower than the electrophysical changes that characterize depolarization and repolarization therefore requires an elapsed time many times that required by depolarization. It follows that this process cannot be represented as a single wave passing over the muscle as was done for depolarization. Figure 26 shows a segment of left ventricular wall represented (in an extremely simplified diagrammatic manner) by four fibers. The fibers are shown undergoing depolarization and then repolarization. For the latter process it is assumed, in this figure, that repolarization begins where depolarization began and that the rate or time course of repolarization is uniform in all the fibers. The tracing shown at the right is for the potential at an electrode, *P*, at such a distance from the wall of the ventricle that there is little difference between the solid angles drawn to the endocardial and epicardial fibers. It is seen that although repolarization begins at the endocardial surface (Fig. 26*d*), soon (Fig. 26*e*) the process is going on throughout the thickness of the muscle at the same time. Thus it is difficult to speak of a "wave" of repolarization in the same sense that we speak of a wave of depolarization.

It is seen that as the dipoles reaccumulate

an electrical effect is produced that causes a deflection of the galvanometer in a direction opposite to that which was produced by depolarization. This deflection is the T wave of the electrocardiogram. At any instant during repolarization except at the very beginning and very end of the T wave, the voltage recorded is the net effect of a balance of electrical forces present in a multitude of fibers occupying the entire thickness of the ventricular wall.

It may be seen that at each stage of repolarization the electrical effect at the electrode *P* may be regarded as if it were produced by a balance between the dipoles on the endocardial surface on the one hand and the dipoles on the epicardial surface on the other. For this reason we may analyze many electrocardiographic problems by representing the total effect as if it resulted from the two opposing surface effects. Each of these opposing surface effects may be represented by a monophasic curve. Experimentally, if we cool the fibers at the epicardial surface to the temperature at which they fail to undergo depolarization (Fig. 27*A*) and record the potential at *P* after stimulating the endocardial surface we record a monophasic action potential curve which represents the effects of depolarization and repolarization of the endocardial surface. As soon as the endocardial surface is depolarized (Fig. 27*A-b*) and during the entire process of depolarization of the block of muscle the potential at *P* is proportional to the electrical moment of seven dipoles. When the wave of depolarization reaches the cooled epicardial surface it is

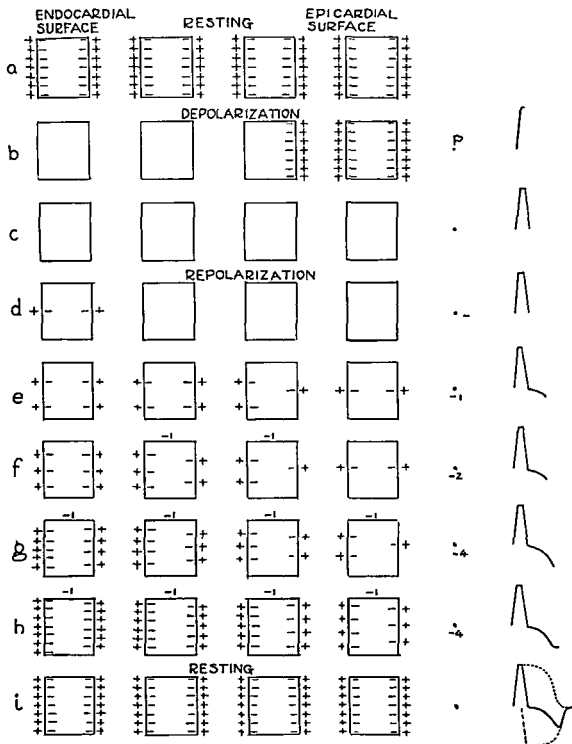


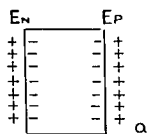
FIG. 26. Simplified representation of repolarization of a segment of ventricular wall. The endocardial surface (where depolarization begins) is on the left; the epicardial surface is on the right. The ventricular wall is represented by four fibers. It is seen that if the rate of repolarization were uniform throughout the muscle as represented here an inverted T wave should occur.

The two dashed curves may be ignored for the moment.

It is important to note that the balance between the dipole effects pointing toward the right and those pointing to the left throughout the muscle is equal to the balance between the dipoles on the epicardial surface and the dipoles on the endocardial surface. In other words it is the surface effects which are all-important.

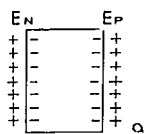
It is understood that the electrode *P* is sufficiently distant from the ventricular wall for there to be little difference between the solid angles subtended at *P* by the endocardial and epicardial surfaces.

The assumption that opposite sides of the same fiber may be in different stages of repolarization at the same time may be questioned. Actually the diagram is an oversimplification, justified by the fact that the myocardium is a syncytium; each of the "fibers" may be thought of as representing a two-fiber block of syncytium so that the two sides represent opposite sides of two adjacent fibers bridged by a joining fiber (see Fig. 9, p. 12).



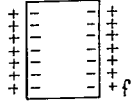
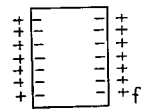
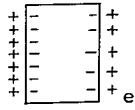
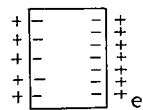
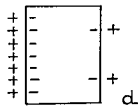
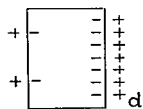
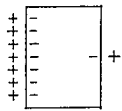
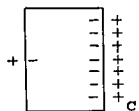
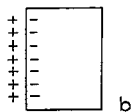
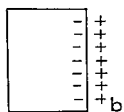
A.

P.



B.

P.



blocked by the cooling (Fig. 27A-b) and the potential remains at this level. As repolarization begins, at first slowly (Fig. 27A-c) the potential begins to fall slowly. Repolarization becomes more rapid as it progresses (Fig. 27A-e and f), the number of dipoles at the endocardial surface increases more rapidly, and the potential at *P* falls more rapidly. Finally, when repolarization at the endocardial surface is complete the potential is again zero (Fig. 27A-f). The monophasic action current curve for the endocardial surface thus may (theoretically) be recorded. Inasmuch as this is an oversimplification of the problem it represents a bit of didactic license. However, as a simplified device to be employed in understanding many of the problems of electrocardiography it has been useful. Its limitations will be discussed later.

If we cool the *endocardial* surface of the ventricular wall and stimulate subjacent to the cooled surface the corresponding monophasic curve representing the electrical effects of the epicardial surface will be recorded (Fig. 27B). During depolarization the potential remains at zero. When the epicardial surface is reached and is depolarized (Fig. 27B-b) the potential drops to a negative value equal to the positive value attained in Fig. 27A-b. As repolarization begins, at first slowly, the potential at *P* slowly rises and with the progressively increased speed of repolarization rises more rapidly, finally reaching zero when repolarization is complete.

If we place the two monophasic curves of Figs. 27A and 27B in the *proper time relationship* to one another represented by the period of time required for the wave of depolarization to pass through the wall to reach the epicardial surface, we see that the curve of Fig. 26 may be regarded as the result of the algebraic addition of the two broken monophasic curves of Fig. 26i.

Thus if repolarization follows the same order as depolarization but is slower, and if the rate of repolarization is uniform throughout the muscle, the electrocardiogram recorded by placing a unipolar electrode at *P* will show an inverted T wave. If we wish to look at the matter more simply the electrical effects of repolarization should be opposite to the effects of depolarization and represent the same quantitative potential changes so that the area (time \times voltage) under the QRS equals the area (time \times voltage) of the T wave. Actually, in normal human electrocardiograms we generally do not find that the T wave is opposite in direction to the QRS complex. As a matter of fact, most normal tracings show an upright T wave in Lead I where the QRS is usually upright and the same holds for most other leads, especially the left precordial (unipolar) leads in adults. This can only mean that repolarization does not follow the same order as does depolarization.

It was F. N. Wilson who first suggested that repolarization may be more rapid at the

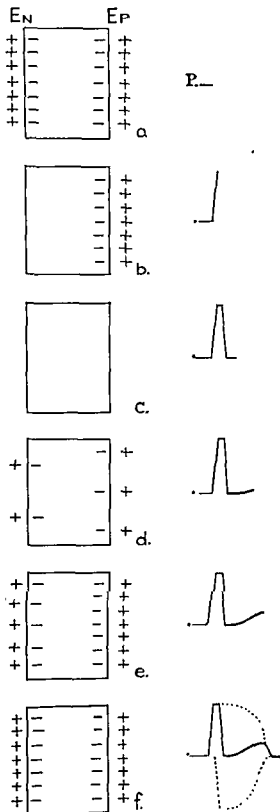
FIG. 27. A. Diagrammatic representation of the monophasic curve produced by depolarization and repolarization of the endocardial surface. The epicardial surface is cooled to a degree that renders it incapable of being depolarized by the wave of excitation.

The potential at *P* rises rapidly when depolarization begins and falls slowly during repolarization. The net effect at *P* is the result of a balance of opposing effects occurring throughout the muscle. It may be represented as a balance between the epicardial and endocardial surface effects.

The monophasic curve representing the depolarization and repolarization of the endocardial surface shows that repolarization is much slower than depolarization; that it begins slowly, becomes more and more rapid, and finally slows toward the end.

B. The monophasic curve showing the electrical effects at *P* of depolarization and repolarization of the epicardial surface. The same order of depolarization is assumed which was shown in A.

Here, because the endocardial surface fails to depolarize due to cooling the potential remains at zero until the epicardial surface is reached. It then drops rapidly to a negative value. When repolarization occurs the potential returns to zero in the manner shown.



epicardial surface of the ventricle than at the endocardial surface, as represented by Fig. 28. In terms of the monophasic curve analysis employed above the same phenomenon may be represented by shortening the duration of the monophasic curve representing the electrical effects of the epicardial surface (see Fig. 28f). It is seen that the direction of the T wave in the human electrocardiogram may be represented as the consequence of the difference between the two oppositely directed monophasic curves.

Some justification for Wilson's speculation is furnished by experiments (Ashman) with turtle hearts from which monophasic action currents were recorded in much the same manner as has been described above. It was found that when one portion of the heart was sufficiently cooled (but not to an extent to produce blocking of the muscle) the rate of repolarization was slowed so that the monophasic curve of the cooled portion of the muscle was prolonged.

If we cool the endocardial surface in this manner the effect is to produce a situation whereby the "epicardial" portion repolarizes relatively more rapidly and produces a T wave which is in the same direction as that of the QRS. This experiment was repeated by Ashman and Toth using dogs. What condition is responsible for this hypothetical increased rate of repolarization in the epicardial fibers of the human ventricle (or decreased rate of repolarization of the endocardial fibers) is a matter for further speculation.

It should be pointed out here that Ashman found that when the heart was repeatedly

FIG 28. Depolarization and repolarization of a segment of myocardium assuming that the epicardial muscular layers repolarize more rapidly than the endocardial. Again, the net effect of all of the opposing effects occurring throughout the muscle may be represented as the balance between the endocardial and epicardial effects.

The more rapid repolarization at the epicardial surface assumed by Wilson may be represented by the monophasic curve of shorter duration shown for the epicardial surface. The result is that an upright T wave is recorded at P.

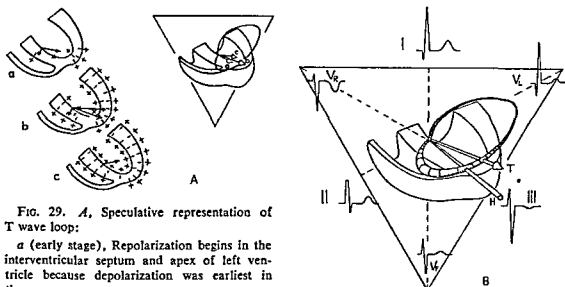


FIG. 29. *A*, Speculative representation of T wave loop:

a (early stage), Repolarization begins in the interventricular septum and apex of left ventricle because depolarization was earliest in these areas.

b (intermediate stage), Combined effects from interventricular septum, apex and lateral wall.

c (final stage), Combined effects from apex and lateral wall.

The speculation follows the order of depolarization and the assumption that the epicardial surface repolarizes more rapidly than the endocardial surface; the right side of the

septum is assumed to repolarize more rapidly than the left but the difference assumed is not as great as the difference between the rates of epicardial and endocardial repolarization in the apical and lateral regions.

B, The mean T wave vector is derived from the assumption described in *A* and from experience with many thousands of electrocardiograms.

excited at rapid rates the monophasic curve for the cooled region approached again the form and duration of the monophasic curve of the uncooled region. The T wave under these conditions would tend to return to the form shown in Fig. 26 (see Fig. 32). This will become important when we come to the consideration of the effect of rate upon the RS-T segments and T waves of the electrocardiogram. It will be seen later that repolarization is influenced by a number of factors that do not materially affect depolarization.

Vector Representation of the T Wave

Since repolarization cannot be represented by a "wave" in the same sense as can be done for depolarization, but results from the net effect of a balance of opposing forces throughout the muscle, it has become customary to deal with the T wave in terms of a net or mean T wave vector. There is a T wave loop (Fig. 29*a*) but it cannot yet be dealt

with on theoretical grounds in a detailed manner.

An anatomic representation of the mean T wave effects (repolarization) consistent with observed electrocardiographic phenomena can only be made by rather broad speculation. Such speculation has been made for teaching purposes as follows: It is assumed that the right ventricle probably contributes little to the formation of the normal T wave. It is further assumed that the septum, being activated from both sides almost simultaneously, is also repolarized on both right and left surfaces almost simultaneously. The two effects almost cancel one another and leave the septum also without a great part in producing the T wave in normal hearts. However, since the T wave is upright in V_2 and V_3 in adults we may assume that repolarization is a little more rapid for the right side of the septum than for the left. This gives the septum some part in the production of the

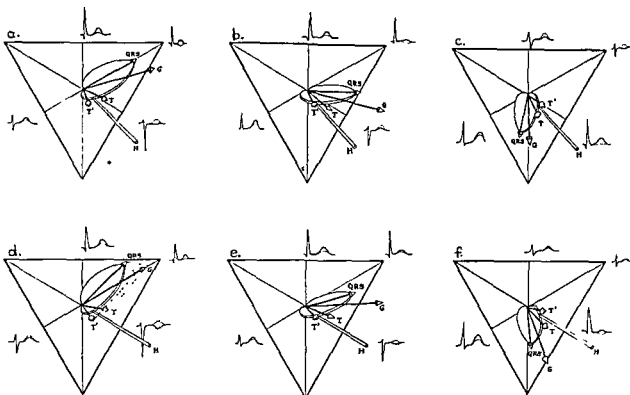


FIG 30 QRS-T relations. The model QRS loop with mean spatial QRS and mean spatial T wave vectors attached. The vectors labeled G and T' and the dotted T waves are to be ignored for the moment.

The top row of drawings shows the model loop in orientations representing (a) markedly counterclockwise rotation about the anatomic axis; (b) a heart counterclockwise, and (c) a markedly clockwise rotated heart. The anatomic axis is the same for a, b, and c (intermediate between transverse and vertical).

The bottom row of drawings shows the same rotations about the anatomic axis when the heart is made more transverse to the same extent in each case.

The figure shows the use of the model to demonstrate the effects of (1) rotation about the anatomic axis, and (2) change of the anatomic axis, upon the QRS, the T waves, and the QRS-T relationship. It therefore constitutes a method of understanding the variations in QRS-T relationships which may be seen in the same and in different normal individuals.

normal T wave. Thus, according to this speculation, in the normal heart the T wave is largely produced by the free wall of the left ventricle and in small part by the septum (Fig. 29a). If the epicardial surface is repolarized more rapidly than the endocardial surface and the T wave is largely produced by the electrical effects of repolarization going on in all parts of the ventricles at the same time we would find that the general direction of the mean T wave vector may be represented by the vector of Fig. 29b. This figure may be regarded as the result of application of Fig. 28 to the human ventricles.

Since the T wave is written when the ventricles are contracted the vector may require some correction from the position shown in the figure. The figure also shows the spatial relationship of the T wave vector to the QRS loop and the anatomic axis of the heart which, roughly speaking, prevails in most normal hearts.

QRS-T Relationship

If we place the T wave vector upon the QRS loop model shown in Figs. 17 and 18 we will have a method by which we can demonstrate the relationship between the T wave

and the QRS complex of the normal electrocardiogram. If the model is now rotated about the anteroposterior and anatomic axes as in Fig. 18 this relationship can be studied (Fig. 30).

The lower row of Fig. 30 shows the effect of making the heart more transverse for each of the rotations represented in the upper row. Such changes in position as are represented by comparing any of the diagrams with its neighbors in any direction may occur in the same individual with change in posture or change in the respiratory phase. Such rotation about the anteroposterior axis seems to produce more change in the T wave axis than does rotation about the anatomic axis because the T axis has so nearly the same direction as the anatomic axis that simple rotation about the latter does not change the T wave direction very much. Thus, vertical hearts, regardless of rotation, most frequently show vertical T axes with low T_I and high T_{III} , whereas transverse hearts are more apt to show transverse T axes, with high T_I and low or inverted T_{III} . In Fig. 30 the T axis as well as the QRS loop and mean QRS axis are seen to become more transverse when the heart becomes more transverse, in all rotations. For example, when a semitransverse counterclockwise heart becomes more transverse (e.g. due to distension of the abdomen), the effect on the T wave and QRS is represented by the change from Fig. 30a to Fig. 30d. R_I becomes lower, S_{III} becomes deeper, T_I becomes a bit higher, and T_{III} , which was only slightly negative, becomes definitely inverted. Corresponding changes occur when the other rotations depicted are made more transverse. The importance of recognizing the effect of such purely nonpathologic changes as are represented in Fig. 30 can hardly be exaggerated. Note, in comparing Fig. 30/ with Fig. 30c that T_{VL} , previously positive (Fig. 30/), becomes negative (Fig. 30c)* with a change in cardiac position which commonly

occurs simply as a result of inspiration or even moderate elevation on a back rest.

Thus, if in serial electrocardiograms a change in the T waves occurs, the QRS should be examined carefully. If a change has occurred in the QRS complex which can account for the change in T by indicating a change in position or rotation (which can be determined by employing the model loop and T vector shown in the figure) then no pathologic significance can be attached to the change in T. A more detailed discussion of variation of the QRS-T relationship resulting from changes in cardiac position and rotation will be taken up later.

If the T wave axis is as depicted in Fig. 30, rotation about the anatomic axis may produce certain changes which deserve recognition. However, it is important to emphasize that these T wave changes are not very striking at ordinary rates and without the effects of food and digitalis because under these conditions the T wave axis is very close to the anatomic axis (H , Fig. 30) and does not change much with rotation of the heart about the anatomic axis. It can be seen that with counterclockwise rotation (Fig. 30a and d) the projection of the T wave vector on the frontal plane is such that it lies slightly to the "left" (the reader's right) of the anatomic axis and to the right of the long axis of the QRS loop which is also the mean axis of the QRS as projected on the frontal plane. As a result the T wave in Lead I is generally higher than the T wave in Lead III when the QRS axis is deviated to the left unless, as stated above, the heart is very vertical. It follows also that the T wave in Lead V_L is upright. With clockwise rotation (Fig. 30c) the T wave vector as projected upon the frontal plane tends to lie slightly to the right of the anatomic axis and to the left of the mean QRS axis. Thus, when the QRS axis is deviated to the right by clockwise rotation of a normal heart the T wave in Lead III tends to increase slightly while the T wave in Lead I becomes slightly lower. As stated above, these effects may not be striking because the

* Obviously, when T_{III} is larger than T_I , either as a normal or a pathologic phenomenon, T in V_L must be negative.

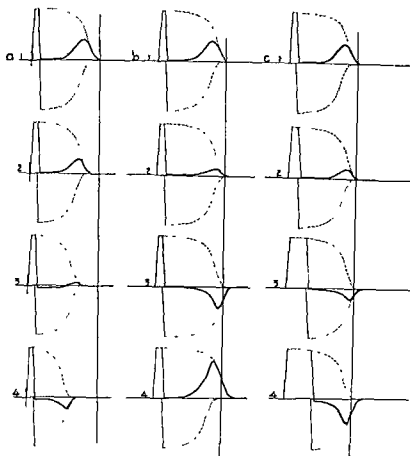


FIG. 31. Monophasic curves for (a) increasing rate; (b 1, 2, 3) epicardial ischemia; b, 4 represents endocardial ischemia and (c) increasing degrees of delay in conduction from endocardial to epicardial surface.

a shows that with increasing rate repolarization becomes more rapid at both endocardial and epicardial surfaces (both monophasic curves become progressively shorter) and that the longer (upper) monophasic curve becomes shorter more rapidly than the shorter (lower) one. The result is a progressive diminution and a final inversion of the T wave. The latter occurs only with very rapid rates in normal hearts. Series *a* follows Ashman's findings in the turtle heart. Note RS-T shift which results when both monophasic curves are steep (final diagram of series *a*).

T axis is of so nearly the same direction as the anatomic axis.

The QRS-T relationship does not remain as fixed as is suggested by our model of a fixed T wave axis glued to a plastic QRS loop. The T wave is a result of a balance of opposing electrical forces throughout the myocardium and it is easily altered by change in rate and by other factors that have little influence upon the QRS.

Further Consideration of QRS-T Relationship

In developing the T wave vector employed in this presentation Wilson's suggestion that the epicardial surface of the left ventricle repolarized more rapidly than the endocardial surface was adopted. This was represented in Fig. 28 and it was shown that this idea could be expressed by the employment of two monophasic curves, one representing the electrical effects of the epicardial surface and the other

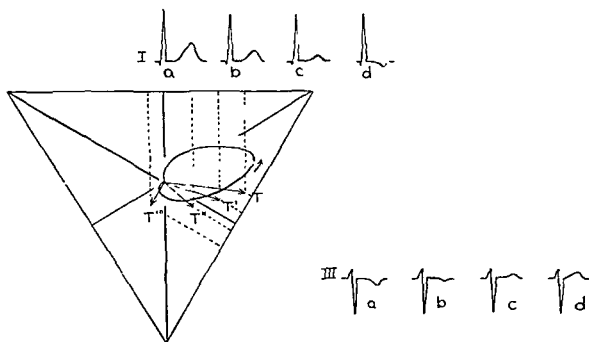


FIG. 32. Given a frontal plane QRS loop and complexes *a* shown in the drawing the vector *T* is constructed by plotting the area of T_I (*a*) against the area of T_{III} (*a*) on the Einthoven triangle. Applying the effect of progressively increasing rate upon the complexes (shown in Fig. 31, series *a*), to this tracing one would expect Lead I to show the series of changes depicted as complexes *b*, *c*, and finally *d*. Lead III can be treated in the same way, noting that the result is simply an inversion of the complexes of Fig. 31, series *a*.

If T_I^b and T_{III}^b are plotted on the triangle the vector T' results. If T_I^c and T_{III}^c are plotted the vector T'' results. If T_I^d and T_{III}^d are plotted the vector T''' results. The general effect therefore, is that the *T* vector changes its direction so that it points more and more away from the long axis of the loop and, therefore, the mean QRS axis.

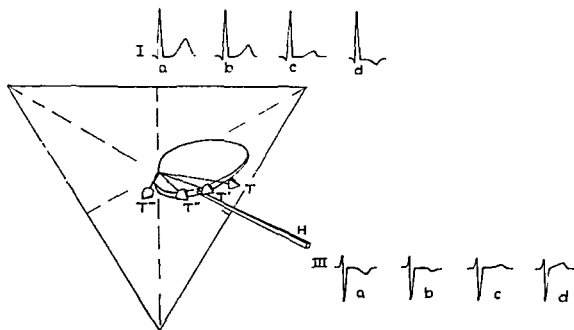


FIG. 33. Translation of Fig. 32 into three dimensions.

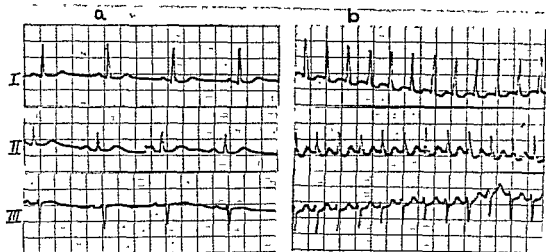


Fig. 34. *a* is an electrocardiogram made on patient whose heart rate was 75/min. *b* is a tracing made on the same patient when the heart rate was 200/min. The change in the T wave axis is attributable to the very rapid rate.

representing the electrical effects of the endocardial surface. It might be well to review again some of Ashman's work with the turtle heart. Ashman found that if turtle heart muscle were cooled (but not to the extent that block is produced) the monophasic curve recorded from the cooled region is longer than that recorded from an uncooled region, i.e., repolarization is slower. Ashman also found that with increasing rate of the heart beat (controlled by artificial stimulation) the monophasic curve for the cooled region and the monophasic curve for the uncooled region both became shorter (repolarization became more rapid in both regions) and the two curves approached an identical form and duration (the monophasic curve for the cooled region became shorter more rapidly than did the monophasic curve for the uncooled region). The application of Ashman's findings to the representation depicted in Fig. 28 is shown in Fig. 31, column *a*. It seems reasonable to apply the same type of analysis to any electrocardiographic lead, for the purpose of speculating upon the expected effect of increasing rate. For example, if the QRS loop is as shown in Fig. 32 the QRS complexes in Lead I and III will be as shown in the same figure and the T waves are

frequently of the form represented by vector *T* and complexes *a*. Application of Ashman's findings (Fig. 31, column *a*) to the QRS and T relationships in Lead I result, with increasing rate, in the progressive changes in the T wave that are shown by the T waves of Lead I in Fig. 32 labeled *a*, *b*, *c*, and *d*. In Lead III the corresponding progressive changes in the T wave which would be expected as a result of increasing rate are shown by the T waves of Lead III, labeled *a*, *b*, *c*, and *d*. If we plot T_I^a and T_{III}^a , T_I^b and T_{III}^b , T_I^c and T_{III}^c and T_I^d and T_{III}^d we obtain a series of T vectors T' , T'' and T''' . Since with increasing rate the T wave direction deviates away from the direction of the mean QRS in any lead the writer has taken the liberty of representing this phenomenon spatially in Fig. 33. This involves the assumption that the T wave vector remains in the plane of the QRS loop (from which it probably deviates to some extent).

As shown in Fig. 34, changes in rate do produce such changes in the QRS-T relationship in the human electrocardiogram. Other factors, such as digitalis and the taking of food have, in a general way, a similar effect. The effect of these factors may be generalized as represented in Fig. 30 (which is developed

from Fig. 33), in which the vector T is a usual T wave vector at ordinary rates, without digitalis, etc., and T' is the spatial T wave vector which may result from moderate rate change, digitalization, or the taking of food. The changes which may result from these factors with several rotations and positions of the heart are represented by the range of T vector direction that might occur between T and T' . In Fig. 30 the T waves shown as solid lines correspond to vector T ; those shown as dotted lines correspond to vector T' . A normal range of variation is thus indicated.

This figure, then, represents a range of QRS-T relationships which is normal to certain circumstances, none of which is pathologic. The range of T directions between T and T' shown in the figure is not intended to represent the extreme normal limits. As indicated in Fig. 33 there are T directions to either side of the T - T' range which may be normal under certain circumstances. No clear concept of the possible range of normal variations can be understood without some attention to the quantitative relationship between the QRS and T deflections of the electrocardiogram.

5. Quantitative Analysis of QRS-T Relationship

If the relationship between QRS and T is to be evaluated quantitatively it is best to begin with the representation offered in Fig. 35. If the rate of repolarization were the same in all areas of the ventricles (if the rates of repolarization at the epicardial surface and the endocardial surface were the same—Fig. 26) the T wave would be opposite in direction to the QRS, and the area of QRS would equal the area of T. Therefore, the algebraic addition of the area of the QRS (AQRS) and the area of the T (AT) would result in zero no matter how we related the two monophasic curves with respect to time and regardless of which monophasic curve occurred first (premature beats may reverse the order of depolarization). This is shown in Fig. 35a. This relationship simply follows from the fact that there is no difference between the monophasic curves representing the rates of repolarization at the endocardial and epicardial surfaces respectively. If the rate of repolarization is different in the two regions then the two monophasic curves representing this state of affairs may be represented as in the corresponding series of diagrams of Fig. 35b. It is seen that the fact that the difference between the two monophasic curves is always present and is always the same is reflected by the fact that the result of algebraic addition of the QRS and T areas is *not* zero and is always the same regardless of how we relate the curves with respect to time. This net area resulting from algebraic addition of the areas of QRS and T in any lead may be regarded as the component in that lead of the net electrical effects of differences in the rates of repolarization in various portions of the ventricles.

This net effect may be measured in any

two limb leads and may be plotted as a vector quantity on the frontal plane. It has been termed by Wilson the *ventricular gradient* and has been represented by the symbol G .

Measurement of the Frontal Plane Gradient

The area of QRS and area of T is measured in two of the three standard limb leads and tabulated as in Fig. 36. The value of $AQRS + AT$ is then obtained by simple addition. The unit of area measurement is the Ashman unit, or one small rectangle on the electrocardiographic ordinates. It is, of course, equal to 0.04 microvolt seconds.

The AQRS, AQRST and AT of any two leads are plotted on the Einthoven triangle (or triaxial system of Bayley) and the manifest vectors are thus obtained (Fig. 36). Of course, the manifest AQRST vector (G) will always form the diagonal of a parallelogram of which the two sides are the AQRS and AT vectors,* because it is the resultant of these two vector quantities.

The vector quantity AQRST represents, as indicated above, the frontal plane projection of the net electrical effects of differences in rates of repolarization in various areas of the ventricular muscle.

The concept may be approached in another way (Fig. 37). Figure 26 shows the electrocardiogram that might be expected if the rates of repolarization throughout the ventricular muscle were identical (in this case the order of repolarization follows the order of depolarization). In this tracing, reproduced

* For experimental work we plot Lead I and II, Lead II and Lead III, and Lead I and Lead III and take the mean of these observations as the final determination.

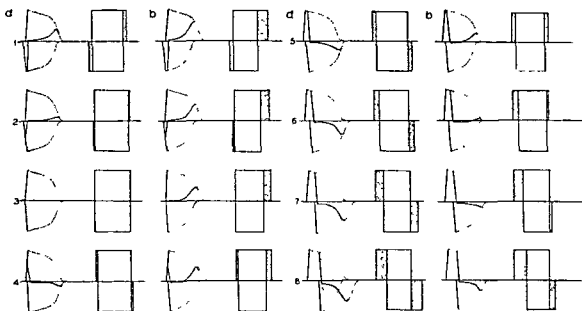


FIG. 35. In series *a* the upper (endocardial) monophasic curve and the lower (epicardial) monophasic curve are identical in every way except sign. The algebraic addition of the two monophasic curves always results in QRS and T complexes which are equal in area but of opposite sign so that they ($AQRS + AT$) always add up to zero regardless of the relationship of the two curves. This is made quite clear by the rectangular figures representing the areas of the complexes and the corresponding curves.

In series *b* the two monophasic curves are of opposite sign but they are not identical; the lower (epicardial) curve is of shorter duration representing a more rapid rate of repolarization at the epicardial surface. In this series the algebraic addition of the two monophasic curves results in QRS and T complexes which are not always equal in area and opposite in sign as in series *a*, and the value of $AQRS + AT$ (as illustrated in the rectangular figures) is always the same value but it is not zero as in series *a*.

Thus in series *a*, $AQRS + AT$ always equals zero while in series *b*, $AQRS + AT$ always equals some finite value which is constant for the series. This difference between the two series results entirely from the fact that in the one case (series *a*) the two oppositely directed monophasic curves, representing uniform rate of repolarization, are identical while in the other (series *b*) the two oppositely directed monophasic curves, representing different rates of repolarization, are different in duration and area.

Since the value of $AQRS + AT$ is zero when the rate of repolarization is assumed to be uniform throughout the muscle, this quantity may be employed to measure the net electrical effect of differences in rates of repolarization in various areas of ventricular muscle as shown above. It is this value which is defined as the ventricular gradient.

Note that the RS-T shifts, when they occur, are always opposite in direction to the QRS complex. These RS-T shifts are the inevitable result of the addition of any two oppositely directed monophasic curves which are not flat at the top.

in its essential form in Fig. 37, the T wave is opposite in direction to the QRS and equal to it in area. The gradient potentials may be regarded as the potentials that must be added to the T wave of this figure (called the regression T wave) to produce the T wave of the form actually observed. Thus the net gradient effect is measured by the area en-

closed by the regression T wave below and the observed T wave above (in Fig. 37). It is, then, equal to the sum of the area of the observed T wave (AT) and the area of the regression T wave. $AT_{R} + AT = G$ where T_{R} is the regression T.

The regression T wave is not measurable since it is actually not observed. However,

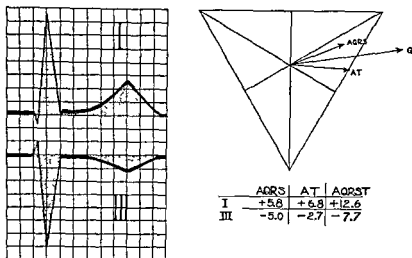


FIG. 36. Plotting the frontal plane ventricular gradient.

The areas of the various deflections of two leads are measured and tabulated. The value of $AQRS + AT$ is obtained by simple algebraic addition. Each of the values ($AQRS$, AT and $AQRST$) is plotted as a vector quantity. $AQRST$ (or G) is the gradient.

it may be recalled that the area of the regression T wave is equal to the area of the QRS (Fig. 26). Thus, substituting in the formula above, we obtain $AQRS + AT = G$.

The frontal plane projection of the gradient is regarded as if it were derived from a spatial gradient (SG or $SAQRST$) which in Fig. 30 is constructed by addition of the two spatial vectors $SAQRS$ and SAT , employing the parallelogram of forces.

Ashman, Gardberg and Byer estimated that the spatial gradient vector lies approximately in the same plane as the mean QRS vector and the anatomic axis of the heart and at a spatial angle of approximately 30° with the mean spatial QRS vector.

The angle between the gradient and the mean QRS can be visualized if it is realized that the wave of excitation passes diagonally through the left ventricular wall (Fig. 14) instead of as shown in the simplified diagrams of Fig. 26. On the other hand, if the epicardial fibers repolarize more rapidly than the endocardial fibers then the gradient points from the endocardial surface to the epicardial surface more or less perpendicular to the wall of the ventricle. Thus for any chosen segment

of ventricular wall, and therefore for the entire left ventricle the direction of the spatial gradient vector would, under these circumstances, be expected to make an angle with the direction of the mean spatial QRS vector.

Thus, if to the model which we have employed to represent the spatial QRS loop, the mean spatial QRS axis and the mean spatial T axis we add a spatial gradient vector at an angle of 30° to the direction of the mean spatial QRS vector it becomes the diagonal of a parallelogram of which the spatial T vector and spatial QRS vectors are the two sides. We now have a means of representing a standard relationship between the spatial QRS loop, the mean spatial QRS, the mean spatial gradient, and the mean spatial T vector. Just as we employed the model loop to study the effects of rotations of the heart upon the QRS complexes of the limb leads we may now in addition employ it to study the various normal relationships between the directions of the gradient, the mean QRS axis, the mean T axis, and the anatomic axis of the heart. If for any tracing we determine the direction and the magnitude of the ventricular gradient and find that the rela-

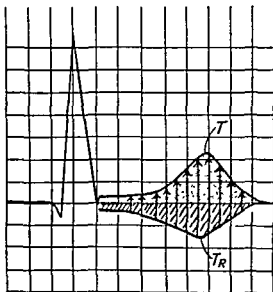


FIG. 37. The ventricular gradient as the net difference between the regression T wave and the observed T wave.

The regression T wave (T_R) is that which is postulated to occur when the rate of repolarization is uniform throughout the muscle and the order of repolarization follows the order of depolarization (Fig. 26). Here the gradient is visualized as the potential that must be added to the regression T wave to produce the observed T wave. In terms of area the measurements can be made because AT_R equals $AQRS$, and $AQRS$ and AT can be measured. The gradient potentials cannot be measured in terms of instantaneous potentials (the vertical arrows) because the regression T is never observed as such and, besides, the instantaneous potentials of the T wave are not related closely in time to the instantaneous QRS potentials. Attempts to so relate them are erroneous at a very fundamental level.

tionship of its direction to that of the mean QRS axis is very definitely not that which is expected from projection (upon the frontal plane) of the corresponding vectors of the model when the model is held in the orientation which corresponds to the limb leads (see pp. 26-29) then that tracing is abnormal. The magnitude of the gradient varies too much from individual to individual and in the same individual under nonpathologic conditions to be of great value in the analysis of single electrocardiograms. Both the direction and the magnitude of the gradient are more valuable in the study of serial electrocardiograms.

Significance of the Ventricular Gradient

The great value of measurement of the ventricular gradient resides in the fact that it furnishes an instrument enabling us to find some order in apparently random T wave changes and to differentiate normal from pathologic T wave changes that are indistinguishable by more superficial methods of examination. It has already been stated that certain nonpathologic factors (rapid rate, food, etc.) cause changes in repolarization, and certainly pathologic changes also cause changes in repolarization.

Since the gradient is an index of the net effect of the difference in rates of repolarization in various portions of the ventricles it may be employed as an instrument for the study of this phenomenon in health and disease. It should not be surprising that disease is capable of causing changes in the direction and magnitude (especially the former) of the repolarization potentials which are not produced by physiologic factors. It should not be surprising also to learn that disease not infrequently produces changes in the repolarization potentials that are similar to those produced by nonpathologic factors. The superiority of gradient measurements over T wave measurements as an index of these changes in repolarization potentials resides in the fact that the direction of the T wave vector is readily changed by even minor changes in the magnitude of the difference between, say, epicardial and endocardial rates of repolarization. In contrast, the gradient, as a more direct method of measuring such effects, reflects closely the real magnitude of the change which has taken place in the relative rates of repolarization in the various regions of the ventricles. For example, in Fig. 34 it will be seen that a simple diminution of the gradient such as may occur under nonpathologic conditions (increase in rate) will cause a considerable change in the direction of the T wave vector and, therefore, of the T deflections of the electrocardiogram. Thus, unless the gradient is measured it is sometimes impossible to know whether an

observed T wave change is due to a physiologic change in gradient *magnitude* or to a change in *gradient* direction characteristic of certain pathologic states.

Figure 38A shows two tracings *a* and *b*, made from the same heart at different times; the change from *a* to *b* is characterized by a decrease in the height of T_I and an increase in the height of T_{III} . In Fig. 38B the change from *a* to *b* is also a decrease in the height of T_I and an increase in the height of T_{III} . As far as the T waves are concerned, the nature of the two changes seems to be the same; yet they are not for in one case (*A*) the gradient potentials are simply of less magnitude such as may occur with increase of rate, while in the other (*B*) the magnitude of the gradient potentials is only slightly less but their *direction* has changed and in a manner which generally occurs only under pathologic conditions.

It is important to note that either tracing *a* or *b* of Fig. 38B *evaluated alone* may be within normal limits. The direction of the frontal plane projection of the gradient in relation to the direction of the frontal plane projection of the mean QRS and the anatomic axis varies in individuals so that a single observation may be determined to be abnormal only if it lies outside a fairly wide range of the normal predicted by the use of the model. However, in serial tracings much change in *magnitude* of the gradient may be due to nonpathologic factors, but even moderate change in the *direction* of the gradient without change in the QRS complexes is likely to be due to pathologic factors.

It must be realized that if the heart undergoes a change in rotation about any axis, the direction of the AQRS, AT, and gradient vectors will not change in their spatial relationship, but the relation of their projections upon the frontal plane may change considerably.

The value of the concept of the gradient can be further emphasized by considering the evaluation of the T wave changes that occur in serial tracings showing changes in intra-

ventricular conduction (Fig. 38C). One tracing on a patient may show no conduction change and the next may show a degree of left bundle branch block, or a moderate grade of hypertrophy due to hypertension or arteriosclerosis may occur so that the QRS becomes larger in height or in width or both. Under these circumstances a marked change may occur in the T waves and even the RS-T segments. If we examine Fig. 38C these T wave changes are seen to be a necessary result of the QRS changes if nothing else has happened to change the relative rates of repolarization in the various portions of the muscle, i.e., if the ventricular gradient (AQRS+AT) remains the same. Obviously in any lead, if the area of QRS+ the area of the T remains constant an increase in the area of the QRS must be accompanied by an equal diminution of the area of T. Conversely, if the area of the QRS is diminished an equal increase in the area of the T must occur.

This principle is illustrated in a very practical way in Fig. 39.

The T wave change observed in Fig. 38C is called a secondary T wave change because it is caused by a change in the QRS and not by a primary change in the repolarization phenomena. The change in the T wave in Fig. 38B is a primary T wave change because it is due to a change in repolarization phenomena entirely independent of the unchanged order of depolarization (QRS).

Thus, when two tracings from the same individual are compared changes in the T wave can only be evaluated in terms of the relationship between the QRS and the T waves. As has been shown it is the net area AQRS+AT (the gradient) that must be employed in making this evaluation. Frequently, it is immediately obvious without making actual measurements that the T wave changes result from QRS changes (due to changes in position or conduction disturbance) and that these changes do not reflect a change in the direction or magnitude of the gradient. In some cases this is not so obvious and actual measurement may be required to determine

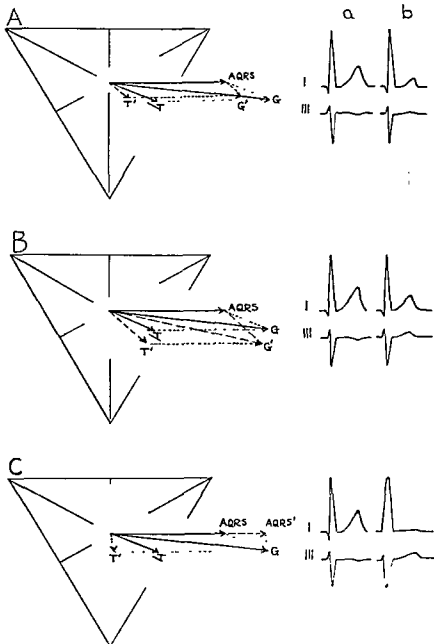


FIG. 38. Relative value of T wave and gradient analysis.

In *A*, *B*, and *C* the change from tracing *a* to *b* consists of T wave changes of the same kind: T_I becomes smaller and T_{III} becomes larger in each of the three cases.

Measurement of AQRS, AT and AQRST (the gradient) in both tracings (*a* and *b*) and plotting these on the Einthoven triangle show that:

1. In *A* the T wave change from *a* to *b* is due to a diminution of the magnitude of the gradient, and since this commonly occurs with increased rate or after a meal it may not be pathologic.

2. In *B* the T wave change from *a* to *b* is superficially similar to that seen in *A* but here it is due to a change in the *direction* of the gradient. Considered alone either *a* or *b* is within normal limits but a change from *a* to *b* in the same individual is suspect for no decided change in the direction of the gradient (with no change in the QRS) occurs except as a result of disease.

3. In *C* the T wave change from *a* to *b* is also superficially of the same kind as that shown in *A* but here it is due to an increase of AQRS, the gradient remaining the same. This occurs in left bundle branch block and in left ventricular hypertrophy. The T wave change is *secondary* to the QRS change; there is no *essential* change in repolarization rates.

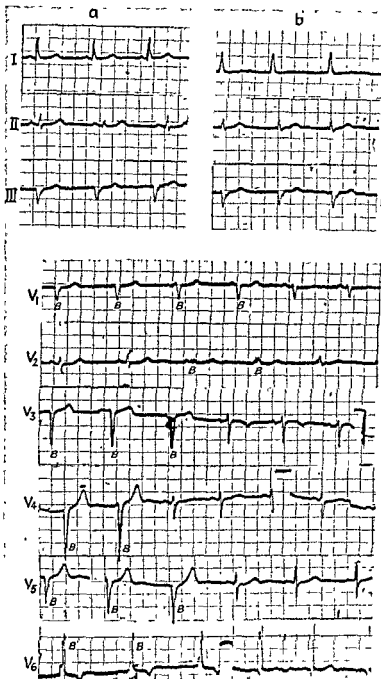


FIG. 39. Secondary T wave changes illustrating the principle of the gradient.

a and *b* are sets of limb leads made on the same patient on different days. The precordial leads belong to tracing *b*.

T_1 has become low in tracing *b* because of the occurrence of just such a change of conduction as was illustrated in Fig 38C. On reasonably careful examination, even without measurement, the area of QRS in Lead I is seen to be greater in *b* than in *a* and accounts for the change in T (AQRS + AT remains constant). The same phenomenon is seen in every one of the precordial leads. The complexes labeled *B* are those in which the conduction disturbance is present. It is seen in every lead that the change in the area of the T always has a reciprocal relation to the change in the area of the QRS, illustrating the principle of the gradient shown in Figs. 35 and 38C.

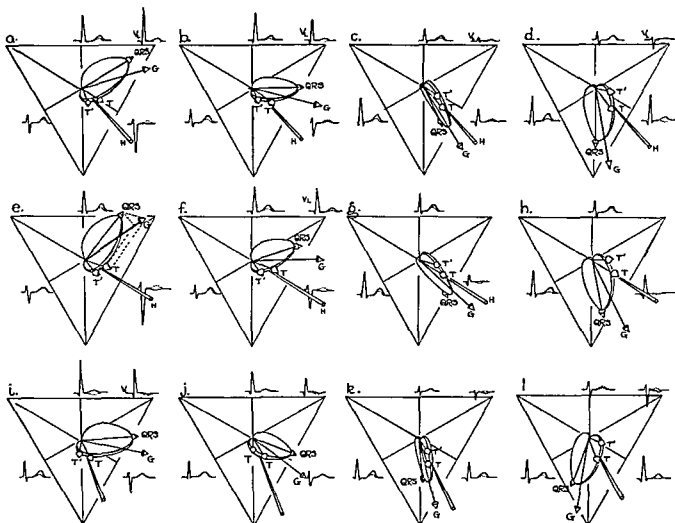


FIG. 40. Various orientations of the model spatial QRS loop showing the relationship of the mean spatial QRS, spatial gradient, and spatial mean T vectors. The change from T to T' results from diminution of the gradient as shown in *e*. The solid T waves correspond to the T vector, the dotted T waves correspond to the T' vector.

In each horizontal row the anatomic axis is the same, being intermediate in the top row, transverse in the second row, and very vertical in the bottom row.

In each vertical row the rotation about the anatomic axis is the same. Beginning with marked counterclockwise rotation in the first row there is moderate counterclockwise rotation in the second row, slight clockwise rotation in the third row, and moderate clockwise rotation in the fourth row.

The figure represents a wide variety of normal QRS-T relationships. It is discussed in detail in the text.

whether the gradient has changed in direction or in magnitude (or both). If a change (obvious or measured) in direction or magnitude of the gradient (or both) has occurred it remains to be decided whether such change may have resulted from nonpathologic conditions.

Summary of QRS-T Relationship Variations that May be Nonpathologic

In order that we may attempt to distinguish changes in QRS-T relationships that are pathologic it is necessary to review normal variations and changes due to variation and change in cardiac position, rate and other

nonpathologic factors in some detail. In Fig. 40 the mean spatial QRS (SAQRS), the mean spatial T (SAT) and the ventricular gradient are represented by spatial vectors attached to the model of the spatial loop which was described in Chapter 2. The loop is here used for purposes of orientation. As stated before the direction of the spatial mean QRS vector (SAQRS) is generally at an angle of 90° to the anatomic axis (H) of the heart; the spatial vector of the ventricular gradient is at an angle of 30° to the direction of the mean QRS vector and forms the diagonal of a parallelogram of which the mean spatial QRS and the spatial T vector are the two sides (Fig. 40e). All three of the vectors are represented as being in the same plane (Fig. 40e).

EFFECT OF CHANGE IN ANATOMIC AXIS OF THE HEART. It is seen that as the heart is made more vertical the projection of all three vectors* upon the frontal plane changes. Thus, when the counterclockwise heart represented in Fig. 40e becomes more vertical and is then represented by Fig. 40a, the spatial vectors for the mean QRS, the gradient, and the mean T potentials change direction with the anatomic axis. The projections of these vectors and of the QRS loop upon the frontal plane change correspondingly. The change in the orientation of the QRS loop is reflected in an increase of the magnitude of the R wave in Lead I and a diminution of the S wave in Lead III. The corresponding change in the orientation of the T axis is reflected in a slight decrease in the height of the T wave in Lead I and a corresponding change in the T wave in Lead III which, previously inverted, becomes isoelectric. If the heart becomes still more vertical (Fig. 40i) the R wave in Lead I becomes still greater, and the S wave in Lead III becomes smaller. The T wave in Lead I decreases still further and the T wave in Lead III becomes upright. Also the T wave in V_L , previously upright, becomes inverted. It is safe to say that such T wave changes are frequently observed and that the QRS changes which are the clue to the posi-

tional origin of such T wave changes are not obvious to superficial examination of the electrocardiogram and are overlooked. As a result significance is erroneously attached to the T wave change.

The above described changes in cardiac position may occur as a result of change in position of the body,* respiratory changes (some of which occur after exercise), and abdominal distention by fluid or gas.

EFFECT OF ROTATION ABOUT THE ANATOMIC AXIS. If the counterclockwise semitransverse heart, represented by Fig. 40e, becomes rotated more clockwise it may then be represented by Fig. 40f, or, with still more clockwise rotation, Fig. 40g. The changes that occur in the orientation of the QRS loop and the T vector are reflected by the changes in the complexes shown in Fig. 40f and 40g. With rotation about the anatomic axis the T axis changes but little because the T axis is generally of nearly the same direction as the anatomic axis. However, since the orientation of the QRS loop is changed considerably by rotation about the anatomic axis the QRS complexes change. When the rotation changes from that represented by Fig. 40e to that represented by 40f the change in the QRS complexes consists chiefly of an increase in the height of R_I and a decrease of S_{III} . When still further clockwise rotation occurs (as possibly with a deep breath in some persons) so that Fig. 40g applies, Q_I disappears and the QRS complex becomes smaller in Lead III, while R_{II} becomes large. Marked clockwise rotation produces the situation shown in Fig. 40h. Thus QRS change may occur as a result of changes in cardiac position without necessarily changing the T deflection of the electrocardiogram.

It is to be noted that rotation about the anatomic axis changes the angles between the frontal plane projections of the anatomic axis, the ventricular gradient vector, the mean QRS vector, and the mean T vector. In counterclockwise hearts (Fig. 40e and f) the projection of the gradient upon the frontal

*The change in body position required to produce such changes is frequently a slight elevation on a hospital bed-rest or a slight rotation of the body to the right or left.

*The T' vector and the dotted T waves of Fig. 40 are to be ignored for the present.

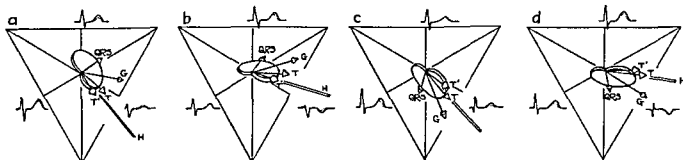


FIG. 41. The apex back heart in terms of the model:

a, sthenic counterclockwise heart (apex back); b, transverse counterclockwise (apex back); c, sthenic clockwise (apex back); d, transverse clockwise (apex back).

The direction of the gradient is so nearly perpendicular to the frontal plane that reduction of its magnitude must be much greater to produce marked changes in the T wave than is true for apex-forward hearts.

For apex back hearts the QRS and gradient measurements are so small that errors are much greater.

plane lies to the right of the mean QRS vector, whereas in clockwise hearts (Fig. 40g and h) the projection of the gradient lies to the left of the mean QRS vector. In an intermediate rotation (no rotation) the projections of these vectors on the frontal plane would be superimposed.

The various diagrams of Fig. 40 may be employed to represent the electrocardiograms in different normal individuals as well as variations in the same individual. One may begin with any of the diagrams shown in Fig. 40 and predict the probable effect of changing the anatomic axis (vertical, transverse) by studying the diagrams in the vertical column containing the diagram selected. Such change in axis is seen as a result of change in posture, of gain or loss of weight, pregnancy or delivery, abdominal distention or its relief, alteration of respiratory excursion, and displacement by pleural effusion or tumor. The probable effect of rotation about the anatomic axis (clockwise or counterclockwise) may be predicted by studying the neighboring diagrams in the horizontal row containing the diagram selected. Such changes in rotation of the heart may be produced by the same factors listed for changes in the anatomic axis and in addition by dilatation of the right ventricle (which produces clockwise rotation).

ROTATION ABOUT THE VERTICAL AXIS. In

addition to these changes in orientation of the heart the apex may be moved backward with relation to the base under certain conditions. In many hearts apex-back rotation is present under all circumstances. A few of these are shown in Fig. 41. A prominent characteristic of the apex-back position is the presence of well-marked negative deflections in all three standard limb leads, and shortening of the frontal plane projection of the mean QRS and gradient vectors.

A deep breath usually changes the anatomic axis toward the vertical and rotates the heart clockwise. The apex may be moved back at the same time. In some persons a deep breath may cause less change in cardiac orientation than in others. Furthermore, the change in one person may be a marked change in the anatomic axis while in another it may be a marked change in the rotation about the anatomic axis, usually clockwise. In pregnancy the heart becomes more transverse, tends to rotate clockwise, and the apex is moved back.

Nonpathological Factors Influencing the Magnitude of the Ventricular Gradient

In Fig. 40e, the T vector corresponds to the mean QRS vector r when the gradient is of the normal direction and of the normal magnitude for ordinary rates and basal conditions in a strongly counterclockwise-rotated

heart. When the rate becomes rapid, after a meal, or with digitalis, the magnitude of the gradient diminishes and a new parallelogram must be constructed. If we use a shorter length of G as shown in Fig. 40e, the T vector perforce becomes T' , and the T waves change from those shown as the unbroken lines to those shown as dotted lines. The QRS, of course, has not changed. T_I becomes lower, T_{III} may become flat or upright and T in V_L becomes much lower or isoelectric. As has been shown previously (Fig. 38) the T wave pattern alone is not very valuable in determining what has actually occurred, for a change in the *direction* of the gradient as shown in Fig. 38B can accomplish a similar lowering of T_I and increase in the height of T_{III} . Furthermore, it is necessary to consider that after *exercise* the rate increases and because of change in the respiratory midposition a change to a more vertical cardiac position occurs. Under these circumstances the tracing before exercise may, for instance, be depicted by Fig. 40f in which T is the T wave axis and therefore the unbroken T waves occur, while the tracing *after exercise* is that of Fig. 40b with T' as the T axis and the dotted T waves are those observed. T_I becomes lower, T_{III} becomes upright (higher), and T in V_L may become inverted. Yet no pathologic condition is present. Furthermore, it is apparent that in many persons a deep breath and also exercise cause rotation of the heart about the anatomic axis. Thus, the tracing before exercise may be represented by Fig. 40e, with T as the T wave axis, and after exercise the tracing may be represented by Fig. 40b, with T' as the T wave axis. Finally, it is possible that the apex may also move back with the respiratory change that follows exercise and the after-exercise tracing may be represented by Fig. 41a, with T' as the T wave vector and the T deflections those which are dotted on that figure. In the evaluation of such tracings it is again obvious that T wave changes must be analyzed by employing the principle of the gradient and the spatial relationship of the mean QRS and

gradient axes to the anatomic axis of the heart whether the gradient is measured or not. At times, measurement of the gradient is necessary. Since we are employing limb leads the evaluations and measurements discussed refer to the frontal plane projections of the spatial vectors. The areas AQRST, AT, and AQRST (G), determined from limb leads, are frontal plane projections. The author knows no method of measurement or recording of spatial vectors (oscillographic or otherwise) that is as nearly accurate as deductions from the limb leads; frequent statements to the contrary notwithstanding.

A careful study of Fig. 40 will reveal that those conditions that diminish the ventricular gradient without significantly affecting its direction (digitalis, food, moderate or greater exercise, and rate changes) affect the T wave in the various leads of individual hearts in different ways. In the counterclockwise heart represented by Fig. 40b, the T wave of Lead I diminishes while the T wave of Lead III is increased; in the slightly clockwise rotated heart represented by Fig. 40c, the T waves of all three leads are diminished equally. In the strongly clockwise-rotated heart represented by Fig. 40d, it is the T wave of Lead III that is diminished and may become inverted, while T_I is less diminished. Figure 42 which is explained in the caption is important in relation to this phenomenon. Figure 43 shows illustrative electrocardiograms. Furthermore, in the apex-back heart, in which the gradient has a smaller projection upon the frontal plane, its diminution produces much less effect upon the projection of the T vector on the frontal plane. Thus in all of the apex-back diagrams of Fig. 41, the T wave is seen to change but little with moderate diminution of the gradient. Thus, with exercise and food, unless a change from the apex-back position or a greater rotation occurs, the T axis may show little change in these hearts.

It is important to point out that these phenomena are mainly a result of the spatial relationship of H , AQRS, and G (see Fig. 40). It is also important to note that when the

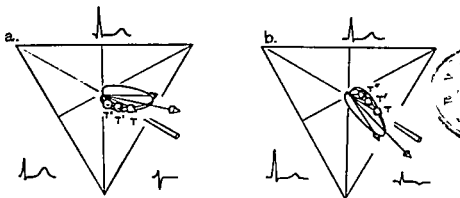


Fig. 42. Figure 42 shows the model of the QRS loop with mean spatial QRS, spatial gradient, and vectors T , T' , and T'' . The vectors T' and T'' result from progressive diminution of the magnitude of the gradient as developed in Figs. 32 and 33 (or Fig. 40) *a* shows slight counterclockwise rotation; *b* shows slight clockwise rotation. The manner in which the rotation about the anatomic axis affects the spatial orientation of the series of T vectors which occurs as the magnitude of the gradient is diminished is illustrated. In the counterclockwise heart (*a*) the change $T-T'-T''$ (as with increased rate or food) causes T_{III} to become higher. In the clockwise heart the same progressive change causes the T in III become smaller and frequently negative.

It is to be expected that at times a heart which appears to be slightly clockwise in rotation as judged from the limb leads, behaves, after exercise, or with rapid rate as if it were counterclockwise. This is due to: misinterpretation of the rotation because of some irregularity in the first portion of the loop, or to change in rotation after exercise or with whatever condition has caused diminution of the gradient. As Fig. 42 or manipulation of the model which Fig. 42 depicts will readily show, it requires but slight change in rotation to change the order of the effect upon T_{III} .

heart is rotated clockwise the effect of diminution of the ventricular gradient upon the direction of the T vector (compare T and T' of Fig. 40*h*) is opposite to the effect of making the heart more vertical (compare T' of Fig. 40*h* with T' of Fig. 40*l*). Thus when both effects occur simultaneously—after exercise, for instance—they may tend to neutralize one another; again, either effect may predominate.

Thus, the T wave may change without change in the QRS complexes; the QRS complexes may change without change in the T waves; and, finally, both the QRS complexes and T waves may change under non-pathologic conditions. When one considers the great number of possible normal variations in cardiac position; the fact that the effects of so many factors, such as posture, rate change, food, tobacco, emotional ten-

sion, etc., are commonly seen in electrocardiograms; and the fact that the latter changes can be evaluated only in terms of the principle of the ventricular gradient, it must be concluded that the empirical approach to the evaluation of electrocardiograms is almost hopeless. It is to be noted the 16 diagrams of Figs. 40 and 41, representing 32 possible normal electrocardiograms (a small fraction of the total number of possibilities), actually were made from a single representation of the QRS-T relationship, namely the model of the QRS loop with the mean spatial QRS vector and spatial ventricular gradient vector attached as described above. This application of the principle of the gradient is the only means presently available of bringing some sort of order to interpretation of T wave changes in the electrocardiogram. The same statement applies to the evaluation of RS-T

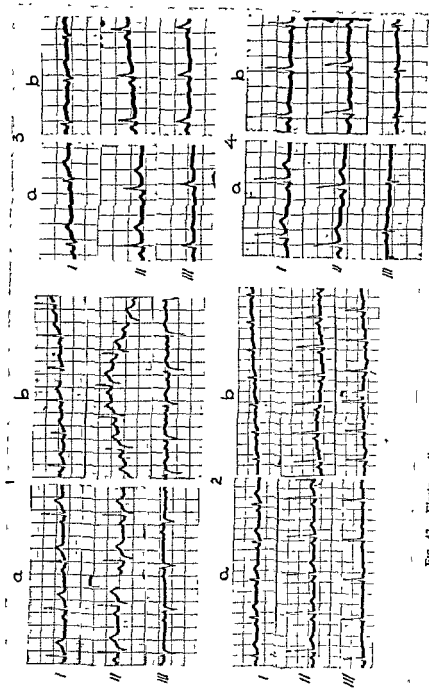


FIG. 43. Electrocardiograms of a normal heart before and after exercise.
 1, Counterclockwise rotation: *a* before, and *b* after exercise.
 2 and 3, Clockwise rotations. Compare with Fig. 40f.
 4, Nonrotated heart.

elevations and depressions which are to be discussed in detail in the chapter on coronary disease.

With respect to the *precordial leads* it should be noted that the effect of diminution of the magnitude of the gradient (by increased rate, exercise, etc.) can be analyzed by employing the two monophasic curve method illustrated in Figure 31a. This figure shows that as the gradient diminishes (when the two monophasic curves approach one another in form and duration repolarization approaches a uniform rate) the T wave becomes lower and then inverted when the QRS is largely upright. Actually, following food and exercise or food and smoking it is not rare to find *inversion of the T waves in all the precordial leads in perfectly healthy young adults*. RS-T depressions are very common under these conditions.

It is to be noted that Ashman found that with increasing rate the ventricular gradient not only diminished in magnitude but its direction usually deviated somewhat to the left.

In some normal persons the magnitude of the ventricular gradient is greater than the usual. This causes the T vector to become large and to point more toward the direction of the gradient (see T, Fig. 33).

As has been indicated in the discussion introducing the ventricular gradient (p. 50 and Figs. 35 and 38 [monophasic curves and vector diagram]) if all other conditions remain the same the direction and magnitude of the net gradient potentials remain the same regardless of changes that may take place in intraventricular conduction. Thus if transitory right or left bundle branch block occurs without other changes the QRS and T waves change but the magnitude and direction of the spatial ventricular gradient tends to remain the same. This is apparent from the observation that in any lead the algebraic sum of the QRS area and the T area (the component of the gradient in that lead) tends to remain the same (Fig. 39). Departures from the rule observed in premature beats probably result from the altered motion of the heart

which results from marked change in the sequence of activation of the two ventricles.

Again, it seems that with the development of left ventricular hypertrophy the gradient usually remains unchanged in magnitude so that when the QRS becomes larger the T wave must become smaller and vice versa.

It is important to realize that a lateral wall ischemia in the proper location may diminish the ventricular gradient in precisely the same manner as depicted in Fig. 40e. When this occurs distinguishing the resulting tracing from one occurring as a result of diminution of the gradient by nonpathologic conditions cannot be left to isolated mensuration of the complexes of the electrocardiogram. If the rate is not rapid, if the patient has not received digitalis, if he has not eaten a meal within three hours, etc., then the change is indicative of a pathologic process. If the patient has had digitalis (and if it is not clear that he needs it) it will be necessary to discontinue the drug for several weeks and then make further observations. The presence or absence of the food factor may be determined by making observations under basal conditions and again one hour after a full meal, preferably before and after breakfast (Fig. 44). If the rate is rapid one can evaluate the electrocardiogram when it has become slower.

In most instances the location of myocardial ischemia is such that it changes the *direction* of the gradient as well as its magnitude. The gradient as projected upon the frontal plane is deviated to the left in diaphragmatic wall ischemia and to the right in lateral ischemia.

Practical Application of the Model Loop and Vectors

Throughout this book, to the extent to which this is possible, electrocardiographic phenomena are presented in terms of the spatial QRS loop and the mean spatial QRS, T, and gradient vectors. The *spatial* constructions are made by projecting the frontal plane loops and vectors into three dimensions. For the normal one simply finds by trial and error

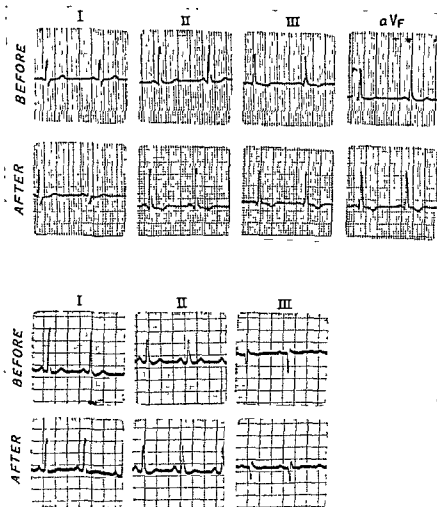


FIG. 44. Electrocardiograms before and one hour after a meal:

Top, Normal clockwise heart. Note inversion of T in aV_F as well as in Leads II and III.

Bottom, Counterclockwise rotated normal heart. T in Lead I is smaller; T in Lead III is more positive after food.

the orientation of the model of the idealized loop which when projected upon the frontal plane, most nearly matches the loop which is constructed from the limb leads. This may be done either by holding the model at eye level and visualizing the projection upon the frontal plane (see p. 26) or by clamping the model in a stand and throwing its shadow upon a triangle employing a source of parallel rays of light (Fig. 45).

When the orientation of the model loop is found that most closely matches the frontal

plane loop constructed from the limb leads the shadow (or frontal plane projection) of the spatial gradient vector gives the predicted direction of the ventricular gradient. This method may be more accurate if the direction of the mean QRS is also constructed and matched by the shadow of the mean spatial QRS vector of the model at the same time that the loop is matched. Some consideration can be given at times even to the magnitude of the constructed mean QRS, which is small in apex-back hearts. Obviously the method

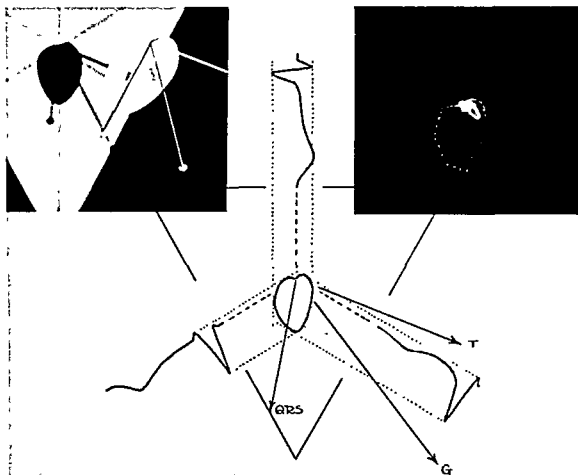


FIG. 45. The drawing shows the frontal plane QRS loop, and the frontal plane QRS, T, and gradient vectors constructed from the standard limb leads.

At the upper right is a photograph of the frontal plane loop recorded with the cathode ray oscilloscope.

At the upper left is a photograph of the model loop held in such a position that its projection (shadow) most nearly matches the constructed frontal plane loop. The direction of the mean QRS is also matched as closely as possible. Note, in this photograph, that the predicted direction of the gradient vector (the shadow) is only 8° to the right of the measured direction in the drawing.

of loop matching is valueless if the loop is abnormal.

It is to be noted that when we plot the QRS loop on the frontal plane as described in Fig. 45 and then orient the model loop in space so as to correspond with this frontal plane loop the projection of the gradient vector of the model upon the frontal plane frequently does not predict accurately the direction of the ventricular gradient as measured from the tracing. One reason for this becomes apparent after some experience with the model

loop. When the apex is back the slightest rotation of the model about the anatomic axis causes enormous changes in the vector directions as projected upon the frontal plane. In these cases, also, the complexes are generally quite small and therefore the greatest errors in measurement are made.

Again, the matching of the constructed frontal plane loop frequently is erroneous because of a slight distortion of the loop which causes its projection on the frontal plane to be much narrower or wider than it would be

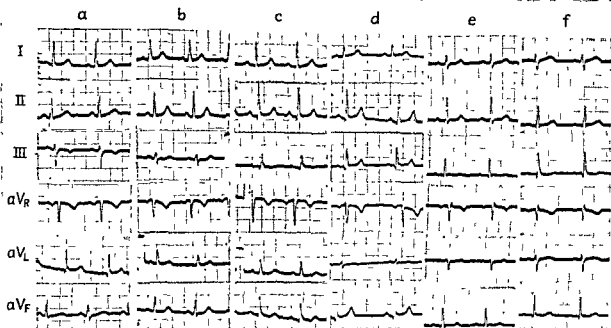


FIG. 46. A number of limb lead electrocardiograms from normal individuals which the reader may employ in practicing with his model QRS loop and T axes. Electrocardiogram *a* will be found to correspond to the loop held in the position and rotation shown in Fig. 40*f*. The limb leads of *b* will be found to correspond to the loop held in a rotation midway between *b* and *c* of Fig. 40; the loop is still counterclockwise but less so than in *b*, and its long axis is just about perpendicular to the line of Lead III. *c* corresponds fairly closely to the loop held in the position and rotation shown in Fig. 40*g*. *d* corresponds to the position and rotation shown in Fig. 40*e* but is probably a little more vertical. *e* corresponds to the loop held in the position and rotation shown in Fig. 40*h*. *f* corresponds fairly closely to the loop held in the position and rotation shown in Fig. 40*d*.

Note that the T waves also correspond to the T vectors attached to the model.

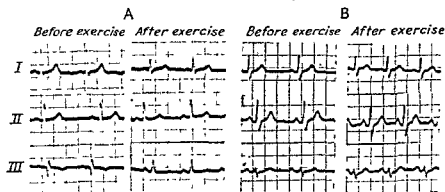


FIG. 46 (Continued). *A*. In *a* the QRS complexes and T waves correspond closely to the projection of the model held as shown in Fig. 41*d*. After exercise the anatomic axis is more vertical so that the QRS complexes correspond to the model held in the position and rotation shown in Fig. 41*c*. However, *T'* is now the T axis, for the gradient has been diminished by the exercise (rapid rate, etc.). In *B* the complexes correspond to the model held in the position and rotation shown in Fig. 41*a*. After exercise the position and rotation seem to have changed very little but *T'* is the T axis (Fig. 41*a*) as a result of diminution of the gradient.

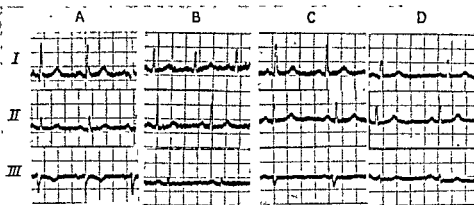


FIG. 47. A series of tracings made on the same patient at the same sitting. A, made sitting up, corresponds to the loop in the position and rotation shown in Fig. 40f. B, made sitting up holding a deep breath, roughly corresponds to Fig. 40g. Note that the T waves and QRS complexes both correspond to the diagrams referred to in Fig. 40g. The deep breath apparently causes a clockwise rotation of the heart. With the patient supine (C) the limb leads correspond to the loop in an orientation somewhat like that of Fig. 40f but a bit more vertical. With a deep breath (D) the heart now becomes more vertical and the loop is in the orientation shown in Fig. 40f but rotated a little more clockwise (the loop as projected on the frontal plane is narrower as evidenced by the small deflection in Lead III).

The example does not establish a rule for changes due to changes in posture. Postural changes vary a great deal and a deep breath sometimes produces counter-clockwise rotation. One factor in the case illustrated is a rather large abdomen, which with the patient sitting on an examining table caused the diaphragm to be pushed upward.

without the distortion. Eccentricity effects play a part in producing these errors.

Thus no narrow limits for the normal direction of the gradient have been established for the single electrocardiogram. However, wide divergence from the direction predicted by the method described above is to be held suspect.

It should never be forgotten that the direction of the ventricular gradient (and of the T wave) can be evaluated *only in relation to the mean QRS*. At times (e.g., after exercise)

the mean QRS and the gradient (as measured from the limb leads) become larger than before (as a result of change in cardiac position). However it will generally be found that the gradient has not become proportionately as large as the mean QRS so that it is relatively shorter.

Figures 46 and 47 represent practical examples of electrocardiographic changes resulting, in Fig. 46, from heart rotations similar to those shown in Figs. 40 and 41, and in Fig. 47 from changes in posture.

Suggested Reading

Ashman, R. The normal human ventricular gradient. IV. The relationship between the magnitudes AQRS and G., and deviations of the RS-T segment. *Am. Heart J.*, 26: 495, 1943.

→ Ashman, R., and Byer, E. The normal human ventricular gradient. II. Factors which affect its manifest area and its relationship to the manifest area of the QRS complex. *Am. Heart J.*, 25:36, 1943.

Ashman, R., Byer, E., and Bayley, R. H. The normal human ventricular gradient. I. Factors which affect its direction and its relation to the mean QRS axis. *Am. Heart J.*, 25:16, 1943.

Ashman, R., Gardberg, M., and Byer, E. The normal human ventricular gradient. III. The relation between the anatomic and electrical axes. *Am. Heart J.*, 26:473, 1943.

Bayley, R. H. On certain applications of modern electrocardiographic theory to the interpretation of electrocardiograms which indicate myocardial disease. *Am. Heart J.*, 27:431, 1944.

Gårdberg, M., and Olsen, F. Electrocardiographic changes induced by the taking of food. *Am. Heart J.*, 17:725, 1939.

Wilson, F. N. T deflection of the electrocardiogram. *T. A. Am. Physicians* 46:29, 1931.

Wilson, F. N., Macloed, A. G., Barker, P. S., and Johnston, F. D. The determination and the significance of the areas of the ventricular deflections of the electrocardiogram. *Am. Heart J.*, 10:46, 1934.

6. Injury

Acute injury to the myocardium such as occurs as the result of application of chemicals to the surface, inflammation, and (most common) deprivation of blood supply produces an increase in the permeability of the cell membrane and a reduction of its electrical resistance so that the injured cell membrane is partially depolarized and a current flows in the resting state. This current is called the *current of injury*. This situation is represented in Fig. 48. The dashed portion of the membrane is the injured portion. A simple method of regarding the electrical effects produced by the injured zone depicted in Fig. 48 is to attribute them to the imbalance between the dipoles on the opposing surfaces of the mass of syncytial muscle. Since there are three more dipoles pointing toward the left than toward the right the potential produced by the current of injury may be represented by a vector, C_i , which points toward the endocardial surface. The injury represented involves the epicardial surface.

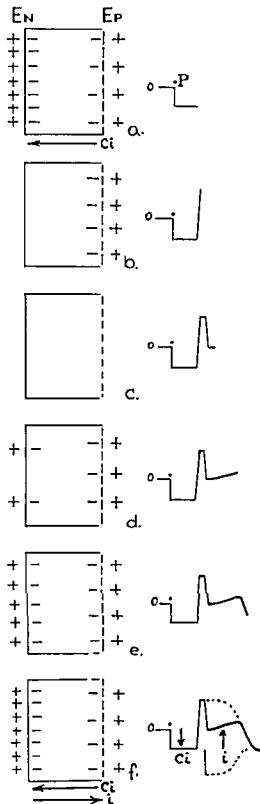
With the onset of the injury the current of injury causes the base line of the tracing made by placing an electrode at P to drop to a negative value as indicated in Fig. 48*a*. It is important to realize that this is not discernible in clinical electrocardiography. When the ventricle is activated in the usual manner (Fig. 48*b*) the wave of excitation produces a potential which in this case is greater than the current of injury and in the opposite direction so that the potential at P rises (R wave) to a positive value (Fig. 48*b*). When activation is complete (Fig. 48*c*) the potential at P is zero. Early in the injured state the rate of repolarization in the injured fibers is apparently not affected or becomes even more rapid than normal and repolarization occurs

in the usual order (more rapidly at the epicardial surface) so that the potential at P rises to positive values during repolarization. The T wave remains upright (Fig. 48*e*). When repolarization is complete the resting state is again achieved and the potential at P returns to the resting negative value resulting from the current of injury (Fig. 48*f*).

Thus it is seen in Fig. 48 that the current of injury produces a downward displacement of all portions of the record except that portion which we know is at zero potential, the RS-T segment. Actually on clinical electrocardiograms the level of the interval between beats is regarded as the base line and the RS-T segment appears to be elevated. Thus the RS-T shift has a direction opposite to that of the current of injury and may be represented in Fig. 48*f* as a vector i opposite in direction to C_i . This reversal of the direction of the vector employed in graphic representation of the shift that results from a current of injury has caused considerable confusion for the beginner. Careful attention to Fig. 48*f* should clarify this matter.

The two monophasic curves representing the electrical effects of the injured muscle are shown in the figure. The curve representing the potential changes of the endocardial surface is unaffected. The injured epicardial surface must be represented by a monophasic curve of smaller amplitude, because fewer dipoles are present on this surface. The relative duration of the two monophasic curves may remain the same as in the normal, but the curve for the injured surface may be of shorter duration (more rapid repolarization than normal).

If the injured muscle regains its full polarization it has recovered from the "injured"



state and will no longer produce an injury current and an RS-T shift. However, the involved fibers may still remain altered or impaired so that their rate of repolarization is slower than normal. Under such conditions (called ischemia) there would be (Fig. 49) an inversion of the T wave at the electrode *P* if the epicardial surface is the one involved. The Q-T interval in ischemia is frequently prolonged.

Frequently, soon after the "injured" state occurs there are neighboring areas of ischemic muscle and the electrical effects are as depicted in Fig. 50. There is a combination of RS-T shifts due to injury and a terminal inversion of the T due to the ischemic zone.

If now the injured zone dies or recovers to the extent that it becomes ischemic the RS-T shift diminishes and the T wave becomes increasingly inverted. If the muscle dies the R wave becomes smaller as the RS-T shift

FIG. 48. A segment of ventricular wall represented in the resting state. *Ep* is the epicardial surface; *En* the endocardial surface. *P* is an electrode placed at such a distance that there is little difference between the solid angle subtended by the endocardial and epicardial surfaces of the segment of ventricular wall.

The epicardial surface (dashed) is injured and is therefore represented as being partially depolarized (fewer dipoles are shown per unit area of membrane) and producing a current of injury represented by the vector *Ci*. The current of injury lowers the baseline of the tracing as shown.

b, Depolarization of the endocardial surface of the segment of myocardium produces the positive deflection (R wave). *c*, Complete depolarization brings the tracing to zero (which is above the baseline)

d and *e*, Repolarization is more rapid at the injured surface in early injury and the T wave is upright.

f, Return to resting state. When the current of injury *Ci* is directed away from the electrode *P* the RS-T shift is upward. Therefore if a vector is constructed for the current of injury (vector *Ci*) the RS-T shift produced by the current of injury must be represented by a vector of the same magnitude but opposite in direction (*I*).

The representation of the net effect by reducing the amplitude (partial depolarization) and shortening the duration of the epicardial monophasic curve is shown in *f*.

diminishes because dead muscle produces no electrical effect. If the muscle does not die but recovers to the extent that it becomes ischemic (or recovers altogether) the R wave remains unaffected.

The complete sequence of changes generally seen following an "injury" is depicted in Fig. 51.

The most common clinical condition in which "injury" occurs is coronary disease. When the blood supply to a segment of myocardium is cut off, the electrocardiogram goes through the series of changes described above.* In man the early injury tracing with the T wave in the same direction as RS-T shift may change within a few hours. The duration of the deprivation of blood supply probably determines the degree of injury of the involved muscle. The "injured" state with partial depolarization as depicted above is generally a temporary condition. Usually the muscle either dies or recovers in some measure. In angina pectoris the muscle usually recovers within a few minutes so that the electrocardiogram is frequently normal between attacks, and shows abnormality (RS-T shifts characteristic of injury) only if made during an attack. During recovery from most attacks of angina the tracing changes from the injury (RS-T shift) type back to the previous appearance without going through an "ischemic" change. In other cases if the anginal attack is sufficiently severe or of long

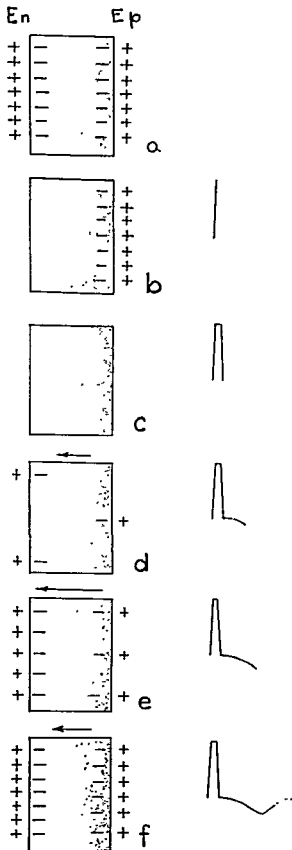
* The primary inversion of the T wave seen by Bayley as the first change occurring in experimental coronary occlusion in dogs is not generally seen in man under clinical conditions.

FIG. 49. Ischemia of the epicardial layers and surface of a segment of ventricular wall. Ischemia slows the rate of repolarization of the affected fibers.

This figure shows how slower repolarization of the epicardial surface produces an inverted T wave at P. The net effect can be represented by lengthening the monophasic curve representing the electrical effect of the epicardial surface (Fig. 31 b, 1, 2 and 3).

Note that ischemia is apt to prolong the Q-T interval.

A vector showing the direction and magnitude of the ischemic effects, as in *e*, is called the ischemic vector (*I_s*).



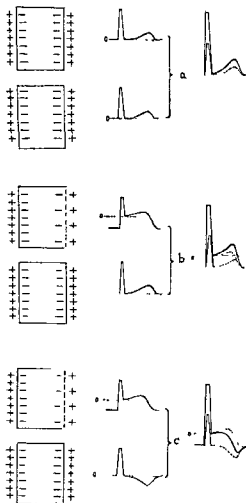


FIG. 50. Epicardial injury and ischemia. *a*, Two neighboring normal segments of ventricular wall. *b*, The upper segment becomes injured. *c*, The upper segment is injured and the lower is ischemic. Simple summation of the effects of the two regions produces the complexes recorded at an electrode corresponding to *P* of Fig. 48.

The figure shows the common sequence of events observed in human electrocardiograms when injury occurs.

duration, the muscle recovers from the injured state but is left in the altered state (ischemia) described above which causes it to be slow in repolarization. In such cases changes may be found in the electrocardiogram between attacks. These changes may of course, depend upon a continued lesser degree of diminution of blood supply (coronary insufficiency, ischemia).

If the deprivation of blood supply to a segment of myocardium is complete and permanent some of the muscle in the center of the area will certainly die (infarction) while a surrounding area will probably be deprived of part of its blood supply (ischemia). If infarction occurs the QRS will be affected because, as stated before, dead muscle can produce no electrical effects. In Fig. 51 one may see as the muscle dies a relationship between the disappearance of the injury effect and the appearance of QRS changes.

Wilson felt that if the coronary blood supply of a segment of left ventricular wall was cut off the epicardial layers of muscle would be affected to a greater extent than the endocardial fibers, which were maintained in good state by the direct blood supply from the cavity of the ventricle. Thus, Fig. 48 may be taken to depict what usually occurs when the vessel supplying a segment of left ventricular wall becomes occluded. However, at times it appears that the endocardial fibers suffer the most (subendocardial injury—see Fig. 52). When this occurs the RS-T shift is downward in a tracing made with the electrode over the epicardial surface of the injured area and the ischemic T wave when it occurs is upright and high (Fig. 53).

Effect of Localized Injury on the RS-T Segment in the Limb Leads

Figure 54 represents an area of "injury" (due to coronary disease) in the lateral wall of the left ventricle. Visualizing the changes depicted in Figs. 48 and 49 as occurring in sequence in the involved area of the myocardium shown in Fig. 54, we construct vectors C_i and i to represent respectively the current of injury and RS-T shifts produced by the current of injury in the earliest stages, and vector I_s to represent the resulting ischemia effects occurring during repolarization in the later stages. If we plot i we obtain the direction of the RS-T shift in the various limb leads. For the early injury effects we may plot the normal T wave following these shifts (*a*). However, during the early stage current

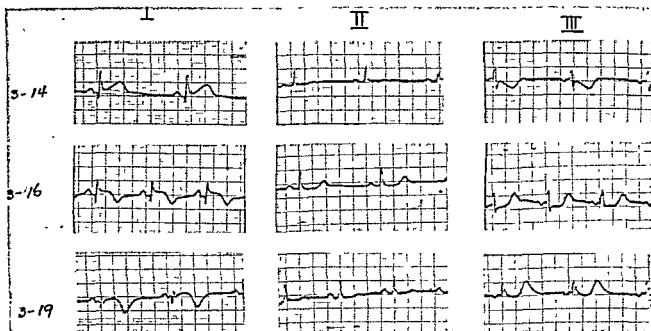


FIG. 51. Series of tracings made on patient with acute anterolateral myocardial injury ending in infarction. Tracings of March 14 and 16, correspond to the *b*, and *c* complexes of Fig. 50. Note lengthening of Q-T on March 16 and 19.

of injury effects may completely oppose and reverse the direction of the normal or previous T wave. If we add to the normal T wave vector the vector I_s (employing the parallelogram of forces) we obtain the resultant T wave vector T' , which occurs as a result of ischemia after the earliest injury stage (*b*). Finally when the injured state has disappeared only the ischemic effects (*c*) remain as shown in complexes labeled *c*. This series of complexes, then, represent the characteristic series of electrocardiographic changes that occur following a lateral wall injury, followed by ischemia. If rapid recovery follows injury the T wave may return to normal.

Figure 55 shows the electrical effects of an area of injury in the diaphragmatic wall of the left ventricle. The derivation of the RS-T shifts is accomplished in the same manner as for Fig. 54. A downward shift in the RS-T_I and upward shift in RS-T_{III} are characteristic, but, of course, the direction and magnitude of the shifts in the limb leads depends upon the direction and magnitude of the vector i , which in turn depends upon the

orientation of the involved area of ventricular muscle. The precordial electrodes generally face the endocardial surface of the injured region and the RS-T segments are usually displaced downward in those in which it is displaced.

Figure 56 shows the derivation of the precordial leads for the areas of injury indicated. The electrodes that face the epicardial surface of the injured area record complexes which show an elevation of the RS-T segment while those that face the endocardial surface show a depression of the RS-T segment. Again, in those leads that show an elevation of the RS-T segment the T wave becomes inverted in the later ischemic stage; and where there was a depression of the RS-T segment the T waves later become high and upright. Note that in pericarditis no precordial electrode looks toward the endocardial surface of the injured area and all of these leads will show elevation of the RS-T segment. In subendocardial injury the reverse is true, i.e. all precordial leads show depression of the RS-T segments.

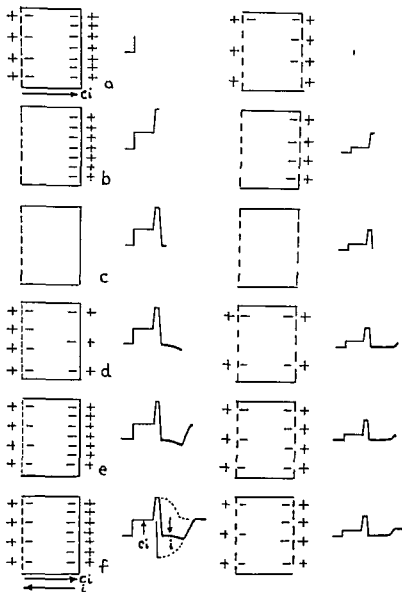


FIG. 52. *Left: Endocardial injury. Right: Transmural injury. a, resting; b, depolarization; c, fully depolarized; d, early repolarization; e, f, repolarization completed. In endocardial injury the current of injury and RS-T shifts are in the opposite direction to those which occur in epicardial injury. The net effect may be represented by diminishing the amplitude and the duration of the endocardial monophasic curve.*

Effect of Localized Injury on the QRS Complexes

If the direction of the current of injury is the same as that of the R wave in a given lead it may cause the tracing to reflect QRS changes that are more apparent than real.

Figure 57B shows an apparent reduction in R as measured from the new base line, which results entirely from the current of injury. If recovery takes place without death of muscle the R will return to its previous height (Fig. 57B). This figure represents an anterior

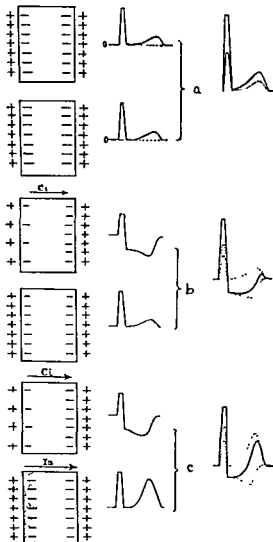


FIG. 53. Endocardial injury and ischemia. Compare Fig. 50 which represents epicardial injury and ischemia.

Note that the RS-T segments are displaced downward for an electrode at the epicardial surface and that the ischemic T waves are excessively high.

subendocardial injury. The forces that normally produce the R wave produce the same positive potential at *P* which they would normally, but because the base line is shifted the R is apparently smaller than normal. Also, the S being written by the uninjured lateral and posterior walls reaches its usual absolute depth and appears to be a larger deflection than normal as measured from the new base line because it occurs after the current of in-

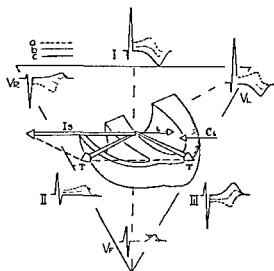


FIG. 54. Lateral wall injury followed by ischemia. The principles developed in Fig. 48, 49, and 50 are applied to the limb leads. The vectors *Ci* and *i* represent the magnitude and direction of the current of injury and the RS-T shifts respectively. The vector *Is* represents the later effects of ischemia of neighboring regions.

jury has been wiped out by depolarization of the apex.

If there is anterior epicardial injury (Fig. 57A), which is common in early anterior myocardial infarction, the current of injury is opposite in direction to the forces which

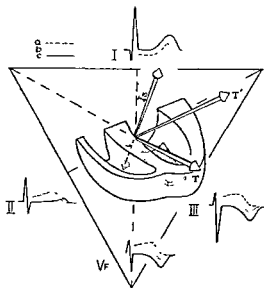


FIG. 55. Diaphragmatic injury followed by ischemia. The construction follows the same method employed for Fig. 54.

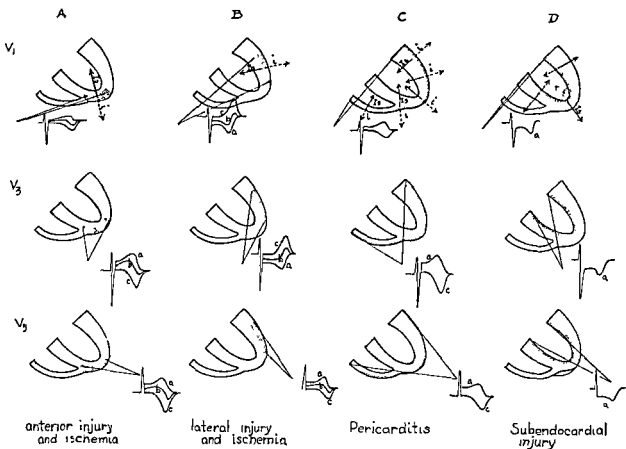


FIG. 56. Summary of RS-T and T effects of injury followed by ischemia in the precordial leads.

The method of analysis is the same as that employed for Fig. 54. Column A, V_1 , V_2 , and V_3 , in anterior injury followed by ischemia. Column B, V_1 , V_2 , and V_3 , in posterolateral injury followed by ischemia. Note that electrode at V_1 is facing one side of the lesion while V_2 and V_3 are facing the other. As a result the sequence of effects at V_1 is the reverse of that seen at V_2 and V_3 . Column C, V_1 , V_2 , and V_3 in pericarditis, (a) acute and (b) subacute. Column D, Diffuse subendocardial injury.

produce the R wave in Lead V_3 represented in the figure. When depolarization occurs there is actually less positivity at P than normal but the downward displacement of the base line makes it appear that R is unchanged. On the other hand, if an S is present which is derived from depolarization of the base and lateral wall of the ventricle, the S wave will be drawn upward; it will appear smaller as measured from the new "base" line. This occurs because depolarization of the injured zone has wiped out the current of injury (temporarily). Under these circum-

stances the negative deflection S must be drawn or constructed from zero as a base line instead of from the altered base line due to the current of injury (Fig. 54A-b). This latter phenomenon is very commonly seen (Fig. 58, leads III, V_2). If infarction occurs, of course, the R will diminish or disappear for it is derived from the involved zone. If R disappears the normal S becomes a "Q" or QS.

If epicardial injury occurs (Fig. 57C) in the posterolateral wall of the left ventricle where the S originates for the lead chosen

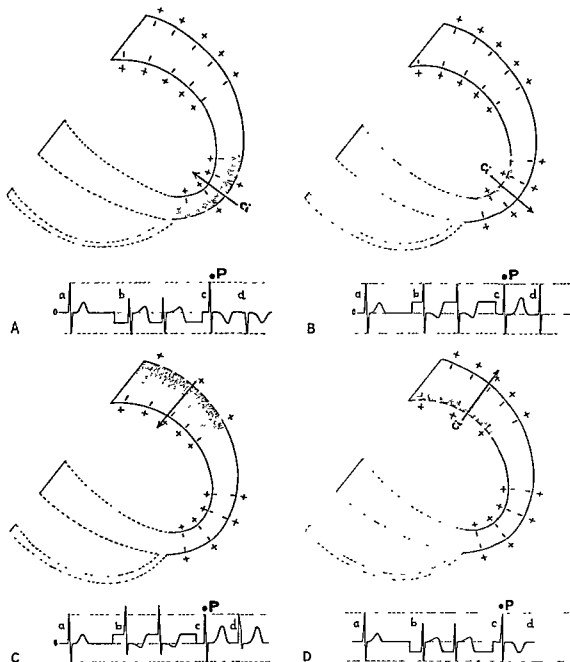


FIG. 57. Secondary QRS effects of injury. *A*, Upward displacement of S wave by anterior epicardial injury current. *a*, Complex before injury. *b*, Injury (two complexes). Note change in baseline. *c*, Recovery from injury, ischemia remaining causing inversion of T. *d*, Complex which occurs if transmural infarction follows injury.

B, Anterior endocardial injury. *a*, Complex before injury. *b*, Injury (two complexes). Note diminution of R and increase of S as measured from new baseline. *c*, Recovery from injury, ischemia remaining causing increase in height of T. *d*, Complex occurring if infarction of the

endocardial layer of fibers occurs. The QRS may be little affected because the overlying epicardial fibers still produce an R and the S is derived from the basal regions and lateral wall.

C, Posterior lateral epicardial injury. *a*, Complex before injury. *b*, Injury (two complexes). Note R and S remain the same as measured from the new baseline. Some change in R occurs at times as described in text. *c*, Recovery from injury; ischemia remaining produces high T waves similar to those occurring in anterior endocardial ischemia (see *B*).

D, Posterior lateral endocardial injury. Note similarity to anterior epicardial injury in every detail.

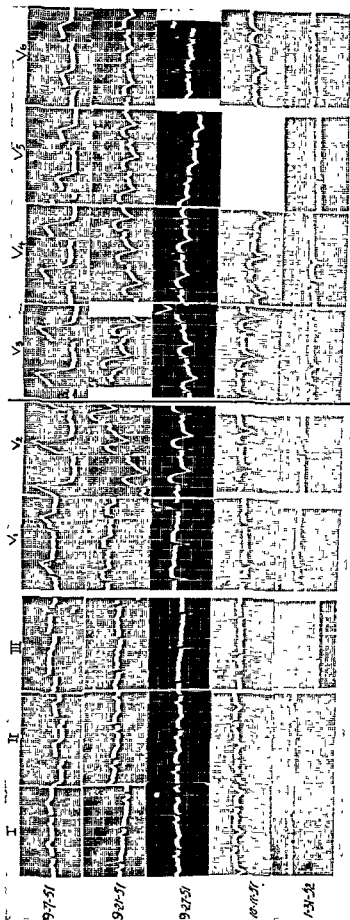


FIG. 58. Serial electrocardiograms on a patient suffering a myocardial infarction. In V₁ one notes the S "drawn up" as described Fig. 57A. The tracings also show all of the effects described for injury in the theoretical presentation.

for analysis, the R will appear to be of normal amplitude. Here the current of injury is in the same direction as the forces producing the R wave and both are in effect at the same time. The base line is displaced upward, the R adds its total effect to the potential at *P* because it is not derived from the injured zone; while the potential at *P* is greater than normal it is apparently unchanged from the normal because the base line is shifted upward.* When the S is inscribed less negativity is produced at *P* than normal but because of the shift of the base line it appears to be of normal magnitude. If infarction occurs S becomes smaller, because it is the portion of the ventricle which normally produces the S which is infarcted. If we place *P* at V_0 the changes become those

* However, R is apt to be wider than normal because for a short period of time the apex and base both contain waves of excitation (0.025 second–0.035 second); the injury at the base, where activation generally opposes the effects of apical activation upon the potential at *P*, causes the potential at *P* to remain positive for a longer period of time (Fig. 112).

which occur anteriorly for an anterior injury or infarction except that there is often little or no S at V_0 .

If a posterior subendocardial injury occurs (Fig. 57D) the changes are quite similar to those of the anterior epicardial injury.

The effects of pericarditis resemble those of a diffuse epicardial injury producing upward shifts in virtually all standard limb leads (except Lead III in horizontal hearts) and precordial leads followed by T wave inversion.

During many acute attacks of angina pectoris it appears that a diffuse subendocardial injury may be present.

It is important to note that actually injury is frequently transmural reaching and affecting both the epicardial and the endocardial surfaces. The net effect as represented here will depend upon which surface is more injured. Furthermore, this balance may change within a short time in any given case. A more detailed discussion will be undertaken in another connection.

Suggested Reading

- Bayley, R. H. An interpretation of the injury and the ischemic effects of myocardial infarction in accordance with the laws which determine the flow of electric currents in homogeneous volume conductors and in accordance with relevant pathologic changes. *Am. Heart J.*, 24:514, 1942; 26:769, 1943.
- Bayley, R. H., and La Due, J. S. Electrocardiographic changes of impending infarction, and the ischemia-injury pattern produced in the dog by total and subtotal occlusion of a coronary artery. *Am. Heart J.*, 28:54, 1944.
- Bayley, R. H., and La Due, J. S. Differentiation of the electrocardiographic changes produced in the dog by prolonged temporary occlusion of a coronary artery from those produced by postoperative pericarditis. *Am. Heart J.*, 28:233, 1944.
- Bayley, R. H., La Due, J. S., and York, D. J. Electrocardiographic changes (local ventricular ischemia and injury) produced in the dog by temporary occlusion of a coronary artery, showing a new stage in the evolution of myocardial infarction. *Am. Heart J.*, 27:164, 1944.
- Bayley, R. H., La Due, J. S., and York, D. J. Further observations on the ischemia-injury pattern produced in the dog by temporary occlusion of a coronary artery. *Am. Heart J.*, 27:657, 1944.
- Wilson, F. N. *The Distribution of the Currents of Action and of the Injury Displayed by Heart Muscle and Other Excitable Tissues*. Ann Arbor, Michigan, University of Michigan Press, 1933.

7. Ischemia

The effects of myocardial ischemia such as results from coronary sclerosis have been described in the chapter dealing with Injury. The characteristic electrocardiographic changes that occur in ischemia result from the slower rate of repolarization in the ischemic zone, particularly at the epicardial surface.

A separate discussion of ischemia is necessitated by the fact that in many cases the ischemic effects are seen alone. Either the patient is not seen sufficiently early to obtain tracings during the "injured" state or the latter state does not occur. Figure 59 represents a zone of ischemia in the lateral wall of the left ventricle constructed precisely as it was for the ischemic effect following injury in Fig. 49. In Fig. 59 the effects of varying degrees of ischemia are represented by a series of ischemic vectors (I_s) of increasing magnitude. The effect of these various degrees of ischemia upon the T wave of the electrocardiogram is developed by adding the vectors representing them to the normal T vector employing the parallelogram of forces.

Figure 60 is a series of electrocardiograms made on the same patient showing the entire range of ischemic changes developed in Fig. 59.

Posterior ischemia may be represented in the same manner employing the ischemic vector of Fig. 55 (see Chapter 6). Figure 61 is a series of electrocardiograms on the same patient illustrating increased ischemic effects produced by an attack of angina in a patient who had had a posterior myocardial infarction some months before and who still had ischemic T waves as a result of that event.

Ischemic T waves may be the only evidence of an attack of angina or of a series of at-

tacks of angina. They may also appear without angina. Having appeared they may disappear within a few days and then reappear. Again they may gradually disappear over a period of several weeks or months or they may remain permanently.

It is important to point out that as shown in Fig. 60b the T waves need not be inverted in Lead I to indicate ischemia. Whenever the direction of the T wave axis is seen to change as from T_0 to T_1 (Fig. 59) without significant change in rate or in the absence of other non-pathologic conditions that may explain it, ischemia should be suspected. The ischemic

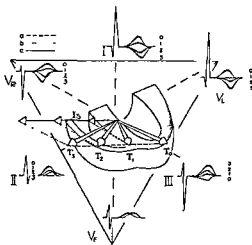


FIG. 59. Lateral ischemia (the stippled area is ischemic).

I_s is the ischemia vector corresponding to that shown in Fig. 54.

T_0 is the normal mean T vector.

The figure shows the effect of increasing degrees of ischemia. As I_s is increased in length its vectorial addition to T_0 produces, successively, vectors T_1 , T_2 , and T_3 . The corresponding T waves in the limb leads are so labeled. Corresponding tracings from a patient are shown in Fig. 60.

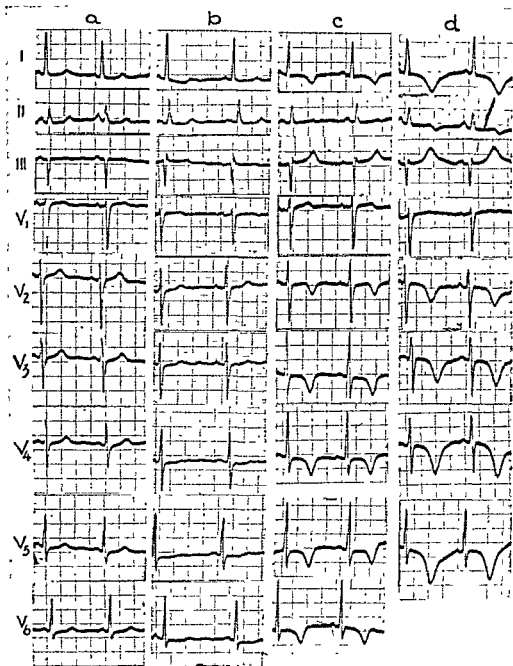


FIG. 60. Anterolateral Ischemia. A series of tracings from a patient with progressively increasing ischemia, producing the series of T wave changes in the limb leads constructed in Fig. 59. In *a* the T axis corresponds to T_s of Fig. 59; in *b* the T axis corresponds to T_2 ; in *c* the T axis corresponds to T_4 ; and in *d* the T axis corresponds to T_6 of the same figure.

effects capable of producing this change may be too small to cause inversion of the T waves in the precordial leads. It was Ashman who first pointed out the pathologic significance of such rightward deviation of the electrical axis of the T wave in the limb leads.

It is of utmost importance to point out here that in the interpretation of T wave changes observed in a series of electrocardiograms the effect of nonpathologic factors must be ruled out. The similarity between the T wave changes produced by ischemia in Fig. 38B

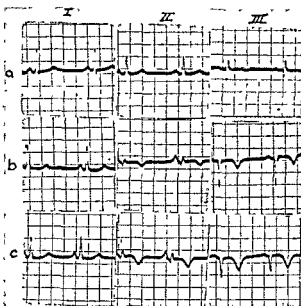


FIG. 61. Diaphragmatic ("posterior") wall ischemia. Series of tracing showing increasing degrees of posterior ischemia due to angina in a patient who had sustained a diaphragmatic wall infarction.

to those produced by rate changes in Fig. 38A must be apparent. Other factors discussed in Chapter 5 must be considered in this connection. The necessity for employing the principle of the gradient and some knowledge of the factors governing the magnitude and the direction of the gradient must again be emphasized.

If the ischemia were more apical in location the effect would simply be to shorten the T-wave vector (Fig. 62) in mild ischemia and finally to reverse its direction for higher grades of ischemia. Thus in the milder degrees of ischemia all the T waves would simply become smaller in magnitude.

In posterior ischemia the evidence is more difficult to evaluate. Inverted T waves in Lead III are common normally and inverted T waves in Lead II may occur. Unless these are very large as in Fig. 61 they cannot be evaluated easily. Once again determination of the direction and magnitude of the gradient is a better criterion than attempting to analyze T wave directions empirically.

If a section of ventricular wall is ischemic

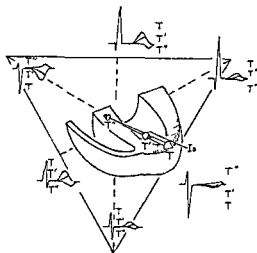


FIG. 62. Apical ischemia (the stippled area is ischemic). The ischemia vector I_s is, fortuitously, opposite in direction to the normal T vector so that with slight ischemia (I_s is short) the T vector simply becomes shorter T' and with more ischemia its direction is reversed (T'').

The T waves of the limb leads carry the label of the T vector to which they correspond.

With a greater degree of ischemia the T'' vector would become longer and large inverted T waves would appear in Leads I, II, V_1 and V_2 .

It is probable that the epicardial and endocardial surfaces are both affected and it is likely that under these circumstances the first portion of the repolarization curve is flat for both surfaces. Under these conditions deviation of the RS-T segment does not occur. It follows also that if such transmural ischemia occurs the direction of the T wave changes depend upon which surface is most ischemic. While we follow Wilson's assumption that the endocardial surface is generally less affected than the epicardial surface when a segment of the ventricular wall suffers diminution of its blood supply because of coronary disease it is probable that the reverse occurs at times. This seems to be the case quite frequently in angina pectoris and occasionally at the onset of myocardial infarction.

The Precordial Leads in Ischemia

The precordial electrocardiogram in myocardial ischemia deserves detailed discussion.

Although vector representation was employed in discussing the effects of injury and ischemia on the precordial electrodes in the preceding chapter it is important to point out that this short cut in presentation may contain errors at a fundamental level. The precordial electrodes are very close to the heart and as has been indicated in Chapter 3 the solid angle method of analysis is the most accurate presently available under these circumstances.

Figure 63B shows a heart in which a low-grade ischemia has developed in the apical region, characterized by a slower rate of repolarization at the epicardial surface in this region. Figure 63B-a shows the early stage of repolarization. The slow rate of repolarization at the apical epicardial surface is represented by a delay of the reappearance of dipoles at this surface (compare with Figure 63A-a which depicts the normal). The effect upon the various precordial leads is shown. All of the electrical effect at this time is produced by repolarization in the interventricular septum, because the effects of repolarization of the endocardial and epicardial surfaces of the apex now counterbalance one another. No solid angles need be drawn because the oversimplified diagram shows only one dipole. However, in considering the effects of this dipole upon the potential at each electrode it is necessary to remember that the potential diminishes in proportion to the square of the distance from the area (dipole) producing the effect.

At a later stage of repolarization of the ventricles (Fig. 63B-b) the slower rate of repolarization at the epicardial surface of the apex is again represented by drawing fewer dipoles on this surface than in the normal (compare with Fig. 63A-b), and again the endocardial and epicardial repolarization effects are represented as counterbalancing one another instead of producing the effects seen in the normal. (Note absence of unbalanced dipoles at apex whose effects are shown in Fig. 63B-b as small vectors pointing toward the epicardial surface). At this stage the electrical effects are derived from septal and

lateral wall repolarization. If we draw solid angles from each electrode position to the septal wall and the lateral wall of the left ventricle (giving each its proper sign) we may analyze the electrical effects in the same way as was done for the QRS complex of the precordial leads. The results are shown in Fig. 63B-b and the completed complexes are found in Fig. 63B-c. The Q-T intervals may or may not be discernibly prolonged beyond the limits of normal.

Ashman was the first to note that in antero-septal ischemia (or infarction) the QT interval may be prolonged in Leads V_2 and V_3 and yet remain normal in the limb leads because the ischemic vector is perpendicular to the frontal plane.

Figure 64b is an illustrative electrocardiogram from a patient with apical ischemia.

Since the important effects are to be found in Figs. 63A-b and 63B-b (and because too detailed speculation regarding the beginning and end of repolarization is not yet warranted) the analysis of ischemia in other locations will be confined to this stage, which corresponds, in the normal, to the peak of the repolarization effects.

The effects that occur with a greater degree of apical ischemia are shown in Fig. 63C-b. Here repolarization is so slow at the epicardial surface that the potential across the apical wall is actually in the reverse direction to that which prevails in the normal. From each electrode solid angles must now be drawn to the septum, the apex, and the lateral wall. When each is given its proper sign and the total effect estimated the results will be as shown in the figure. Actually most of the effects will be obvious at a glance.

It must be noted that it is not believed that the precordial electrode records only or even mainly effects occurring subjacent to the electrode. Employment of the solid angle principle attributes to every portion of the heart an effect on the electrode; the magnitude of the effect of each portion of the heart upon the electrode depends upon the orientation of the electrical effects occurring in that por-

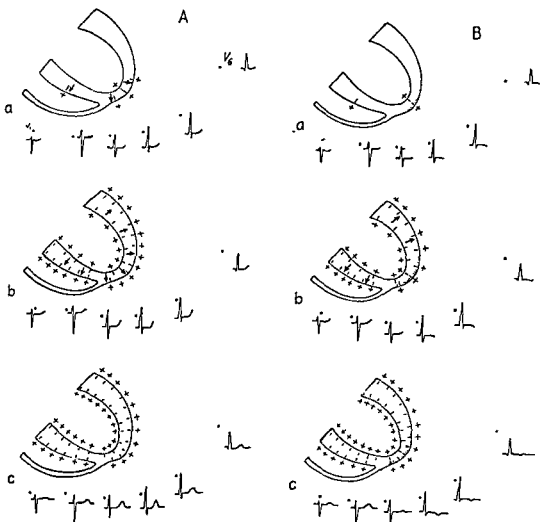


FIG. 63. *A*, The normal T waves in the precordial leads. *a*, Early repolarization effects. The small vectors indicate the balance between epicardial and endocardial repolarization. *b*, Later stage of repolarization. *c*, Full repolarization.

The more rapid rate of repolarization at the epicardial surface causes the net effects to have the direction indicated by the small vectors. It is to be re-emphasized that the T effects result from a rather fine balance between opposing effects.

It is apparent that as constructed the repolarization effects produce positive T waves in all the precordial leads. Common variations are described in Chapter III.

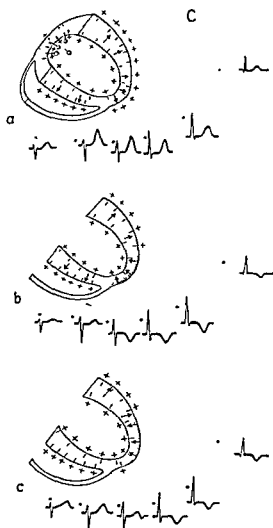
B, Precordial leads in apical ischemia. *a*, *b*, and *c* are the same stages depicted in *A*. The stippled area is sufficiently ischemic for the rate of repolarization at the epicardial surface to be nearly equal to that at the endocardial surface instead of being more rapid. As a result the T

effects of the apex of the left ventricle are lost. Thus the T waves in the precordial leads are produced entirely by the normal repolarization effects of the unaffected regions.

Under these circumstances the T waves may be unaffected at V_1 and V_2 , lowered at V_3 , small and inverted at V_4 and V_5 , and small diphasic or upright at V_6 (see figure 64B). This is evident if one considers the effects of the remaining vectors of *A* upon the electrodes. With slightly less ischemia the T waves in V_1 , V_2 , V_3 , and V_4 would all be low and upright.

C, Precordial leads in ischemia. *a*, Diaphragmatic or posterior wall epicardial ischemia. If repolarization is slower at the epicardial surface of the diaphragmatic or posterior wall the net repolarization effects point anteriorly and upward (solid tipped vectors). The result is an increase of the height of the T waves in the precordial leads. If the ischemia reaches the posterolateral wall the T in V_1 may be inverted.

b, Marked apical ischemia. Repolarization is



so slow at the epicardial surface of the apex that the repolarization effects are reversed. This causes inversion of the T wave in V_4 , V_5 , V_6 , and V_a . If the ischemia extends a bit more to the right all of the T waves in the precordial leads are inverted.

c. Anterolateral ischemia. The reversed repolarization effects are pointing toward V_1 and V_2 causing the T waves in these leads to become higher than normal while the T waves in V_4 , V_5 , and V_6 are inverted.

tion of the heart and upon the distance between that portion of the heart and the electrode. It is important to point out that the application of vector analysis (implying single dipole representation) would not give the results for Fig. 63B (mild ischemia) that are depicted in that figure.

Figure 64a shows the effects of anterolateral ischemia. It is important to point out that the T in V_1 and V_2 are apt to be *higher* than usual. It is also important to note that in mild degrees of anterolateral ischemia the findings are similar to those that occur in left ventricular hypertrophy and incomplete left bundle branch block, as well as after digitalis. The orientation of this area of the left ventricular wall is such that the effect of ischemia here directly opposes and therefore diminishes the normal ventricular gradient.

In "posterior" myocardial ischemia the effects depend as always, upon the orientation of the ischemic area. If only the diaphragmatic area of the left ventricle is involved in a transverse heart there will be no effects upon the precordial leads. If the posterior and not the posterolateral wall is involved the effects will be as depicted in Fig. 63C-a. It is to be noted that the effect of epicardial ischemia in the wall of the ventricle opposite to that subjacent to the electrode is to increase the magnitude of the T wave at the electrode under discussion. If the ischemia is posterior and does not extend to the lateral wall the T waves may be increased in all the precordial leads. Unfortunately large T waves occur normally and it is impossible to establish a criterion of normalcy. Again, serial observations of T wave potential may reflect more the effect of change in electrode position than the effect of change in T potentials.

The effect of ischemia on the gradient can be constructed for Figs. 59, 61, and 62 by adding I_s vectorially to the normal gradient vector.

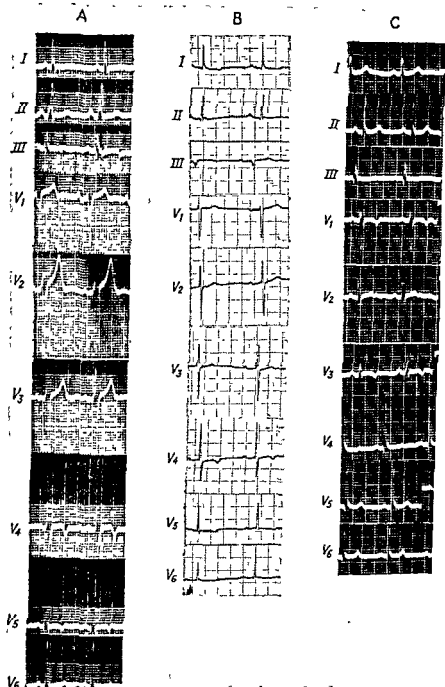


FIG. 64. *A*, Antero-lateral ischemia. Note increase in height of T in V₁ and V₂, while T in V₄ and V₅ is inverted.

The greater effect on V₂ than on V₄ is due to the fact that V₄ is much closer to the heart.

B, Apical ischemia corresponding to Fig. 63B.

C, It is to be recalled that in children, young women, and occasionally in men the T waves are normally inverted in V₁, V₂, and V₄. At times, because of the placement of the electrode the inversion is recorded only in V₄. *C* is such a tracing; it is entirely normal.

8. Left Ventricular Hypertrophy

When hypertrophy of the left ventricle occurs the wall of the ventricle is, by definition, thicker than it is normally. This change has been observed frequently by the writer when little enlargement of the heart has occurred. Frequently the apex is thicker in relation to the base than in the normal although at times even in very much enlarged left ventricles the apex remains quite thin while the lateral wall and base becomes much thicker than normal.

Figure 65 represents the effect of a moderate increase in the size of the left ventricle and of increasing the thickness of the apex. Normally the short length of the vector that occurs at 0.025 second depends upon the early penetration of the thin apex by the wave of excitation. When this portion of the ventricle becomes thicker the early penetration of the apex of the left ventricle does not occur. This leads to a lengthening of the vector at 0.025 second and gives it a more anterior direction. The persistence of a wave of excitation in the apex causes the vectors that follow also to have a more forward direction and greater length. The general effect is to cause the spatial QRS loop to have a more circular shape than is found normally, for the last portion of the loop produced by the base of the ventricle tends to remain unchanged.

In some instances when the apex remains thin the loop may not become more circular but may simply be elongated as a result of the increased size of the ventricle and therefore increased size of the wave of excitation.

It is important to note that the persistence of the wave of excitation in the apex of the ventricle as described above accounts for considerable increase in the size of the complexes without the necessity of postulating noticeable enlargement of the heart. This occurs as a

result of the fact that there are, under these circumstances, large vectors which are parallel to the frontal plane. In the normal spatial loop of Fig. 15 the longest axis (0.04 second) points backward as much as to the left.

While large complexes are the chief sign of left ventricular hypertrophy in the limb leads it is important to note that rather large complexes may be seen in normals, especially in thin young adults and adolescents. It is also important to point out that very much enlarged and hypertrophied left ventricles may sometimes produce relatively small complexes in the limb leads even when no edema or hydrothorax is present. *No arbitrary standard for magnitude of complexes, therefore, should be set up as a criterion.* It is really the duration of S in V_1 , V_2 and V_3 and the duration of R in V_5 and V_6 that is important.

Generally when the ventricle is considerably thickened its depolarization requires more time than in the normal. Unfortunately a prolonged QRS duration of even 0.10 second may occur in some normals. If both the duration and magnitude of the QRS phenomena described above are greater than are commonly expected, we may be more sure of the presence of left ventricular hypertrophy. The QRS duration may reach 0.12 second without the presence of left bundle branch block.

The Precordial Leads in Left Ventricular Hypertrophy

In the precordial leads, as shown in Fig. 66, the depth and duration of the S waves in V_2 and V_3 are apt to be exaggerated and the height and duration of R in V_5 and V_6 are apt to be greater than is generally seen in the normal. On the other hand it is important

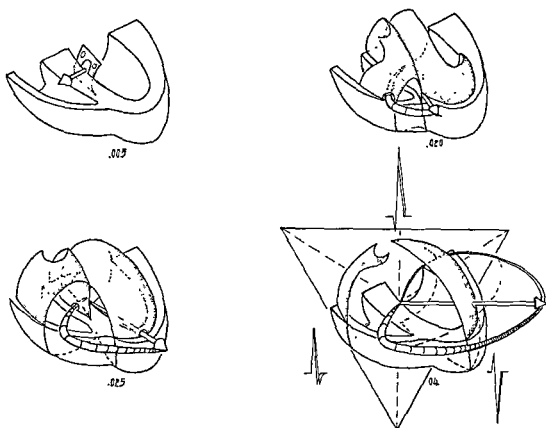


FIG. 65. Development of loop in left ventricular hypertrophy. Depolarization of the ventricles is represented in four of the stages employed for the normal. The thickened apex assumed to be present here causes a delay in the penetration of this region by the wave of excitation. This causes each of the vectors present at .02 second, .025 second and .04 second to be longer and to have a more forward direction. As a result the spatial loop bulging more forward becomes more rounded than the normal. The limb lead complexes which result are apt to be larger than the normal because the vector at, for instance, .04 second is more nearly parallel to the frontal plane than the .04 second vector in the normal and therefore has a larger projection on the frontal plane unless the apex back position occurs. The QRS is usually wider because depolarization of the thickened wall requires more time than in the normal.

to point out that the R in V_4 and V_3 may be quite high (25 mm. is not unusual) in healthy children and young adults.

A very common occurrence in left ventricular hypertrophy is a loss of the R wave in V_1 and very small R waves in V_2 and at times V_3 are not uncommon. The explanation of this phenomenon is not clear. It may result from a very slight left bundle branch delay (see Chapter 10). Distinction from the precordial leads in anteroseptal infarction may be impossible. The abrupt transition from large S waves in the right precordial leads to

large R waves in the left precordial leads may occur in all three conditions.

Although most hearts with hypertrophied left ventricles seem to be rotated counter-clockwise and are transverse so that the limb leads show left axis deviation (electrical axis to the left of 0°) the fact remains that many normal hearts also produce limb leads indicating left axis deviation. Furthermore, many hypertrophied hearts do not show left axis deviation. This depends upon the anatomic position and rotation of the heart. Obviously the QRS loop of Fig. 65 may be

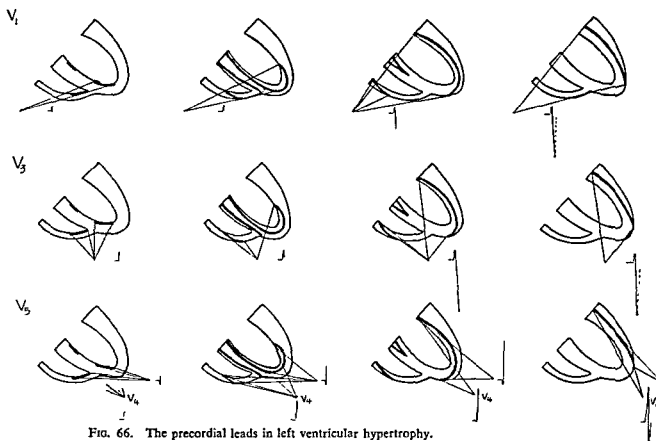


FIG. 66. The precordial leads in left ventricular hypertrophy.

Comparison with the corresponding figure for the normal (Fig. 23) reveals that the increased depth of S in V_1 and V_3 , the diminished magnitude of R in V_1 and V_3 , and increased height of R in V_5 and V_6 (not shown) result from the larger waves of excitation which occur because the apical wall is not penetrated as rapidly as in the normal.

If the heart is enlarged the waves of excitation may be larger for this reason also.

rotated clockwise just as was done with the normal loop (see Figs. 67, 68).

The T Wave in Left Ventricular Hypertrophy

The T waves in left ventricular hypertrophy may be entirely normal. Frequently, however, they undergo a series of changes with advancing hypertrophy (Fig. 170), which theoretically may result from the increased time required for the wave of excitation to traverse the increased thickness of the ventricle. If we approach this problem in the manner employed in presenting the normal T wave (Fig. 28) and assume that depolarization—and therefore repolarization—of the epicardial surface is delayed because more time is required to traverse the thickened wall the situation may be represented as in Fig. 31c. The epicardial monophasic curve

must occur later than normally. The result is a lowering of the T wave. With greater delay (Fig. 31c) a depression of the RS-T segment and an inversion of the T wave occurs if the QRS is largely upright; and an elevation of the RS-T and increase in the height of the T wave occurs if the QRS is largely negative. This phenomenon simply follows the principle of the ventricular gradient and is applicable to the precordial as well as the limb leads. If there is no ischemia or other lesion the gradient is unaltered in magnitude and direction and the increase of the area of the QRS which occurs in left ventricular hypertrophy must be accompanied by a compensatory change in the T wave (so that $AQRS + AT$ remain constant). While more work needs to be done on this problem, measurement of the gradient in some 50

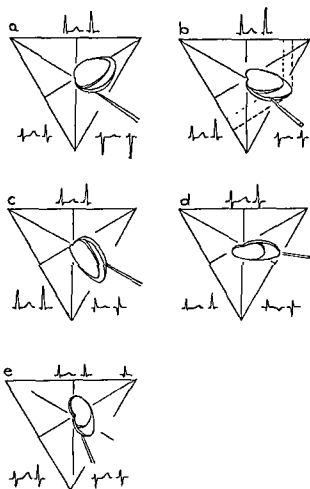


FIG. 67. The QRS loops of the normal and of left ventricular hypertrophy in various positions and orientations *a*, Marked counterclockwise rotation; *b*, slight counterclockwise rotation; *c*, slight clockwise rotation; *d*, transverse apex back slightly clockwise rotation; *e*, vertical apex back slightly counterclockwise rotation.

cases of left ventricular hypertrophy seems to indicate that the magnitude and direction of the gradient in relation to the mean QRS are about the same as in the normal.

Application of this principle to all leads results in the prediction that the T wave in leads with a large S wave as the prominent deflection (III, V_1 , V_2 , V_3) will become large and upright in most hypertrophies and that in leads in which a large R is present (I, V_6) the T will become flat and then inverted. When digitalis is administered the Q-T is shortened and further diminution of the gradient exaggerates these RS-T and T wave effects (Fig. 68).

The onset of congestive heart failure is generally accompanied by a diminution of the gradient and the RS-T shifts and T wave inversions become exaggerated.

In some cases of left ventricular hypertrophy the limb leads are surprisingly small. The duration of the QRS complex in such cases is apt to be greater than normal. In some of these cases the small complexes result from infarction. In others this is clearly not the case. It is possible that in some of these cases the effect of eccentricity is important.

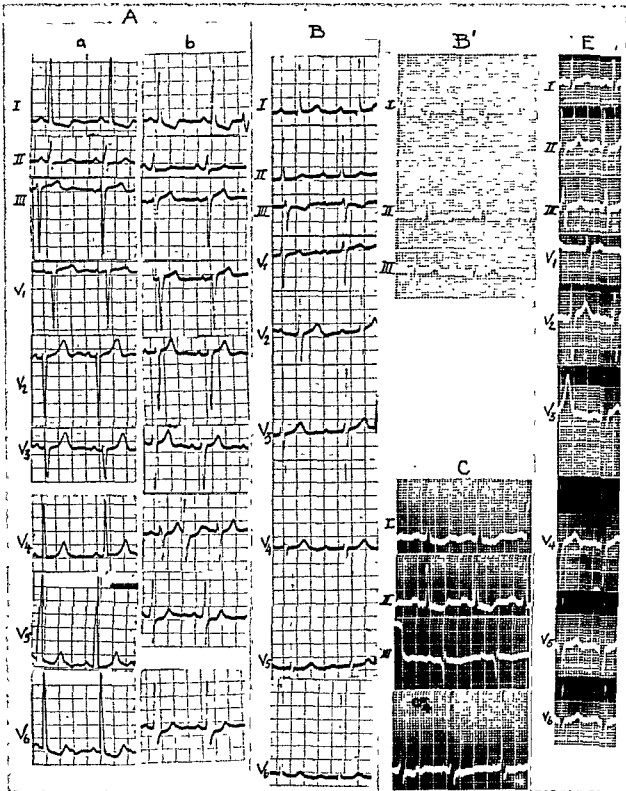


FIG. 68. Left ventricular hypertrophy. *A*, Marked counterclockwise rotation; corresponds to diagram *a* of Fig. 67. (*a*, before digitalization; *b*, after digitalization.) *B*, Counterclockwise rotation; corresponds to diagram *b* of Fig. 67. *B'*, Nonrotated; corresponds to a rotation between that of diagram *b* and *c* in Fig. 67. *C*, Clockwise rotation; corresponds to diagram *c* in Fig. 67. *E*, Apex-back vertical counterclockwise rotation; corresponds to diagram *e* in Fig. 67.

9. Right Bundle Branch Block

In this presentation we will adhere to the classical concept that in bundle branch block there is delay or complete blocking of the impulse in the right branch of the bundle of His. Under the latter circumstance the impulse can only reach the right ventricle by traversing the thickness of the septum. For our purposes we assume that the time required for activation of the interventricular septum from one side is about 0.06 second.

Fig. 69 represents a visualization of the activation of the ventricles in right bundle branch block. The same phenomena that are postulated for the normal are pictured, but in the left ventricle alone until the septum has been traversed. Following this the appropriately timed waves appear in the right ventricle. The septum is activated only from the left side and the wave of excitation traverses it from left to right.

The early 0.005-second stage does not differ from the normal. At 0.015 second the partial excitation of the left side of the septum and the more complete excitation in the left apex combine to produce a vector which points toward the right and forward. At 0.02 second the left side of the septum is probably not yet fully activated so that the wave of excitation may be represented as in Fig. 69, 0.020 second.* The vector constructed for this stage is the result of the addition of two vectors, one for the septal portion of the wave and the other for the portion of the wave of excitation in the apex of the left ventricle. The re-

sultant vector as shown in the figure probably points to the right of the anatomic axis. However, if the excitation spreads more rapidly on the endocardial surface of the lateral wall of the left ventricle or more slowly over the surface of the left side of the septum this vector may not differ by much from the normal vector for this stage.

At 0.03 to 0.035 second activation has proceeded to the stage depicted in Fig. 69, 0.030 second. The entire endocardial surface of the left ventricle has been activated. At the apex where the ventricle is thinnest (and probably along the interventricular groove) the epicardial surface has been reached. If we construct a vector to represent the septal portion of the wave and another to represent the portion of the wave in the lateral wall of the left ventricle and add these vectorially (parallelogram of forces) the resultant will be as depicted in the figure. The resultant vector points toward the lateral wall of the left ventricle because the wave in this portion is larger in all dimensions than that in the septum. This vector is frequently shorter than that depicted in the figure for the difference between the size of the wave of excitation in the lateral wall of the left ventricle and that in the septum is not very great unless the left ventricle is hypertrophied.

The wave of excitation in the septum remains rather large during the succeeding several hundredths of a second while that in the lateral wall of the left ventricle becomes progressively smaller. At 0.06 second, as shown in Fig. 69, 0.06 second, the wave of excitation in the septum is larger than that in the lateral wall of the left ventricle. Vectors constructed separately for these two waves make such an angle with one another that the

* For the normal (Chapter 2) this stage of activation of the left side of the septum was drawn as a confluent wave of excitation because this made it possible to eliminate a complication in drawing technic. It was felt that this was permissible since it made little difference in the ultimate result in the normal.

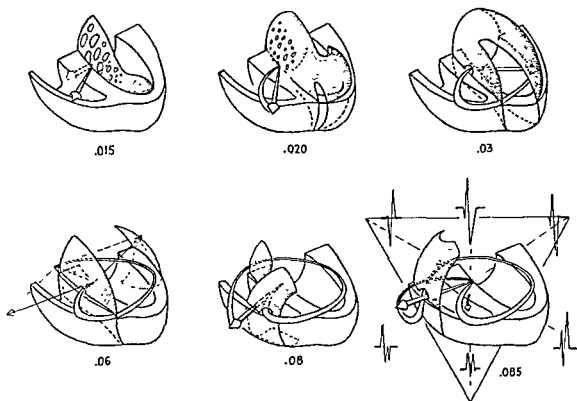


FIG. 69. Right bundle branch block.

Activation of the right ventricle is delayed by 0.06 second. The waves of excitation that normally occur in the right ventricle are, therefore, delayed in their appearance by that interval. Thus for the first 0.06 second the electrical effects are produced by the free wall of the left ventricle and by the interventricular septum. The latter structure being activated only from the left side and being rather thick throughout exerts a moderately large effect directed toward the right after the initial stages from 0.025 second to 0.06 second (until 0.025 second the net effect is not greatly different from the normal; see text for details). At 0.03–0.035 second the wave of excitation in the free wall of the left ventricle is greater than that in the septum but by 0.06 second it has become smaller and the resultant points to the right and frequently backward. After 0.06 second the effects result from the waves of excitation in the right ventricle which produces vectors directed forward and to the right.

The characteristics of the limb leads are a wide S in Lead I and often a wide R' in Lead III, though the latter may be absent. As the figure shows, these deflections are inscribed by the activation of the interventricular septum and the late activation of the right ventricle.

resultant points backward and to the right. However, at times the shape of the heart is such that the angle is 180° and the resultant therefore points to the right and forward. At other times the shape of the heart is such that the angle between the vector for the wave on the lateral wall of the left ventricle and that for the wave in the septum is such that the resultant points more forward than to the right (Fig. 70).

At 0.05 to 0.06 second the wave of excitation has penetrated most of the septum and

reaches the Purkinje network near the apex of the right ventricle. From this time on the electrical effects result from activation of the latter structure. At 0.08 second there is probably no residual activation in the septum, as shown in the figure, unless hypertrophy or slow conduction is present in the septum. Therefore, ordinarily one would expect the vector shown in Fig. 69, 0.08 second to be shorter than that shown in figure if there is no ventricular hypertrophy. At 0.085 second the wave that occurs normally at 0.025 second

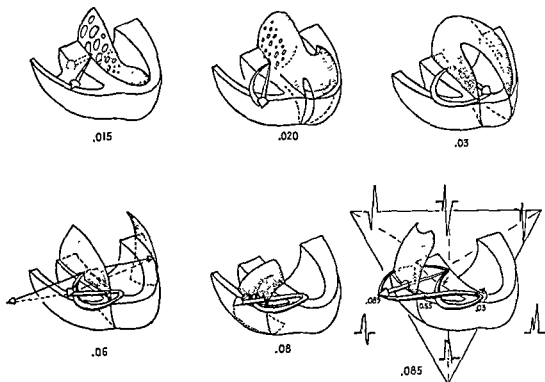


FIG. 70. An alternate form of the QRS loop in right bundle branch block. The difference between the loop developed here and that developed in Fig. 69 is produced by assuming a different shape for the left ventricle.

is present in the right ventricle and this produces a vector as shown in Fig. 69, 0.085 second. The length of this vector will also depend upon the thickness of the right ventricle.

After 0.085 second the vector rapidly diminishes and swings backward in direction. By 0.10 second there is little activation remaining except in the conus. This may proceed for another two hundredths of a second or more but its vector probably points so much forward as to register little on frontal plane leads. Thus the writer believes that complete right bundle branch block may occur though the total QRS duration in the standard limb leads is little more than 0.10 second (Fig. 71B).

The spatial QRS loop (as depicted in the figures) may have alternate forms resulting from the anatomic variations mentioned above. Other variations, resulting from right and left ventricular hypertrophy and infarction, will be discussed under those heads.

Variations in the limb leads (standard or unipolar) occur as a result of the variations of the positions and rotations of the heart described in dealing with the normal QRS loop. If the apex is back and the anatomic axis is rotated clockwise the loop of Fig. 69 attains the orientation shown in Fig. 72. Under these circumstances the limb leads will be like those of left bundle branch block. However, the precordial leads, as we shall see, will be quite dissimilar. In each such case in the writer's experience the heart has been enlarged. It is also important to note that comparison of tracings of the same patient before and after the development of right bundle branch block may show lack of correlation of rotation about the anatomic axis. This may result from difference of cardiac position or from the fact that when the left ventricle contracts before the right it changes the orientation of the right ventricle during depolarization.

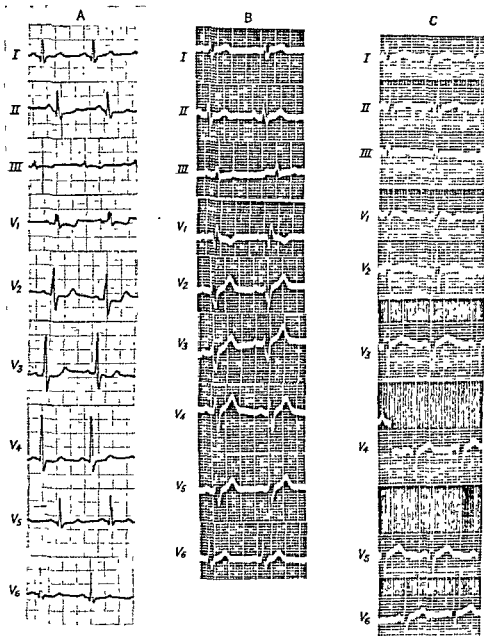


FIG. 71. *A*, Right bundle branch delay. Note correspondence of precordial leads to those of Fig. 77. *B*, Right bundle branch block. Note that QRS duration is not over 0.105 second. *C*, Right bundle branch delay.

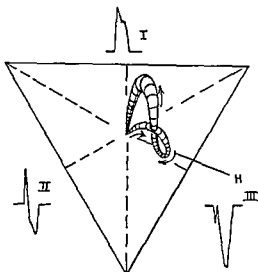


FIG. 72. The spatial loop of Fig 70 rotated clockwise about a transverse anatomic axis, *H*. Note similarity of limb leads to those of left bundle branch block. The precordial leads would make the distinction in such a case.

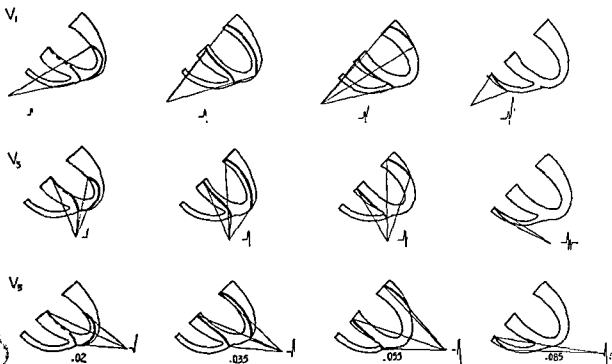


FIG. 73. Precordial leads in right bundle branch block.

The same solid angle method analysis is employed as was shown in Fig. 23 for the normal precordial leads. The waves of excitation shown in Fig. 69 at 0.02 second, 0.035 second, 0.055–0.06 second and 0.085 second are employed as a sequence of activation.

The top row of diagrams depicts the development of potentials in Lead V_1 , the middle row depicts the development of the potentials in Lead V_2 , and the bottom row depicts the development of the potentials in Lead V_3 .

It is noted that it is the late development of the waves of excitation in the right ventricle and the late left-to-right excitation of the interventricular septum that accounts for the wide R' in V_1 and the wide S in V_3 which are typical of right bundle branch block.

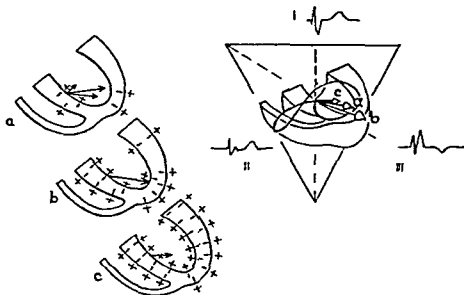


FIG. 74. The T wave in right bundle branch block. *a*, Early stage of repolarization. Of the three vectors forming a parallelogram the smallest represents the early septal effects, the next longest represents the early apical effects, and the diagonal is the resultant of the two.

b, Repolarization at the peak of the T wave. The right side of the septum repolarizes more rapidly than the left and its effects now equal or almost equal those of the left side which began early. Actually septal effects possibly are directed toward the left at this time. Most of the effects, however, are due to the apical effects as shown.

c, Final repolarization effects attributable to the base of the free wall of the left ventricle.

The QRS loop and T wave effects in the diagram indicate that the mean T vector in right bundle branch block is probably a bit to the left of the normal T wave vector. The gradient approach holds.

Precordial Leads

The precordial leads in right bundle branch block are developed in Fig. 73. At 0.005 second the deflections developed by a solid angle analysis are like those seen in the normal. At 0.015 second (not shown in the figure) deflections in V_1 , V_3 , and V_5 are developed that are appropriate to the sign and the approximate size of the solid angle subtended at the electrode. At this stage very incomplete activation of the left side of the septum makes it necessary to make the deflection much smaller than would be expected if this activation were confluent. As a result in the early stages the deflections do not differ much from the normal.

At 0.020 second the activation in the septum has spread but is not as completely con-

fluent as in the apex of the left ventricle. The solid angle subtended at the electrode in the V_1 -position by the wave in the apex of the left ventricle is negative, while that in the septum is positive. Even considering the fact that the septal activation is not yet confluent it probably overbalances the effect of the wave in the apex of the left ventricle so that the potential at V_1 is probably positive though not very great. However, a slight change in the position of the heart may alter these relationships and make the potential at V_1 negative at this stage. At the same time (0.02 second) the solid angles subtended at V_3 are both smaller but the positive angle to the septum is distinctly larger and a higher positive potential at V_3 may be expected. At V_5 at the same time the positive solid angle to the wave in the apex of the left ventricle

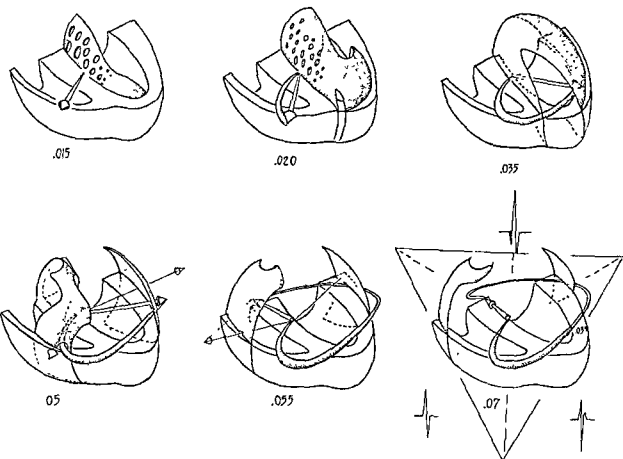


FIG 75. Right bundle branch delay (0.03 second). Delay of conduction in the right bundle branch by 0.03 second is assumed causing the waves of excitation that normally occur in the right ventricle to appear after a delay of that interval

The first two stages and even the third do not differ from those of complete right bundle branch block. However, at 0.05 second and 0.055 second the late effects from the right ventricle oppose the effects in the left ventricle which are normally unopposed. This tends to make the loop shorter than the normal loop. Again in the later stages (0.055–0.070 second) it is noted that simultaneous waves of excitation of nearly the same size occurring in the bases of the two ventricles tend to give a resultant that points backward. This causes the loop to be more rounded than the normal. It is to be noted that unless the late conus effects are reflected in a lead in an important manner there is less increase in the duration of the QRS than one might expect.

The effect on the limb leads is the appearance of an S in Lead I which is not so wide as in complete right bundle branch block and often but not always an R' appears in Lead III.

which is completely confluent is much larger than the solid angle to the more incomplete wave in the septum and the potential here is represented as correspondingly higher than at V_3 .

At 0.035 second the solid angles to both the septal and left ventricular waves are about equal at V_1 and the potential is zero at this

electrode. However, in those hearts in which the left ventricle is a bit larger or in which the rotation of the heart is such that the left ventricle exerts a greater effect on the electrode than does the septum the potential will be negative as represented by the dotted trace. At V_3 at the same time the positive solid angle to the septal wave is smaller than

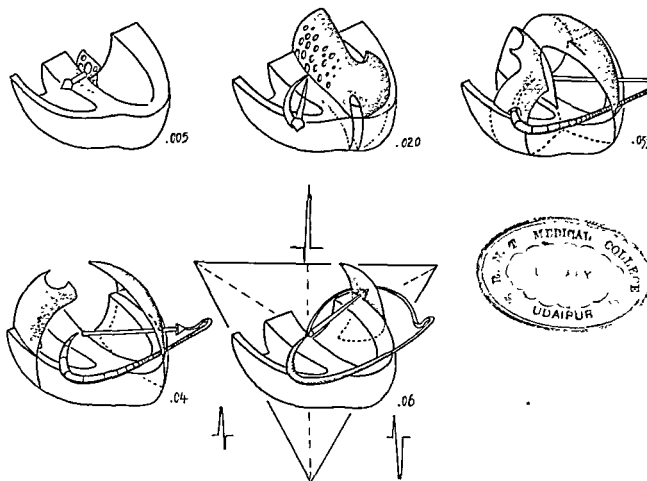


FIG. 76. Right bundle branch delay (0.02 second). The delay of 0.02 second in right ventricular activation produces a loop that is shorter and rounder than the normal and yet may produce just as great effects upon the limb leads as the normal sequence of activation because the vectors at 0.035 second are more nearly parallel to the frontal plane. There may be a notch in the R in Lead I. No S appears in Lead I and no R' is seen in Lead III.

the negative solid angle to the wave in the free wall of the left ventricle and the potential at this time is represented as falling to a negative value. However, if the position of the heart is changed even slightly the solid angles will change so that the potential at V_4 is more negative, zero, or even positive. The reader may consider that if the apex of the heart is pushed back the relation of the electrode V_3 approaches that represented in the figure for V_1 . At V_3 , at the same time, the solid angles to the wave in the septum and the wave in the left ventricle are again almost equal and the potential falls to zero. However, again

even slight enlargement of the left ventricle or slight changes in the position of the heart will cause the potential at this time to change even in sign at this electrode.

At 0.055 second the wave of excitation is much larger in the septum than in the free wall of the left ventricle so that the potential at V_1 is definitely positive. At the same time at V_3 the position of the electrode is such that the positive solid angle to the septal wave is only a little larger than the negative solid angle to the remaining wave in the free wall of the left ventricle. Therefore the potential at V_3 is only slightly positive. At the same

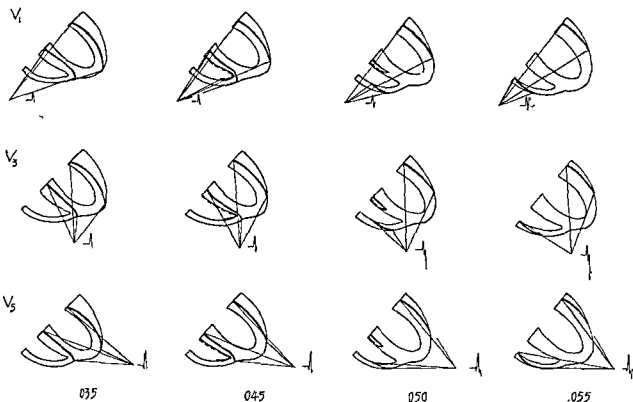


FIG 77. Precordial leads in right bundle branch delay (0.03 second).

The solid angle analysis is the same as for complete right bundle branch block for the first 0.035 second. A 0.045-second stage is interpolated which does not appear in Fig 75.

In the diagram for 0.045 second there are three waves of excitation. With respect to V_1 , the wave in the middle of the septum is positive and the other two are negative. The positive solid angle to the midseptal wave is greater than the negative solid angle to the wave in the free wall of the left ventricle. At first glance it might appear that the wave in the right septal surface would more than nullify the net positive effects of the other two waves. However, it is necessary to remember that this wave is extremely patchy at this time and that the balance of effects is probably close to zero.

V_1 shows a deep notching of the R wave and ends in an S wave due to late effects from the left ventricle after 0.06 second (not shown). This S can be deeper than drawn in many cases. The notch in V_2 is also notable. The S in V_3 is also characteristic.

time the potential at V_3 is quite negative for the position of the electrode is such that it faces the negative side of both waves.

The remainder of the figure (0.085 second) is self-explanatory.

T Wave

The T wave in right bundle branch block uncomplicated by disease differs but little from the normal T wave in the limb leads. Since the free wall of the left ventricle is the only structure activated at the normal

time and in the normal manner in right bundle branch block the small influence upon the T wave which results from right bundle branch block suggest that it is the free wall of the left ventricle that accounts largely for the normal T wave. The only structure of any volume that is activated in a different manner from the normal in right bundle branch block is the interventricular septum. If the rates of repolarization of the two surfaces were equal one would expect right bundle branch block to cause a marked in-

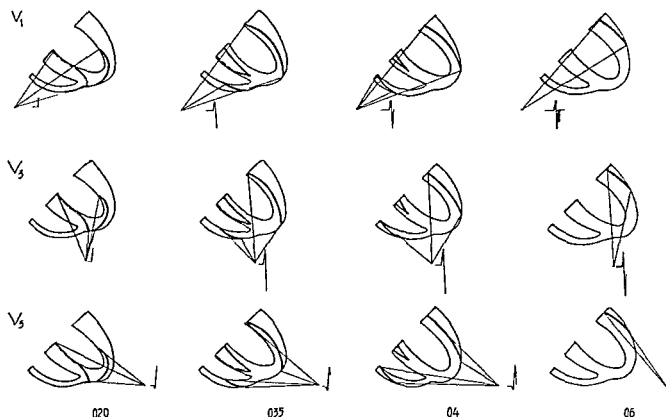


FIG. 78. Precordial leads in right bundle branch delay (0.02 second). The complex in V_1 begins little different from the normal. However, the late appearance of and rapid disappearance of the right ventricular effects causes a notch in the S of V_1 .

crease in the height of the T waves in Lead I. Since this does not occur it may be plausible to speculate that the rate of repolarization is more rapid in the right layers of the septum than the left for only thus can the sequence of septal activation which occurs in right bundle branch block fail to produce a pronounced change in the T wave over the normal. Following this speculation the T wave in right bundle branch block is constructed as in Fig. 74. Here repolarization in the septum is represented as producing a smaller vector pointing to the right than occurs during the normal sequence of repolarization.* This combines with the usual effects from the free wall of the left ventricle to produce T wave vectors which point a little

* Actually, in the earliest stages the electrical effects of septal repolarization may produce a small vector pointing to the *left*, because the left side of the septum is depolarized so much earlier than the right side.

further to the left than do the normal T wave vectors.

Entirely aside from the theoretical speculation described above it is a matter of actual observation that when right bundle branch block supervenes without other change in the heart (as when it appears and disappears in the same tracing) the T wave follows the principle of the gradient in all leads including the precordial; the gradient does not change in magnitude or direction in a significant manner.

Incomplete Right Bundle Branch Block

Figures 75 and 76 represent application of the same postulates employed throughout this presentation to the problem of lesser delays in the right bundle branch. Figures 77 and 78 represent the corresponding precordial leads which occur under these conditions.

It is important to point out that with the

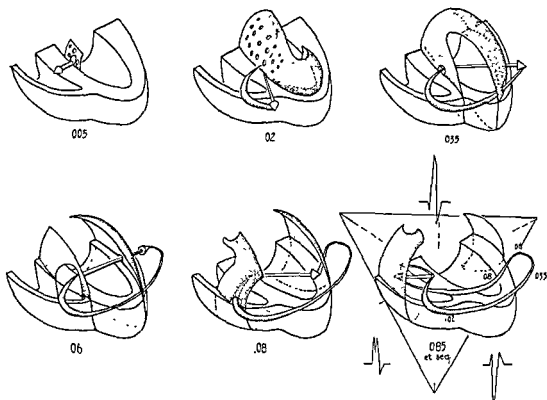


FIG. 79. Right bundle branch block and left ventricular hypertrophy. The prolongation of left ventricular effects as a result of hypertrophy tends to oppose some of the effects of the delay of right ventricular excitation. However, the magnitude of the S in I and the R' in V_1 are usually more reduced than their duration. In addition the height of R in I is greater than in right bundle branch block without left ventricular hypertrophy. Less often the S in III is deeper.

shortest delay (0.015 second) represented (Figs. 76 and 78) there occurs a notching of the upstroke of the S in V_1 and at times a corresponding notching of the down-stroke or peak of R_1 instead of an S in Lead I. In Lead III a notch may appear in the upstroke of S (Fig. 76).

In the next greater degree (0.03 second) of right branch block depicted (Figs. 75 and 77) the complexes assume the appearance shown in the figures.

In all cases the time of appearance of the effect of activation of the right ventricle determines whether there is a notch in the upstroke of S in V_1 or an R' . The same applies to the appearance of a notch in R_1 and the appearance of an S in Lead I.

The T wave in incomplete right bundle branch block follows the gradient principle.

Right Bundle Branch Block and Left Ventricular Hypertrophy

When left ventricular hypertrophy coexists with right bundle branch block depolarization of the ventricles is hypothetically as depicted in Figs. 79 and 80. The notable features are the probable longer persistence of depolarization effects in the lateral wall of the left ventricle which more than counterbalance effects occurring in the septum. At a corresponding time (0.05–0.06 second) in the normal heart the septal effects predominate and at a later time (0.07–0.08 second) the left ventricular effects which are still prominent in the hypertrophied heart have disappeared in the normal heart. It may be argued that in left ventricular hypertrophy the septum is much thickened and this is so. However, it is

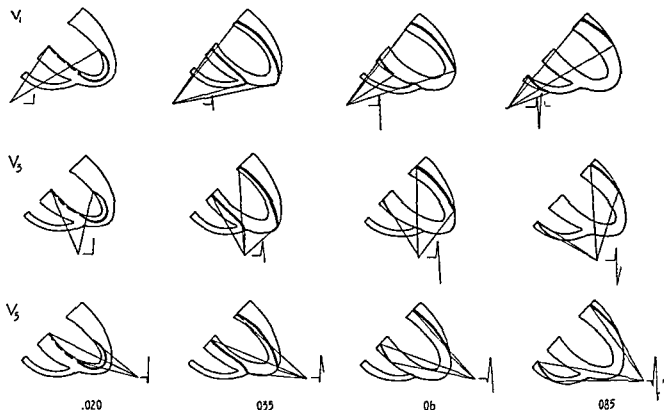


FIG. 80. The precordial leads in right bundle branch block and left ventricular hypertrophy. Compare with Fig. 73. Note depth of S and height of R' in V_1 and the height of R in V_4 .

not as large as the free wall of the left ventricle and even if a wave of excitation were still present in the upper septum in Fig. 80 at 0.08 seconds the large left wave still present in the free wall of the left ventricle would still 'more than counterbalance it and the

small wave in the right ventricle (insofar as the limb leads are concerned). V_1 and V_2 , however, would be more affected as R' would be made larger and wider than as depicted in Fig. 77. Such tracings do occur.

Suggested Reading

- Sodeman, W. A., Johnston, F. D., and Wilson, F. N. The Q_1 deflection of the electrocardiogram in bundle branch block and axis deviation. *Am. Heart J.*, 28:271, 1944.
- Sodi Pallares, D. *Nuevas Bases del Electrocardiografía*. Mexico, D. F., 1945. Also, *El Electrocardiograma Intracavitario Humano*, 1948.
- Sodi Pallares, D., Thomsen P., and Soberón, J. New contributions to the study of the intracavity potential in cases of right bundle branch block in the human heart. *Am. Heart J.*, 36:1, 1948.
- Sodi Pallares, D., Vizcaino, M., Soberón, J., and Cabrera, E. Comparative study of the intracavity potential in man and in dog. *Am. Heart J.*, 33:819, 1947.
- Wilson, F. N. The order of ventricular excitation in human bundle branch block. *Am. Heart J.*, 7:305, 1932.
- Wilson, F. N., Johnston, F. D., and Barker, P. S. Electrocardiograms of an unusual type in right bundle branch block. *Am. Heart J.*, 9:472, 1934.

10. Left Bundle Branch Block

Figure 81 depicts the application to left bundle branch block of the method employed in the analysis of right bundle branch block. The earliest activation is at the apex of the right ventricle and the apex of the right side of the septum producing a small vector pointing in the same direction as that shown in the figure for 0.015 second but shorter. At 0.015 second (Fig. 81) the wave of excitation is such as to produce a vector that points toward the apex of the left ventricle as represented. At 0.020 second the wave in the right ventricle is not quite as effective as the larger though less complete wave in the septum and the vector again points a bit to the left and forward. Again the resultant of the two elements of the wave is determined by vectorial addition. At 0.025 second the wave in the right ventricle almost directly opposes that in the septum but is much smaller and the net effect is directly toward the left in direction and about as depicted in magnitude. When activation of the right ventricle is complete a wave of excitation remains in the septum as depicted at 0.05 second and its vector is represented as perpendicular to the surface of the septum and larger than at 0.025 second because it is no longer opposed by a wave in the right ventricle. This wave remains of almost constant size for several hundredths of a second. At about 0.06 second it breaks through into the endocardial surface of the left ventricle and the vector shortens abruptly. Activation of the left ventricle then begins. At 0.08 second the activation of the apex of the left ventricle produces a vector as shown and at 0.10 second the wave of excitation normal at 0.04 second is seen. The final stage occurs as in the normal and the loop represented in the figure is completed as for the normal.

The apex of the left ventricle in complete left bundle branch block is activated both from the endocardial surface and from the right side (its junction with the septum). It thus becomes activated more rapidly than in the normal once the impulse reaches the Purkinje fibers of the left side. Therefore, no left ventricular wave comparable to the left-sided wave for 0.025 second of the normal occurs.

The deflections on the limb leads as developed in the figure are characteristic of left bundle branch block. If we move the apex a bit forward the first portion of the loop crosses the zero point of Lead III and an R_{III} appears. Left axis deviation is not always present in left bundle branch block. If we rotate the heart of Fig. 81 in a clockwise manner as we did with the normal loop the left axis deviation can be made to disappear, and a wide and usually heavily slurred R will appear in all three leads. Actually such a tracing as shown in Fig. 81 may occur in right bundle branch block. As Wilson pointed out the precordial leads must make the distinction between the two.

Figure 82 shows the potentials that develop at V_1 , V_2 , and V_3 in left bundle branch block. The first activation (not shown) occurring at the junction of the right ventricular wall to the right side of the apical end of the septum, produced negativity at V_1 . At 0.02 second the potential at V_1 is even more negative because of the broader area of activation of the right side of the septum. The positive solid angle to the wave in the right ventricular wall is not sufficient to overcome this. At the same time V_3 , which may have been slightly positive under the influence of the earliest stage of activation described above, is even

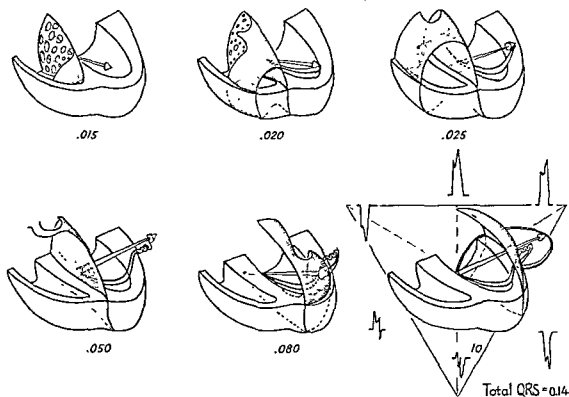


FIG. 81. Left bundle branch block.

The waves of excitation that normally occur in the left ventricle are delayed by 0.06 second, the time assumed to be necessary for penetration of the septum.

In the early stages (0.015-0.025 second) the vector results from the combination of effects from the septum and the free wall of the right ventricle. From 0.03 to 0.06 second there is a moderately large wave of excitation of constant dimensions in the interventricular septum. When this reaches the left ventricle (probably first in the apical region if the septum is not badly diseased) excitation of the left ventricle begins and the waves of excitation that normally occur will appear, though they are 0.06 second late.

Frequently the septal vector shown in the diagram for 0.05 second is as large as any that occur and the curly portion of the loop (which simply indicates that the tip of the vector spends considerable period of time in the same location) is at the tip of the loop. The temporary shortening of the vector at the time that the break through into the left ventricle is reached is common though not always present. The forward swing shortly afterward is also not constant.

The two prominent features are: (1) The loop begins toward the left so that there is usually no Q in I. (2) There is a period in which the direction and magnitude of the vector changes but little (0.03-0.06 second) so that R in Lead I commonly shows a wide slur or plateau at its apex and S in Lead III may show the same. (3) The QRS is prolonged.

more negative. V_3 , on the other hand, is positive at this time because it faces the positive side of the wave in the septum and because its solid angle to this wave is larger than the negative solid angle to the wave in the right ventricle. The remaining diagrams of the precordial leads in left bundle branch block are self-explanatory.

In left bundle branch block the slightest

movement of the electrode over the left chest (V_5 or V_6) is apt to cause a great change in the appearance of the complexes. This makes these leads almost useless for interpretation of serial changes.

A comparison of Fig. 82 with the corresponding Fig. 73 for right bundle branch block makes it clear that there is seldom any difficulty in distinguishing the ventricle that

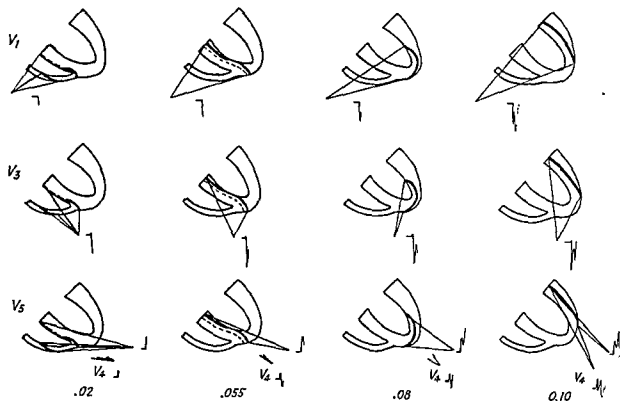


FIG. 82. The precordial leads in left bundle branch block. The solid angle method of derivation is employed. The notable features are the very small R or absence of R, and the wide often notched S in V_1 and the wide, usually notched R in V_6 .

Approximately the first half of the S in V_1 is inscribed largely by the interventricular septum, the latter half by the free wall of the left ventricle. The same statement applies to the R in V_6 .

In the apex-back heart, especially if it is enlarged, there is a narrower R and a large wide S in V_6 and V_4 . Both types of complexes can frequently be recorded at the same sitting from the same patient by moving the electrode or having the patient take a deep breath.

is activated first. The distinguishing characteristics are seen in leads made over the right ventricle. The absence of R in V_1 in left bundle branch block and the usual presence of a broad R' in right bundle branch block makes distinction between the two rather sharp regardless of the appearance of the limb leads.

Right bundle branch block on occasions has the appearance of left bundle branch block in the limb leads. Figure 72 represents such a case.

Some variations which occur in left bundle branch block probably result from variations in the manner in which the impulse traverses the interventricular septum. If the impulse

reaches the left ventricle near the apex the activation of that structure will be somewhat different than if the impulse first reaches a basal area.

Incomplete Left Bundle Branch Block

Figure 83 depicts the activation of the ventricles with 0.020-second delay in the left bundle branch. In each diagram the wave of excitation in the left ventricle is that which normally occurs 0.02 second sooner. The diagram of the events, at 0.025 second in Fig. 83 should show beginning activation in the left ventricle such as is shown for the normal at 0.005 second. This is omitted from the diagram because it would be diffi-

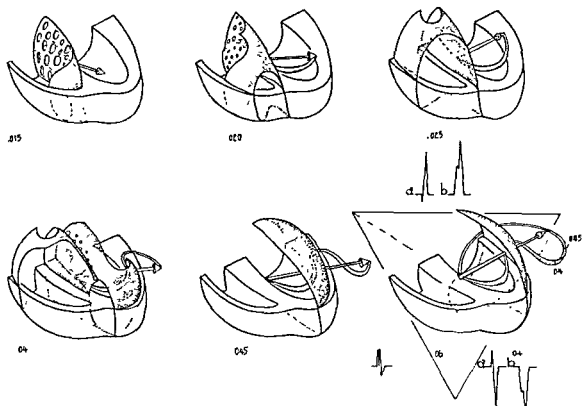


FIG. 83. Incomplete left bundle branch block. A 0.02 second delay of activation of the left ventricle is shown.

The loop begins exactly as does the loop of complete left bundle branch block, but at 0.04 second the activation of the left ventricle and of the left side of the septum has proceeded to the stage normally reached in 0.02 second. The wave in the septum that originated on the right side is much more complete than that which originated later on the left side. Therefore the net septal effect at this stage is directed toward the left. The apical wave produces a vector which points forward and toward the left. The net result of all effects, therefore is a vector which points forward and toward the left (probably a bit more forward than shown in the figure).

At 0.045 second the vector obviously must point toward the left and more forward than any large vector in either the normal or the complete bundle branch block loop. As a result R in I (at times S in III) is apt to be larger than in the normal or in complete left bundle branch block. The absence of Q in Lead I and at times of R in Lead III may occur as in complete left bundle branch block. The QRS duration is increased. The total here is 0.10 second.

cult to incorporate in the drawing. Its effect is simply to shorten the vector at this stage. At 0.04 second activation has begun in the left ventricle and reaches the stage occurring normally at 0.02 second (see Fig. 15, p. 18). The greatest electrical effect derives from the wave of excitation in the apex of the left ventricle. Additional effect results from the balance between the septal waves. Since the wave of excitation in the septum moving to the left as a result of right ventricular activa-

tion is more complete than that associated with the later left ventricular activation the net effect of septal activation at this stage is a small vector pointing to the left. Application of the parallelogram of forces to the vectors representing the apical and net septal effects produces the resultant vector shown in the drawing.

At 0.045 second the wave of excitation in the left ventricle is that which occurs in the normal at 0.025 second except that the septum

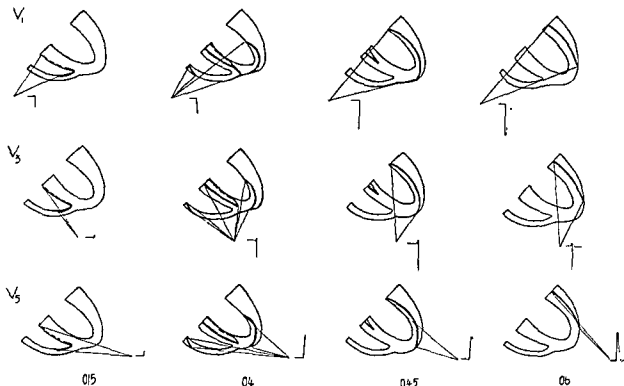


FIG. 84. Precordial leads in incomplete left bundle branch block. The same disappearance or small magnitude of R in V_1 and Q in V_2 and V_6 (not shown) is seen as in complete left bundle branch block.

is now completely depolarized. The resultant vector is large and is nearly parallel to the frontal plane as was the preceding vector. Since this is a larger wave of excitation than any which occurs normally, and its direction is nearly parallel to the frontal plane it produces a larger deflection in Lead I and in the left precordial leads than is seen without the delayed conduction.

At 0.06 second and later the situation is similar to that which occurs normally.

With the heart in the position and rotation shown the notable features in the limb leads resulting from 0.02 seconds delay in conduction in the left bundle are widening of the QRS complex and disappearance of the Q in Lead I. There may be loss of the R in Lead III. If the heart were a bit more vertical or the apex a bit more forward the first portion (or first vectors) of the loop would inscribe an R_{III} . The upstroke of R_I is apt to be slurred or notched. At times there is

notching or slurring of the peak of R_I . Frequently R_I is higher than before the inception of the conduction defect, while S_{III} is not affected in magnitude. If complete bundle branch block supervenes the magnitude of R_I becomes smaller again. A comparison of Figs. 81 and 83 shows that this finding should not be surprising. The 0.045-second vector of Fig. 83 is larger than any vector that occurs normally or in complete left bundle branch block.

In the precordial leads the same loss of R in V_1 and possibly of the R in V_2 and V_3 occurs that was noted in complete left bundle branch block. As indicated above, other conditions being equal, R in V_4 , V_6 , and V_6 is apt to be larger than in the normal or complete left bundle branch block (Fig. 84).

Most left bundle branch block occurs in hearts with left ventricular hypertrophy. Since the duration of the QRS complex may reach 0.12 second in the absence of left bundle

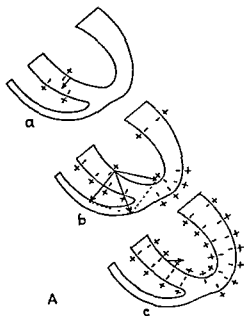
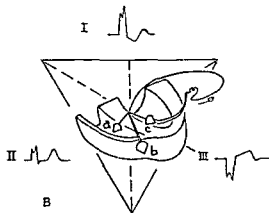


FIG. 85. The T wave in left bundle branch block. *a*, *b* and *c* of *A* show three stages of the repolarization of the septum and left ventricle. The right ventricle is assumed to have no detectable effect.

The earlier repolarization of the right side of the septum follows from the assumption that this is the first area to be depolarized. Since the right side of the septum is assumed to be repolarized more rapidly than the left it is assumed to produce a rather large electrical effect directed toward the right soon after repolarization has begun (*b*). At the same time the usual large apical effects occur and the resultant is as shown by the diagonal of the parallelogram. The final effects (*c*) are due to repolarization of the base and the free wall of the left ventricle.

The three vectors developed in diagrams *a*, *b*, and *c* of *A* are shown as spatial vectors *a*, *b*, and *c* in *B*. A T wave loop may be drawn about them. The corresponding complexes are derived from QRS loop and the T wave vectors drawn.



branch block some difficulty is encountered in distinguishing the effects of hypertrophy and of bundle branch block. Following the hypothetical principles employed here the distinguishing features of hypertrophy are the presence of a distinct Q in Lead I when the tracing is of the usual form shown in the basic drawing (Fig. 65), and the presence of a distinct R wave in V_1 and V_2 (Fig. 66).

Unfortunately in massive transmural septal infarction a Q wave in Lead I may occur in the presence of left bundle branch block. Furthermore, septal infarction which involves mostly the left side of the septum may cause a loss of the Q in Lead I as well as the R in V_1 , V_2 , and V_3 in the absence of left bundle branch block. The QRS may be widened by left ventricular hypertrophy and thus left bundle branch block will be simulated. Therefore it is frequently impossible to distinguish left bundle branch delay, left ventricular hypertrophy, and septal infarction.

The T Wave in Left Bundle Branch Block

If we accept for the moment the assumption that the right ventricle contributes little to the T wave under ordinary conditions it must also be assumed that it also may be neglected in considering the T wave in left bundle branch block. The interventricular septum, which was assumed to contribute to the T wave to a less extent than the free wall of the left ventricle, in the normal, must play a different role in left bundle branch block. When the sequence of activation is from right to left instead of from both sides simultaneously it is reasonable to suppose that the right side of the septum will begin repolarizing before the left. As a matter of fact repolarization has already begun here and to a measurable extent before the QRS complex is completed. As a result, there are RS-T segment deviations in left bundle branch block. It will be recalled, also, that it was assumed that the right side of the septum repolarized a bit more rapidly than the left. As a result the septal effects must be represented by a fairly large vector pointing to the

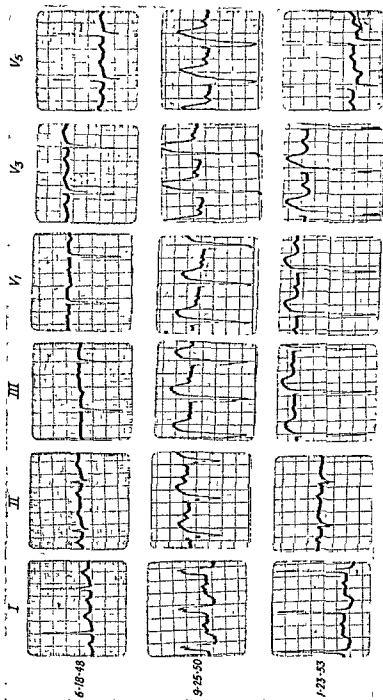


FIG. 86. Three tracings from the same patient. 6-18-48, Left ventricular hypertrophy. 9-25-50, Left bundle branch block, 1-23-53, Left bundle branch delay.

Note that the R in I is larger with the left bundle branch delay than with complete left bundle branch block, or in the original tracing. The RS-T segment shifts and T wave changes in both of the later records are partly secondary to the QRS changes and partly are due to digitalis. Anteroseptal infarction cannot be ruled out.

right. Repolarization of the free wall of the left ventricle begins in the usual order but at a later time than repolarization of the septum because it is depolarized at a later time. However, a superimposition of effects quickly occurs. Thus, repolarization in left bundle branch block is represented as in Fig. 85A. The vector *a* represents the early septal effects, *b* represents the combined later septal effects and free wall effects, and *c* represents the final free wall effects.

Seen in three dimensions the T loop is constructed as in Fig. 85B. Vector *a* actually occurs before the QRS is completed so that an RS-T shift occurs. The QRS loop continues into the T loop without returning to the zero point.

Variations in QRS and T in left bundle branch block tracings are due to variation in position and rotation and to the presence of disease. So commonly is left bundle branch block associated with left ventricular hypertrophy, ischemia, and infarction that it is difficult to find a case free of one of these. Rarely left bundle branch block occurs in a heart with no other evidence of disease. Right bundle branch block occurs much more frequently under these conditions.

Of course, insofar as the QRS-T relationship for the whole heart are concerned the gradient principle holds. If a patient develops left bundle branch block without other changes the gradient remains the same as it was before.

The net T wave reduction shown in Lead I in Fig. 86 (9-25-50) may be regarded as secondary to the increase in area of the QRS due to left bundle branch block. T must become smaller if $AQRS+AT$ (the gradient) is to remain constant. This relationship tends to hold true in all leads including the precordial.

If left bundle branch block is incomplete the septal effects shown in Fig. 85A are present but are less, corresponding to the degree of block, and the T will be less markedly affected. Again in any lead the magnitude of the change in the T wave (in terms of area) will be proportionate to the magnitude of the increase in QRS area.

As shown in Fig. 86, the degree of bundle branch block frequently varies in the same individual from time to time and at times in the same tracing. In either case a relationship between the block and heart rate is frequently seen. Often it is apparent that conduction in the affected bundle branch depends upon the time permitted for recovery. When the rate is rapid less time is permitted for recovery and block occurs. When the rate is slow the bundle branch has ample time for recovery and it may conduct normally. This accounts for the QRS aberrations that are so common in auricular tachycardia, auricular fibrillation with rapid ventricular rate, and other tachycardias.

11. Coronary Disease

It is in the diagnosis of coronary disease that the electrocardiogram, properly used, has its greatest usefulness. It is equally true that it is in its application to this problem that, improperly used, it has done the greatest harm. It is safe to say that most of the errors result from the employment of empirical criteria and that most of these errors might be eliminated by the employment of a physiologic approach to the electrocardiogram, at least to the extent to which this is possible. Only then is it possible to know the full capacity as well as the limitations of the method. It is for this reason that the writer has developed the formation of the QRS complex, the T wave, and the QRS-T relationship on the physiologic basis presented in the early chapters. On no other basis is it possible to acquaint the reader with the wide range of normal findings in different individuals and in the same individual under different circumstances. It is frequently impossible to distinguish the normal from the abnormal with the methods presently at our disposal but it is far better to know this than to believe that we know that which we do not know.

For purposes of discussion coronary disease will be divided here into two main categories: coronary insufficiency and myocardial infarction.

Coronary Insufficiency

Under this heading are included all cases of paroxysmal coronary insufficiency presumably due to vascular spasm or claudication (angina pectoris) and all other cases of ischemic heart disease whether acute or chronic excepting myocardial infarction. The term angina pectoris or anginal attack will

refer to a paroxysmal attack of coronary insufficiency regardless of whether it occurs in a patient who has had recurrent attacks for years or in the first attack. Attempts to divide these cases in any other manner leads to confusion. Pain usually accompanies the paroxysmal attack, but may not. Chronic coronary insufficiency with resulting chronic myocardial ischemia occurs frequently, and often paroxysmal attacks also occur in the same patient.

The patient with angina pectoris most frequently shows a normal electrocardiogram between attacks. The electrocardiogram made during the attack will usually (but not always) show definite changes. These changes are due to the effects of "injury", Figs. 48, p. 70 and 52, p. 74). Curiously enough, in most cases of angina pectoris the precordial leads show depression of the RS-T segments as if the injury were largely endocardial. Usually within a few minutes after the attack has subsided the injury effects disappear without leaving ischemic effects in the electrocardiogram. This circumstance makes the diagnosis extremely difficult. In some cases the electrocardiogram shows no RS-T shift during the attack but only ischemic T wave changes.

In other cases, or at other times in the same case, especially if an attack has lasted a long time or if attacks have occurred frequently, ischemic changes may be left which are evidenced in electrocardiograms made between attacks. However, the mere presence, between attacks, of an abnormal electrocardiogram in a patient who is having paroxysmal pain does not necessarily prove that the pain is of cardiac origin. Many persons have abnormal electrocardiograms due to left ventricular hypertrophy, myocardial fibrosis, or old

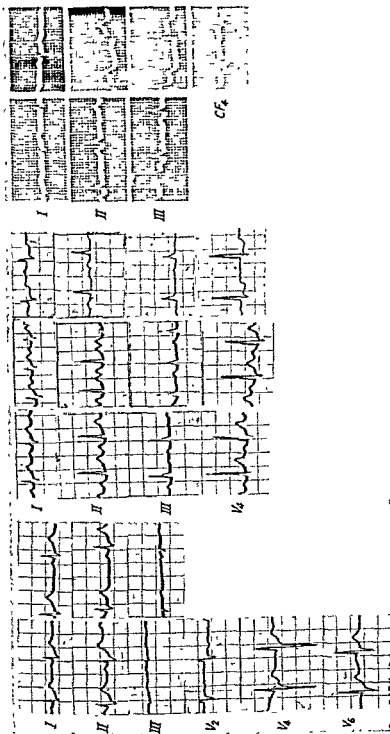


FIG. 87. *Left*, The first tracing was made on a 27-year-old man during pain in the chest accompanying an anxiety attack. The RS-T shifts indicate that coronary spasm was present. The second is an interval tracing.

Center, The first tracing is an interval tracing made on a woman aged 42 with a history of pain in the chest and both arms. The second tracing was made during a severe attack. Except for increased rate no change is seen. The third tracing was made during an attack which differed in no discernible way from the attack during which the second tracing was made. The RS-T shifts are due to injury.

Right, An interval tracing and a tracing made during an attack of chest pain in a third patient. The elevation of the RS-T segment in Leads II and III and the RS-T depression in CF_4 are diagnostic.

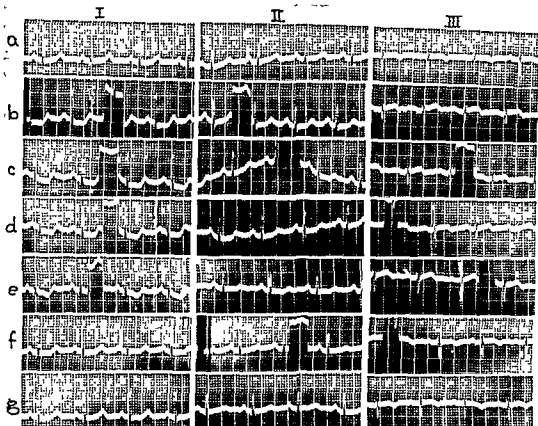


FIG. 88. Serial tracings before, during, and after an attack of angina. The patient gave a history of pain only upon lying down after a meal.

a was made immediately upon lying down after lunch *b* was made within one minute (pain had just begun) after *a*. *c* was made after another minute when pain was severe. Nitroglycerine was given at this time. *d* was made three minutes later. *e* was made five minutes later; pain was gone. *f* and *g* were made at five-minute intervals.

myocardial infarction and have pains due to some other cause. An evolution of changes in serial tracings can be helpful in diagnosis only when analyzed properly.

ELECTROCARDIOGRAPHIC DIAGNOSIS OF CORONARY INSUFFICIENCY WHEN REPEATED INTERVAL TRACINGS ARE NORMAL. If the electrocardiogram of the patient suspected of having angina is normal between attacks and the attacks are occurring frequently it is wise to await the next spontaneous attack in order to obtain tracings during a seizure, (Fig. 87). If the attacks are of short duration this may require hospitalization as it may not be possible otherwise for the apparatus to be used before the pain has subsided. When the attacks are infrequent and of short duration attempts

are made to induce attacks for the purpose of obtaining diagnostic evidence. The first method employed, if feasible, is reproduction in the office of the circumstances under which the spontaneous attacks occur. The tracings of Fig. 88 were made after inducing an attack by having the patient lie down immediately following a meal, for such was the history of her spontaneous attacks. This is a classical *anginal tracing showing fleeting RS-T shifts*. It is interesting to note that the electrocardiographic changes persisted for a few minutes after the pain had disappeared, indicating that it may not be futile to make a tracing even if one arrives shortly after the attack has subsided.

When the pains are too infrequent to make

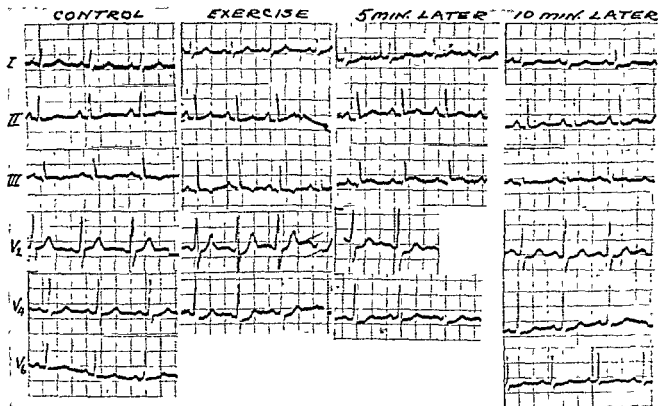


FIG. 89. Serial exercise tracings in angina; delayed effects. The exercise tracing shows only an RS-T depression in V_6 which is not conclusive. Five minutes later elevation of RS-T in Leads II and III occurs which is diagnostic since they are in the same direction as the QRS complexes in those leads. The depression of RS-T in V_6 is also important. Ten minutes later the change has not entirely disappeared.

Only a slight pain occurred 5 minutes after the exercise. Seven years later this patient had a large anterolateral myocardial infarction.

it practical to wait for a spontaneous attack or if an attack cannot be induced by reproducing the precipitating circumstances described in the history the exercise test is employed. Tracings are made before and after 15–20 deep knee bends done as rapidly as possible. The patient is warned to stop if pain occurs at any time during the exercise. Observations are made immediately after the exercise and at 5-minute intervals for 10 minutes or more. Such exercise has frequently served to induce attacks which are proven electrocardiographically to be due to coronary disease (Fig. 89). At times the changes occur in the later tracings and are absent or not very pronounced in the immediate and 5-minute tracing. The exercise test has even more frequently failed to induce attacks or significant electrocardiographic changes in

persons who are soon proven to have coronary disease by observations made during a subsequent attack. Furthermore, very frequently changes occur in the electrocardiogram following exercise that are mistaken for changes due to coronary disease.

Normal Versus Pathologic RS-T Shifts. It is necessary at this point to call attention to the fact that with sufficient diminution of the gradient an RS-T shift frequently develops (Fig. 31a, p. 46). Such RS-T shifts are very common with diminution of the gradient due to rapid heart rate or exercise. They tend, in any lead, to be opposite in direction and proportionate in magnitude to the main deflection of the QRS complex in that lead. It seems, however, that occasionally, especially in chest leads very close to the right side of the heart, nonpathologic shifts may at times

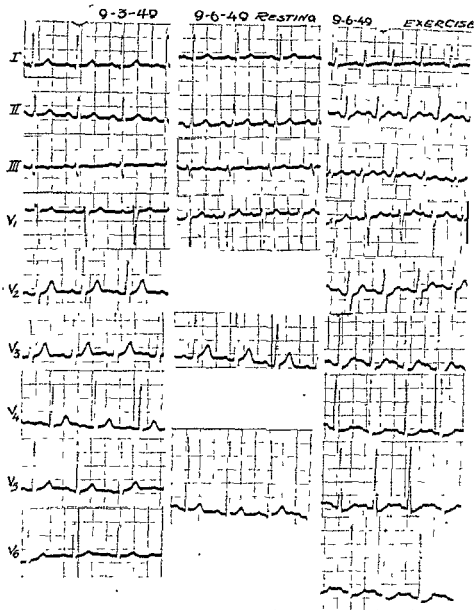


FIG. 90 A. Electrocardiograms after exercise. The subject was a healthy male 29 years of age. On 9-3-49 a resting tracing was made. On 9-6-49 an exercise test was made. The exercise tracing on that date shows a marked lowering of T_{II} and increase in T_{III} and definite downward RS-T shifts in V_1 , V_2 , V_3 , and V_4 . The change in the T waves in the limb leads are due to marked diminution of the magnitude of the gradient and change to a more vertical position of the heart (R_{III} larger and S_{III} smaller). The RS-T shifts occur in those leads with the largest QRS complexes and are opposite in direction to the main deflection of the QRS complexes of those leads. They are of no pathologic significance.

The difference between the resting tracings of 9-3-49 and that of 9-6-49 is accounted for by the fact that the former was made 4 hours after the last meal and that 9-6-49 was made forty-five minutes after a meal. Note that due to diminution of the gradient and a more vertical position of the heart the T axis has changed so that T_{III} , previously inverted, has become upright in the resting tracing of 9-6-49 (see Fig. 40).

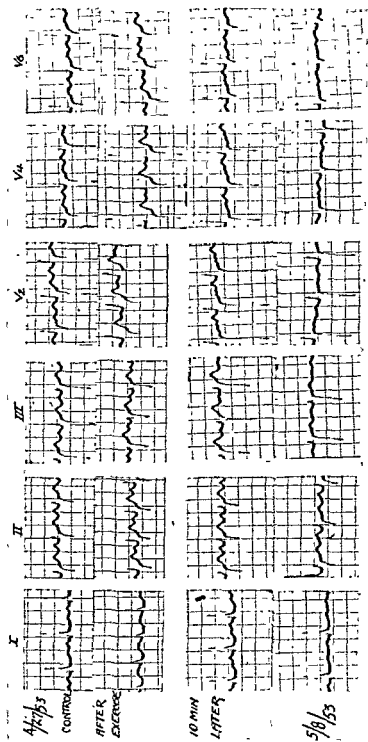


FIG. 90 B. An abnormal exercise record. In contrast to the exercise tracing of A note that in the precordial leads, the RS-T shifts are not opposite in direction to the main deflection of the QRS complexes.

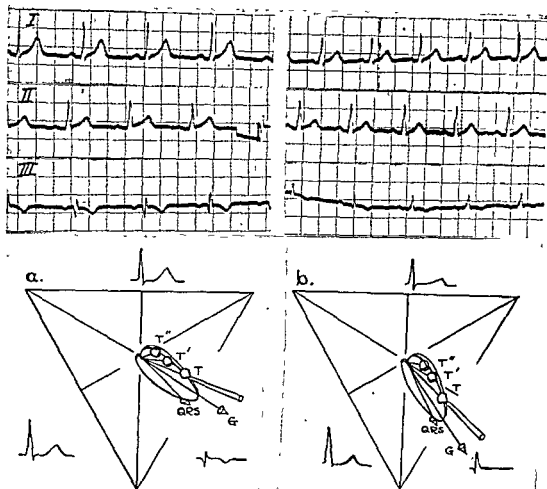


FIG. 91. Here the exercise tracing (*right*) shows changes due to a reduction of the gradient and a more vertical position of the heart due to dyspnea. Diagram *a* with *T* as the T vector represents tracing immediately above Diagram *b* with *T'* as the T vector represents the tracing on the right. Note full correspondence of QRS complexes and T waves.

Had the tracing on the right been made first (as well may have occurred) tracing on the left, made subsequently, might be interpreted as showing evidence of posterior infarction.

be seen which are in the same direction as the main deflection of the QRS complex. This is especially noted after digitalis but may occur with increased rate.

RS-T Shifts Following Exercise. Figure 90A shows RS-T shifts following exercise. It is noted that the shifts are opposite in direction and proportionate in magnitude to the main deflection (in terms of area) of the QRS complex and they are, therefore, not unexpected when the gradient magnitude is diminished by exercise. Figure 90B is an exercise electrocardiogram showing RS-T

shifts due to disease. There is no essential difference in the appearance of the shifts themselves, but in the precordial leads of 90B the shifts are not opposite in direction nor proportionate in magnitude to the main deflection of the QRS complexes. Generally, but not always, the nonpathologic shift is related to the rapid rate following exercise. Again the time of appearance of the shift may be of importance. Nonpathologic shifts are usually most marked in the tracing made immediately after exercise because the rate is most rapid at this time. However, the exer-

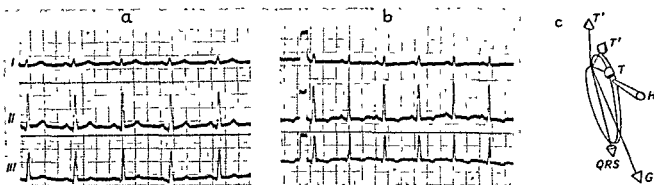


FIG. 92. Exercise effects in a young normal subject. *a*, resting; *b*, after exercise. Note inversion of T waves in all three standard limb leads. As shown in the diagram (*c*), this results from diminution of the gradient when the loop is orientated as shown. T' is the T vector which resulted from marked diminution of the gradient as a result of exercise in this subject.

cise shift is not entirely dependent upon rapid rate. The pathologic shift accompanies the pain (if any) and while it may be most marked in the tracing made immediately after exercise it may make its first appearance or become greater, if already present, in the tracing made 5 or 10 minutes after the exercise is completed (see Fig. 89).

When RS-T shifts occur as a result of rapid rate, after exercise, after food, and (most marked) when exercise effects are superimposed on the effects of food, the relationship of the magnitude of the RS-T shift to the QRS complex is of the greatest importance. This phenomenon makes empirical attempts at limitation of the magnitude of nonpathologic RS-T shifts without regard to the relationship of such shifts to the magnitude or direction of the QRS complex quite erroneous and dangerous. A very small shift in the same direction as a large QRS complex may be very significant, and a small shift in the opposite direction of a very small QRS complex may be equally significant.

Because T wave changes will be noted in the electrocardiograms made after exercise it may be well here to review *the effects of exercise (20 deep knee bends) on the T wave of the electrocardiogram in the normal* and to show several examples. Following such exercise the heart generally beats at an increased rate and undergoes some change in position and rotation as a result of the higher respiratory

midposition characteristic of dyspnea. This subject has been pursued in some detail in Chapter 5. The diminution of the gradient which characteristically seems to follow exercise (and which does not entirely depend upon rapid rate) together with the change in cardiac position and rotation (as revealed by comparison of the QRS complexes before and after exercise) produce changes in the T wave which may be misinterpreted as evidence of disease. One need not necessarily measure the gradient to determine that T wave changes have resulted from diminution of the gradient. Figure 40 (p. 57), representing the effect of diminution of the gradient upon the T wave vector and upon the T waves of the limb leads when the heart is in various positions and rotations, illustrates the use of the model of the spatial QRS loop with the attached mean spatial QRS vector, spatial gradient vector, and the series of T wave vectors, T to T' , resulting from progressive diminution of the gradient. In general, if the heart is rotated clockwise the T wave axis as projected on the frontal plane is deviated to the left by diminution of the gradient. If the heart is in counterclockwise rotation the T axis is deviated to the right by diminution of the gradient. If the heart is nonrotated or only slightly rotated the T axis remains unchanged in direction. In such cases the T axis as projected upon the frontal plane becomes smaller unless a change in cardiac position

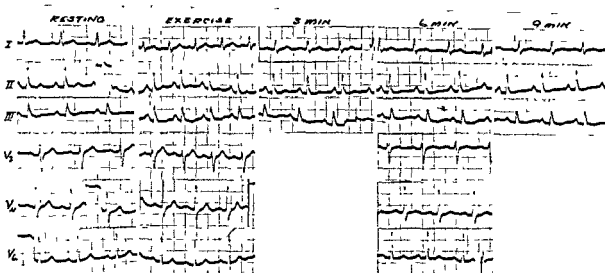


FIG. 93. Persistence of exercise effects The significance of the persistence of the T wave changes shown here has not yet been determined. The patient is a 45-year-old woman with no evidence of heart disease—unless this be it.

counterbalances the effect of diminution of the gradient. In apex-back hearts the degree of the change in the magnitude of the T axis is less than in apex-forward hearts.

If the QRS loop model is placed in the proper orientation, so that its projection upon the frontal plane produces the limb leads occurring in the patient's tracing, the effect of diminution of the gradient can be learned by comparing the effects on the limb leads of the projection of the vectors T and T' upon the frontal plane. If the QRS complexes have changed following exercise it will usually be found that the change in the orientation of the model which is required to correspond to the new QRS complexes is a change of the anatomic axis to a more vertical direction and/or a clockwise rotation of varying degree. It is important to note that when the heart is clockwise and remains so after exercise diminution of the gradient causes the T axis to deviate to the left (from T to T' , Fig. 40d, p. 57) while a change to the more vertical position tends to cause the T axis to deviate to the right (for the T axis tends to follow the anatomic axis, Fig. 40e). Since both the diminution of the gradient and the change in anatomic axis frequently occur

after exercise (and under other circumstances) it is important to point out that the two opposing effects may counterbalance one another and that sometimes one predominates and sometimes the other. Figure 91 shows such a combination of effects analyzed by means of the model employed in Fig. 40. It is safe to say that if the tracing b of Fig. 91 had been obtained first (as well it might have been) and that shown as tracing a been obtained later some might erroneously conclude that a "posterior" infarction had occurred. Figure 92 shows that if the loop is in the orientation shown (diagrammed) the change from T to T' may cause inversion of the T wave in all three limb leads. The T wave in V_4 , V_6 , and V_6 may also be inverted.*

It is commonly observed that the U wave becomes larger after exercise. This has no pathologic significance.

The possible significance of the duration of the exercise effects has not yet been determined. They are presently under investigation. Figure 93 demonstrates prolongation of the duration of the exercise effects. They seem

* All these effects result from the diminution of the gradient and are also predictable from the two monophasic curve analysis presented in Fig. 31, column a (p. 46).

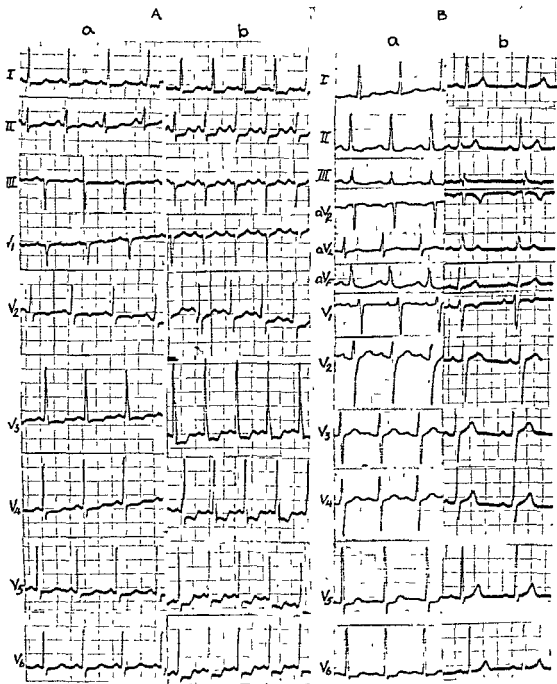


FIG. 94. *A*, Tracings made at interval observation (*a*) and during an attack of pain (*b*).
B, Tracings of another patient made during (*a*), and after (*b*) an anxiety attack. The patient was a 26-year-old male. Pain in the chest was present during the anxiety attack.

Both cases show RS-T shifts. While these are greater in the tracings of patient *A* when we compare her tracing *b* to *B*'s tracing *a*, this is *not* true when we compare the tracings in which the rate is the same (tracing *A-a* and *B-a*). Thus if *B*'s rate had risen to almost 150 beats/minute the RS-T shifts might have become larger.

The distinction between the tracing showing disease (*A*) and that which is normal (*B*) is that in *B-a* all shifts are opposite in direction and proportionate in magnitude to the main deflection of the QRS complexes, while in *A* they are not; Lead II in *A-b* shows a large shift though the R in that lead is not large, and in Lead III the RS-T shift is in the same direction as the main deflection of the QRS complex.

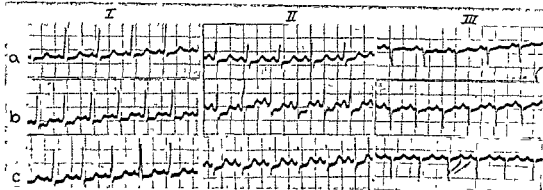


FIG. 95. *a*, An interval tracing on a 68-year-old woman with hypertension. The RS-T shifts are probably due to relatively rapid rate (120/min.). *b* was made when patient developed epigastric pain while in the office.

Comparison of *c* with *b* shows a definite diminution in the shifts following nitroglycerine. There is little change in rate. The pain also disappeared. The shift in Lead II in tracing *b* is too great to attribute to rapid rate, for it does not follow a large R wave.

to persist longer after the taking of food (in the same individual).

At times exercise induces a nodal rhythm. This has no pathologic significance.

Occasionally the exercise induces left bundle branch block. This must be regarded as a definite and important sign of disease.

RS-T Shifts Due to Rapid Rate. Frequently electrocardiograms are made on persons suspected of coronary disease when the heart is beating rapidly because of emotional factors or shock. RS-T shifts associated with rapid rate are common in such tracings. Such RS-T shifts which tend to be opposite in direction and proportionate in magnitude to the main deflection of the QRS complex may be due entirely to the rapid rate as described in the discussion of exercise tracings. Unfortunately, RS-T shifts due to injury may also be opposite in direction to the main deflection of the QRS complex and again the distinction between the normal and the abnormal may be difficult. Figure 94A shows two tracings made on the same patient within a few days, one (*a*) without pain and the other (*b*) with pain. The RS-T shifts in *b* are opposite in direction to the main deflection of the QRS complex except in Lead III in which the RS-T shift and the main deflection of the QRS complex are in the same direction. The flat depressions of the RS-T segment

including the displacement of the RS-T junction is empirically very suggestive of disease but it can be closely mimicked by nonpathologic shifts when the rate is rapid (Fig. 94B). The shift in Lead II in 94A-b is a bit large in proportion to R to be explained on non-pathologic basis. Nitroglycerine was administered and observations were made at frequent intervals. A diminution in the shifts without significant rate change accompanied relief of the pain, (Fig. 95).

It must be stated that frequently the decision regarding the degree of RS-T shifts that should be regarded as pathologic depends upon the experience of the observer.

Figures 96a and b are tracings made on two patients whose heart rates were rapid every time they were examined. The RS-T shifts tend in most of the leads to be proportionate to and opposite in direction to the main deflection of the QRS complexes. These tracings, therefore, may be entirely normal. However, in both of these tracings the RS-T shift in V_2 appears to be in the same direction as the main deflection of the QRS complex. In *b* the S is deeper, but the R is wider and R actually has a greater area and may be responsible for the direction of the RS-T shift. This is not true of *a*, however, and it is necessary to consider whether the shift is pathologic or, as has been described above,

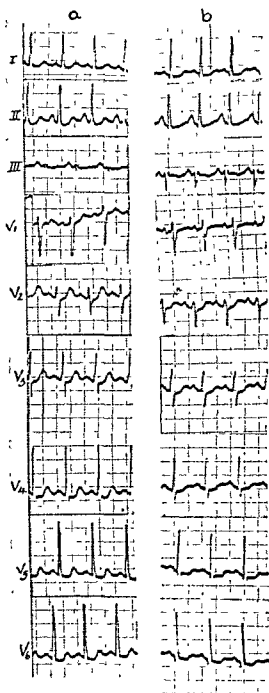


Fig. 96. Two patients whose hearts were always rapid due to emotional causes. RS-T depressions follow all large R waves and are probably due to small gradients resulting from rapid rate. V_2 may be an exception in *a*. In *b* the R of V_2 is not large in amplitude but is wide while the deeper S is very narrow. Since it is the area which is important and the area of R is greater than that of S, the downward shift of the RS-T still follows the rule.

whether it represents an example of the contrary behavior of a nonpathologic shift in a lead made by an electrode close to the heart. In many such cases no final conclusion may be justified. Further observation may be necessary. If following such observations the electrocardiogram undergoes changes that are distinctly abnormal the conclusion must be based on these findings and not upon such tracings as shown in Fig. 96*a* and *b*. In this connection it is necessary to warn the reader that in the normal heart after prolonged tachycardia due to ectopic rhythm the electrocardiogram may show inverted T waves that may persist for several days after the rate is slowed (Fig. 97). No diagnostic significance can be attached to T wave changes under these circumstances.

An upward shift of the RS-T segment in leads with large R waves, is, at times, due to the presence of a *large gradient* (Chapter 5) in a perfectly normal heart (Fig. 98). At times it is possible to be certain of this only after repeated observations over a period of time show that the shift does not change. Shifts due to pathologic changes only occasionally remain stationary. RS-T elevations due to a large gradient may diminish after exercise (Fig. 98). However, it is also possible for injury shifts to be reduced by exercise and therefore this method of distinguishing the shifts is useless as well as dangerous. Again, in some cases the nonpathological shift may persist after exercise but the T wave becomes inverted producing a cove-shaped diphasic T wave which may be mistakenly interpreted as abnormal. It will be seen in Fig. 99 that this phenomenon occurs not only after exercise but also when a deep breath is held.

It is important to mention here that RS-T shifts are common in electrocardiograms of patients taking digitalis. At times patients do not know they are taking this drug and errors can be made on this account. These digitalis shifts are exaggerated by rapid rate. More detail is furnished in another section. Figure 100 shows a tracing made on a patient who

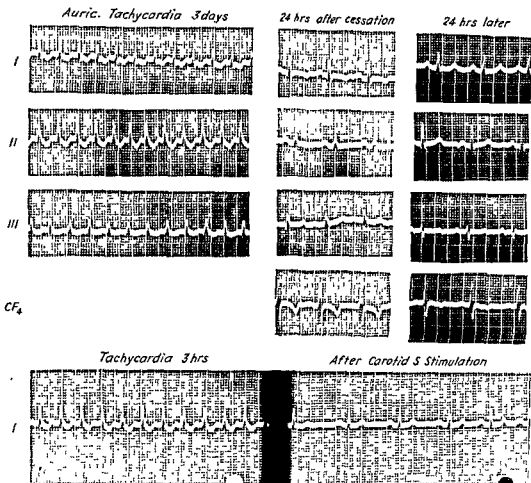


FIG. 97. Tracings during and after two attacks of auricular tachycardia in the same patient. After the prolonged attack the T waves in Lead I and CF_4 are inverted 24 hours later the T wave in Lead I is upright but the T wave in CF_4 is diphasic. There is no heart disease. After the short attack the T wave in Lead I is not inverted.

had been taking digitalis. It is impossible to evaluate the changes shown here until the digitalis effects have disappeared. This may not occur until the digitalis has been discontinued for several weeks.

ELECTROCARDIOGRAPHIC DIAGNOSIS OF CORONARY INSUFFICIENCY FROM SERIAL CHANGES IN INTERVAL TRACINGS. The electrocardiogram *a* of Fig. 101 was made on a 50-year-old man who had had a pain in the chest following moderate exertion several days before. This tracing reveals no striking findings. On the following day electrocardiogram *b* was made. In this tracing we find that T_I has become

larger and that T_{III} has become inverted. In other words, the T wave axis has swung to the left. Just as the recording of this electrocardiogram was completed the patient had another pain in the chest and another tracing, *c*, was made. In this tracing the T wave axis has swung far to the right; T_I is very small and T_{III} is very much larger. If V_L had been recorded it would have shown an inverted T wave. The T wave in the precordial lead shows a definitely abnormal form. The tracing retained this form for about a week but by another 15 days it had almost reverted to the form shown in Fig. 101*b*. Following this the

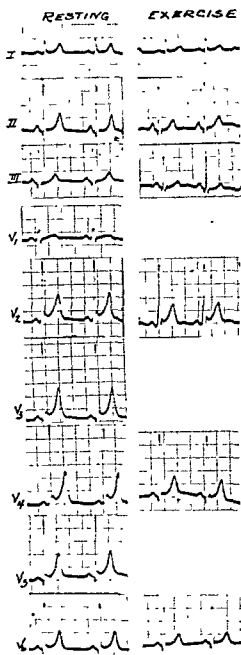


FIG. 98. Diminution of nonpathologic RS-T shift after exercise. Unfortunately pathologic RS-T shifts may at times also be diminished after exercise.

patient had no further symptoms although he was completely active and four years later his electrocardiogram was unchanged. Six years following the first tracing he suffered a myocardial infarction.

Frequently, when no electrocardiogram can

be made during an attack or when such tracing do not show diagnostic changes, serial tracings made between attacks over a period of several days or weeks may show changes that are diagnostic. These are due to the persistence of ischemia after the attacks are over and to subsequent recovery. If tracing *c* of Fig. 101, had not, fortuitously, been obtained during an attack the series of tracings *a*, *b*, *d*, *e*, and *f* would represent such a serial change and it will, therefore, be employed to illustrate this phenomenon in detail. It is important to note that in these tracings the T axis swings to the left (*a* to *b*) then to the right (*d*), and finally to the left again (*f*). There is not sufficient change in the QRS complexes of the limb leads to make it possible to explain this phenomenon on the basis of change in cardiac position, nor is it possible to explain them on the basis of nonpathologic change in the gradient due to change in rate, etc. It is important to note that tracings *a* and *b*, considered individually, are both within normal limits. The QRS-T relationship (the gradient) in each of these tracings is within the bounds of normal individual variations. As stated before the magnitude of the ventricular gradient varies from individual to individual (Chapter 5). However, when such tracings as *a* and *b* occur in serial observations on the same patient and if the change in the T axis cannot be accounted for by nonpathologic factors (change in cardiac position and rotation, change in the magnitude of the gradient due to rate change, exercise, food, tobacco, or digitalis) then such change in the T axis is suggestive of disease. The subsequent appearance of tracing *d* showing a marked change in the T axis is conclusive even if the precordial lead had not shown the markedly abnormal form.

Figure 102 shows a series of interval tracings on a patient who was having pains in the chest and in whom several areas were involved in the ischemic process. The serial change in the T wave axis is diagnostic.

In the evaluation of any T wave change in serial tracings the measurement of the

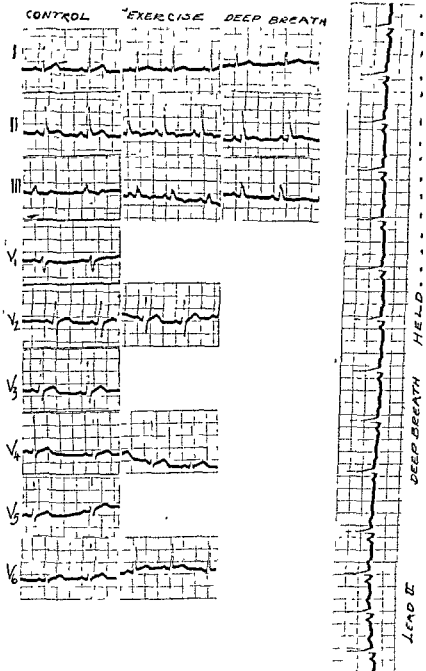


FIG. 99. Effect of exercise and deep breath on a patient with non-pathologic upward shifts of RS-T. An unusual case in which in Lead II the shift persists but the T wave becomes inverted.

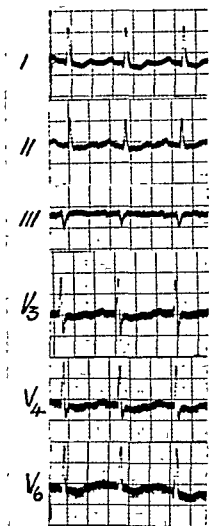


FIG. 100. RS-T shifts due to digitalis. The reason for administration of digitalis could not be ascertained. Interpretation of the tracing in the presence of such digitalis effects is impossible.

Q-T interval may be of great importance. The Q-T interval may not be or become prolonged in such tracings but if it does the prolongation is of great diagnostic significance in the absence of electrolyte disturbances and of quinidine.

Figure 103 shows a series of tracings made on a patient who was having pains in the chest of bizarre distribution. The first record shows a large T_I and a small T_{III} pattern characteristic of a semitransverse heart in

counterclockwise rotation (Fig. 103, 2-8-53a). The second tracing shows a marked change in the T axis so that T_I is now smaller than T_{III} although both are upright. This at a glance represents at least a diminution of the magnitude of the gradient. Actual measurement might show that the direction of the gradient has also changed. However, even if the gradient is simply diminished to produce this rightward deviation of the T axis the absence of change in cardiac position (the QRS remains the same), of rate increase (the heart is actually slower), and of other non-pathologic factors make it necessary to conclude that the change resulted from disease (ischemia). At times, as when some non-pathologic factor cannot be ruled out, it may be necessary to measure the gradient. In the case illustrated in Fig. 103 it is found that the gradient has deviated some 15° to the right from tracing a to tracing b (2-8-53). This cannot be normal unless the cardiac rotation has changed. The subsequent tracings bore out this conclusion. As indicated in the discussion of Fig. 102 a change in T axis from right to left in serial tracings may be equally important when it cannot be explained on a nonpathologic basis. It is important to note that when T_{III} is greater than T_I , whether in normal or in pathologic states, then T_{V_L} will be negative; when T_I is greater than T_{III} then T_{V_L} must be positive. T_{V_L} has no greater or less significance than the $T_I : T_{III}$ ratio. It is also important to note (Fig. 103) that ischemic changes may be present in an electrocardiogram even though all of the T waves are upright including those in the precordial leads.

Figure 104 shows a series of tracings obtained over a period of several days from a patient who had attacks of pain in the chest on walking. No opportunity to make tracings during an attack presented itself. This series shows a progressive change in the T wave axis toward the right due to change in the direction of the gradient (though here it was not necessary to determine this by measurement). Another finding is inversion of the

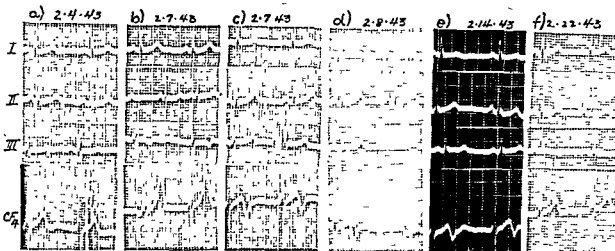


FIG. 101. Tracing *a* was made two days following an attack of chest pain that occurred while this 50-year-old male was working in the garden. *b* was made three days later and *c* a few minutes after *b*, the latter during pain which occurred just after the recording of *b* was completed. *d*, *e*, and *f* were made on the dates indicated as follow-up observations.

The change in the T wave axis from tracing to tracing (discussed fully in the text) is regarded as diagnostic even in the absence of the characteristic change in the precordial lead seen in *c*, *d*, and *e*.

U waves in the precordial leads. This does not occur in normal hearts. Except for this finding the precordial leads in the first tracing are within normal limits. This patient died of an acute anterior infarction several months after these tracings were made.

It would be well to recall here that interpretation of serial precordial leads is full of pitfalls (see Chapter 3). Changes in the T waves as well as changes in the QRS complexes may be and frequently are due to change in the placement of the electrodes. While changes in the T waves of the limb leads due to changes in cardiac position can be detected by examination of and analysis of corresponding changes in the QRS complexes, the same cannot be done for T wave changes in precordial leads of the same series of tracings. Although the QRS complexes of the two corresponding serial chest leads may show sufficient difference to indicate that the electrode was placed differently for each, such comparison is very crude and, therefore, is often completely unreliable. Even if the electrode positions are marked on the skin with silver nitrate the position of the heart

with relation to the electrode may be altered as a result of abdominal distention, slight change in posture, or change in the respiratory midposition. It frequently requires but a small change in the position of the electrode to produce a marked change in the electrocardiogram. This is true for both the QRS complexes and for the T waves.

When one considers the fact that so many persons have pains about the chest and in the epigastrium which they think unimportant or which they attribute to "gas" it becomes apparent that it is necessary to realize that the electrocardiogram made on any patient under any circumstances might be found to be a member of such a series as presented in the above figures if repeated observation over a period of time were made. Thus the value of repeated observations over a period of several days to weeks is emphasized.

SIGNIFICANCE OF NONPATHOLOGIC FACTORS IN INTERPRETATION OF SERIAL ELECTROCARDIOGRAMS WHEN CORONARY DISEASE IS SUSPECTED (WITH EMPHASIS ON EFFECT OF FOOD). In the evaluation of the serial electrocardiographic observation recommended here

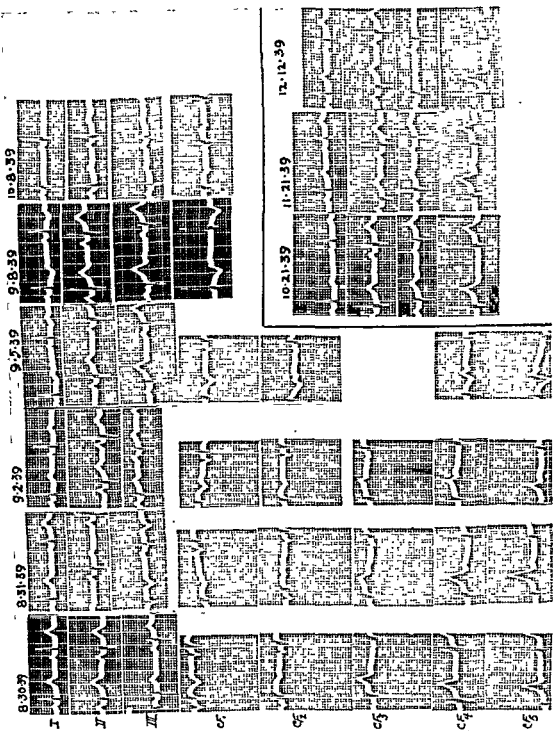


FIG. 102. Serial change in T wave axis pathognomonic of disease.

From 8-30-39 to 8-31-39 the T axis changes markedly toward the left. From 8-31-39 to 9-2-39 the T axis has changed direction toward the right again. During this time there have been no diagnostic changes in the precordial leads. On 9-5-39 the T axis is further to the right than it had been at any time previously. The precordial leads show definitely abnormal T waves for the first time. On 9-8-39 it is still further to the right. On 10-8-39 it is less to the right but is smaller (all T waves are small). From this time until 12-12-39 the T wave axis is less and less to the right. The tracing on 12-12-39 is entirely within normal limits.

Such changes in T axis either to the left or the right occurring within a short time in the same individual and if not due to rate change, exercise or food, are diagnostic of disease.

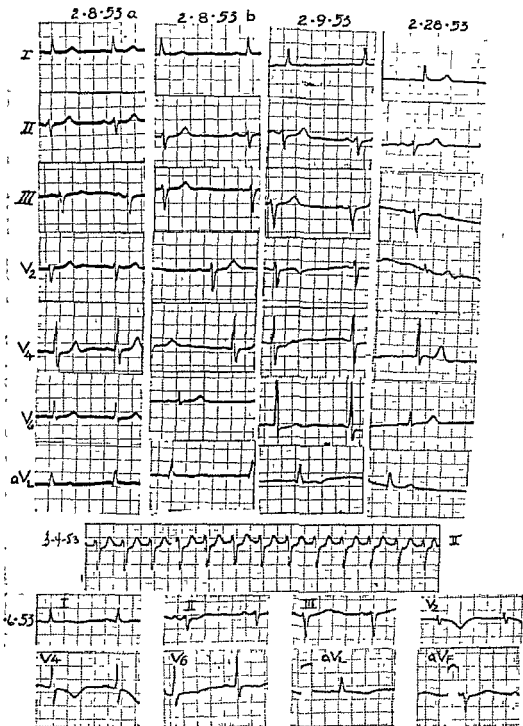


FIG. 103. Change in T axis in serial interval tracings in angina. The tracings were made on a patient having repeated pains in the chest. No observation was made during an attack. The change in T axis toward the right from 2-8-53a to 2-8-53b could be due, in a counterclockwise heart, to diminution of the gradient by rapid rate, food or exercise. Since the patient was at bed rest, the rate is actually slower in b, and the tracing was made fasting, the change is diagnostic of disease. Subsequent tracings bear out this conclusion. Furthermore, measurement of the gradient shows that it deviated 15° to the right from a to b. This seldom occurs as a result of nonpathologic factors without change in cardiac position or rotation. It is evident from the QRS complexes that no significant change in cardiac rotation occurred between a and b.

By 2-28-53 the tracing was normal again. On 3-4-53 the patient had an attack of auricular tachycardia. The tracing made on 3-6-53 shows the effects of quinidine and of the attack of auricular tachycardia.

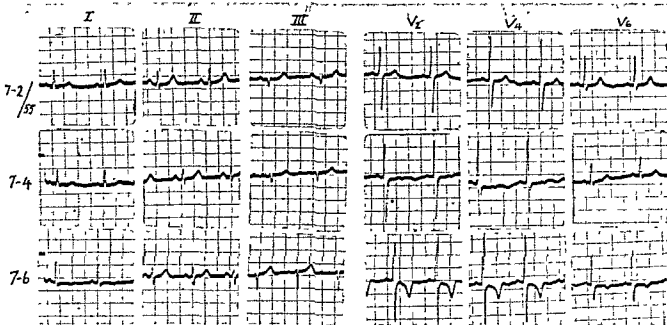


FIG. 104. Change in T axis in serial tracings in angina. Progressive deviation of T axis toward the right pathognomonic of myocardial disease. No observations could be made during an attack.

The diagnosis was suspected from the first tracing because the T axis is such as to indicate that the gradient lies too far to the right for a mean QRS which is at roughly 0° , though this can be normal in some apex-back vertical hearts. The inverted U waves in V_1 and V_2 were also highly suspicious. Subsequent change of the T axis even further to the right confirms the suspicion even without the markedly abnormal T wave changes in the precordial leads in the last tracing.

and shown in Fig. 103 (in which the changes are notably in the T waves) it is necessary, as has been stated before, to take into account the possible influence of nonpathologic factors. Postural change, abdominal distention, and ascites may cause such change in cardiac position and rotation as is depicted in Fig. 40 (p. 57). Even the difference between the back rest and the supine position may be important. The higher respiratory midposition of hysterical hyperpnea or of great pain is often important in this connection. The detection of change in position and rotation depends upon close examination of the QRS complexes (see Fig. 91). Hemorrhage, shock, and anxiety may cause great rate change; RS-T shifts and the T wave changes depicted in Fig. 94B occur under these circumstances as a result of diminution of the ventricular gradient.

The effects of exertion summarized in the

preceding discussion of the effects of exercise on the electrocardiogram (p. 119) are of great importance in this regard. Electrocardiograms are frequently made (without realizing it) a few minutes after rapid walking or other activities which may produce exercise effects (Fig. 105). Unless one is cognizant of these effects errors can be made. Again, the effects of digitalis, tobacco, and of electrolyte disturbances as well as of other factors must be taken into consideration. Description of some of these must be left to the other sections.

In addition to other factors the writer has found and reported in 1939 that the taking of food causes pronounced changes in the T waves of the electrocardiogram in the majority of persons. These also seem to result from diminution of the magnitude of the gradient, and may, therefore be summarized by the diagrams of Fig. 40. These changes are at their peak at about one hour after the

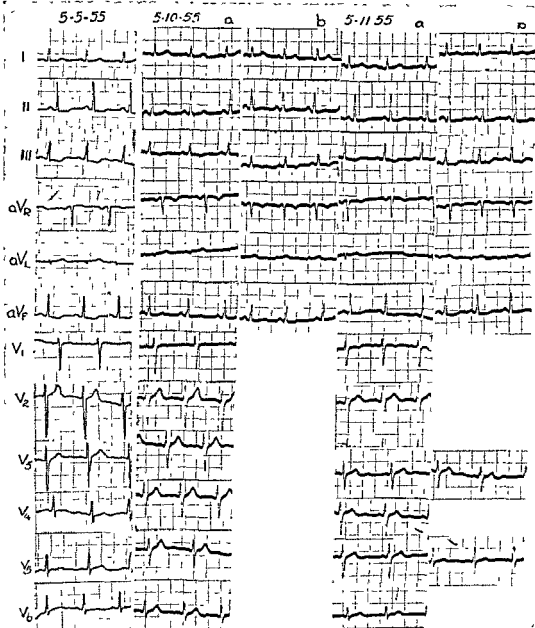


FIG. 105. Effects of food and exercise. 5-5-55, Electrocardiogram made on young woman for clinical purposes. 5-10-55a, Electrocardiogram made four hours after the last meal. 5-10-55b, Electrocardiogram made at same sitting as a after 20 deep knee bends. 5-11-55a, Electrocardiogram made one hour after a large meal. 5-11-55b, Electrocardiogram made at same sitting after 10 deep knee bends.

Note that the tracing made with exercise following a meal is almost exactly like that of 5-5-55. It was subsequently learned that the latter tracing (5-5-55) was made after walking two blocks very rapidly one hour after a meal.

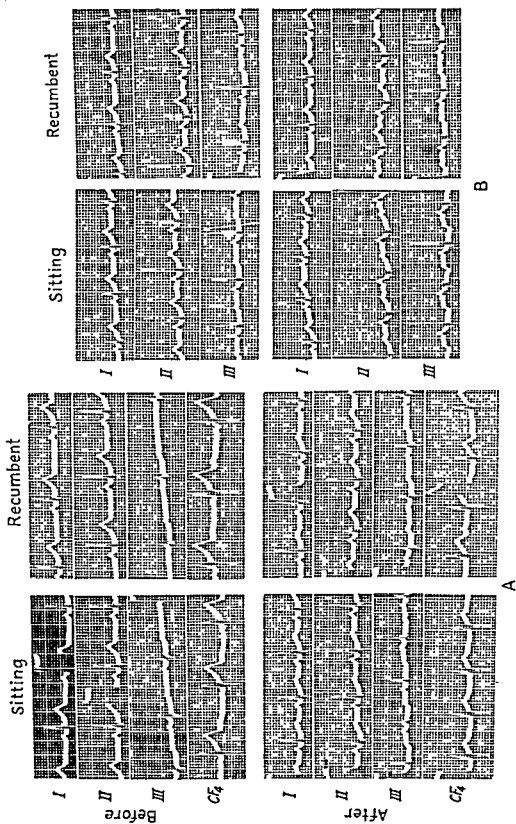


FIG. 106. Effect of food on the electrocardiogram. *A*, Marked diminution of the T waves in all leads due to food. *B*, Diminution of the T waves and change in T wave axis due to food. Note that T_{III}, previously upright, has become inverted. T_{II} may also become inverted. In *A* there is a marked increase in rate after food; in *B* the rate increase is not significant. (From Gardberg, M., and Olsen, J. *Am. Heart J.* 17: 725, 1939.)

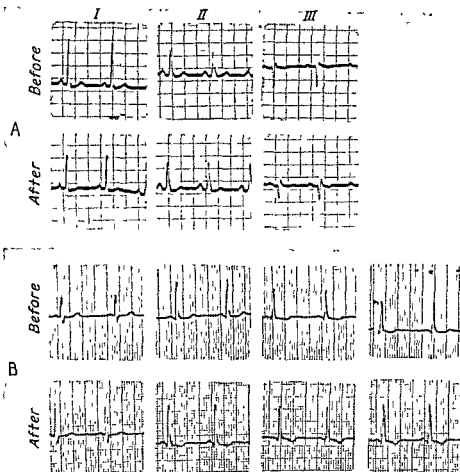


FIG. 107. *A*, Effect of food when the heart is rotated counterclockwise: T_I is most markedly lowered while T_{III} increases. *B*, Effect of food when heart is rotated clockwise. T_I is affected less; T_{III} and T_{II} are diminished and may become inverted. Note that the T in aV_r is inverted by the meal.

The common denominator is the ventricular gradient which, in both cases, is diminished by food but changes little in direction.

taking of the meal and seem to persist as long as two and one-half hours. Figures 106A and B are from the original work. Exercise after the taking of food seems to increase the effects, producing a more marked diminution of the magnitude of the ventricular gradient than is produced by either factor alone. More RS-T deviation is, therefore, also produced under these circumstances.

Figure 107A shows the effect of the taking of food upon the electrocardiogram of a man whose tracing shows left deviation of the QRS axis.

Figure 107B shows two observations made on the same patient on different days. The

change might have been due to myocardial ischemia which may also diminish the magnitude of the gradient. There is no significant rate change and no digitalis had been given. Tracings made fasting and one hour after a full breakfast reproduced exactly the two tracings made previously.

Figure 108 shows electrocardiograms made before and one hour after breakfast; the subject was a young woman with no evidence of heart disease of any kind. It is the only example of RS-T depression in Lead I of this type which the writer has seen in the absence of disease or digitalis, or rapid rate.

It should be mentioned in passing that the

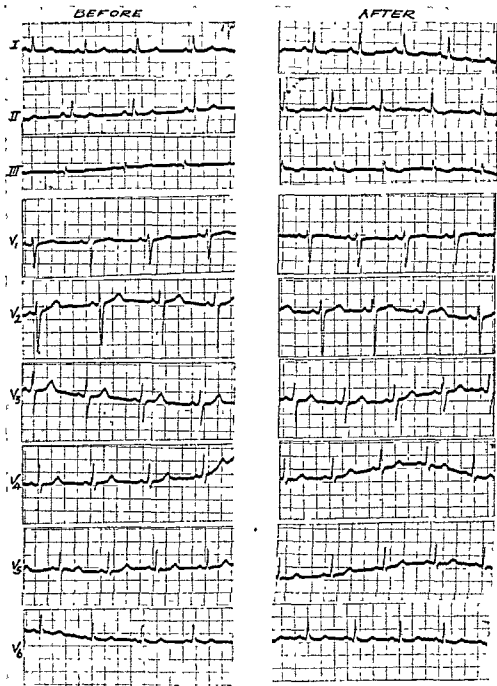


FIG. 108. Effect of food on the electrocardiogram. Depression of the RS-T segment in Lead I due to food.

electrocardiographic changes which follow cigarette smoking and anxiety cannot logically be interpreted differently from the same changes following any other factor which simply diminishes the magnitude of the ventricular gradient such as increased rate (which is a frequent accompaniment of smoking and of anxiety), digitalis, or the taking of food.

T wave changes can never be interpreted except in terms of the QRS-T relationship.

T WAVE CHANGES FOLLOWING VENTRICULAR PREMATURE BEATS. At times, as demonstrated in Fig. 109, complexes which follow the compensatory pause of premature beats show T wave changes. This does not occur in nor-

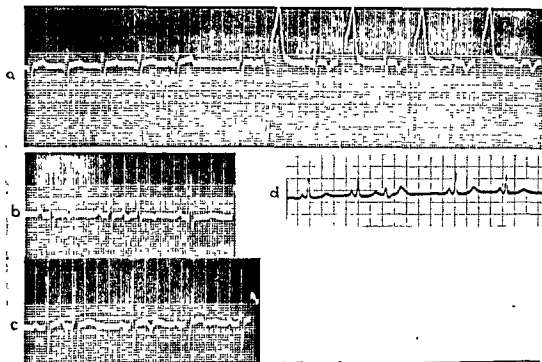


FIG. 109. T wave changes following premature beats *a*, Note T wave becomes inverted after each pause following a premature beat. *b*, In this record T previously inverted becomes upright following the premature beat. *c*, T wave previously upright becomes inverted following the premature beat *d*, The T wave becomes larger following the premature beat.

mal hearts unless the original rate is rapid. The T wave change may be a diminution, even an inversion (as in Fig. 109*a*) or an increase as in Fig. 109*b*. This phenomenon was observed by Ashman some years ago. It is an important diagnostic sign of myocardial disease.

Azamora elicited the same effect of increasing cycle length by employing carotid sinus stimulation. He showed that in diseased hearts previously upright T waves became inverted when the rate was slowed. By employing exercise he produced the opposite effect.

*Myocardial Infarction**

If one is to trace the effects of myocardial infarction upon the electrocardiogram from their inception it is necessary to begin with the injury effects which have been described

* With the collaboration of Louis Levy, II, M.D., Heart Station of Charity Hospital, New Orleans.

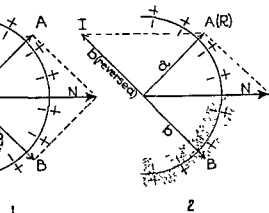


FIG. 110. Principle involved in analyzing the effect of infarction on the representative vector of a wave of excitation.

in Chapter 6, which the reader should review at this time. As has been stated in Chapter 6 the QRS changes generally appear as the injury shifts diminish. The reciprocal change most often requires about five days to become complete but is more rapid in some cases and much slower in others.

In order to construct the RS-T shifts and T wave changes which occur early in myocardial infarction in any area one simply constructs (as described in Chapter 6) the vector I , representing the current of injury, perpendicular to the surface of the injured area. The vector i (the reversal of I) is then constructed to represent the direction of the RS-T injury shifts. I may also be employed to represent the ischemic vector Is and the T wave effects are constructed as shown in Figs. 54 and 55 (pp. 75-77). In the succeeding diagrams employed in the analysis of the QRS complexes in myocardial infarction the infarct vector, I , when it represents the effect of the entire infarct, may be employed as the current of injury vector I as described above. Conversely the RS-T shift may be measured in two limb leads and plotted as the vector quantity, i . The reverse of this vector quantity gives us the vector I representing the direction and magnitude of the current of injury. Some aid in determining the location of the infarct may be afforded by determining the direction of the current of injury, for the spatial vector representing it is perpendicular to the injured area (see Fig. 54, in which I is labelled Ci).

The same hypothesis of sequence of activation employed throughout this presentation is applied to the analysis of the QRS complexes in myocardial infarction. It is assumed that the area of muscle that has undergone necrosis is incapable of producing electrical effects. Therefore it is assumed that the wave of excitation which is drawn for each stage of depolarization shown in Fig. 15 (p. 19) should show, as a result of infarction, a defect in that part occupied by the infarct. In order to determine the effect of the infarct upon the spatial vector representing any stage of activation it is necessary to subtract the

electrical effect normally exerted by the area which has become infarcted from the electrical effect of the total wave of excitation. In order to do this we erect a spatial vector which represents the estimated electrical effect of that portion of the wave of excitation which fails to occur as a result of the infarct. The direction of this vector representing the absent portion of the wave of excitation (the defect) is reversed (I , Fig. 110) and it is then added vectorially (parallelogram of forces) to the normal vector (N) to obtain the resultant vector (R) which represents the electrical effect of the dipole layer after infarction has occurred.

In Fig. 110 A and B are two parts of a wave of excitation. The electrical effect of each part is represented by a vector (a , b) drawn perpendicular to the surface of each part and the total effect of the entire wave of excitation is obtained by vectorial addition (the parallelogram of forces) to obtain the resultant vector, N . If now the area normally occupied by B is destroyed it is seen that reversal of the direction of the vector which normally represented the dipole layer B and its vectorial addition to the vector N gives us the vector R which represents that portion of the dipole layer which remains (A), and which, obviously is identical with the vector a .

It is important to remember that for the same infarct the size of the defect which occurs in the wave of excitation is different at the various stages of activation. As a result the magnitude and direction of the vector which represents the defect in the wave of excitation varies from stage to stage. This becomes clearer when we consider Fig. 111 in detail.

LATERAL MYOCARDIAL INFARCTION. The first group of infarctions to be presented will be infarctions in the lateral wall of the left ventricle. The general location of the infarct is shown as the missing portion of the ventricle in Fig. 111. The reader is to understand that the infarct extends into the upper half of the heart (not shown in the first stage) as far as it does in the lower half.

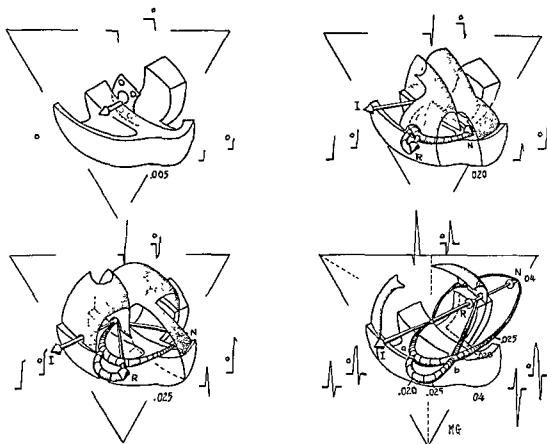


FIG. 111. The heart is again represented in the semitransverse position and counterclockwise rotation seen in Fig 15.

Since the infarct is in the lateral wall of the left ventricle the first stages of activation, 0.005 second and 0.015 second (not shown) are unaffected since the wave of excitation at these stages has not yet reached the infarcted area. At 0.02 second the defect in the wave of excitation can be estimated by comparing with the corresponding stage of Fig 15. The vector representing this defect (the infarct vector *I*) points to the right and somewhat toward the base. As shown in the diagram the construction of this vector is necessarily different for each stage. Vectorial addition of this infarct vector *I* to the normal vector, *N*, for each stage of activation produces the resultant vector, *R*, representing the electrical effect of the wave of excitation as it occurs after infarction. Throughout the process of depolarization as shown in the figure, it is the succession of resultant vectors, *R*, which inscribes the deflections of the electrocardiogram as it appears after infarction. The earthworm-like structure which traces the path of the head of the cone-shaped vectors *R* is the spatial QRS loop which occurs after infarction in the semitransverse counterclockwise rotated heart while the earthworm-like structure which traces the path of the normal vectors, *N*, is the normal QRS loop for the semitransverse counterclockwise rotated heart (as may be recognized from Fig 15).

Figure 111 depicts the effects of a lateral wall infarction upon the spatial QRS loop and the standard limb leads of the electrocardiogram employing the basic diagrams developed in Chapter 2. Both the normal spatial QRS loop and the loop which occurs after in-

farction are developed simultaneously. In describing the effect of infarction upon the spatial loop it is of fundamental importance that we pay attention not only to the change in the *shape* of the loop and its orientation in space but also to the *timing* of the various

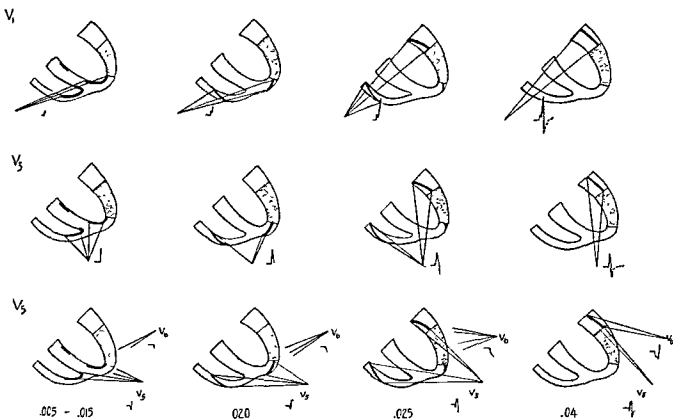


FIG. 112. The precordial leads in lateral and posterolateral infarction. The four stages of the process of excitation employed in Fig. 111 are represented in two-dimensional diagrams. The distinguishing features are the increase in height and duration of R in V_1 and the diminution of S in V_1 . A wide Q and inverted T in V_1 may appear, but if the infarct occupies a more basal position than shown here the precordial leads over the left chest are not remarkable. Diagnostic difficulty can be caused by the similarity of the precordial leads that occur in lateral and posterolateral infarction to those which occur in right bundle branch delay and in right ventricular hypertrophy.

portions of the loop. Two loops may be of similar shape but the timing may be considerably different.

The characteristics of the spatial QRS loop which may be expected when lateral infarction occurs in a semitransverse counterclockwise-rotated heart are as follows: (1) the first portion of the loop (from a to b) extends further forward and a bit further to the right than does the first portion of the normal loop; (2) this portion of the infarct loop is of longer duration than the first portion of the normal loop because vectors occurring at 0.02 second and 0.025 second are found pointing to the right as compared to similarly timed vectors in the normal loop.

The longer duration of the first portion of the loop, as shown in the basic diagram, increases the duration of the Q in Lead I even though it does not deepen it greatly. The same changes produce a deepening and widening of the Q in V_L (not shown in Fig. 111). At the same time the R wave in Lead III is increased in height and duration. Especially in high lateral infarction and in apex-back hearts the effect on the Q in Lead I is not nearly so marked as is the effect on R in Lead III.

Precordial Leads. In Fig. 112 the precordial lead pattern associated with lateral myocardial infarction is depicted. The essential points are an increase in duration and amplitude of

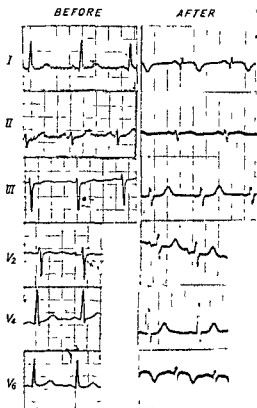


FIG. 113. Electrocardiograms made on a patient (whose heart is in approximately the position and rotation shown in the diagram of Fig. 111) before and after the development of a lateral wall infarction. Note the increased duration of Q_I and increased height and duration of R_{III} , as well as the decreased magnitude of S_{III} and increased magnitude and duration of the R in V_2 . All these effects of the infarct are predicted in Figs. 111 and 112 on the basis of the hypothesis that we employ.

the R in V_1 and the decrease in the amplitude of R in V_5 and V_6 . There is also an increase in the duration of Q in V_6 .

The initial stage of activation (at 0.005 second) is represented in Fig. 112 by the small wave of excitation on the left side of the septum. The sides of the solid angle are not drawn for this stage but the deflection produced by it begins the QRS complex drawn for each lead in the figure. The obliteration by the lateral wall infarction of a large part of the waves of excitation normally occurring in the lateral wall of the left ventricle at 0.02–0.04 second permits the preponder-

ance of the effects of the waves of excitation in the right ventricle on the electrode at V_1 (and V_2) at these stages: the positive solid angle subtended at V_1 by the wave of excitation in the right ventricle is much larger than the negative solid angle subtended at the same electrode by the much reduced wave of excitation in the lateral wall of the left ventricle (see 0.020 second and 0.025 second of Fig. 112). This causes an increase in the height and duration of the R wave in V_1 . The reduction of the size of the later waves of excitation occurring at 0.04–0.06 second by the infarct causes the S in V_1 and V_2 to become reduced (compare Fig. 112 to Fig. 23).

Figure 113 shows tracings before and after lateral wall infarction in a patient whose cardiac position is that of Fig. 111.

Effect of Various Rotations upon the Limb Leads. It is seen that clockwise rotation of the heart (Fig. 114b) causes the Q in Lead I to disappear and causes a Q to appear in Lead III. As a study of the timing of the loop reveals, the width of the Q is more important than its depth. The reader would do well at this point to fashion the loops shown in Fig. 114 and an anatomic axis from a piece of wire and experiment with the rotations himself. With the loop in clockwise rotation the infarct tracing assumes the form commonly associated with "posterior" infarction (Fig. 114b,c). Actually, of course, clockwise rotation does make the infarct assume a more "posterior" (diaphragmatic) orientation in space. It requires but little clockwise rotation to change a frontal plane loop so that the tracing changes from a $Q_I R_{III}$ to a $Q_{III} R_I$ pattern, especially when the apex is moderately back.

When the heart is in the position and rotation shown in Fig. 114d, the tracing shows, after infarction, a deepening of the Q_{III} . Whether a detectable widening of Q_{III} will become evident is problematic because with the heart (and loop) in this position the Q_{III} is already moderately wide. Widening, if it occurs, is of great significance. It is clear, however, that from the limb leads alone the

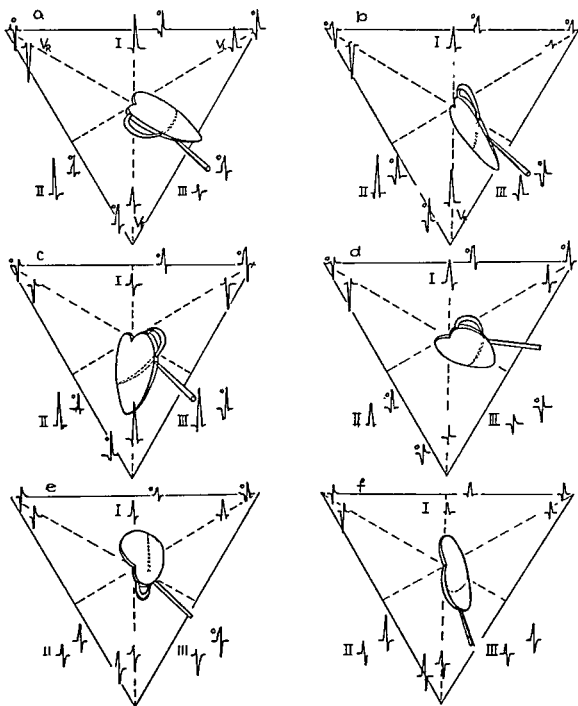


FIG. 114. *a*, Effect upon the loop and QRS complexes when the heart is less counterclockwise than in Fig. 111. *b* and *c*, Effect of clockwise rotation of the heart about its long axis. In *c* there is more clockwise rotation than in *b*. The marked complexes correspond to the infarct loop. *d*, Effect of making the heart transverse, moving the apex back with relation to the base, and rotating it slightly clockwise. *e*, Effect of moving the apex back and rotating the heart slightly counterclockwise. *f*, Effect of left ventricular hypertrophy (which increases the width of the spatial loop) in a vertical slightly counterclockwise heart. *No infarction is present*. Note similarity between the complexes of the vertical heart with a hypertrophied left ventricle and those of the lateral wall infarct of *e*.

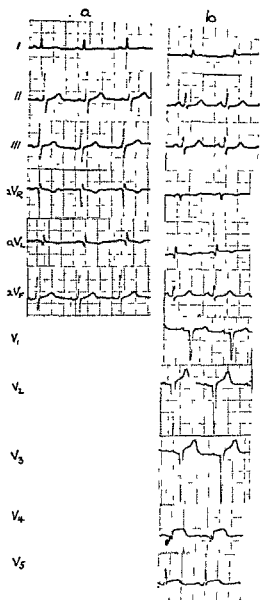


FIG. 115. *a*, Normal tracing, apex-back, vertical, counterclockwise. Precordial leads were normal. *b*, High anterolateral infarction producing similar standard and unipolar limb leads. Only the precordial leads distinguish the two tracings.

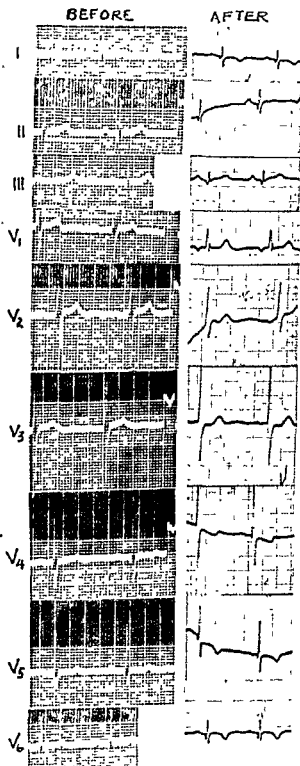


FIG. 116. Electrocardiograms before and after lateral myocardial infarction when the preinfarction tracing corresponds approximately to the position and rotation shown in Fig. 114*b* (there is probably slightly less clockwise rotation). Note that after infarction Q_s becomes wider and all of the R waves in the limb leads are lower as in the infarct leads shown in Fig. 114*b*.

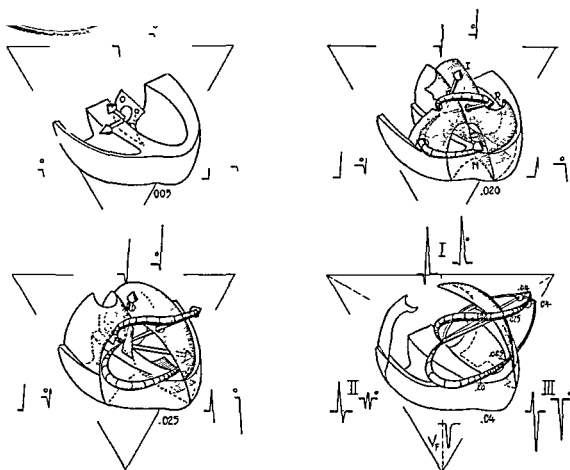


FIG. 117. A diaphragmatic wall infarct is represented by the gridded area on the floor of the left ventricle and the adjacent portion of the left side of the interventricular septum (not marked). The same method of analysis is employed as described for Fig. 111. Note that the chief effect of diaphragmatic infarction is the upward displacement of the first portion of the loop from the plane of the normal loop.

infarct may not be discernible. When the heart is in the position and rotation shown in Fig. 114e, the lateral wall infarct produces only two notable changes. These are an increase in the height and duration of R in III and a deepening and/or increase of the duration of Q in V_L . If one has previous tracings on the patient or if these changes are marked, they are diagnostic. It is necessary in this connection to consider the situation represented in Fig. 114f. Since hypertrophy of the left ventricle enlarges the loop anteriorly the effect will be to increase the duration of Q in V_L . This tracing may be indistinguishable from that of the lateral wall infarct or high anterolateral infarct

(see Fig. 115). It frequently shows a Q in Lead I and this makes the distinction even more difficult (see Fig. 67e).

Figure 116 shows electrocardiograms obtained from a patient whose heart position corresponds closely to that shown in Fig. 114b.

DIAPHRAGMATIC MYOCARDIAL INFARCTION. Infarction of the diaphragmatic wall of the left ventricle is very frequently accompanied by infarction of the diaphragmatic portion of the interventricular septum. Figure 117 depicts the effect of such an infarct upon the waves of excitation, the spatial QRS loop, and the limb leads of the electrocardiogram. In general the effect upon the spatial QRS loop

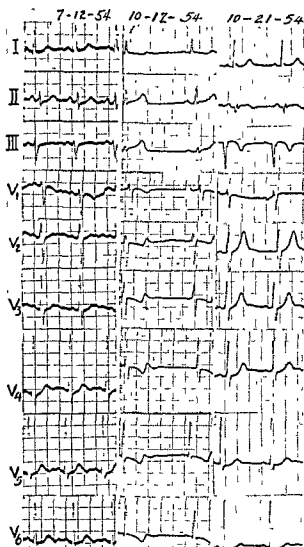


FIG. 118. Electrocardiograms of a patient before and after the development of an infarction of the diaphragmatic wall of the left ventricle. The limb leads before infarction (7-12-54) indicate that the heart is approximately in the position and rotation shown in the diagram of Fig. 117. The limb leads after infarction correspond closely to those shown for the infarct tracing of Fig. 117. The precordial leads show no striking changes in the QRS complexes.

is to displace the first portion of the loop upward. The infarct spatial loop can be fashioned from the normal loop by folding the anterior half of the normal loop upward on the posterior half which is kept stationary. The frontal plane loop assumes a figure-of-

eight form and becomes narrow. With the heart in the position shown in this basic diagram, the prominent changes are in Leads II, III, and V_F , where the initial R is replaced by a Q.

Precordial Leads. The precordial leads will generally show no characteristic QRS changes in the presence of a diaphragmatic infarction without anterior septal involvement.

Figure 118 is an illustrative set of electrocardiograms from a patient with a diaphragmatic wall infarction whose heart is in approximately the same position and rotation as that of the basic diagram.

Effect of Variations in Rotation. Figure 119 shows the normal and infarct loops in their proper relation to one another for various degrees of rotation on the three axes. Figure 119a depicts the effect of diaphragmatic infarction upon the QRS loop and limb leads when the rotation is slightly counterclockwise. The Q in Lead I and in V_L disappears and a wide Q appears in Lead III and V_F . However, a larger area of infarction would throw the initial portion of the loop still higher and result in a larger Q in Leads II and III (Fig. 120). The same effect is produced by making the position of the heart more horizontal.

Figure 119b depicts the effect of slight clockwise rotation upon the normal and infarct loops. It will be noted that the initial portion (0.005 second through 0.04 second) of the QRS loop is displaced to the left, upward, and somewhat posteriorly as a result of the infarction. This is reflected in the limb leads by a deepening of the Q in Lead III with only slight increase in its duration. The Q in V_F increases slightly in duration and amplitude. The initial R in V_R disappears, largely as a result of the septal involvement.

Figure 119c depicts the effect of a slightly more vertical position with an increase in the degree of clockwise rotation over that shown in Fig. 119b. In this position the normal frontal plane loop and the frontal plane loop for diaphragmatic infarction can almost be superimposed. The leftward and posterior devia-

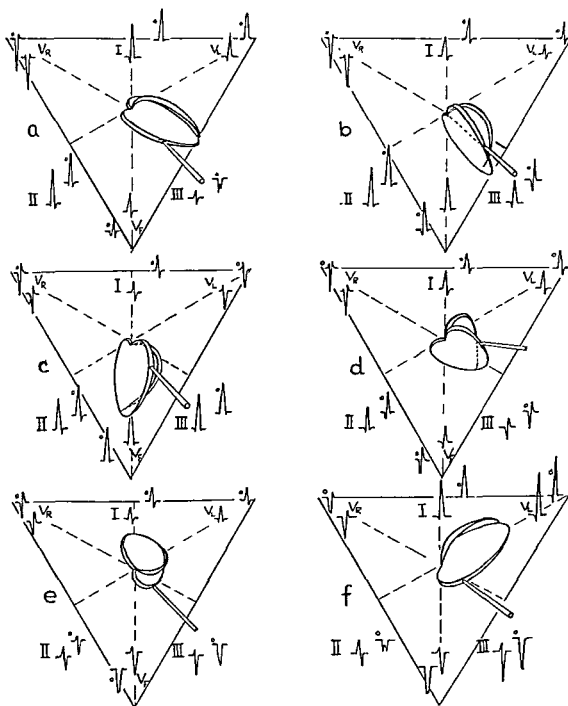


FIG. 119. *a, b, c, d, and e* depict the same cardiac positions and rotations depicted in Fig. 114, only now the infarct is in the diaphragmatic wall of the left ventricle. *f* depicts a slightly more counterclockwise rotation than that shown in Fig. 117.

tion of the 0.015-second portion of the loop increases the magnitude of its projection on the frontal plane and causes a small increase in the height of R in Lead I. If a normal spa-

tial QRS loop in this position (Fig. 119c) were subjected to a moderate degree of apex-back rotation it is apparent that the first half of the loop (0–0.04 second) would almost

coincide spatially with the corresponding portion of the infarct loop (Fig. 119c). Since such a normal loop would then have a similar shape and spatial orientation in its first half as the infarct loop of Fig. 119c it is clear that no single lead or combination of leads could differentiate the two loops.

In Fig. 119d the QRS loop is in the horizontal, apex-back, slightly clockwise position frequently seen in persons of the hypersthenic habitus and in pregnant women. Here the effect of a diaphragmatic wall infarction tends

to displace the first portion of the loop upward and a bit posteriorly, resulting in a slight decrease in the amplitude of R in Lead I, and an increase in depth and duration of Q in Leads II, III, and V_F .

Careful study of Figs. 119b, c, and d makes it possible to appreciate the magnitude of the difficulty which arises in attempting to differentiate the normal tracing from diaphragmatic infarction tracings when a clockwise rotation is present. Once again the importance of electrocardiograms before and after infarction is emphasized. In a heart in the position shown in Fig. 119c a normal Q in Lead III may not be greatly affected with the development of a diaphragmatic infarction; whereas in hearts in the position shown in Fig. 119b and d a normal Q becomes larger in Lead III and V_F with the development of a diaphragmatic infarction. It is demonstrated that a single unipolar lead (V_F) cannot be utilized to distinguish between the normal electrocardiogram and one with infarction. In a clockwise horizontal position (Fig. 119d) a normal Q of considerable depth may be present in V_F .

In this connection it is important to point out that when diaphragmatic infarction occurs without involvement of the septum the first portion of the loop (nearly to 0.015 second) probably remains unaltered from the normal

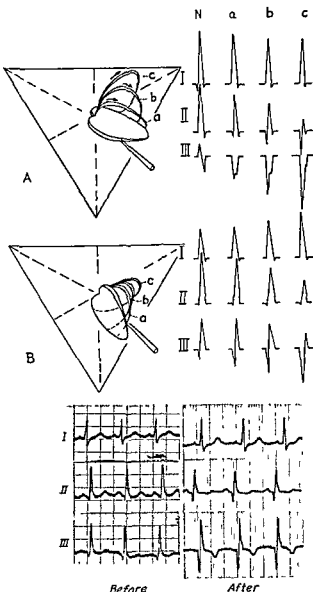


FIG. 120 The upper triangle (A) contains the normal loop in slightly counterclockwise rotation as shown in Fig. 119a. The loop a is the same infarct loop shown in Fig. 119a. Loops b and c result from increasing progressively the size of a diaphragmatic infarct. The complexes of the three limb leads designated a, b, and c correspond to the similarly labeled loops. The lower triangle (B) contains the same group of spatial loops showing the effect of clockwise rotation of the heart. It is to be noted that Q_I may not become prominent (though it would with slightly less clockwise rotation) and that R_I may increase and R_{III} become much smaller; Q_{III} becomes larger, as before. The accompanying electrocardiograms (before and after infarction) correspond to B-b.

It is to be expected that with increasing area of infarction the infarct loop joins the normal loop depicted at a later time, as shown in the figure.

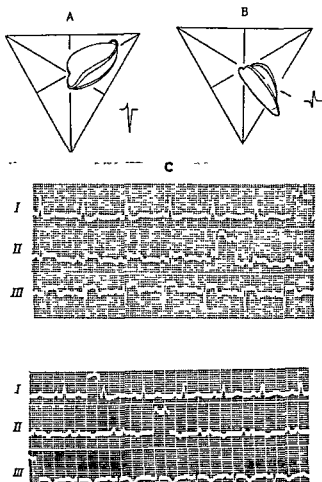


FIG. 121. QRS loops of a counterclockwise heart (A) and a clockwise heart (B), with identical diaphragmatic infarcts that do not involve the septum. The first portion of the loop (0-0.015 second) is not affected because the septum and anterior walls are not infarcted. When the heart is rotated counterclockwise the R in Lead III is retained. When the heart is clockwise the R in Lead III is lost and a Q appears. C shows serial electrocardiograms in posterior infarction with retention of R_{II} and R_{III}.

(Fig. 121). In counterclockwise hearts the R in Lead III and in Lead II would then be retained (Fig. 121c). However, when the heart is rotated clockwise the effect would be little different from that when the septum is involved, except possibly in the precordial leads.

Figure 122A depicts a normal loop in an apex-back, counterclockwise position. A diaphragmatic wall infarction in a heart with this

position (see Fig. 119e) results in a QS deflection in Lead III and V_F, a lowering of the R in Lead II, and a disappearance of the normal Q in V_L. A septal infarct in a heart with this position will result in the same limb leads; however, Leads V₁, V₂, and V₃ frequently show changes in septal infarction.

Figure 122B depicts a horizontal, apex-back, counterclockwise-rotated normal loop with the first portion of the loop bent upward. This is one type of loop which may be seen with left ventricular hypertrophy and occasionally in normal persons (Fig. 122C). A QS complex is present in Lead III and also in Lead V_F; they do not signify diaphragmatic infarction. Comparison of this loop with that of Fig. 119e demonstrates, once again, that the normal and infarction loops may differ only slightly from one another.

Thus when the tracing shows a Q_{III} (with or without a Q_{II}) it may be impossible to determine whether an infarct is present or not. Frequently the accompanying injury changes (RS-T shifts) and T wave changes are relied upon to make the diagnosis. Since T_{III} is commonly inverted when a large Q_{III} is normal only a deeply inverted T_{III} (preferably accompanied by inversion of T_{II}) is significant. Even this sign may be fallacious because a patient with a normal Q_{III} may suffer a diaphragmatic ischemia (see Fig. 157, p. 183). When R_{II} and R_{III} are large T_{II} and T_{III} may be inverted when the rate is rapid or after food (Fig. 107B) and tracings showing these effects are almost indistinguishable from some of those which are due to infarction (see Fig. 123). Serial observations during the attack is the only certain method of diagnosis in many cases.

The esophageal lead is worse than useless and is mentioned only to be condemned. If the electrode lies opposite the valve opening it is bound to show a large Q wave in the normal heart and since its position cannot be accurately determined, the lead is useless.

Finally, it is important to point out that when left ventricular hypertrophy occurs and the heart remains in clockwise rotation about

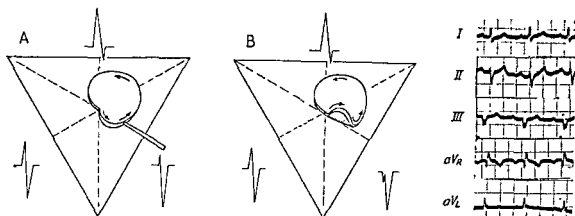


FIG. 122. *A*, Normal spatial loop in the apex-back, semitransverse, slightly clockwise position. *B*, Same loop with the initial portion turned upward slightly. Such variations in the first portion of the loop are not rare in the presence of left ventricular hypertrophy and occasionally may be seen in normal persons. The effect upon Lead III of such variations is shown and the difficulty in distinguishing such tracings from certain infarction tracings (see Fig. 119*e*) is apparent.

The accompanying electrocardiogram is from a healthy subject, and corresponds to diagram *B*.

the anatomic axis (as in rheumatic mitral insufficiency but at times in nonvalvular disease) a rather large and wide Q occurs in Lead II and III. This, as shown in Fig. 67*c* (p. 90), is due to the larger than normal first portion of the loop which occurs in left ventricular hypertrophy. With the inverted T waves which commonly follow the large R waves occurring in hypertrophy (if the gradient remains normal) the tracing is indistinguishable from that which may occur in diaphragmatic infarction.

At times following diaphragmatic infarction changes are noted in the last portion of the QRS complex. An R wave following the QS frequently appears in Lead III. One explanation offered for this phenomenon has been a delayed wave of excitation in an undamaged layer of muscle overlying the epicardial surface of the infarct. However, in some instances it seems clear that the phenomenon simply results from a change in cardiac position and rotation. In some cases such an R wave following the Q is present before infarction but disappears following it. This may be due either to a change in rotation or to the infarct itself.

Figure 123 shows electrocardiograms obtained from a patient with a diaphragmatic infarction. The heart rotation is similar to that depicted in Fig. 119*c*.

SEPTAL MYOCARDIAL INFARCTION. Figure 124 depicts the effects of a septal infarction upon the waves of excitation, the spatial QRS loop and the limb leads of the electrocardiogram. Only the left portion of the septum is involved in the infarction, as is frequently found at postmortem examination. The electrical effect of such infarction is to leave the wave of excitation normally occurring in the

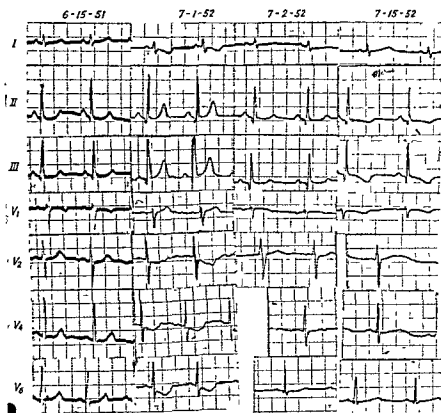


FIG. 123. Series of tracings made on the same patient before (6-15-51), during (7-1-52, 7-2-52), and after the development of what was undoubtedly a diaphragmatic infarction. There was fever, leukocytosis, and sustained drop in blood pressure. The tracing before and after infarction corresponds closely to the complexes shown for Fig. 119c. Note that except for a consistent, though not diagnostic, small increase in Q_{III} there are no QRS changes. Comparison of 7-15-52 with Fig. 107B (normal with food effects) shows that a prolonged Q-T in Fig. 123 is the only important difference.

right side of the septum unopposed. There is, therefore, a loss of vectors that contribute to the anterior and rightward direction of the first portion of the normal spatial QRS loop. Once again, however, the timing of the loop is of fundamental importance. The first portion of the loop points to the left. This results in a disappearance of the Q in Lead I and often also of the initial R in Lead III. An electrocardiographic pattern of the type described for septal infarction may be seen in left ventricular hypertrophy or left bundle branch delay with or without infarction. The precordial leads (Fig. 125) show a QS complex in V_1 through V_3 .

When *transmural septal infarction* occurs

and is massive, the first (0.005 second) vector would be absent but by 0.015 second the normal vectors would appear virtually unchanged for the reason that the effects of activation of the two sides of the septum tend to counterbalance one another and if both are destroyed there is little net effect. Thus a transmural infarction of the septum may have little discernible effect upon the QRS complexes (after the stage of injury has passed) unless it causes A-V or bundle branch block (Fig. 126) or it extends to the apex of the right ventricle. In the precordial leads the effect of transmural infarction may also be less discernible than the effect of the left sided septal infarction depicted in Fig. 125.

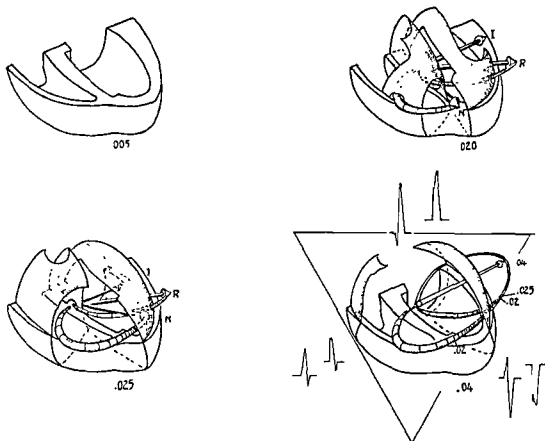


FIG. 124. Septal infarction, involving largely the left side of the septum: The effects shown are only partial if the infarct is patchy. If transmural infarction occurs the effects of the infarct may be considerably different from that shown here.

It is to be noted that with the common type of septal infarct depicted here the first rightward portion of the QRS loop is lost. This loss of the first portion of the normal QRS loop causes a disappearance of the Q_r and often of the R_{II} which normally occurs when the heart is in the counterclockwise rotation and semitransverse position shown in the figure.

Since the peak of R_1 is reached at about the same time as in the normal the upstroke of R_1 is slower than in the normal, occupying all of the time normally used in inscribing the Q. At times the slur appears at the apex of R_1 and also at the nadir of S_{III} for the same reason.

The leads on the left are the normal; those on the right result from the infarction.

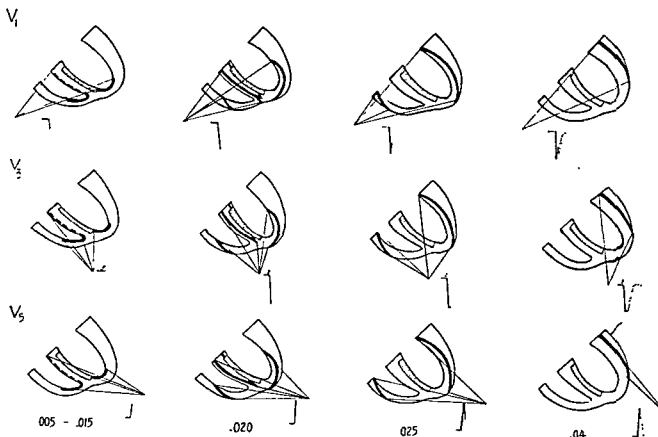


FIG. 125. The precordial leads in the common variety of septal infarction are depicted employing the solid angle approach. The initial and rapidly increasing negativity at the electrode at V_1 is shown to result from the retreating wave in the right side of the interventricular septum and in the left ventricle which is more than sufficient to overcome the positive effect of activation in the right ventricle. At V_2 the R wave is smaller for the same reason and may disappear or be notched, especially if the apex is back. At V_3 (and V_4) the disappearance of a small Q previously present is due to the same effects.

In the latter the undestroyed right side of the septum has electrical effects that tend to neutralize the effects of the right apical myocardium on the electrodes at V_1 , V_2 , and V_3 , but if both sides of the septum are destroyed the electrical effects of the wave of excitation in the apex of the right ventricle will not be neutralized. Thus a transmural or partially transmural septal infarct may retain a small R in V_1 , V_2 , V_3 .

It is important to note that such septal infarctions (which commonly extend to the anterior wall of the left ventricle near the interventricular groove) produce electrocardiograms that are indistinguishable from those of left ventricular hypertrophy with or without early bundle branch delay. In both condi-

tions there occur similar spatial loops, similar deflections in the various limb leads and in the precordial leads. V_1 , V_2 and V_3 may show QS deflections or very small R waves followed by deep S waves in both conditions. Finally, similar findings in the chest leads also occur in high anterior infarction, in right ventricular dilatation, and in chronic pulmonary disease.

Figure 127 is an illustrative set of electrocardiograms from a patient with a septal wall infarction whose heart is in the same electrocardiographic position and rotation as that of the basic diagrams.

Effects of Variations in Rotation. Figure 128 demonstrates the normal and septal wall infarct loops in their proper relation to one

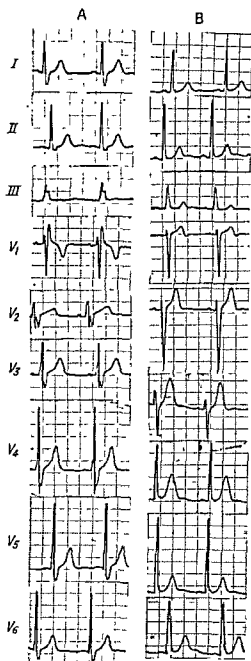


FIG 126 *A* is from a patient with severe chest pain and shock. *B* was made on the following day. Fever and leucocytosis were present. Right bundle branch block present in *A* had disappeared when *B* was obtained. It was the only detectable electrocardiographic effect of a transmural septal infarct.

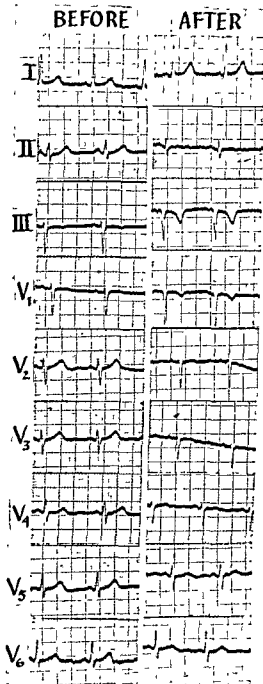


FIG 127. Electrocardiograms before and after infarction (mainly septal) when the original tracing shows that the heart was in approximately the same position and rotation depicted in Fig 124. Note the similarity of the limb leads to those following diaphragmatic infarction when the heart is in this rotation. The Q in *V*₁ and low R waves in *V*₅, *V*₆, and *V*₄ correspond to the complexes derived for septal infarction in Fig. 125. This infarct probably extends onto the anterior wall.

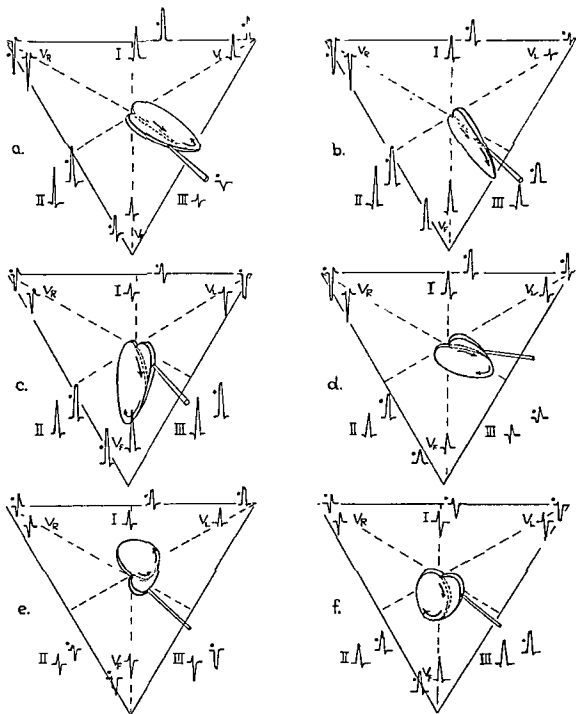
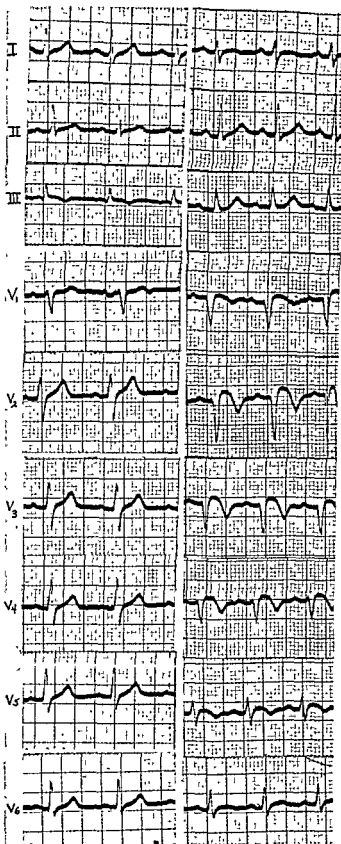


FIG.128. Normal and septal infarct loops corresponding to various positions and rotations of the heart.



another for various degrees of rotation on the three axes. The same positions of rotation have been utilized in Figs. 114 and 119, the corresponding diagrams for the previous areas of infarction. In the counterclockwise-rotated loop with septal infarction (Fig. 128a) the Q becomes smaller or more frequently disappears in Lead I and V_L and the R in Lead III becomes smaller or may be replaced by a QS. In the clockwise-rotated heart (Figs. 128b and c) the effects of septal infarction may result in a disappearance of the Q in Lead III and V_F . In addition, the initial R may disappear in V_L when the position depicted in Fig. 128c is present. When septal infarction occurs in the clockwise, horizontal, apex-back position (Fig. 128d), the Q may disappear in V_F and may become smaller or disappear in Lead III. In Fig. 128e, an apex-back, counterclockwise-rotated loop with septal infarction results in a lowering of the amplitude of the R in Lead II and V_F and the disappearance of the R in III and the Q in V_L . This is essentially the same frontal plane loop as the one depicted for a diaphragmatic infarction with the same heart position. A loop similar to that of Fig. 128e, except for clockwise rotation, is depicted in Fig. 128f. It will be noted that the Q disappears in Lead III and V_F and the R becomes smaller in Lead I and V_L .

Figure 129 shows illustrative electrocardiograms obtained from a patient whose heart corresponds to Fig. 128b.

None of the limb lead patterns mentioned above are strongly suggestive of myocardial infarction when seen on a single electrocardiogram. However, when on serial electrocardiograms the changes in QRS configuration described above occur in the limb leads, then myocardial infarction may be suggested. The

FIG 129. Electrocardiograms before and after infarction on a patient whose heart is approximately in the position and rotation depicted in Fig. 128b. The infarct extends to the anterior wall near the interventricular groove. The disappearance of Q_s , as depicted in the theoretic diagram of Fig. 128b, is noteworthy.

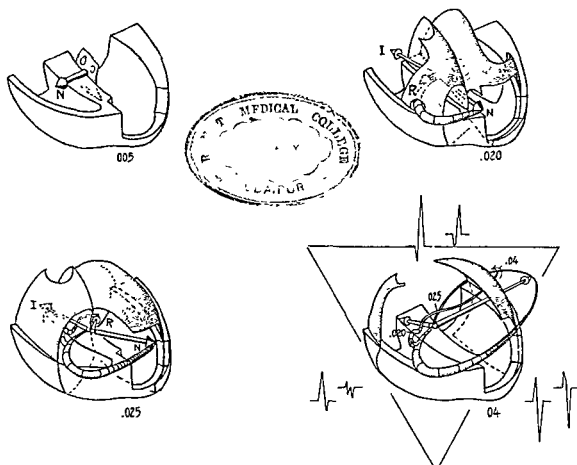


FIG. 130. The same method is employed for analysis of the effect of apical infarction as shown for infarcts in other locations. Special attention is drawn to the timing of the infarct loop. The normal complexes are on the left, the infarct complexes are on the right. A larger infarct produces a more marked effect.

confirmatory evidence is usually found in the precordial leads (Fig. 125).

APICAL MYOCARDIAL INFARCTION. Figure 130 depicts the effect of an apical infarction upon the waves of excitation, the spatial QRS loop, and the limb leads of the electrocardiogram when the heart is in the counter-clockwise rotation and semitransverse position. The first portion of the loop is shortened as a result of apical infarction, and is swung posteriorly. The frontal plane loop assumes a figure-of-eight configuration and is much narrower than the normal loop. The longer duration of the initial portion of the loop increases the duration of the Q in Lead I with slight if any increase in its depth. The short-

ening of the 0.04-second vector results in a decrease in the amplitude of the R in Lead I. The directions of the vectors at 0.015 through 0.025 second are such that there is a decrease in the R and the appearance of an early S wave in Lead II. The configuration and timing of the first portion of the apical infarction loop results in a decrease in the amplitude and increase in the duration of the R in Lead III, and a narrowing of the S wave in Lead III.

Precordial Leads. The precordial leads in the presence of an apical infarction are represented in Fig. 131. The wave of excitation at 0.005 second and the corresponding initial portions of the QRS complexes are included although the solid angles for this stage are

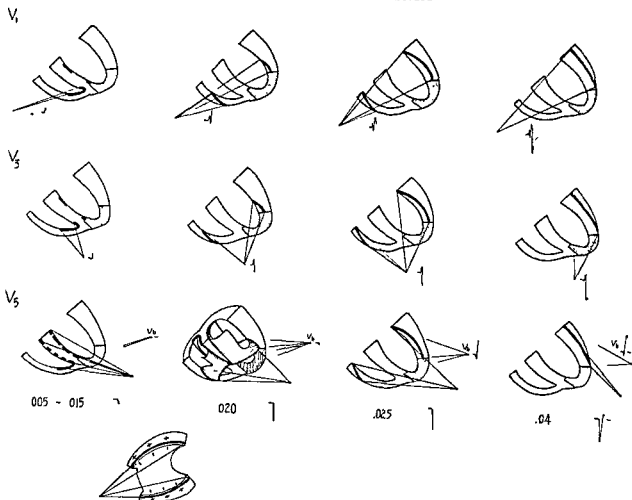


FIG 131. The precordial leads in apical infarction, using, as before, the solid angle method. The 0.020-second diagram for V_3 is drawn in three dimensions and while solid angles to all the waves of excitation are not drawn they can perhaps be visualized with the aid of the longitudinal diagram of the left ventricle below the figure. That the electrode faces a good deal of negative surface and little positive surface is evident.

not drawn Visualization of the solid angles for the 0.015-second stage at the V_3 position is very difficult. Inclusion of the incomplete septal waves of excitation in the diagram is necessary for discussion of the potential developed at V_3 at this time. The very approximate method of analysis employed indicates that there are two opposing effects, the positive solid angle to the wave of excitation in the apex of the right ventricle and the patchy wave of excitation on the right side of the septum opposing the negative solid angle to the less patchy wave of excitation on the left

side of the septum. The latter is represented as producing the greater effect in the diagram because the wave of excitation on the left side of the septum is less patchy than that on the right side of that structure even though the negative solid angle, as drawn, is smaller than the positive solid angle. However, the right-sided effects may at times be the greater and the deflection at this stage may be positive, though smaller than normal. Unless the interventricular septum is involved (see *septal infarction*) these right-sided effects cause a retention of the initial R wave in Leads V_2

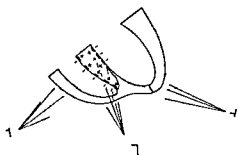


FIG. 132. An apical infarction with transmural involvement of the apex of the septum extending up the left side of the septum. An initial negative deflection occurs at V_2 because of the septal effects (as in septal infarction) but an R may not follow, especially if conduction to the apex of the right ventricle is slightly delayed by the infarct or if the apex of the right ventricle is infarcted. If neither of these events occurs an R may follow the Q.

and V_3 (see diagrams for V_3 in the figure).

If the apex of the septum and of the right ventricle are involved the net effect at 0.015 second is seen to be an initial negative potential (Q wave) in most of the precordial leads. If the infarct is not large the Q may be followed by an R in these leads (Fig. 132).

At 0.02 second the diagrammatic representation of Fig. 131 shows a secondary positive deflection in V_1 which is due to the lateral extension of the infarct. This is not a common finding with strictly anterior infarcts. In V_3 reduction of the R wave is not difficult to visualize if one compares the diagram with the corresponding one for the normal (see Fig. 23, p. 33). The 0.02-second stage for V_3 is drawn in three dimensions and while solid angles are not drawn to all of the waves of excitation they can perhaps be visualized with the aid of the longitudinal diagram of the left ventricle shown in the lower part of the figure. That the electrode faces a great deal of negative surface and little positive surface is evident. This causes a deep negative deflection in the QRS complexes at V_4 and V_5 at this time.

If an apical infarct is not large and does not extend as far laterally as is shown in the diagram of Fig. 131 but is confined to the region adjacent to the interventricular groove

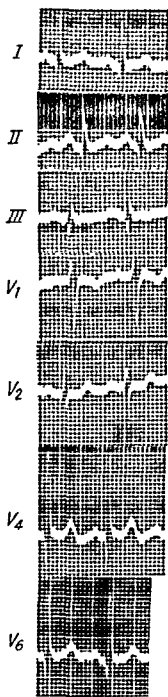


FIG. 133. Normal electrocardiogram with Q waves in V_2 , V_3 , and V_4 .

and does not involve the septum the 0.015-second stage would be as shown in the diagram. However, at 0.02 second the waves of excitation depicted for the normal would be

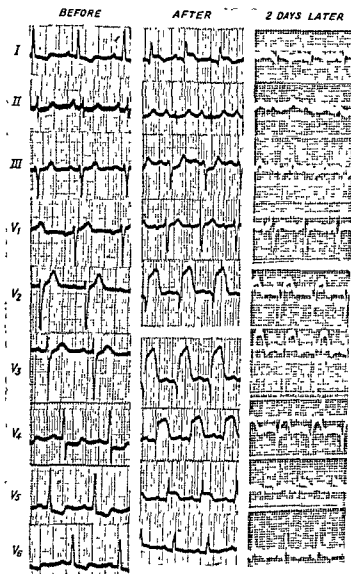


FIG. 134. Electrocardiograms before and after infarction of the apical portion of the left ventricle of a patient whose heart was in approximately the position and rotation as Fig. 130. The infarct extends a bit more into the lateral wall than shown in Fig. 130, causing the loop to shorten more. The close correspondence of both the limb leads and the precordial leads to those shown in Figs. 130 and 131 is evident.

little affected by the infarct because the area infarcted is normally so quickly penetrated by the wave of excitation. The waves of excitation at 0.025 second and all succeeding stages would not be affected at all. Therefore, it is theoretically possible for an apical infarct

that is confined to the region adjacent to the interventricular groove to produce little or no detectable change in the QRS complexes of the precordial leads. If such an infarct extends into the apex of the septum and involves or delays conduction into the apex

of the right ventricle a very small Q wave may appear in precordial leads V_2 , V_3 , and V_4 . Unfortunately such a small Q may at times be seen in the normal (Fig. 133). If the usual septal infarction is combined with such an infarct we have the very common "anteroseptal" infarct producing electrocardiographic changes that are due largely to the septal involvement (see *septal infarction*). It is important to note that without the more extensive septal involvement apical infarctions confined to the region adjacent to the interventricular groove also produce little changes in the QRS complexes of the limb leads, and may therefore be "silent" in the electrocardiogram. This has been verified at autopsy.

If an infarct in the apical region is not very large one may find no diagnostic Q waves in the precordial leads but the R waves may be reduced sufficiently to arouse suspicion of the presence of infarction. If the R wave in V_6 is large the tracing is like that of left ventricular hypertrophy. If it is not the tracing may be indistinguishable from that of chronic pulmonary disease. At times such a tracing may be due to high anterior infarction and this may be detected by exploring the chest at a higher level. Not infrequently a patchy infarct of fairly extensive distribution produces the same type of tracing.

Figure 134 is an illustrative set of electrocardiograms from a patient with an apical wall infarction whose heart is in the same position and rotation as that of the basic diagram. Figure 135 is another.

Figure 136 shows the normal and infarct loops in their proper relation to one another for various degrees of rotation on the three axes. With the loop counterclockwise (Fig. 136a) there is an increase in the duration of the Q in Lead I, II, and V_L . With the loop clockwise (Fig. 136b) there is an increase in the duration of the Q in Leads II, III, and V_F , and a small M- or W-shaped QRS configuration in Lead I. With the apex-back, intermediate, counterclockwise heart position (Fig. 136c) a W-shaped complex appears in Lead I and the normal Q in V_R is markedly

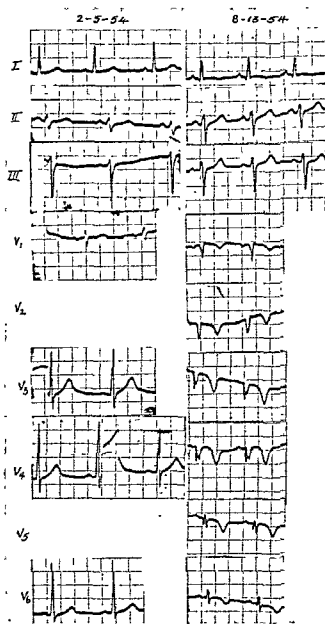


FIG. 135. Left, before, and right, after apical infarction that does not extend to lateral wall of the left ventricle to as great an extent as depicted in Fig. 134. QRS changes in the limb leads are minor but the appearance of Q_1 which was not present before is significant.

decreased in amplitude. Figure 137 shows electrocardiograms before and after infarction which correspond to Fig. 136e.

High Anterior Infarction. All of the infarcts presented thus far, except the diaphragmatic, have been orientated so that the infarct

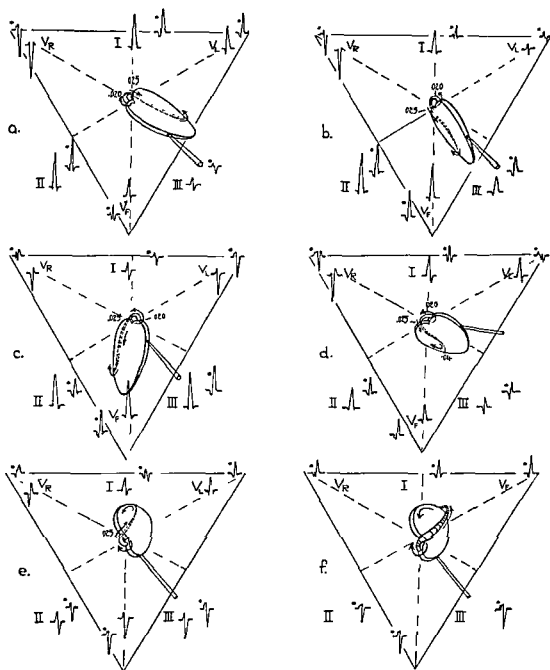


FIG. 136. The QRS loop in apical infarction. The positions and rotations are the same as those which were employed for other areas of infarction, with the exception of *f*, where the position and rotation is identical with that of *e* but an apical and diaphragmatic infarct is depicted.

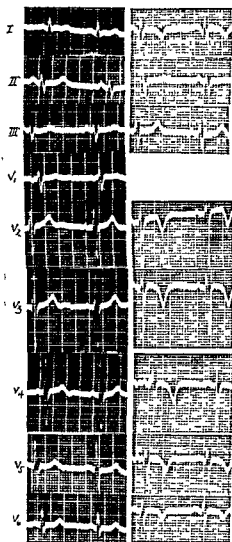


FIG. 137. Electrocardiograms before (left) and after (right) apical infarction from a patient whose heart was in approximately the position and rotation depicted in Fig. 136e. Note the close correspondence of the QRS complexes to those depicted in Fig. 136e. The small R waves in the precordial leads are of the same significance as Q deflections when the left ventricle is hypertrophied (as here) and the infarct is patchy. At times they result from a low placement of the electrodes.

vector lies in the plane of the QRS loop. It is important to point out that infarction occurs high in the anterior wall of the left ventricle as well as in combined locations. An infarct in the high anterior lateral area A of Fig. 140

(but extending laterally) is depicted in the series of diagrams shown in Fig. 138. The effect is similar to that of the lateral wall infarct shown in Fig. 111 except that the infarct loop deviates downward and backward from the plane of the normal loop. The loop cannot be drawn on the basic diagram but is presented as the loop of Fig. 140, ③. These infarcts may be missed on the precordial leads unless the electrodes are placed at a level higher than that usually employed (Fig. 139). Actually such an infarct may be suspected from the limb leads if one thinks in terms of the loop and if the R waves in the precordial leads, V_1 , V_2 , V_3 , and V_4 , are small. If they are small in V_5 and V_6 the suspicion of infarction should be very strong. If only V_1 , V_2 , V_3 , and V_4 have small R waves the tracing may be indistinguishable from that of left ventricular hypertrophy without infarction (as described for apical infarction). Precordial leads made one interspace higher may reveal infarction (see Fig. 139). However, it should be remembered that if the electrode is carried too high toward the left upper chest the precordial electrocardiogram approaches that of the left shoulder (V_L) and since this lead may normally show a deep Q (vertical hearts and vertical apex-back hearts) errors will be made because of empirical interpretation of such high precordial leads. The same principle applies to inverted T waves.

Figure 139 shows illustrative electrocardiograms obtained from a patient whose heart position corresponds closely to Fig. 138.

INFARCTS IN COMBINED LOCATIONS. The majority of infarcts are not confined to the distributions presented in the preceding basic diagrams but are found in combinations of such locations. Figure 140 is a diagram of the ventricles showing various common areas of infarction, A, B, C, D, E, and F. The numbered loops ①-⑥ show the normal and infarct loops for infarction in combinations of these areas. For the most part each area has its effect. However, the presence of septal infarction does not always have the same

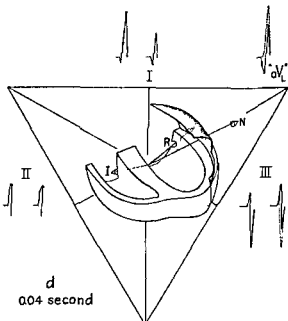
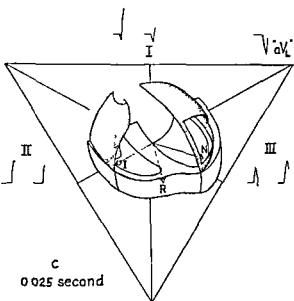
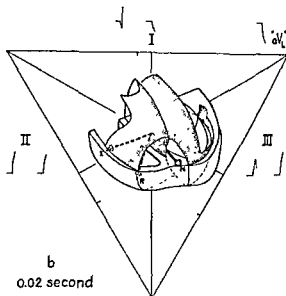
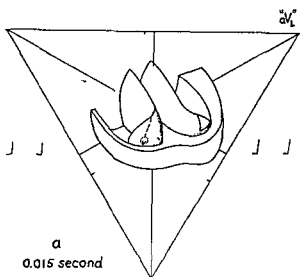


FIG. 138. High anterolateral infarction. The vector loop is not drawn because of technical difficulty. The loop begins normally (a) but at 0.02 second the presence of the infarct causes the vector to point downward and somewhat to the right. This prolongs the Q in Lead I and the R in Lead III. The latter is also made to be higher than it was before infarction. At 0.025 second the resultant vector is directed largely downward and somewhat to the left. It may also be pointing somewhat backward at this time. The upstroke of R_I is beginning (late) and R_{III} is still being inscribed at a time when normally the S_{III} has begun. At 0.04 second the resultant vector is shorter than the normal vector of the same timing but the downward effect of the infarct upon its direction is much less than in previous stages because of the spatial orientation of the defect.

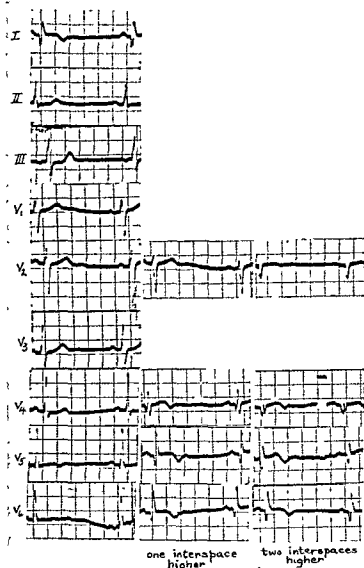


FIG. 139. High anterolateral infarction with no Q waves in conventional precordial leads. One interspace higher, wide Q waves are encountered. All the leads shown were made at the same sitting. The Q in I and the wide R in III followed by an S are diagnostic.

simple effect, for the infarct may be largely leftsided, or transmural.

A study of the various loops of Fig. 140 shows how infarction in various combined locations may result in frontal plane loops and therefore limb leads that are quite similar, even in timing, to loops produced by infarction in other locations. Compare Fig. 140, ① and Fig. 140, ②. The spatial loops are, as indicated, different since the early ascending

limb of the loop ③ dips down and backward; yet the frontal plane projections of the two loops are indistinguishable.

Figure 140a represents the loops before and after infarction in a patient whose transverse, apex-back, counterclockwise heart sustained an infarction in areas E, A, and B. The electrocardiograms are shown in Fig. 141.

Figure 140b represents the loop before and after infarction in the septum (F), anterior

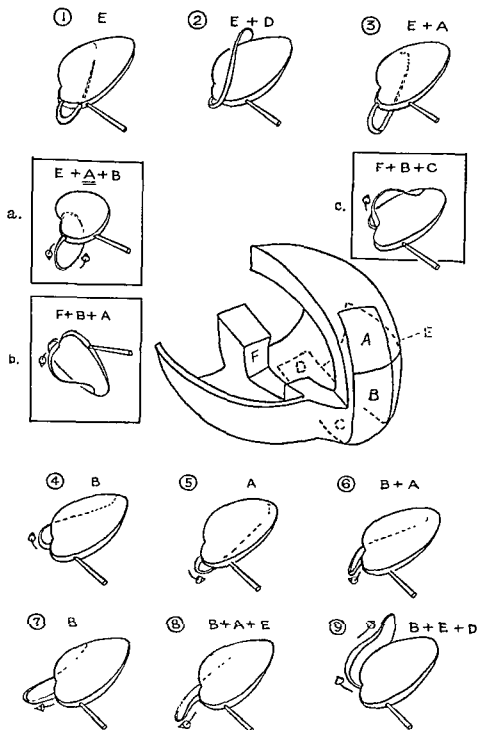


FIG. 140. Cutaway drawing of ventricles showing common locations of infarcts. The numbered diagrams are for infarction in the area or areas designated by the accompanying letters. All represent counterclockwise semitransverse rotation of the heart as indicated by the normal loops of the diagrams. If the reader will attach a piece of wire to the model of the normal spatial loop and bend it into the shape and orientation of the infarct loop desired he can study the effect of changing the anatomic axis and of rotating the heart about the anatomic axis.

a, b, and c represent the normal loop and infarct loops for the cases whose tracings are seen in Figs. 141, 142, and 143 respectively.

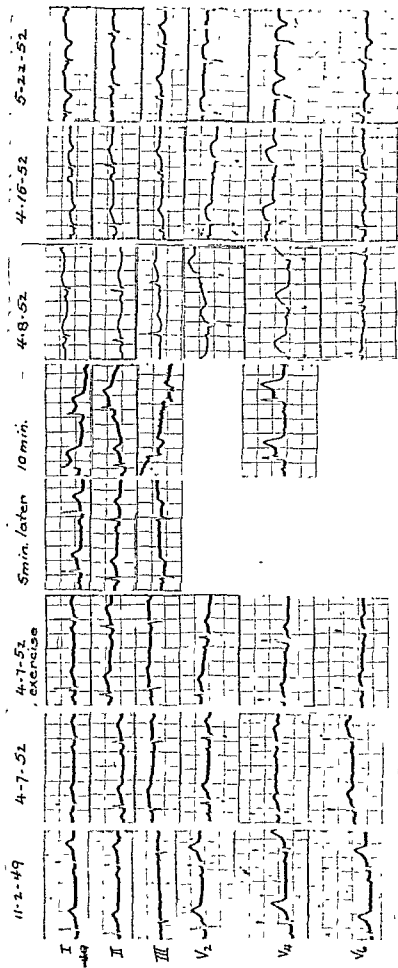


FIG. 141. Electrocardiograms made before, during, and after infarction of high anterolateral (area A of Fig. 140) lateral (E), and anterior (B) portion of the left ventricle. Diagram a of Fig. 140 was drawn for this set of tracings.

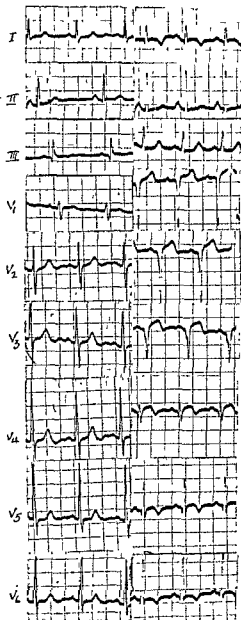


FIG. 142. Electrocardiograms made before and after infarction of the septum (F of Fig. 140), the anterior (B), and high anterior portions of the wall of the left ventricle. See diagram b of Fig. 140.

(B), and high anterior (A) portion of the left ventricle. The electrocardiograms are shown in Fig. 142.

Figure 140c represents the loops before and after infarction in a patient whose counter-

clockwise hypertrophied heart sustained an infarction in the areas F, B, and C. The anterior wall was infarcted (B) and the infarct extended into area C (the diaphragmatic wall) and also involved the septum. The electrocardiograms are shown in Fig. 143.

It is evident, when one infarction is followed by another, that the combined effect of the two produces the net result. The effect upon the spatial QRS loop is easily analyzed as depicted in Fig. 140. However, the effect upon the precordial leads is, at times, not a simple matter. With an infarct that involves the diaphragmatic and apical portion of the left ventricle the limb leads frequently show the deep Q_{III} and Q_{II} , typical of diaphragmatic infarction and the precordial leads show the typical findings of the apical or anterior portion of the infarct. These two areas of infarction, although they are frequently called "posterior" and "anterior" respectively, do not necessarily oppose one another electrically. At other times, however, the electrical effects of one area of infarction may be opposed by those of another. This is best seen when a second infarction occurs (Fig. 144). This patient first suffered an anterior infarction (11-22-52) and some time later had a large diaphragmatic wall infarction which more than counterbalanced the effect of the apical infarction on the left precordial leads.

VARIATIONS IN INJURY PHENOMENA WITH AND WITHOUT INFARCTION. The foregoing description of myocardial infarction employs the simplest possible concept of the injured state and the simplest possible presentation of the QRS effects and residual T wave effects. Considerable experience with the electrocardiogram in injury and in myocardial infarction makes it clear that some additional discussion is necessary.

It seems clear that most injury that later confirms its location by becoming infarcted may be represented as shown in Chapter 6. The limb leads and the precordial leads show RS-T shifts that correlate well with the concept of mainly epicardial injury depicted in the simple diagrams of Figs. 48 and 50.

(Chapter 6), and with the representation shown in Fig. 54 for lateral wall injury and in Fig. 55 for diaphragmatic wall injury. However, in some cases the effect of injury may be more marked at the *endocardial* surface of an area that soon undergoes transmural infarction. In such cases the RS-T shifts are opposite in direction to those that commonly precede infarction in this area (see Fig. 53). Again, it is quite common for persons with angina to exhibit electrocardiographic findings during attacks (and sometimes between attacks) which suggest endocardial ischemia, and yet, when they subsequently suffer infarctions, the electrical effects are typical of epicardial injury.

It appears that the injured state in any cell and even in a large area is reversible. It must also be true that commonly the injury is transmural and the external electrical effects depend upon which surface is most injured.

The reversibility of the injured state make it possible for the electrical effects to become completely reversed within a short period of time or to show complete recovery from the injured state. This concept is depicted in Figs. 145 and 146. Figure 145 represents the injured area in the resting state; the dipoles are those which account for the current of injury. According to the conventional theory described in Chapter 6 the number of dipoles per unit area on any border of an injured area varies inversely with the degree of injury of the cells at that border. Since the two borders *x* and *y* are continuous with normal muscle they carry the normal distribution of dipoles.

Figure 145a represents an area of early injury following the conventional description; the endocardial surface is relatively uninjured. The RS-T shift recorded at the electrode *P* is upward. If the injury becomes more severe

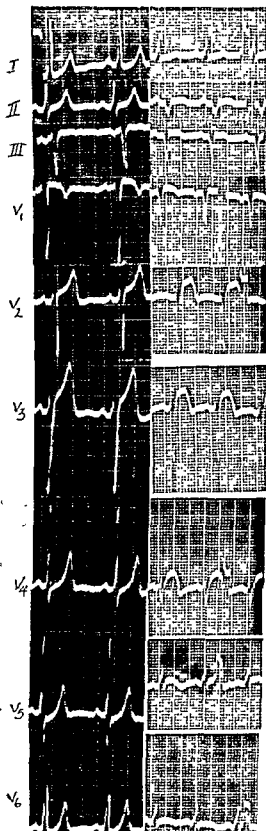


FIG. 143. Electrocardiograms made before and after infarction of the diaphragmatic (area C of Fig. 140), the anterior (B), and septal (F) portion of the walls of the left ventricle. Diagram c of Fig. 140 was drawn for this set of tracings.

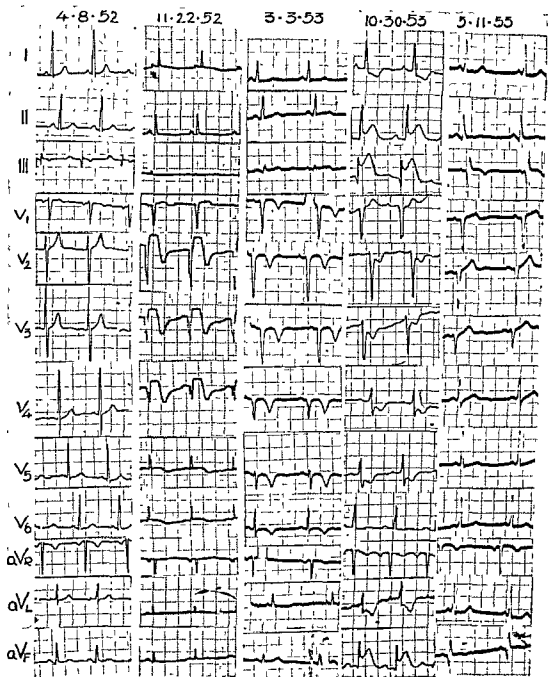


FIG. 144. 4-8-52, Tracing before infarction (Lead III is upside down). 11-22-52, Injury tracing during anterior infarction. 3-3-53, Tracing made following anterior infarction Note Q waves in V₂, V₃, V₄, and V₅. 10-30-53, Injury tracing during diaphragmatic wall infarction. 3-11-55, Tracing following the diaphragmatic infarction. On both 10-30-53 and 3-11-55 it may be seen that the occurrence of the diaphragmatic infarction caused a return of the R waves in V₂, V₄, and V₅.

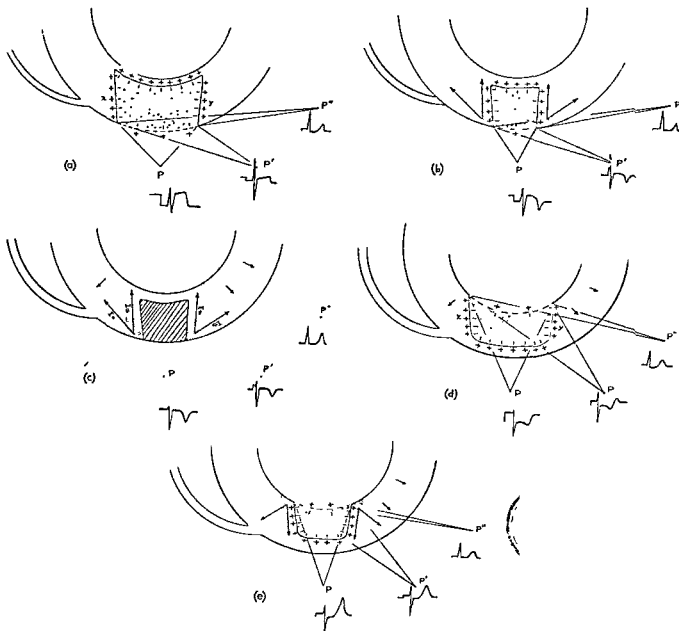


FIG. 145. Variations in injury phenomena. (a), Classical representation of myocardial injury due to coronary occlusion. The dipoles at the epicardial surface are fewer in number because here the surface is injured. The borders x and y and the border near the endocardial surface are bounded by normal muscle so that here the normal number of dipoles is present.

(b), Here the periphery of the injured zone has improved except at the epicardial surface. This peripheral zone is now ischemic (Fig. 54), and the ischemia is greatest in the area which was most injured (near the epicardial surface). The vectors of the drawing represent the predominant repolarization potentials and correspond to the ischemic vector I_s of the fundamental diagram (Fig. 54).

In both (a) and (b) the RS-T shifts depicted in the leads drawn are those expected if we apply solid angle analysis to the epicardial margins of the injured zone. Each solid angle represents two solid angles of identical geometric size, one positive and one negative (e.g., at the electrode P the positive solid angle derives from the epicardial surface of the injured zone, the negative solid angle from the continuous border represented by x , the endocardial border of the injured zone, and y). Since the latter have more dipoles per unit area the negative solid angle is the more effective and the resting potential at P is negative; therefore the RS-T shift is upward. At P'' the opposite is true.

In (b) the ischemic vectors produce inverted T waves following the RS-T shifts.

(c), Classical representation of infarction with Q waves or very small R waves and inverted T waves.

(d), Classical representation of "endocardial" injury sparing the epicardial layers.

(e), Classical representation of "endocardial" injury and peripheral margin of ischemia.

The same methods of analysis are applied to d and e that were employed for a and b .

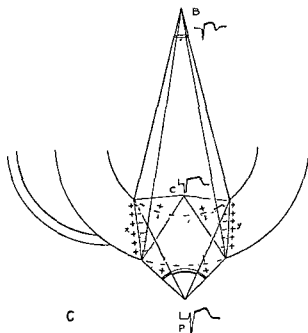
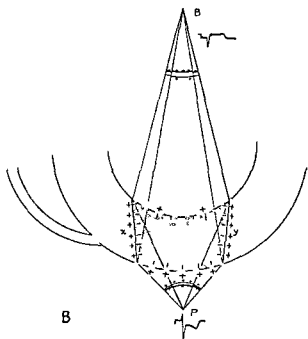
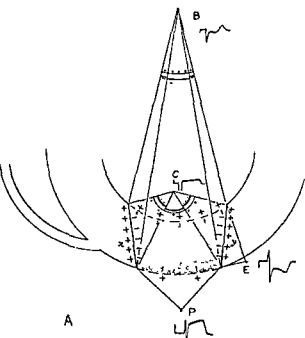


FIG 146. *A*, Concept of transmural injury involving both the endocardial and epicardial surface but the latter to a greater degree. The effect upon electrodes at *P* and *E* is rather obvious, differing little from that seen in Fig 145a.

The effect upon an electrode at *C* (intracavity) requires proper weighting of geometric solid angles to *x*, *y*, the epicardial surface, and

the endocardial surface. The net injury effect here is depicted as negative (so that the shift is upward) largely because of the powerful negative effects of borders *x* and *y*, which are great enough to overcome the positive effects of the endocardial surface of the injured zone. The weak effects upon this electrode of the epicardial injury currents are also negative. However, the relative degree of injury of the endocardial and epicardial surfaces, the short circuiting effect of the blood, and the shape of the injured zone are all variable factors which affect the net injury potentials. The author does not subscribe to the notion that injured or infarcted zones confine themselves to the regular or irregular wedge-shaped designs depicted in the figures. He employs them only for sake of simplicity of description.

The distant electrode *B* (on the back) is represented as recording an injury potential opposite in direction to that recorded at *C* simply because the distance causes the geometric solid angles to *x* and *y* to diminish greatly in relation to the geometric solid angle to the endocardial surface of the injured zone. Here again a slight difference in the shape of the injured zone would have a marked effect.

B, Transmural injury greater at the endocardial surface than at the epicardial surface.

C, Transmural injury with endocardial and epicardial surfaces equally involved. Note that virtually all of the effects are exerted by borders *x* and *y*. Here also the shape of the injured zone would make some difference.

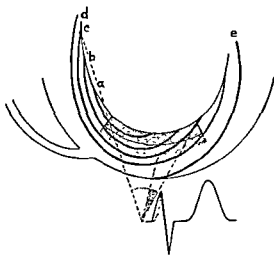


FIG. 147. Endocardial infarction is represented by the stippled area. *a*, *b*, *c*, *d*, and *e* are successive waves of excitation. The dashed lines embrace solid angles to the same wave of excitation *c* before and after infarction. The portion of the solid angle destroyed by the infarct is stippled. Applying this same method to all of the waves of excitation leads to the result that the R wave at *P* would begin a bit later and possibly its ascent would be a bit slower but this would be difficult to detect in precordial leads made with present-day equipment.

Similarly, a thin layer of epicardial infarction might produce only a quicker downstroke of the R and an intramural infarct might produce a notch.

the situation may change rapidly to that represented by Fig. 146*b* in which the entire thickness of the ventricular wall is more injured than before but the endocardial surface has suffered the most. The RS-T shift is now downward.

Let us now suppose that the injury remains more severe at the endocardial surface but recovery occurs at the periphery so that the areas bordering the now smaller area of injured muscle are ischemic and that this ischemia is more severe near the endocardial surface than at the epicardial surface (as one might expect under the circumstances described). This state of affairs is depicted in Fig. 145*e*. The RS-T shift is now downward and the T wave (resulting from the bordering areas of ischemic muscle) is large and upright.

If, starting with the state of affairs depicted

in Fig. 146*b*, recovery occurs more rapidly at the endocardial surface the situation depicted in Figs. 146*a* or in 145*b* may result. Here we again have an upward direction for the RS-T shift and in Fig. 145*b* an inverted T wave. Most commonly the situation depicted in Figs. 145*a* or 146*a* changes to the one shown in Fig. 145*b*. However, considering the reversibility of the injured state it should not be surprising to find that conditions of injury and ischemia have changed rapidly from those represented in any of the diagrams of Figs. 145 and 146 to those represented in any of the other diagrams of those figures. Furthermore, any of the conditions represented may also change rapidly to one of apparent complete recovery on the one hand or to infarction (Figs. 145*c* and 147) on the other.

Figure 146*c* represents a segment of transmural injury in which both endocardial and epicardial surfaces are *equally* affected. The effect of the *x* and *y* borders as well as of the endocardial and epicardial border are analyzed by the solid angle method. It is seen that the precordial leads over the surface of the injured zone would show an upward shift of the RST segment while an electrode off the margin of the injured zone would show a depression of the RS-T segment.

Figure 147 is a diagrammatic representation of an area of endocardial infarction with a neighboring zone of endocardial ischemia. Since the epicardial layers of muscle are not infarcted their depolarization produces QRS effects which are recorded at the precordial electrode as an R wave. The precordial lead, therefore, shows only the T wave changes due to the bordering area of ischemia. The question regarding the production of recognizable QRS changes (in any lead) by infarction of the endocardial layers of muscle is not yet completely settled. If the endocardial layers of muscle normally produce no recognizable electrocardiographic effects (Prinzmetal)—due possibly to penetration of the Purkinje network through a considerable portion of the thickness of the ventricular wall—then

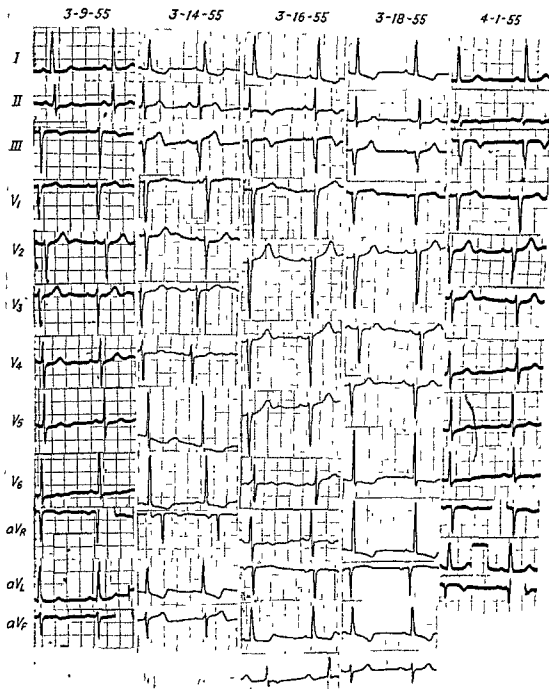


FIG. 148. Rapid appearance and disappearance of injury effects 3-9-55, Electrocardiogram made just before onset of series of chest pains 3-14-55, Electrocardiogram made after chest pains lasting several hours. Note injury shifts, especially in limb leads. 3-16-55, Injury changes disappearing; effects of ischemia are evident. T_{II} and T_{III} are inverted and the Q-T is long (aV_F is mounted upside down). 3-18-55, With another attack of pain injury changes recur. 4-1-55, Injury changes have disappeared; some ischemic changes remain. These disappeared within a few weeks.

No fever and no leukocytosis occurred. The sedimentation rate remained normal.

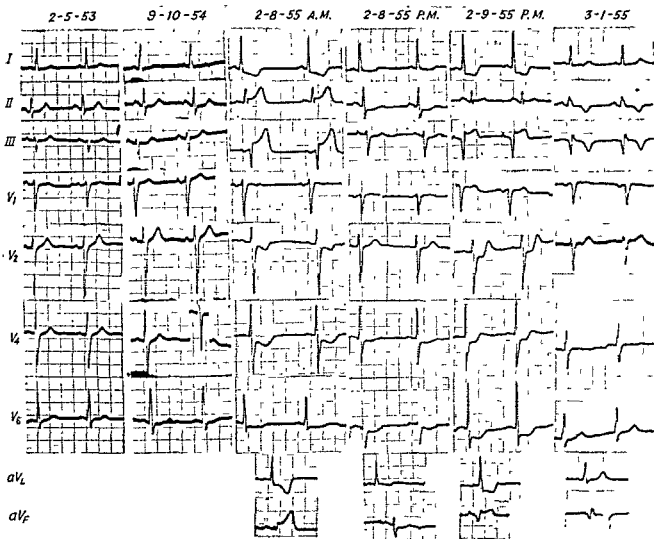


FIG. 149. Appearance, subsidence, and reappearance of injury followed by infarction. Patient had had previous difficulty. On 2-8-55 *A.M.* severe pain in chest occurred. By that afternoon (2-8-55 *P.M.*) the injury effects had largely disappeared. On 2-9-55 *P.M.* another pain in the chest occurred which was no more severe nor more prolonged than that on the previous day. Injury effects reappeared together with QRS signs of diaphragmatic infarction.

infarction of this layer produces no QRS changes. On the other hand, what prevails in the dog may not prevail in man and the difficulty in recognizing endocardial infarction may reside in the fact that, as described above, the QRS changes are necessarily so small as to be difficult of discernment under any circumstances. They are "covered up" by the overlying uninfarcted layers of muscle.

It may be well here to present a few cases that illustrate some of the phenomena described in the above discussion:

Figure 148 shows a series of tracings on a patient who was hospitalized because of a series of rapidly repeated pains in the chest. The rapid appearance and disappearance of the injury effects illustrate their reversibility. No fever, no leukocytosis, and no change in sedimentation rate occurred.

Figure 149 shows a series of tracings on a patient who had had one coronary event (5-7-48). Seven years later he had severe pain in the chest with injury effects in the electrocardiogram (2-8-55 *A.M.*) followed

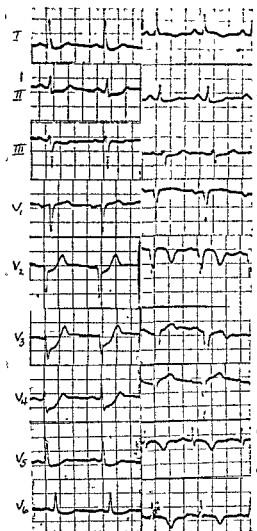


FIG 150. Endocardial injury followed by infarction. The first tracing was made during severe chest pain. The large downward shifts of the RS-T segments indicate predominantly anterior subendocardial injury. The second tracing made 24 hours later indicates that the lesion had progressed to transmural anterior infarction.

by rapid recovery. Twenty-four hours later the injury effects again occurred following another severe pain no greater nor of longer duration than that of 2-8-55. This time, however, infarction followed (2-9-55 P.M., 3-1-55).

Figure 150 shows two tracings made twenty-four hours apart following severe chest pain. The first is typical of endocardial

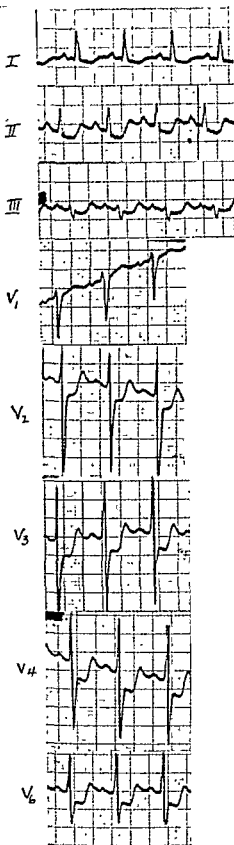
injury and ischemia (or possibly endocardial infarction has already begun). The second tracing shows the typical findings that occur in transmural infarction. Figure 151 shows a similar tracing followed rapidly by death. Autopsy showed extensive infarction, chiefly of the endocardial layers of muscle.

In some instances a pain in the chest may occur, with an abnormal injury tracing appearing only after normal tracings have been recorded over a period of several days. This is probably due to the fact that in the earlier period the injury is entirely intramural and fails to reach the surface. Under these circumstances it can produce no external electrical effects unless it interferes with conduction. When the injury finally extends to the surface it produces effects. It is also necessary to consider the possibility that injury occurs that never reaches the surface and that may then go undetected. It is probable that in some cases the injury does not reach the surface for a period of time but a surrounding area of ischemia does extend to the surface and produces ischemic T waves. Evidence of infarction may appear in the following tracing (Fig. 152). The injury changes were missed because tracings were not made at sufficiently frequent intervals.

It seems apparent that reversible injury may actually be so severe that the affected area of muscle remains depolarized to such a degree that no appreciable QRS effects are derived from that area for several days. It is otherwise difficult to explain the rapid reversion to normal of QRS changes characteristic of infarction that are seen in some cases.

In some cases, notably in persons with ventricular aneurysms (but not exclusively), the injured state seems to remain as a chronic condition (Figs. 153a and b). This phenomenon may be mimicked by the effects of digitalis and of hypertrophy of the left ventricle.

On occasion the injury shift has less the appearance of an RS-T shift than that of a prominent T wave (Fig. 154, 4-20-55). Again



at times it is impossible to distinguish the effects of digitalis from injury effects (Fig. 155). It may also be difficult to distinguish injury shifts from RS-T shifts due to left ventricular hypertrophy, and to left bundle branch block. These and pericarditis will be discussed later.

In the evaluation of injury shifts it is important to realize that nonpathologic shifts tend to be proportionate to the magnitude of the QRS deflection and of opposite direction in most leads (with some exceptions). Thus when even a small RS-T shift occurs following a small QRS deflection it is a matter of more importance than when a similar shift follows a large QRS deflection.

When ventricular premature beats occur in injury tracings the injury shift tends to be the same for the premature beats as in the sinus beats except when a large R or S deflection (in terms of area) occurs in the premature beat in such a direction that the RS-T shift associated with it opposes or enhances the injury shift (Fig. 156).

T WAVE CHANGES FOLLOWING INFARCTION. As described in Chapter 6, when myocardial infarction occurs following injury the disappearance of the injury shifts is generally accompanied by the appearance of QRS changes and T wave changes (see Fig. 54, p. 75). The T wave changes that occur in

FIG. 151. Tracing made during severe chest pain showing marked downward shifts of the RS-T segment in almost all leads, characteristic of diffuse subendocardial injury. See theoretical diagrams of Figs. 53 and 146b. Death followed shortly. Autopsy revealed that "the anterior, lateral and posterior walls of the left ventricle show a light and dark red mottling through the thinner portions of the epicardium. The left ventricle is 12 to 13 mm. in thickness. The anterior, lateral, and posterior walls of the left ventricle and the left half of the interventricular septum show complete infarction as exhibited by softening and a red mottling with slight roughening of the underlying endocardium. The only portion of the ventricle excluded from the infarction are the upper or basal 1 cm. on the posterior wall and the upper or basal 5 cm. on the anterior wall. The infarction extends up the interventricular septum to within 2 cm. of the atrio-ventricular junction."

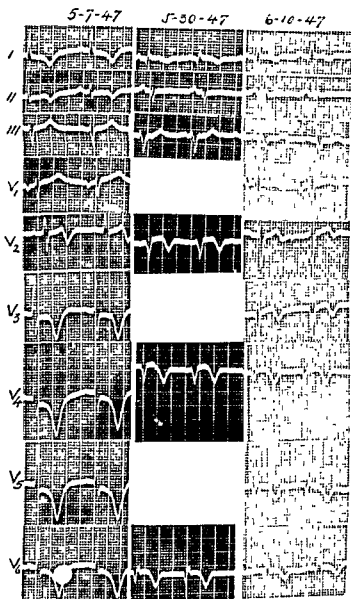


FIG 152 Progression from ischemic to infarction tracing
 Few symptoms occurred following tracing of 5-7-47 and very probably the injury changes might have been recorded if tracings had been made more frequently. Such a change as occurred between 5-7-47 and 5-30-47 may indicate that it is not improbable that intramural injury was present on 5-7-47, at which time only the epicardial ischemia produced effects in the electrocardiogram

infarction are largely due to ischemia in the region surrounding the infarcted muscle. The ischemic zone may be at the margins of the infarcted area or the ischemic effects may result from the relatively greater recovery of the endocardial layer of muscle subjacent to the infarct and lesser recovery of a layer of muscle overlying the epicardial surface of the infarct. Both sources of ischemic T wave effects may be present.

Following infarction the T wave changes may persist or may disappear within several weeks or months. They are commonly not evident after one year. When this occurs it may be difficult or impossible to recognize the tracing as abnormal, for the QRS changes (which are more persistent) may not be sufficiently characteristic. As has been described in detail, the recognition of infarction from QRS changes alone is not infrequently very difficult or impossible. This is most commonly true of diaphragmatic infarction (q.v.). Figure 157 is a series of tracings from such a patient. Of course, the diagnosis of infarction should not be based upon T wave changes alone. While it is common practice to regard the T wave changes as additional presumptive evidence of infarction when the QRS complexes are compatible, this practice may lead to error. The tracings of Fig. 157, 1-26-51 show changes typical of diaphragmatic infarction. However, the previous tracings show that the QRS changes were present long before the attack occurred. Furthermore, there was no fever, leukocytosis, or other clinical evidence of infarction and the attack undoubtedly was an episode of ischemia. The writer has no way of knowing whether an infarction had occurred prior to the time the patient came under his observation. Obviously ischemic T waves can occur in other types of tracings that are indistinguishable from those of infarction (left ventricular hypertrophy), and may lead to the same error.

It is well to point out that if an infarct is large recovery of all of the ischemic muscle may leave the T wave axis in an abnormal direction because a large area of ventricular

wall which has undergone transmural infarction cannot produce T effects. The absence of T effects from a large area should alter the direction of the T axis in the same way that the absence of the depolarization effects alters the QRS loop and deflections. This may furnish part of the explanation of the permanence of the T wave changes in some cases, though the problem is complex.

Furthermore, it should be pointed out that the disappearance of the T wave changes following infarction (especially of the diaphragmatic wall) does not necessarily mean that the T wave axis has returned to the normal magnitude and direction for that patient. If a pre-infarction tracing is not available it is impossible to ascertain what the precise magnitude and direction of the normal T axis was. Thus it is important to recognize that when we state that the T wave changes following infarction have "disappeared" we simply mean that they are no longer recognizable as such. On the other hand, if a pre-infarction tracing is available one has some basis for comparison. However, here it is necessary to exercise caution, for, especially in diaphragmatic infarction,—which, except in the acute stage is unrecognizable from the precordial leads—the T axis as projected upon the frontal plane may return to that which prevailed prior to infarction, and yet the spatial T axis is different. Figure 158 is a series of tracings made on the same patient before, during, and following the development of a diaphragmatic infarction which did not involve the interventricular septum in an important manner, so that R_{III} was retained. The occurrence of an infarct in this location in a counterclockwise heart is accompanied by the change in the spatial QRS loop shown in Fig. 159. The tracing dated 10-17-52, showing the T waves much as they were before infarction, may have been produced by a T vector T' (Fig. 159a), which has the same direction as that of the previously normal T vector as projected upon the frontal plane, but which spatially has a more forward direction due to absence of normal "posterior"

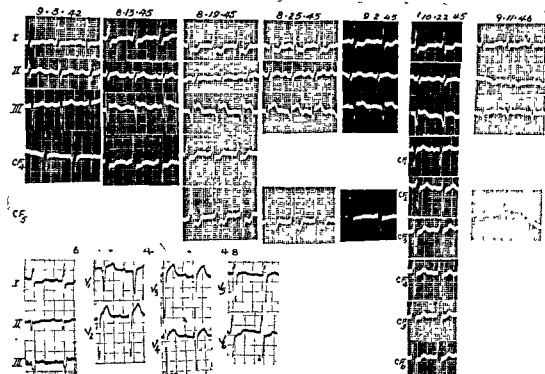


FIG. 153. Persistence of RS-T shifts after anterior (left) and diaphragmatic (right) infarction. In the latter case the RS-T elevations seen on 10-30-54 were persisting 8 months following the infarction. Note inverted U wave in tracings of 10-15-54 early in the attack.

wall effects or to the presence of ischemic "posterior" wall effects. Figure 159b and c show the effect of change to less and less counterclockwise rotations. It is seen that whereas vector T does not change in its projection upon the frontal plane, T' changes very rapidly so that an inversion of T_{III} occurs with even a slight change in rotation and therefore, slight changes in the QRS complexes (Fig. 159b). Examination of the tracing dated 10-17-52 shows that it corresponds well to the diagram of Fig. 159a (T')* and examination of the tracing dated 4-24-53 shows that it corresponds just as closely to the diagram of Fig. 159c. Actually

* Actually T' as drawn would produce a slightly negative T in Lead III. If the figure were rotated a bit more counterclockwise T' and T would be superimposed and the T_{III} resulting from vector T' would be positive. The figure is drawn as it is because the author found it impossible to make a clear drawing showing the two T vectors exactly superimposed.

no events occurred since the original infarction; the tracings were made for the purpose of observation. It is not necessary to conclude that the changes occurring in the series of electrocardiograms are of pathologic significance since, as has been shown, they may be explained by moderate changes in heart position.

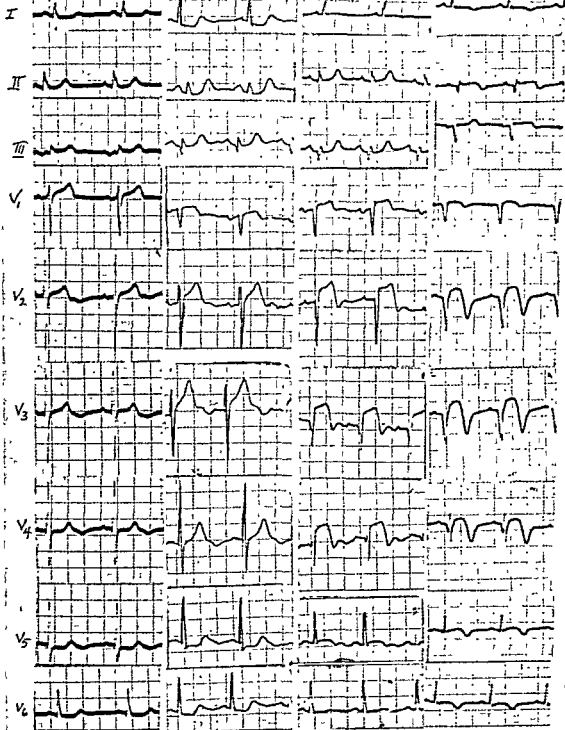
It is because of the importance of the spatial direction of electrical effects, as exemplified above, that some have attempted to record the spatial vector QRS and T quantities with the cathode ray oscilloscope. Others have employed various methods of "calculating" the spatial direction and magnitude of these vector quantities and of the ventricular gradient. In the writer's opinion (which will be developed further later) no method employed thus far has been nearly as accurate as the inferences of the spatial directions and magnitudes that are drawn from an analysis

10-15-54 AM.

10-15-54 P.M.

10-16-54

10-30-54



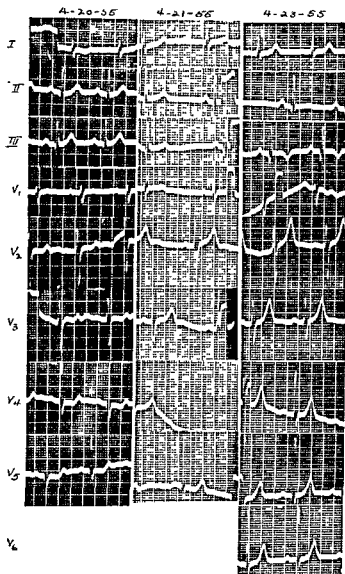


FIG. 154 The large T waves in Leads II and III are revealed as injury effects by the appearance of changes suggesting diaphragmatic infarction during the next few days.

of the frontal plane phenomena on the basis of the model loop and the physiologic approach which comprise this presentation.

The phenomena observed in the series of tracings of Fig. 158 and illustrated by the diagram of Fig. 159 suggest that it may at times be possible to detect abnormalities by making observations with different cardiac rotations. This may be accomplished by having

the patient take a deep breath. However, the approach would differ from the empirical method which has been employed heretofore. The empirical notion that an infarction Q wave will not disappear as readily as a normal Q wave when a deep breath is taken is quickly discarded even after a very small experience. It is, however, possible as shown in the series of tracings of Fig. 158 that a

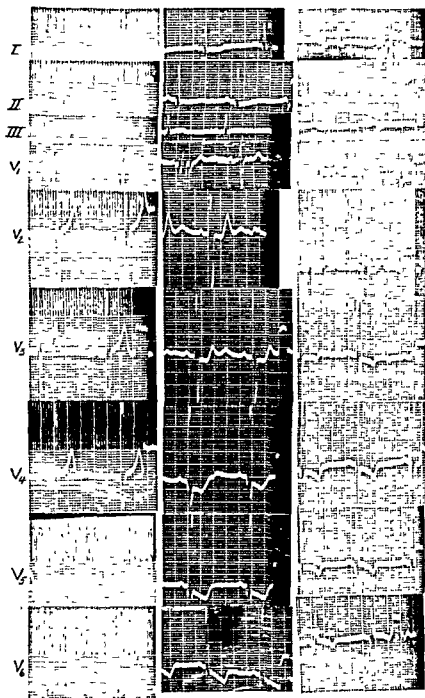


FIG. 155. Injury effects having appearance of digitalis changes. The first tracing was a previous tracing showing left ventricular hypertrophy. The second tracing was made on a subsequent admission to the hospital after vague chest pain. The RS-T shifts in the precordial leads are not unlike those due to digitalis. However, a tracing made on the following day indicated that these changes were due to diaphragmatic injury.

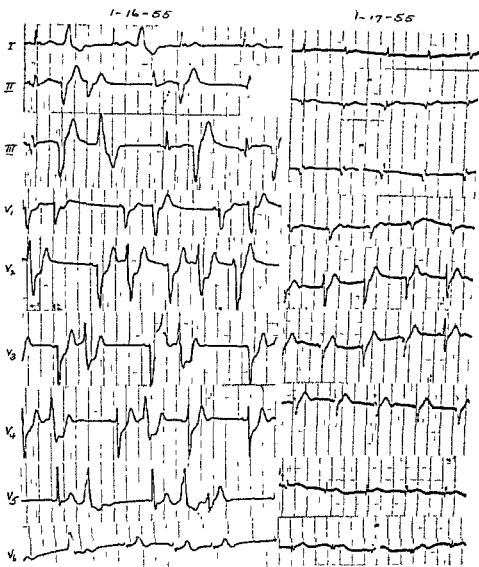


FIG 156 Ventricular premature beats and injury shifts 1-16-55, Acute injury stage of an apical and posterolateral infarction. In the ventricular premature beats in which a large wide R or S wave occurs the RS-T shift expected to follow a wide R or S has its effect just as it does in bundle branch block. Thus the RS-T shift may be greater or less in the premature beats depending upon the change in the QRS as compared to the sinus beat. In those leads in which the injury shift is large it predominates (as in the precordial leads of 1-16-55) In those leads in which the injury shift is small the secondary RS-T shift resulting from the wide R or S takes precedence

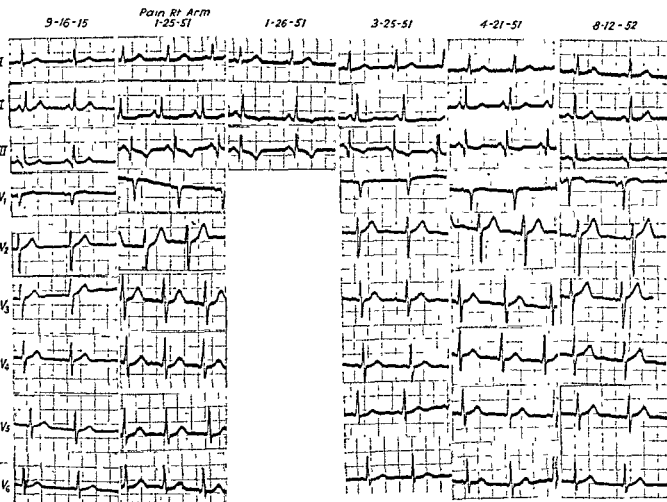


FIG. 157. Ischemic T waves occurring in patient with preexisting Q waves producing appearance of infarction. Pain occurring on 1-25-51 was accompanied by appearance of inverted T waves in Lead II and III so that the diaphragmatic infarction pattern results. The previous tracing (9-16-50) shows that the QRS complexes have not changed. No fever, leukocytosis, or increased sedimentation rate occurred. It was concluded that infarction had not occurred.

QRS-T relationship may occasionally be revealed which is very unusual in the normal. Unfortunately even in the normal the T vector is at times out of the plane of the QRS loop just as shown in Fig. 159. The distinction from the abnormal may rest upon the degree. This matter is under investigation.

QRS CHANGES FOLLOWING MYOCARDIAL INFARCTION IN THE ABSENCE OF ADDITIONAL CORONARY EVENTS. Changes in the QRS complexes observed in serial electrocardiograms made following myocardial infarction may be due to one or more of several causes. Those

changes which may be expected to occur as a result of changes in cardiac position and rotation are outlined in Figs. 114, 119, 128, and 136. The extent to which changes in rotation can account for changes in configuration of the QRS complex and the QRS-T relationship may be seen in Figs. 158 and 159.

Changes in the QRS complexes which may result from changes in intraventricular conduction (right or left bundle branch block) are common early in infarction, when they are likely to be temporary. In other cases conduction disturbances may appear only

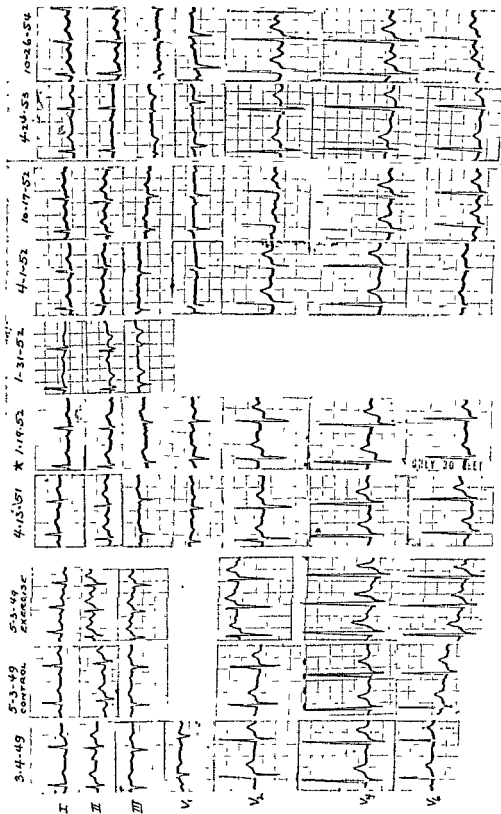


FIG 158. A series of electrocardiograms made before, during (1-19-52) and after a diaphragmatic infarction. Note change in T waves so that by 10-17-52 the only remaining change due to the infarction is the presence of Q in II which was absent before infarction. Note that from 10-17-52 to 4-24-53 there is a change in the QRS and T waves which corresponds to the change due to clockwise rotation depicted in Fig. 159 and which may be of no other significance.

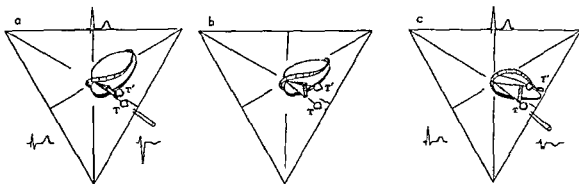


FIG. 159. The effect of clockwise rotation upon the QRS-T relationships when the T vector is out of the plane of the normal QRS loop.

In *a*, *T* is the normal mean T vector and *T'* is the T wave vector after its direction has been thrown upward and forward from the plane of the QRS loop by diaphragmatic wall ischemia or infarction. In infarction which does not involve the septum the QRS loop is also altered as shown. In *a* the heart is in counterclockwise rotation.

b is the same diagram with the heart rotated less counterclockwise than in *a*, and in *c* the heart is still less counterclockwise.

It is seen that the clockwise rotation of the anatomic axis causes no change in the projection of *T* upon the frontal plane. However, this same rotation causes *T'* to swing upward and to the left. The complexes drawn are for the infarct loop and *T'*. Thus in *a*, *T'* projected on the frontal plane produces about the same T waves as are produced by the normal vector, *T*. However, in *c*, *T'* projected upon the frontal plane produces an inverted T wave of considerable magnitude.

Further clockwise rotation would cause *T'* to swing back down again, because rotation of the anatomic axis causes the tip of vector *T'* to describe an arc.

In some normals the tip of the *T* vector lies above the plane of the QRS loop much as in *a*. However, further investigation may make it possible to detect some abnormalities if the degree of change caused by such rotation (produced by taking a deep breath) is not approached by the normals.

with left ventricular hypertrophy or with added myocardial damage (Fig. 160).

Not infrequently the QRS changes that follow myocardial infarction may diminish considerably within a few days. As has been stated before, it is a bit difficult at this time to understand such rapid return of QRS effects without assuming that severely injured muscle, incapable of producing electrical effects, may recover within a short time. Not infrequently the same disappearance of the evidence of infarction occurs after a much longer period of time (Fig. 161).

Left ventricular hypertrophy frequently follows myocardial infarction and may contribute significantly to the changes seen in the electrocardiogram. While in some cases only the magnitude of certain deflections will be affected, in others the form of the com-

plexes is changed, so that it may become difficult or impossible to detect the presence of the infarct (see Fig. 177).

When the left ventricle becomes quite large some of the QRS changes which occur may be referred to change in the cardiac position and rotation. Most often considerable enlargement of the heart causes a more apex-back position and a slight counterclockwise rotation about the anatomic axis. This latter rotation may be sufficient to cause an R in Lead III to reappear in the presence of a diaphragmatic infarction without extensive septal involvement (see Fig. 121, p. 147). The counterclockwise rotation accompanying enlargement may be more apparent than real because of the effects of eccentricity. These effects, however, are still of the order depicted in Figs. 114, 119, 128, and 136, showing the effect

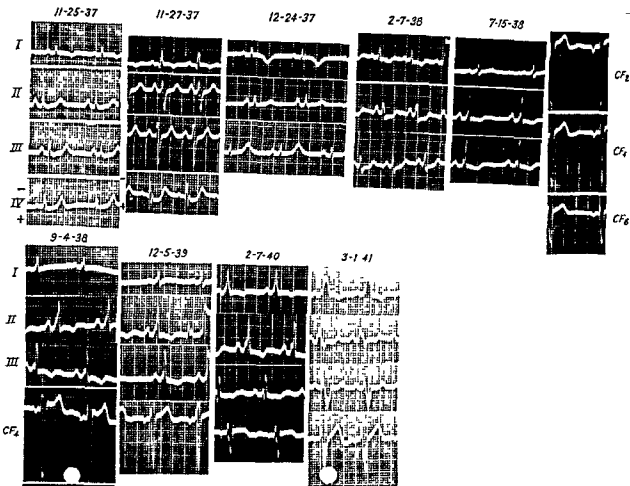


FIG. 160. Series of electrocardiograms made on a patient during and after two coronary events showing temporary (11-27-37) and finally permanent changes in conduction affecting the QRS complexes. The precordial leads made in 1937 are reversed in polarity.

of various positions and rotations. At times, enlargement naturally causes the anatomic axis to become more transverse.

It is probable that the occurrence of hypertrophy and enlargement of the left ventricle after a myocardial infarction may alter the architecture of the heart sufficiently to change the effective location of the infarct. Detailed discussion of this subject at this time would be entirely speculative. It is apparent, however, that enlargement of the ventricle about an infarct may diminish the relative electrical effects of the infarct unless the infarct stretches correspondingly. Many large infarcted areas do stretch when they are replaced by fibrous

tissue and the electrical effect of the infarct is retained. In these cases the changes in the electrocardiogram are due to greater effect from hypertrophy of the uninfarcted areas (Fig. 162a).

In many instances the infarct is patchy and when hypertrophy occurs the fibers which were not destroyed and which lie between the patches of scar tissue become enlarged and the area is again capable of QRS effects which were not detectable before hypertrophy occurred. A similar mechanism involving recovery of badly injured muscle in the interstices of a patchy infarct may account for recovery of QRS effects within the first

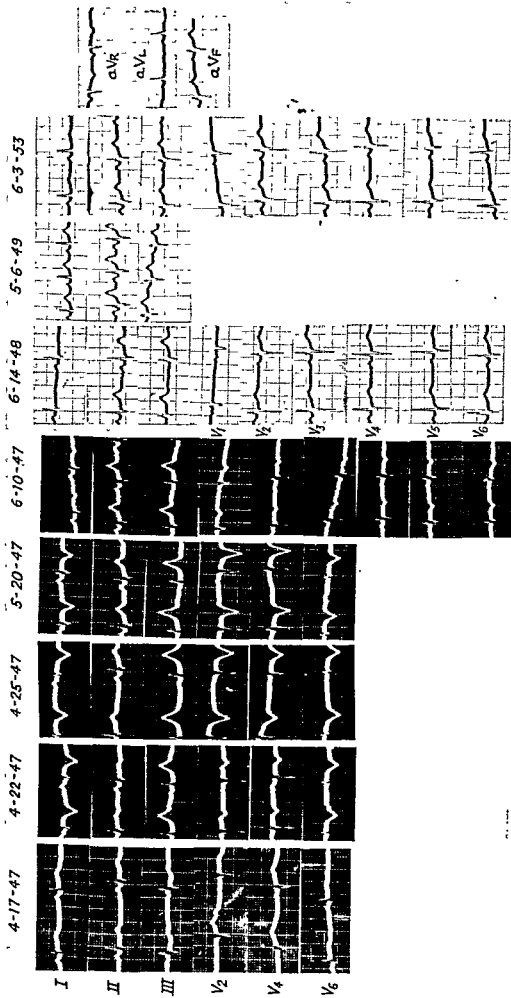


FIG. 161. Series of tracings made during and following an apical myocardial infarction showing complete disappearance of detectable effects of infarction. No tracing made prior to infarction was available.

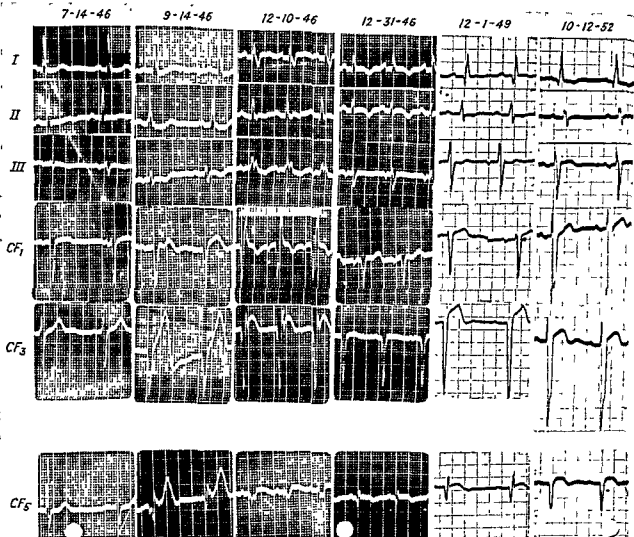


FIG. 162. Effect of left ventricular hypertrophy occurring following infarction. *A*, Tracings made before (7-14-46), during (9-14-46), and after a large apical infarction. On 12-10-46 right bundle branch block occurred during an attack of congestive heart failure. The progressive increase of the magnitude of the QRS complexes is due to enlargement and hypertrophy of the left ventricle.

The T wave changes and RS-T changes (especially RS-T elevations and upright T waves in Leads III, V_2 , and V_4) seen on 10-12-52 are secondary to the increase of the S waves (due to hypertrophy) which they follow. In part the RS-T elevation at V_4 is due to ventricular aneurysm.

The "reappearance" of R waves at V_2 and V_4 is also probably due to hypertrophy, but in part results from alteration of the relationship of the electrodes to the infarct. As the heart becomes greatly enlarged the apical infarct was probably moved to the left.

few weeks following an infarction. In some such cases the QRS effects are recovered to the extent that the tracing cannot be distinguished as abnormal (see Fig. 161). In others the recovery of QRS effects is only

partial and the presence of an old infarct may be suspected. In some of these, notably old anterior lateral infarctions, the small R waves in the left precordial leads as well as the limb leads are indistinguishable from the

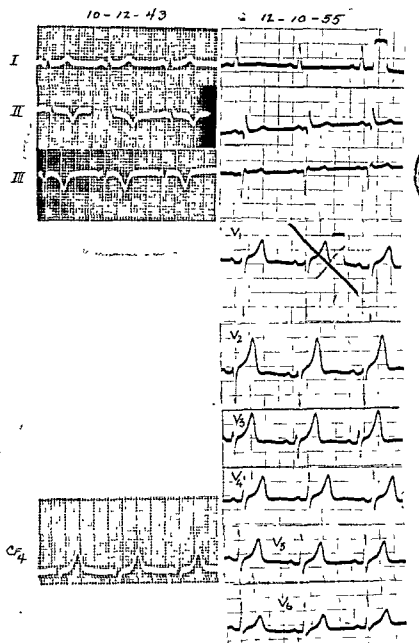


FIG. 162 (Continued). B, T wave changes due to hypertrophy of left ventricle following posterior infarction.

similar findings seen in chronic pulmonary disease or in apex-back vertical hearts.

Some of the changes accompanying hypertrophy of the left ventricle result from the development of left bundle branch block. With left bundle branch block an infarct in most locations is, thus far, undetectable. When right bundle branch block develops, the in-

farct is generally as detectable as it was without right bundle branch block.

It is important to point out that with the development of left ventricular hypertrophy and with left bundle branch block the T wave tends to change in a direction opposite to that of the QRS and usually in proportion to the magnitude of the increase of the QRS.

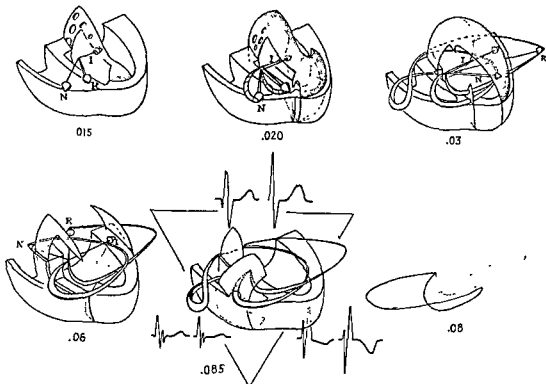


FIG. 163 Representation of spatial QRS loop when septal infarction occurs in the presence of right bundle branch block. The effect on the first portion of the QRS loop and the limb lead complexes as well as precordial leads is similar to that observed when right bundle branch block is absent (see Figs. 124 and 125).

The two loops in the last diagram are for the septal infarct (dotted) when the right bundle branch block is of the alternate form shown in Fig. 70.

This effect upon the T wave may actually be greater than the effect of the infarct upon the T wave and may thus aid in its concealment (see Fig. 162b).

MYOCARDIAL INFARCTION AND BUNDLE BRANCH BLOCK

Right Bundle Branch Block. In the presence of right bundle branch block infarcts generally produce a change in the first portion of the spatial QRS loop similar to that produced by the same infarcts in the first portion of the normal loops (Figs. 163, 164, 165, and 166). As a result, examination of the first portion of the QRS complexes in the presence of right bundle branch block reveals the same QRS changes seen in the absence of right bundle branch block. Of course, the fact that

the left ventricle is activated first and the similarity of the first portion of the right bundle branch block loop to the first portion of the normal loop accounts for this phenomenon.

Furthermore, in the precordial leads the first portions of the QRS complexes are also similar to those produced by the same infarct in the absence of right bundle branch block. It is only the last portion of the QRS complex that is altered by the bundle branch block (Figs. 163, 164, 165, and 166).

Left Bundle Branch Block. Since in left bundle branch block the left ventricle is activated last and only after the interventricular septum has been traversed by the impulse, it is only the later portion of the QRS loop (and complexes) which is affected by infarctions of the free wall of the left ventricle.

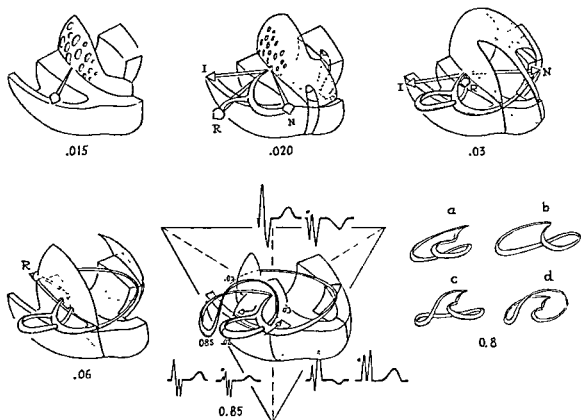


Fig 164. Lateral wall infarct in the presence of right bundle branch block. The infarct causes the first portion of the loop to be extended to the right and forward much as it does in the absence of right bundle branch block (see Fig. 111). At 0.03 second the septal effects are (because of the infarct) greater than those of the free wall of the left ventricle and the resultant vector still points to the right. At 0.06 second and beyond the vectors are much as they are without the infarct for they are derived from uninjured regions.

The first portions of the limb leads and the precordial leads are affected in the same way as they are in the absence of right bundle branch block (see Figs 111 and 112).

a is the corresponding infarct loop for the alternate form right bundle branch block loop *b* as developed in Fig. 70. *c* and *d* are other variants of the infarct loop.

This makes it very difficult to recognize myocardial infarction in the presence of left bundle branch block.

If a wide area of the interventricular septum is involved and especially if the involvement is transmural the first portion of the QRS loop may be affected sufficiently to make the infarction recognizable (Fig. 167). This causes the loop to start to the right instead of the left so that a wide Q occurs in Lead I and a corresponding R in Lead V_1 . If the infarct is largely left sided in the septum this sign will be lost but a large notch may be produced in the early portion of the QRS loop

(and in the R of Lead I) which may or may not be sufficiently marked to be recognized. Occasionally when the apical wall of the left ventricle is also involved the notch may be sufficiently pronounced to arouse suspicion.

Figure 168 represents the expected effect of a diaphragmatic wall infarction upon the QRS loop in the presence of left bundle branch block. Similar speculations may be made regarding the expected effects of infarcts in other portions of the free wall of the left ventricle. It is apparent that the recognition of such infarctions in the presence of left bundle branch block is virtually impos-

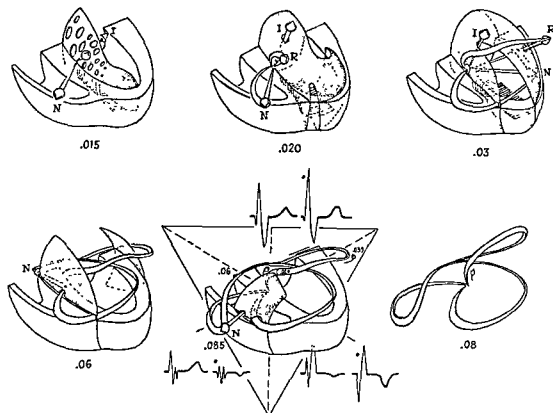


FIG. 165 Diaphragmatic wall infarction in the presence of right bundle branch block. The effect upon the first portion of the QRS loop and on the limb leads is the same as that which occurs in the absence of right bundle branch block. The last diagram is for a larger diaphragmatic infarct.

sible unless the spatial loop can be recorded with some accuracy. The present methods of recording spatial loops involve large errors in the anteroposterior component of the vectors and it is not yet possible to apply this method to the investigation of the problem.

Evaluation of Changes Due to New Coronary Events in Patients with Initially Abnormal Tracings

A variety of factors which may account for the changes seen in serial electrocardiograms have now been described. In most of the above discussions changes are described in relation to the normal. Unfortunately it is frequently necessary to attempt to determine the significance of changes observed in serial tracings when every tracing in the series is

definitely abnormal. Some of the problems involved in this area of electrocardiography are presently unsolved.

CHANGES IN PATIENTS WHOSE TRACINGS SHOW LEFT VENTRICULAR HYPERTROPHY AND LEFT BUNDLE BRANCH BLOCK. The tracing of the patient with left ventricular hypertrophy or left bundle branch block (frequently hypertensive) often shows a rather marked RS-T depression following large R waves and RS-T elevations and upright T waves in those leads with large S waves. When a later tracing is made and a change in this RS-T shifts, and also possibly the T waves, occurs, interpretation of this finding requires careful attention to the possible effect of several factors. First, careful examination of the QRS complexes should be made to determine whether a

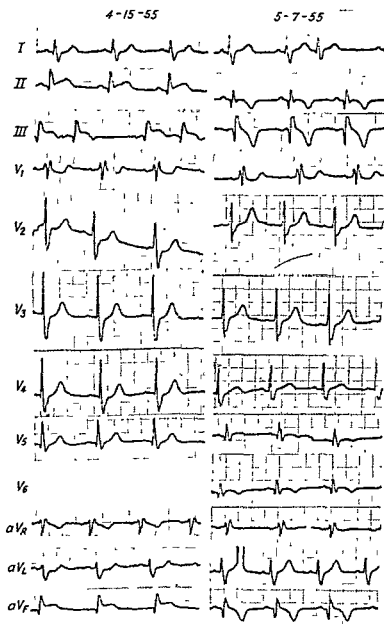
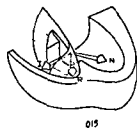
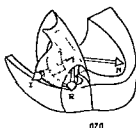


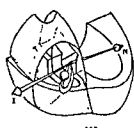
FIG. 166. Electrocardiograms from a patient with a diaphragmatic wall infarction in the presence of right bundle branch block. 4-13-55, Injury and early infarction. 5-9-55, Later tracing. Note deep Q in Leads II and III, like those that occur in diaphragmatic wall infarction in the absence of right bundle branch block.



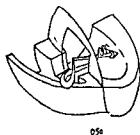
015



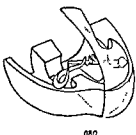
020



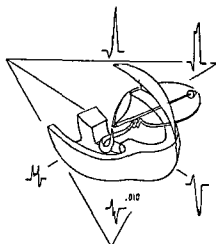
025



050



080



010

a

b

c

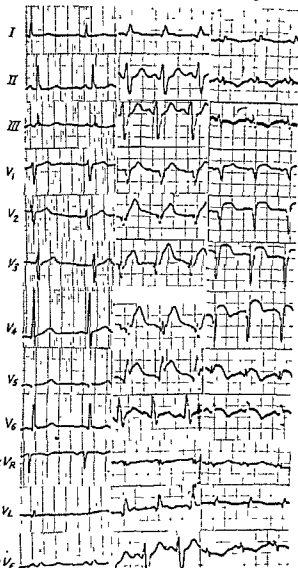


FIG 167 *Top*, Transmural septal infarction in left bundle branch block. The waves of excitation of left bundle branch block (see Fig 81, p 105), are depicted with large defects in those parts occupying the septum. The electrical effect of the defect resulting from the infarction is analyzed in the usual manner.

Only the infarct loop is drawn. Since the first vectors now point to the right a Q appears in Lead I and an R may appear in Lead III. These are largely due to electrical effects from the wave of excitation in the wall of the right ventricle. The same effects result in an appearance of an R in V_1 and V_2 and a Q in V_4 (commonly absent in left bundle branch block—see Fig. 82). If the apical wall of the left ventricle is also infarcted a Q may appear and be very wide in V_4 , V_5 , and V_6 .

Bottom, Anterior and transmural septal infarction in the presence of left bundle branch block. *a*, Tracing before myocardial infarction. *b*, Injury tracing due to myocardial infarction; transient left bundle branch block is present. *c*, Left bundle branch block has disappeared. Compare *b* with limb leads developed for figure above.

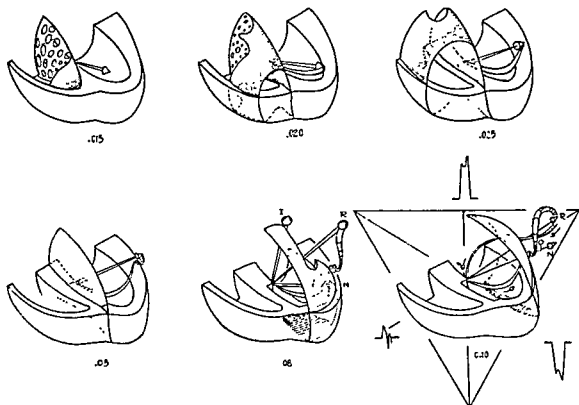


FIG. 168. Diaphragmatic wall infarction in left bundle branch block. The method of analysis is the same as that employed for other infarcts. Here it is seen that infarction of the free wall of the left ventricle affects the later parts of the spatial QRS loop when left bundle branch block is present (septal infarction affects the early portion). The same applies to infarction of the lateral wall of the left ventricle.

The figure serves to show why it is difficult to detect infarction in the diaphragmatic (and lateral wall) of the left ventricle. A sufficiently accurate method of recording spatial loops with the oscilloscope may make it possible to recognize some of these cases.

change in cardiac position or rotation has occurred, for such a change is accompanied by a change in the RS-T shifts and/or T waves (Fig. 169). However, changes in the QRS complexes may be due to an increase in left ventricular hypertrophy or dilatation (Fig. 170) or to change in intraventricular conduction (usually left bundle branch block) which also affect the RS-T shifts and T waves according to the principle of the gradient (Fig. 171). These RS-T and T wave changes tend to be opposite in direction to (and their magnitude is proportional to the magnitude of) the main deflection of the QRS complex (measured in area).

Since the magnitude of the gradient is diminished by rapid rate and by digitalis it follows that these RS-T shifts occurring in left

ventricular hypertrophy and left bundle branch block are usually greater with increased rate and with digitalis. With the latter the Q-T becomes shorter. (Figs. 172, 173, and 174).

The relation of rate to the RS-T segment and T wave changes is seen in Fig. 175 showing the effect of carotid sinus stimulation upon the cardiac rate. With slowing of the rate the inverted T wave becomes smaller and the RS-T shift tends to be less; when the rate increases the inversion of T again becomes greater and the RS-T displacement tends to be greater.

Further controlled studies of the effects of rate, of food, and other factors upon such tracings are being made at this time. Some opportunity to study these phenomena is af-

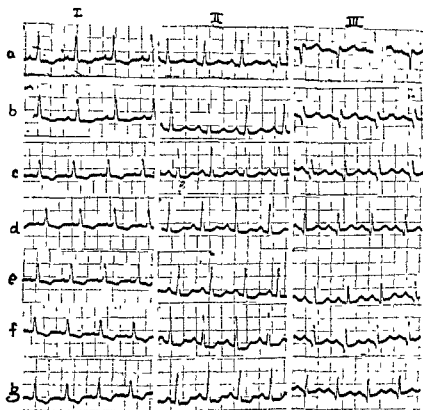


FIG. 169. QRS changes due to change in cardiac position combined with RS-T shifts due to angina. At the time this patient was seen she would have an angina attack upon lying down. All tracings were made at home at the same sitting.

a, Sitting up; *b*, Upon lying down; *c*, Dull pain beginning; *d*, Pain worse; *e*, Pain severe; *f*, Pain very severe; *g*, Pain unbearable.

The pain could be rapidly relieved by nitroglycerine.

The QRS complexes changed with change in posture. This is especially noticeable in Lead III and the relative heights of R_1 and R_{II} . However, with the onset of pain they changed more, and still more when the pain became quite severe. These changes result from elevation of the respiratory mid-position resulting from anxiety and severe pain; the heart became more vertical. The RS-T and T changes might have resulted from the increase in rate. However, the shifts disappeared without change in rate when nitroglycerine was given.

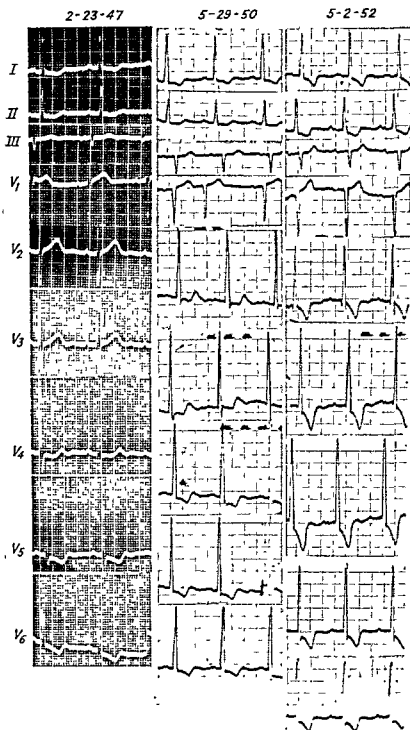


FIG. 170. A series of electrocardiograms on the same patient with left ventricular hypertrophy. 5-29-50, Increased left ventricular hypertrophy. The increase in the QRS has resulted in more marked RS-T shifts and more marked inversion of the T waves in Leads I, V₄, V₅, and V₆. 5-2-52, Digitalization has produced more marked RS-T shifts and greater T wave changes. The Q-T is shorter.

It is impossible to determine the extent to which ischemia may contribute to the change in some of these cases. This patient had angina.

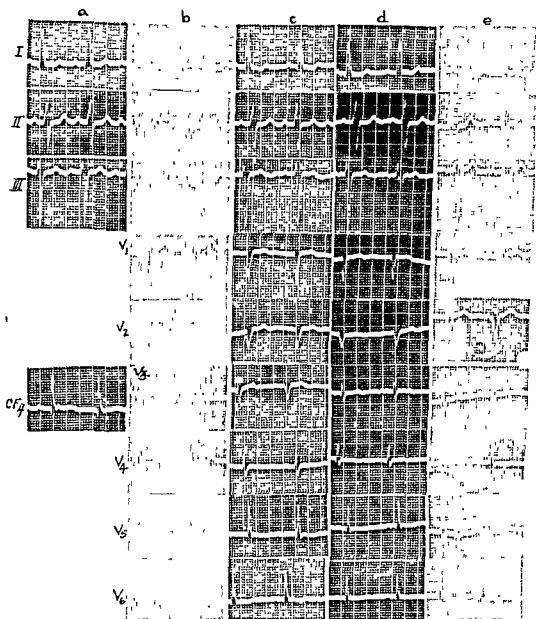


FIG 171 A series of electrocardiograms on the same patient. Varying degree of left bundle branch block is seen. It is noted in any lead that when the QRS becomes greater (in area) the RS-T segment shift in the opposite direction becomes greater. The T wave also changes in a direction opposite to that of the QRS at the same time. These phenomena follow the principle of the gradient.

fording by seeing these patients through non-cardiac illnesses and from observation of cardiac mechanism disturbances.

When rapid rate occurs in combination with the effects of digitalis in these cases the total effect tends to be exaggerated.

It has been found that frequently with congestive failure the gradient is diminished and the same effects are observed that are seen with increased rate. In some cases of acute pulmonary edema this effect is marked and it may be difficult to distinguish it from injury effects. The latter would indicate that acute pulmonary edema is initiated by coronary spasm or occlusion (Fig. 176).

Unfortunately "posterior" or subendocardial myocardial injury may occur in persons with this type of tracing. The direction of the RS-T displacement in such lesions may be opposite to that of the direction of the QRS deflection in all leads (Fig. 151) and because the rate is rapid the false conclusion might be drawn that the RS-T displacement (or increase in existing RS-T displacement) is due to the rapid rate. Thus, under any circumstances conclusion may have to be deferred until serial observations furnish additional information (Fig. 177). Anterolateral ischemia causes the same difficulty in these cases and can only be evaluated properly in serial studies.

At times RS-T shifts previously present which increase during an attack of pain may be seen to become progressively larger as the attack proceeds in spite of the fact that the rate does not change significantly. When this occurs over a period of a few minutes it is highly suggestive. If the shift is sharply diminished by nitroglycerin the evidence is virtually conclusive, especially if the rate is not appreciably slowed. Figure 178 shows two tracings made on the same patient at different times; *b* is an interval tracing; *a* was made during an attack of epigastric pain. The change in the RS-T segments cannot be attributed to the insignificant change in rate.

If in any electrocardiogram a significant RS-T shift appears which is in the same

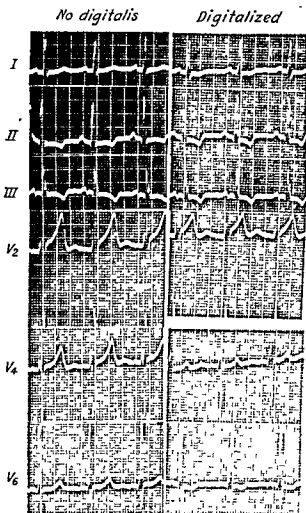


FIG. 172. Electrocardiograms before and after (4 days later) digitalization of a 40-year-old man with left ventricular hypertrophy due to aortic stenosis. The RS-T shifts in the second tracing are due to digitalis. Note that although the rate is changed but little the Q-T is much shorter. This is a characteristic digitalis effect.

direction as the main deflection of the QRS complex in most of the leads the diagnosis of injury is warranted even on a single tracing, (Figs. 179 and 180). Whether this injury depends upon coronary disease or upon pericarditis must be determined by serial study. These tracings should not be confused with normals with large gradient.

What has been said of the RS-T shifts also applies to the T waves, which in these cases are most often, but not always, of the same direction as the RS-T shifts.

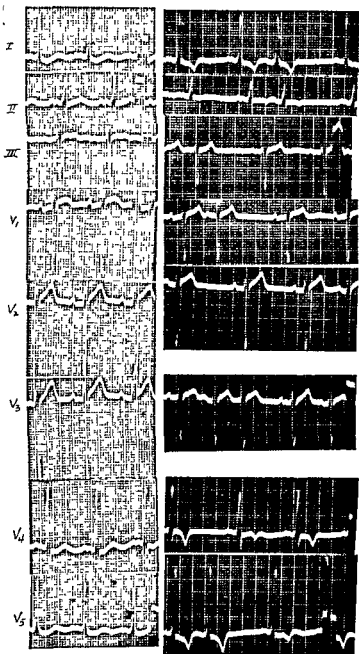


FIG 173. A not unusual effect of digitalis. Both tracings were made under digitalis therapy. The second was made three days after the first and after the dose of digitalis had been increased. The marked change in the T waves seen here is fairly common after digitalis. Note the shorter Q-T interval in the second tracing even when the rate is slower.

4-19-55

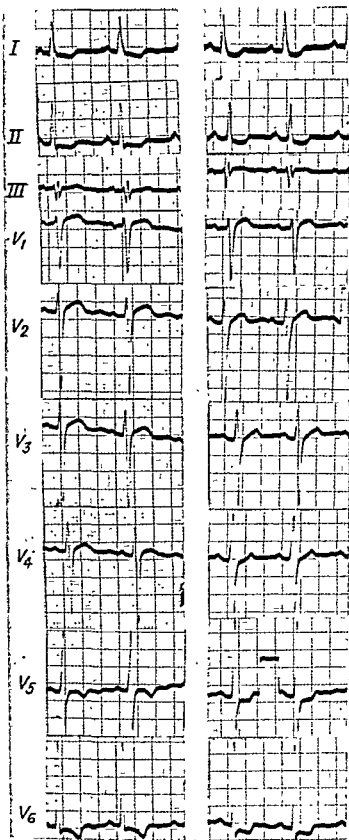
digitalized
5-30-55

FIG. 174. Left ventricular hypertrophy due to arteriosclerotic heart disease before and after digitalization. Here the most marked effect is the shortening of the Q-T interval and the curved depression of the RS-T segment.

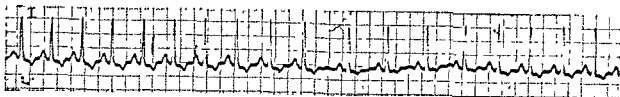


FIG. 175. Effect of rate upon RS-T and T waves in a patient with arteriosclerotic hypertensive heart disease and left ventricular hypertrophy. Note that when rate is slowed by carotid sinus stimulation the inverted T wave is much smaller and the RS-T junction is less depressed.

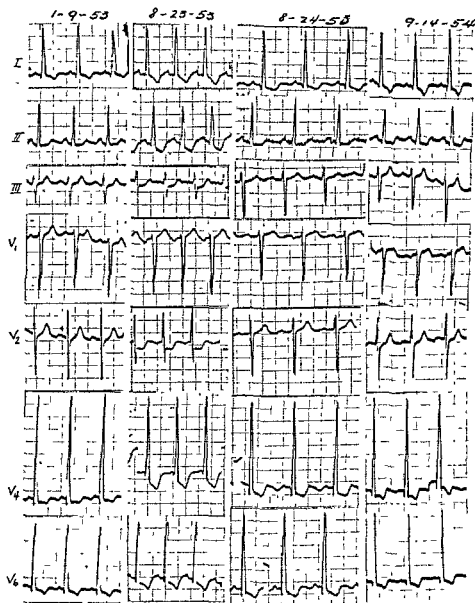


FIG 176. A series of electrocardiograms on a patient who had left ventricular hypertrophy due to hypertension for many years and who suddenly developed acute pulmonary edema on 8-23-53 while in the hospital with a fractured hip. The tracing on this date shows increased RS-T shifts and T wave changes. The rate is more rapid than on 1-9-53. However, the RS-T shift in Lead III is quite large and downward although the net QRS area in that lead is practically zero. The RS-T shift in V_4 is also out of proportion to the net QRS. This suggests injury changes probably due to diffuse subendocardial injury. In follow-up tracings as on 9-14-54 the rate is as rapid yet the RS-T shifts are not like those seen on 8-23-53. The tracing of 9-14-54 shows digitalis effects.

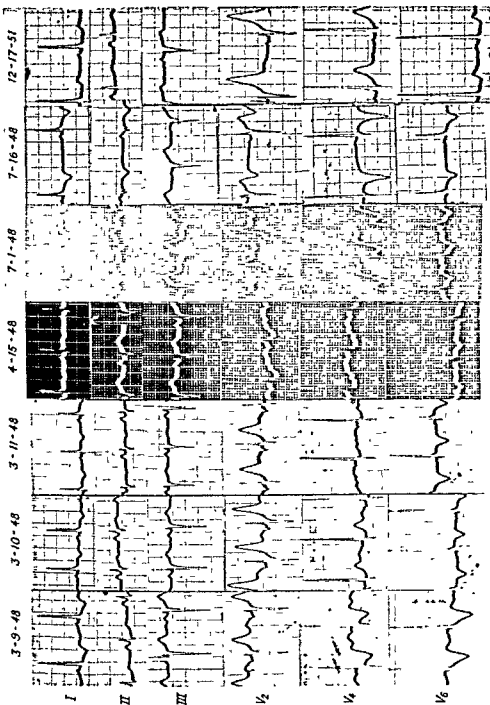


FIG. 177. 3-9-48, Electrocardiogram from hypertensive patient following chest pain. The RS-T shifts are opposite in direction to the main deflection of the QRS complexes, as in left ventricular hypertrophy and digitalis. On 3-10-48 the RS-T shifts have virtually disappeared. R is smaller in Lead I, and Q is wider in Lead I on 3-11-48. Thus serial observation established the fact that the RS-T shifts were injury shifts due to posterior lateral infarction. Actually it was strongly suspected that in tracing on 3-9-48 the RS-T shift in V_4 was out of proportion to the area of the R wave in that lead, but such evaluations require experience.

Tracings on 7-1-48 and 7-16-48 show that the patient sustained a posterior infarction a few months later and 12-17-51, made three years later, shows left ventricular hypertrophy with no detectable signs of infarction remaining.

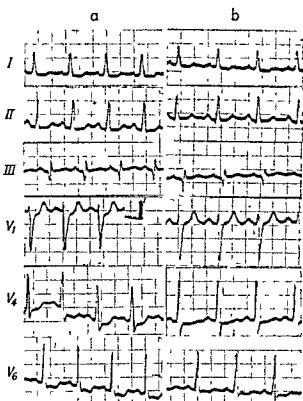


FIG. 178. Hypertensive heart disease with RS-T changes *a*, Electrocardiogram made during pain. The RS-T shift in V_1 is in the same direction as the main deflection of the QRS but the shift in V_4 and V_6 are not and cannot easily be evaluated. The marked change induced by nitroglycerine without significant change in rate (*b*) makes it clear that the RS-T shifts were due to angina.

It is important to point out that in abnormal cases a small change in the location of the precordial electrode produces a greater change in the appearance of the tracing than can occur in the normal. Therefore interpretation of serial precordial leads in these cases is filled with difficulties and great caution should be exercised (Fig. 181). There is no way to assure identical placement of the electrode (in relation to the heart) on two successive examinations.

Figure 182 shows the electrocardiograms of a patient with hypertensive heart disease before and after an attack of angina. Tracing *a* may show only the signs of hypertrophy but the serial T wave change seen between *a*

and *b* is due to ischemia. No digitalis is present.

At times injury shifts may occur which are due to angina or early infarction and are opposite in direction to previously existing changes due to hypertrophy and ischemic changes so that the tracing may actually appear more normal than it did before. (Fig. 183).

In summary, when new injury changes are suspected in these abnormal tracings serial studies must be made in order to search for evidence of relation of the change in the electrocardiogram to rate change and to the administration of nitroglycerin and to detect QRS changes indicating infarction. In the evaluation of the latter, the effect of change of cardiac position and rotation must be allowed for (Fig. 158), as should the effect of congestive failure and of digitalis.

In this connection some mention should be made of QRS changes occurring in congestive heart failure which are apparently due to change in cardiac position resulting from right ventricular enlargement, change in posture, and unknown factors. Similar changes seem at times to accompany rapid heart rates with and without cardiac mechanism disturbances. The changes consist of reduction of the R waves which when left axis deviation is present may cause the remaining S waves to appear to be Q waves. The R waves in the precordial leads may, at times, be considerably diminished.

CHANGES IN THE ELECTROCARDIOGRAMS OF PATIENTS WITH OLD MYOCARDIAL INFARCTIONS. Some of the changes following myocardial infarction have been described. We are presently interested, however, in those which may be due to new coronary events. Since the injury shift is most frequently (but not always) the effect of new events in the heart of coronary origin it will be dealt with first.

If a patient has given a history of myocardial infarction some months before and his tracing following chest pains shows RS-T shifts (Fig. 184) the usual diagnosis would be that he has suffered a fresh occlusion.

Actually this is not necessarily so. Both of the patients whose tracings are shown in Fig. 153*a* and *b* had had infarctions several months before and had retained the shifts during the following months. The presence of ventricular aneurysm had not been established in either case. If one sees such a tracing under the circumstances described and without the opportunity of examining a number of interval tracings the change must be regarded as acute until it has been established that the tracing does not change over a period of time.

New changes occurring in patients who have myocardial infarctions must be approached much as has been described for the electrocardiograms of patients with left ventricular hypertrophy and left bundle branch block. Here again one must not be deceived by changes due to alteration in cardiac position and rotation (see Fig. 158, p. 184). Congestive failure and rapid rate may be responsible for QRS changes which result from changes in cardiac rotation and which may be misleading. Digitalis may produce RS-T shifts and T wave changes as a result of diminution of the gradient.

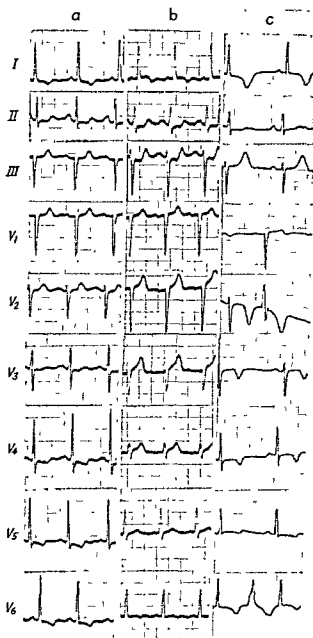
When new coronary events supervene it may be extremely difficult to distinguish these from changes attributed to the above factors.

FIG. 179. The patient is a 74-year-old female with hypertension (blood pressure, 220/100), who has been seen by the writer over a period of 16 years and who had no cardiac symptoms during that time. Tracing *a*, showing left ventricular hypertrophy, was made on routine check-up. Tracing *b* was made (at home) during her first and only severe chest pain. The RS-T shifts in Leads I and III are in the same direction as the QRS complexes and are, therefore, undoubtedly due to injury. The upright T waves and upward shifts of the RS-T segment in the precordial leads in tracing *b* are also due to injury. The QRS complexes are not comparable to those of tracing *a*, entirely because of different placement of the electrodes. There was no fever and no leukocytosis.

Tracing *c* was made 24 hours after tracing *b* and shows the ischemic changes which followed the injury. Recovery from these changes occurred within 5 weeks. It was concluded that no infarction had occurred. The transaminase level remained normal.

It may also be difficult to know whether injury occurs and heals or progresses to additional infarction. Additional anterolateral infarction is easier to detect than additional diaphragmatic wall or septal infarction.

The presence of left bundle branch block makes the recognition of additional changes extremely difficult. The variations that occur in left bundle branch block tracings from time to time due to change in the degree of



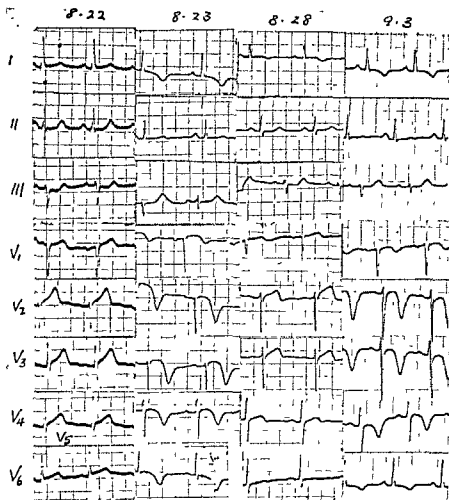


FIG 180 8-22, Tracing from a 64-year-old white female (hypertensive) with pain in the chest. No previous tracing was immediately available. The RS-T shifts in Leads I and III, which are in the same direction as the main deflections of the QRS complexes in those leads, were regarded as diagnostic of acute injury. The upward RS-T shifts in the chest leads and high upright T waves also suggested injury. The patient was hospitalized and the tracing dated 8-23 was obtained 24 hours later. Injury effects recurred on 8-28 and were again followed by ischemia. There was no fever and no leukocytosis. The QRS changes in the limb leads are regarded as being due to change in cardiac position. No significant change in the QRS complexes of the precordial leads is discernible. No infarction is believed to have occurred.

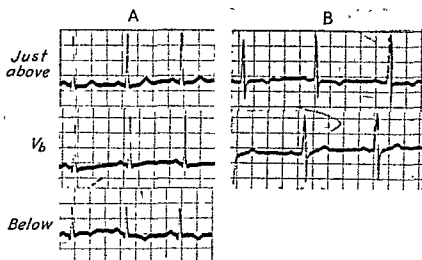


FIG. 181. *A* shows three leads made on the same patient in the same lateral position of V_6 , but at different vertical levels. The marked variation of the T waves obtained in this way at the same sitting illustrates a limitation of serial precordial lead interpretation. *B* is another example. Both of these patients had had myocardial infarctions in the past.

the block may be mistaken for more important changes. The recognition of new QRS changes when infarction occurs in left bundle branch block may be impossible.

The more abnormal the electrocardiogram the more difficulty there is in recognizing new changes.

The present subject may be best pursued by reviewing several cases: Figure 184 is a series of electrocardiograms made on a woman who was 73 years of age at the time the first tracing (8-30-48) was made. On 9-24-52 she had a severe pain in the chest, and developed fever and leukocytosis. The electrocardiogram changed in a manner characteristic of diaphragmatic infarction. She recovered and the ischemic T wave effects had largely disappeared by 6-9-54. On 3-30-55 she suffered another severe and prolonged pain in the chest and again the signs of diaphragmatic injury appeared. A second diaphragmatic infarction was anticipated. However, within five days a trace like that of 9-28-52 was recorded. In the meantime, no fever, leukocytosis, or rapid sedimentation rate had occurred. It is impossible to be cer-

tain from the electrocardiogram alone whether she had had another infarction or not.

Figure 185 shows electrocardiograms of a man who was 44 years of age when the tracing of 4-14-45 was made. He had been having pains in the chest. A diagnosis of coronary insufficiency was made. The subsequent tracings show varying changes in the T wave axis indicative of ischemia of the anterolateral wall of the left ventricle. On 1-13-48 a severe pain in the chest was followed by the appearance of injury shifts which over a period of several days disappeared while at the same time a wide Q appeared in Lead I and all of the chest leads. A large apical infarction had occurred. On 4-5-48 the tracing had changed further toward a left axis deviation and a widening of the QRS had occurred. This may be partly due to a change in cardiac rotation due to enlargement of the heart which occurred at this time but a change in conduction (incomplete left bundle branch block) had also occurred.

For a time the tracing remained essentially unchanged except for the fact that the hypertrophy of the remainder of the left ventricle

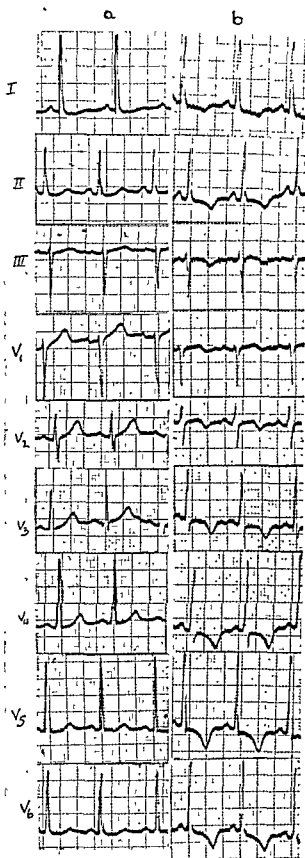


FIG. 182. Tracing *a* was made as an interval observation on a hypertensive female 57 years of age who had had angina for 4 years. Tracing *b* was made after a series of rapidly repeated severe anginal attacks. Ischemia has produced marked T wave changes which are not dissimilar to those which might occur with rapid rate or digitalis with the exception that in Lead III the T wave is inverted. Rapid rate, digitalis, increased hypertrophy, or early left bundle branch block would not have caused the T wave in Lead III to become inverted, they would have made it more positive if any change occurred. No digitalis had been given, nor had the rate increased. There is also no evidence of change in cardiac position.

and digitalis have caused the inverted T waves which commonly follow large Q waves in the precordial leads (V_4) to become upright.

On 2-20-49 the patient had another severe chest pain and the tracing showed RS-T shifts in the same direction as the main deflection of the QRS in Lead I and III. On 2-20-49 and 2-21-49 the Q in Lead I and the R in Lead III are seen to become progressively larger. Additional lateral infarction had occurred.

On 8-15-49 the final attack occurred and the patient expired within the week. Left bundle branch block is present in spite of which the wide Q is retained in Lead I and the R is retained in Lead III, probably due to the presence of infarction in the septum.

Autopsy disclosed extensive infarction of the interventricular septum, the apical half of the anterior and diaphragmatic walls, and the apical two thirds of the lateral wall of the left ventricle.

At times a second infarction occurs in an area of different orientation from that of the first (Fig. 186). Under these circumstances the interpretation is not difficult. Here the reader should review *infarcts in combined locations*. (pp. 161-166).

When multiple infarction has occurred the QRS complexes may become small and heavily slurred or notched and it may be quite difficult or impossible to interpret serial tracings following another attack of pain in the chest.

After repeated infarction right bundle branch block or (more frequently) left bundle

branch block supervenes. In the latter case diagnosis of new QRS changes is extremely difficult.

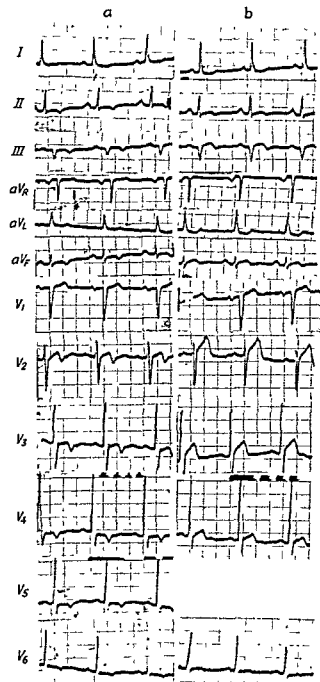


FIG. 183. *a* is an interval tracing made on a 70-year-old white male who had paroxysmal attacks of pain in the left shoulder and circumoral region. The tracing is abnormal, possibly as a result of previous infarction in the anterosseptal region with extension to the diaphragmatic surface. *b* was made during an attack of the above-described pain. The injury effects have caused the previously inverted T waves to become upright in most of the leads. Following the attack the tracing returned to its previous appearance (*a*) within a few minutes. The entire sequence was observed several times.

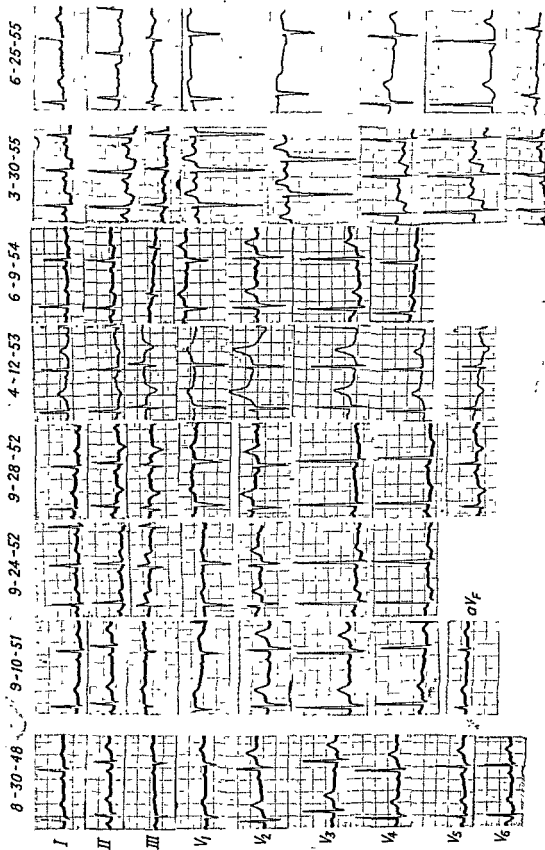


Fig. 184. 8-30-48 and 9-10-51, Routine normal check-up electrocardiograms.

9-24-52, Tracing made following severe chest pain. Note RS-T shifts typical of diaphragmatic injury, and appearance of Q_s and Q_r typical of diaphragmatic infarction. On 9-28-52 the evolution of the electrocardiographic changes is also typical of diaphragmatic infarction.

By 6-9-54 the ischemic T wave changes are much less evident. It would not be certain from this tracing alone that infarction had occurred.

On 3-30-55 another severe chest pain occurred and again injury shifts appear which are typical of posterior injury. A few days later the T waves in Leads II and III are again inverted. It is not possible to be certain that fresh infarction had occurred. There was no fever and no leukocytosis and it was inferred that measurable fresh infarction had not occurred.

Suggested Reading

- Barnes, A. R. Electrocardiographic patterns following acute coronary occlusion complicated by pericarditis. *Am. Heart J.*, 9:728, 1934.
- Eliaser, M., Jr., and Konigsberg, J. Electrocardiographic findings in cases of ventricular aneurism. *Arch. Int. Med.*, 64:493, 1939.
- Johnston, F. D., Hill, I. G. W., and Wilson, F. N. The form of the electrocardiogram in experimental myocardial infarction. II. The early effects produced by ligation of the left coronary artery. *Am. Heart J.*, 10:889, 1935.
- Myers, G. B. Correlation of electrocardiographic and pathologic findings in antero-septal infarction. *Am. Heart J.*, 36:535, 1948.
- Myers, G. B. Correlation of electrocardiographic and pathologic findings in antero-posterior infarction. *Am. Heart J.*, 37:205, 1949.
- Myers, G. B. Correlation of electrocardiographic and pathologic findings in lateral infarction. *Am. Heart J.*, 37:374, 1949.
- Myers, G. B., Klein, H. A., and Hiratzka, T. Correlation of electrocardiographic findings in large anterolateral infarcts. *Am. Heart J.*, 36:838, 1948.
- Pruitt, R. D., and Valencia, F. The immediate electrocardiographic effects of circumscribed myocardial injuries; an experimental study. *Am. Heart J.*, 35:161, 1948.
- Riseman, J. E. F., Waller, J. N., and Brown, M. G. The electrocardiogram during attacks of angina pectoris; its characteristics and diagnostic significance. *Am. Heart J.*, 19:683, 1940.
- Rosenbaum, F. F., Wilson, F. N., and Johnston, F. D. The precordial electrocardiogram in high lateral myocardial infarction. *Am. Heart J.*, 32:135, 1946.

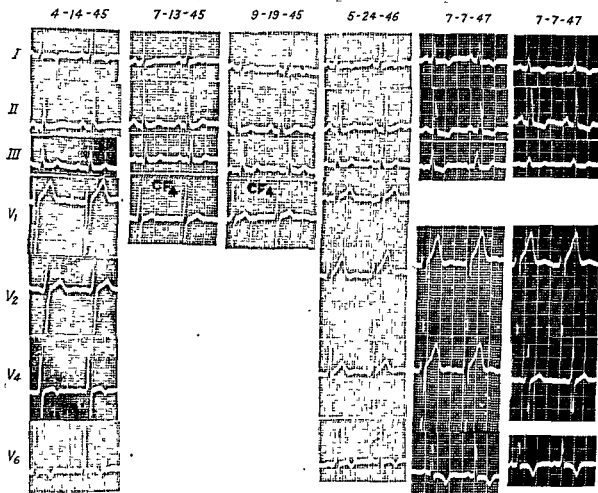


FIG. 185. Tracing made between 4-14-45 and 7-7-47 show changes due to myocardial ischemia. Note that the T axis varies in direction. No digitalis was administered.

On 1-13-48 and 1-14-48 a severe chest pain was accompanied by large injury shifts and QRS changes typical of anterolateral injury and infarction. Note especially appearance of a wide Q in Lead I and the Q waves in the precordial leads. On 4-5-48 there is a change to marked counterclockwise rotation and slight change in intraventricular conduction (left bundle branch delay).

On 2-20-49 another severe chest pain occurred and there are RS-T shifts in Leads I and III which are in the same direction as the main deflection of the QRS complexes. Following this in two tracings made on 2-21-49 the Q in Lead I is larger and the R in Lead III is higher. This change signifying additional infarction in the anterolateral wall was permanent.

On 8-15-49 the final attack occurred, the left bundle branch delay became greater and the complexes smaller in the limb leads.

The variations in the form of V_6 until 8-15-49 result entirely from difference in electrode placement. Any inference that the serial change in V_6 from 4-12-48 to 6-8-48 or from 2-21-49 AM to 2-21-49 PM results from myocardial change is erroneous.

7-15-47

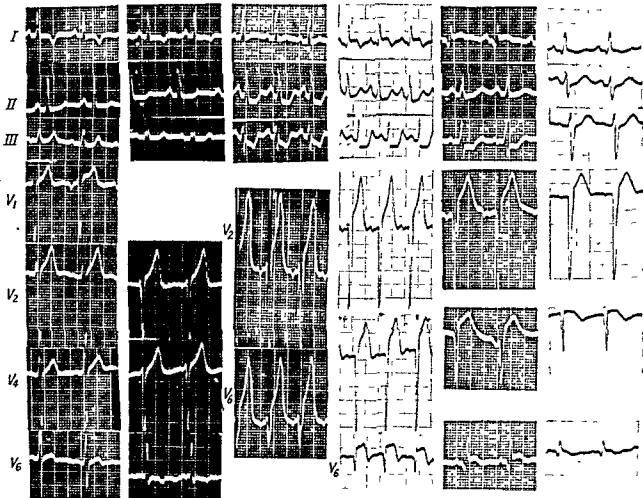
1-13-48

1-13-48

1-14-48

1-19-48

4-5-48



4-12-48

6-8-48

2-20-49

2-21-49

2-21-49

8-15-49

8-18-49



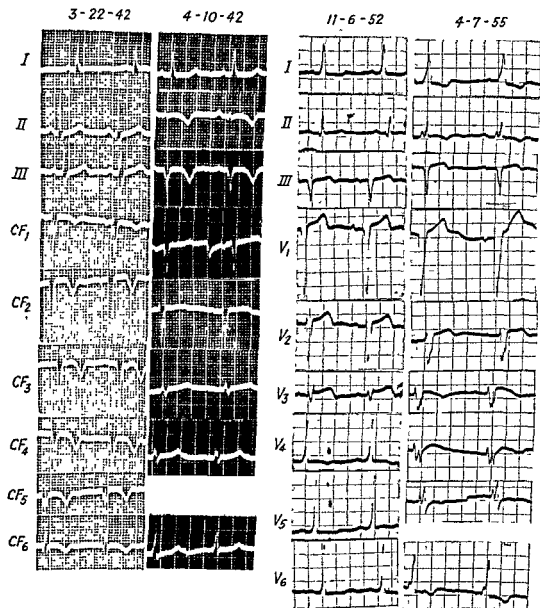


FIG. 186 3-3-42, Tracing made 9 months following an anterior myocardial infarction 4-1-42, Same patient following a diaphragmatic (posterior) infarction 11-6-52, Same patient after hypertrophy and dilatation of the remainder of the left ventricle had occurred. Note that the T wave changes in practically all of the leads are those which, according to the principle of the gradient, would be expected from increase of the area of the QRS (due to hypertrophy). Of course some ischemic T effects may also have disappeared. 1-7-55, Left bundle branch block has ensued. Note that T wave changes of the type described above have become exaggerated.

12. Right Ventricular Hypertrophy*

We approach right ventricular hypertrophy with the same hypothesis employed in the analysis of the normal, of right and left bundle branch block, and of left ventricular hypertrophy.

Figures 187, 188, and 189 represent the application of the hypothesis to mild, moderate, and marked right ventricular hypertrophy. The spatial QRS loops and the precordial leads are developed at the same time. Vector analysis is employed in developing the QRS loops while the solid angle method is employed in developing the precordial leads.

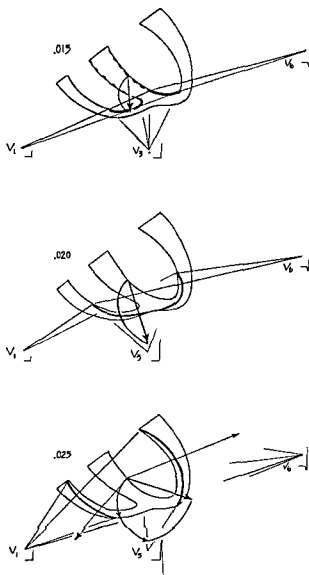
In each case it is first assumed that hypertrophy of the right ventricle involves thickening of the apex of the ventricle and therefore a delayed "break-through" in this area during depolarization (see *0.02 second* in each figure). However, it is necessary to realize that this area of the right ventricle may remain thin though the rest of the ventricle becomes much thicker than the normal. Many hypertrophied right ventricles, like most normal and even some hypertrophied left ventricles, are thin at the apex and become progressively thicker towards the base. Under such circumstances the vector at *0.02 second* in Fig. 187, 188, and 189 may be little or no longer than the normal at this time. In such cases the first portion of the loop becomes smaller and may be represented by an alternate form; in the mild and moderate hypertrophies one simply follows (on those figures showing the completed loops) the normal loop in the first portion until the point is reached where the originally drawn hypertrophy loop first crosses it. From here on the hypertrophy loop is followed.

* In collaboration with Louis Levy, II, M.D., Heart Station of Charity Hospital, New Orleans.

With the right ventricle markedly hypertrophied, this alternate form is represented by a short bridge drawn in to shorten the first portion of the loop.

It is evident in Figs. 187, 188, and 189, as in the development of the normal QRS loop, that the direction and magnitude of the resultant vectors (after the first *0.02 second*) depend upon opposing effects in the two ventricles. Theoretically, therefore, as the right ventricle becomes thicker the loop becomes rounder (Fig. 187) and soon (Fig. 188), because of the basal curvature of the two ventricles, its latter portion begins to point more backward as the loop becomes flatter from right to left. When the right ventricle becomes as thick and as large as the left, the loop should be aligned with the anatomic axis as shown in Fig. 189 (*0.07 second*). If the right ventricle becomes larger and thicker than the left the loop should begin to point more to the right as shown by the dotted loop of Fig. 189 (*0.06 and 0.07 second*). Obviously the larger the vector D in this figure the greater will be the rightward direction of the resultant vector. The precordial leads are shown in the figure.

In Fig. 190 the loops which have developed in Fig. 187, 188 and 189 are shown in *a*, *b*, and *c* respectively, in clockwise rotation and semitransverse position, and in *d*, *e*, and *f* in clockwise rotation and apex-back transverse position. In *g*, *h*, and *i* the anatomic axis is the same as in *a*, *b*, and *c* but there is more clockwise rotation about the anatomic axis. The relation of the hypertrophy loop to the normal loop is shown for purposes of orientation. In *j* the spatial loop of Fig. 189 (marked right ventricular hypertrophy) is represented with the heart very transverse and in slight



clockwise rotation. In *k* the spatial loop of Fig. 189 is shown with the heart rotated slightly counterclockwise with a transverse anatomic axis.

Ordinarily when the right ventricle becomes enlarged, as in pulmonary embolism and in mitral stenosis) the heart tends to rotate clockwise and it is for this reason that the figures are drawn largely for clockwise rotations. It is also difficult to avoid the conclusion that enlargement of the right ventricle of more than mild degree must cause the apex of the heart to be pushed backward, for the

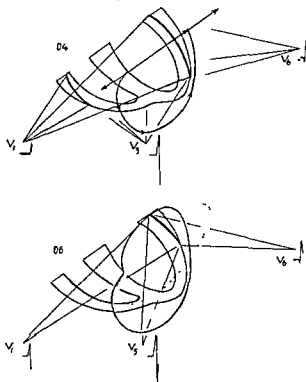


FIG 187. Mild right ventricular hypertrophy. The waves of excitation in the right ventricle are assumed to persist longer than in the normal due to the increased thickness of this structure (compare with Fig 14). This results, as shown, in an increase in the magnitude of the vector at 0.02 and at 0.025 second (unless the apex of the ventricle, as frequently happens, is not thickened). After 0.025 second the electrical effects of the waves of excitation in the two ventricles oppose one another and the vector at 0.04 second is shorter than the vector normally occurring at this time. At 0.06 second (assuming that activation of the mildly hypertrophied right ventricle is completed at this time) the vector is the same as that seen in the normal. If the apex of the right ventricle is not thickened with the base the dotted normal loop is followed to the point at which it crosses the loop for right ventricular hypertrophy; from here on the hypertrophy loop is followed.

The precordial leads are derived by the solid angle method, and, as shown, may reveal no diagnostic changes. The limb leads are derived in Fig 190.

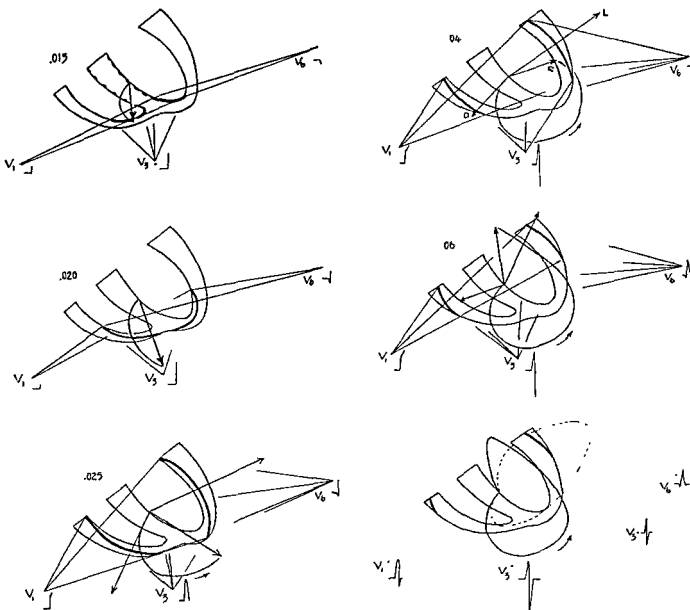


FIG. 188. Moderate right ventricular hypertrophy. The derivation of the first portion of the loop is similar to that of Fig. 187. At 0.04, 0.06, and 0.07 second (the sixth diagram) however, the right ventricular effects are shown to be greater and to persist longer. This shortens the resultant vectors directed to the left. In addition, at 0.06 second it is seen that the waves of excitation in the bases of the two ventricles are such as to produce a resultant which points more backward than any of the vectors of the normal loop.

The precordial leads derived by the solid angle method show a wide and possibly large R in V_1 and small R and deep S in V_6 .

The limb leads are derived from the loop constructed in these diagrams as shown in Fig. 190.

(See next page for third part of Fig. 188)

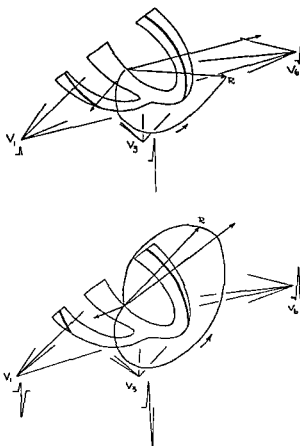


FIG 188 (Continued) The alternate figures for 0.04 and 0.06 second represent what may be expected to occur if to the moderate degree of right ventricular hypertrophy we add a similar degree of left ventricular hypertrophy. The loop returns to the form developed in Fig. 187 but is larger. The precordial leads also tend to return to the form seen in Fig. 187 but are also larger.

right ventricle has no room to occupy anteriorly. On the other hand, in congenital heart disease with great right ventricles and frequently quite small left ventricles, the architecture of the heart is such that the concept of clockwise and counterclockwise rotation as generally employed loses its meaning. If the right ventricle is very large and the conus and pulmonary artery are very large it may well be that the surface of the electrically active mass of the right ventricle points mainly *forward*, somewhat *downward*, and to the right; the surface of the smaller left

ventricle may point down and back and to the left, or simply backward and to the left. It is not inconceivable that it may point a bit upward. At any rate it is not impossible, as far as the right ventricle is concerned, that the effects are such that they may be represented by counterclockwise rotations of the loop as in Fig. 190k.

Right Ventricular Hypertrophy and Right Bundle Branch Delay

It is important to note that the spatial QRS loop and QRS complexes (in all leads) developed for mild hypertrophy of the right ventricle (Fig. 187) such as may occur in some cases of cor pulmonale or rheumatic heart disease differ little from those developed for right bundle branch block of slight degree (see Fig. 76, p. 99) or from the normal. Also, the spatial loop and complexes developed for moderate right ventricular hypertrophy (Fig. 188) differ little from the spatial loops and complexes developed for moderate right bundle branch delay (see Fig. 75, p. 98). Finally, the similarity between the shape of the loop and of the complexes developed for extreme right ventricular hypertrophy (Fig. 189) and those developed for complete right bundle branch block is evident. It must also be remembered that right bundle branch delay does not necessarily increase the duration of the QRS remarkably so that this measurement may be of no help in distinguishing it from right ventricular hypertrophy.

One of the most important problems facing electrocardiographers today is the recognition of right ventricular hypertrophy. The difficulties encountered in this problem are largely due to the common occurrence of various degrees of right bundle branch delay, frequently in the total absence of organic heart disease. Not only do various degrees of right bundle branch delay frequently mimic the limb leads and the precordial leads of right ventricular hypertrophy in every detail but also it is well known that right bundle branch block frequently occurs in the presence of

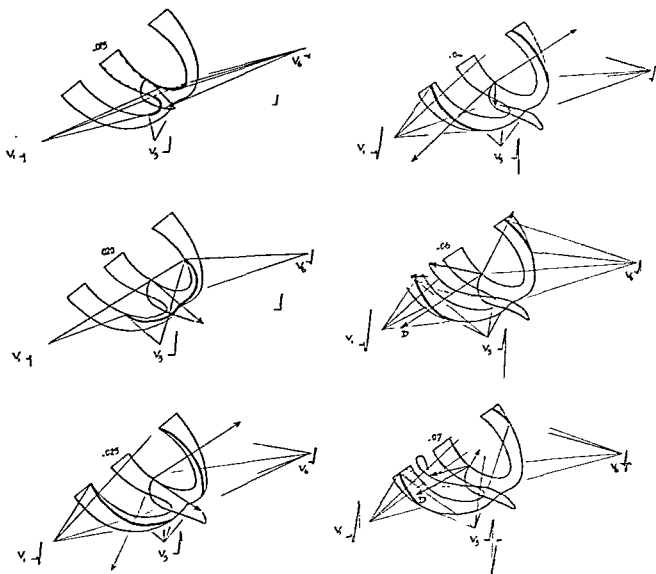
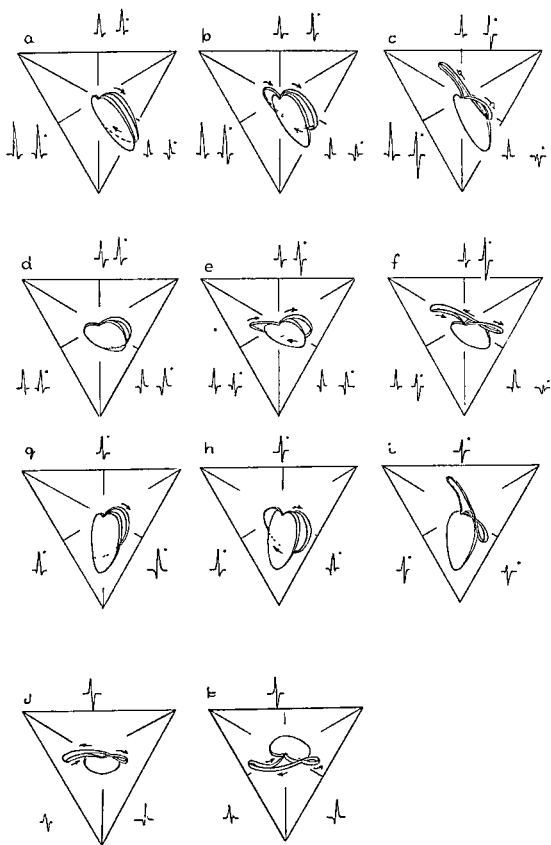


FIG. 189. Marked right ventricular hypertrophy. The same principles are followed which were employed for Figs. 187 and 188. Here the right ventricle is thicker than the left and after 0.02 second the right ventricular effects exceed the left. After 0.04 second the resultant of the vectors representing the waves of excitation in the two ventricles is directed backward and to the right. The larger and thicker the right ventricle the more rightward direction is assumed by the resultant vector. The dotted loop is for a larger or thicker right ventricle than the solid line loop. Even more extreme degrees than this may occur. Again, if the apex of the right ventricle is not so thick and is quickly penetrated the anterior portion of the loop may be much shorter.

The precordial leads are derived by the solid angle method. Note the very large and wide R in V_1 and the very small R and large S in V_3 .

The limb leads are derived in Fig. 190.



right ventricular hypertrophy. Under these circumstances it is not possible to know to what degree the characteristics of the tracing are due to hypertrophy and to what degree they are due to right bundle branch delay (Fig. 191). Furthermore, there is no correlation between the degree of right bundle branch delay and the degree of right ventricular hypertrophy in these cases.

It seems to require very little to produce right bundle branch delay in many persons. Possibly this can occur simply as a result of a rise in intraventricular pressure. However this does not occur at all uniformly. In normal infants it has been observed by Ziegler and by the writer that the right bundle branch delay varies in degree from beat to beat. It may be important that most of these subjects are screaming when the records are being made.

Electrocardiograms from patients with *marked right ventricular hypertrophy* fall into two groups exemplified by Figs 192a and b. Both may be represented by the loop and precordial leads developed in Fig. 189, the loop being oriented as depicted in Fig. 190j or k (it requires but little rotations to change from 190j to 190k). The difference between the two is that the height of the R in Lead I and of the R in the precordial leads is much smaller in Fig. 182b, possibly as a result of failure of the apex of the right ventricle to become hypertrophied so that the

loop has the alternate form described in the hypertrophy loops. Eccentricity effects may play a part. On the other hand the height of the R in Lead I and in the left precordial leads is also greater when the left ventricle is hypertrophied as well as the right (see below). Tracings such as Fig. 192b are more frequently seen in pure right ventricular hypertrophy (pulmonic stenosis).

The QR in V_1 seen in Figs. 192a and b is pathognomonic of marked right ventricular hypertrophy, except in young infants.

With more *moderate right ventricular hypertrophy* the tracing corresponds to the loop developed in Figs. 187 or 188. Figure 193a corresponds to the loop of Fig. 187 and is oriented as in Fig. 190g. Here again the tracing shows a lower R in I than is drawn for the theoretical Fig. (190g); the loop is of the alternate form discussed in the theoretical development of Fig. 187 (Fig. 194a). Figure 193b is another tracing from a patient with moderate right ventricular hypertrophy. Here, however the loop is, at first glance, that developed in Fig. 188 and is practically nonrotated so that it is viewed on edge (Fig. 194b), and the later portion is of long duration and is bent to the right (note R' in Lead III instead of an S). This latter characteristic combines with the rather wide R' in V_1 to make it possible that we are dealing with the loop of Fig. 191 (p. 222) or with the loop of Fig. 75 (p. 98) for moderate right

Fig. 190. The QRS loops of figures 187, 188, and 189 are shown in the usual spatial orientations *a*, *b*, and *c* are the loops of Figs. 187, 188, and 189 (respectively) in semitransverse position and clockwise rotation. *d*, *e*, and *f* are the same loops in transverse, apex-back position and clockwise rotation. *g*, *h*, *i* are the same spatial loops of mild moderate and marked right ventricular hypertrophy respectively, now in greater clockwise rotation than in *a*, *b*, and *c*. *j* is the more marked right hypertrophy loop for a very transverse, slightly clockwise heart. *k* is the marked right hypertrophy loop for a very transverse, slightly counterclockwise rotation. Only the hypertrophy complexes are drawn for *g*, *h*, *i*, *j* and *k*.

The normal QRS loop of the same orientation is shown in each diagram for purposes of orientation. The complexes to the left are normal; those for right ventricular hypertrophy are to the right in each diagram. It must be remembered that alternate forms of the right ventricular hypertrophy loop (when the apex of the right ventricle is not thickened) are drawn by following the normal loop until the point is reached where the hypertrophy loop crosses it; from this point on the hypertrophy loop is followed. Again it is emphasized that the size of the loop has little meaning for the individual case. Only the form is dealt with except when comparing the effect of hypertrophy of one or both ventricles with a previously established loop for the same individual.

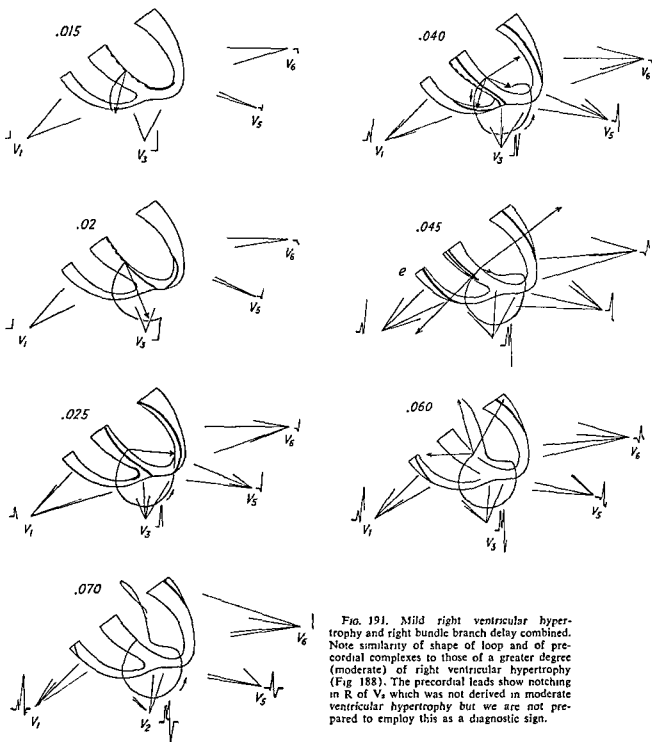


FIG. 191. Mild right ventricular hypertrophy and right bundle branch delay combined. Note similarity of shape of loop and of precordial complexes to those of a greater degree (moderate) of right ventricular hypertrophy (Fig. 188). The precordial leads show notching in R of V₃ which was not derived in moderate ventricular hypertrophy but we are not prepared to employ this as a diagnostic sign.

bundle branch delay without hypertrophy. Very probably right branch delay and right ventricular hypertrophy are both present. Figure 193a is from a patient with patent ductus and Fig. 193b is from a patient with the Eisenmenger complex.

When right ventricular hypertrophy occurs in rheumatic mitral disease it is frequently not very marked and may not be detectable electrocardiographically. Again it may produce loops characteristic of moderate hypertrophy. It is frequently accompanied by left ventricular hypertrophy (due to mitral or aortic insufficiency) and will be discussed under the heading of hypertrophy of both ventricles.

V₁ in Right Ventricular Hypertrophy

A point of great importance is the QRS complex of V₁ as drawn for marked right ventricular hypertrophy in Fig. 189. Actually in most such cases the small primary R wave (due to early left septal activation) does not occur and the complex is characterized by a Q followed by a very large and wide R' wave. The absence of the small R wave may in part be due to clockwise rotation of the heart so that the surface of the left side of the septum does not face the electrode at V₁. However, it may in part be due to the fact that these hearts are generally in a marked apex-back position so that the electrode faces the surface of the left side of the septum tangentially. The effect of this factor upon the potential at V₁ may be further enhanced by the boundary effects of the chest wall as depicted in Fig. 195. Here it is shown that the eccentricity of the source dipoles produces an electrical field such that the potential at V₁ is zero even though the electrode is still facing the positive surface of the dipole layer. This demonstrates one of the inaccuracies of the solid angle method. The same factors may be in part responsible for the absence of the initial R in V₁ in left ventricular hypertrophy.

The appearance of V₁ discussed above is pathognomonic of marked right ventricular hypertrophy. It is not seen to occur in right bundle branch block without hypertrophy.

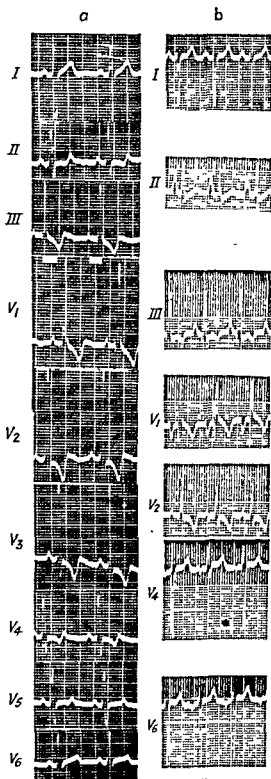


FIG. 192. *a*, Tracing from a patient with marked right ventricular hypertrophy due to atrial septal defect. *b*, Tracing from a patient with marked right ventricular hypertrophy due to pulmonic stenosis.

a

b

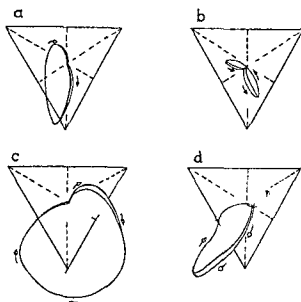
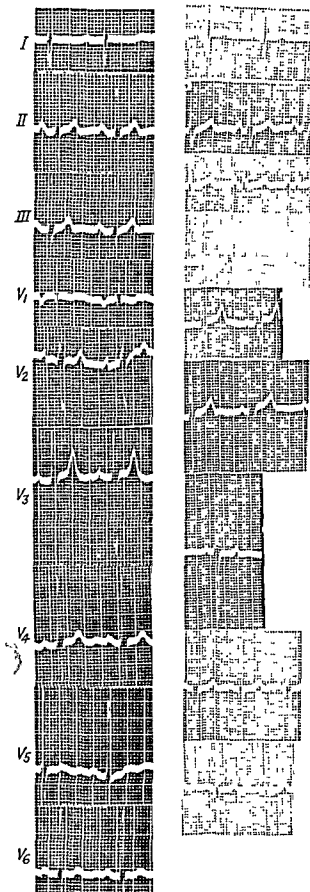


FIG 194. *a*, QRS loop constructed from the limb leads of Fig 193*a*. *b*, QRS loop constructed from the limb leads of Fig 193*b*. *c*, QRS loop constructed from the limb leads of Fig 205*a*. *d*, QRS loop constructed from the limb leads of Fig. 192*b*.

A large S in V₆ generally accompanies this finding. The characteristics of the other precordial leads in the various degrees of right ventricular hypertrophy are shown in Figs. 187, 188, and 189.

Lead V_{3R}. At times the characteristic appearance of Lead V₁ in right ventricular hypertrophy is seen only at points much further to the right. To detect this finding a lead (V_{3R}) is made with the electrode on the right chest at a position corresponding to that of V₃ on the left. Unfortunately high R waves occasionally occur in V_{3R} in normal persons.

Hypertrophy of Both Ventricles

If we add to the right ventricular hypertrophy depicted in Fig. 188 a degree of left

FIG 193. *a*, Tracing from a patient with patent ductus with reversal of flow. There was moderate right ventricular hypertrophy and, as indicated by the large R in V₁ and V₄, some left ventricular hypertrophy. *b*, Tracing from a patient with Eisenmenger's complex. There is moderate right ventricular hypertrophy and possibly right bundle branch delay.

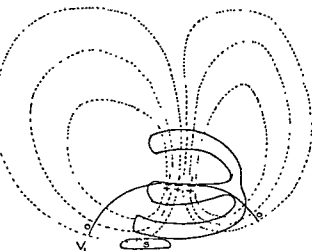


FIG 195. Possible explanation of absence of initial positive deflection in V_1 in marked right (and left) ventricular hypertrophy.

ventricular hypertrophy such as depicted in Fig. 65 (p. 88) each vector in the series of diagrams which represents a wave of excitation in the left ventricle would be made larger and have a bit more forward direction in the early stages and a bit more backward direction in the later stages. The loop representing such hypertrophy of both ventricles would thus be enlarged to the left and forward and would approach the form of the loop drawn in Fig. 187 for a lesser degree of right ventricular hypertrophy *but it would be larger in all dimensions* (see Fig. 188B).

Again, if we add to the right ventricular hypertrophy depicted in Fig. 189 the degree of left ventricular hypertrophy depicted in Fig. 65 (p. 88) the effect would be to cause the loop to approach the form shown for the lesser degree of right ventricular hypertrophy shown in Fig. 188 *but again the loop would be larger in all dimensions*.

These combined hypertrophy loops are most commonly found in the clockwise rotations shown in Fig. 190 (see Fig. 196). However, occasionally they are found in counter-clockwise rotation (Fig. 196c, d), especially when the left ventricular hypertrophy is marked.

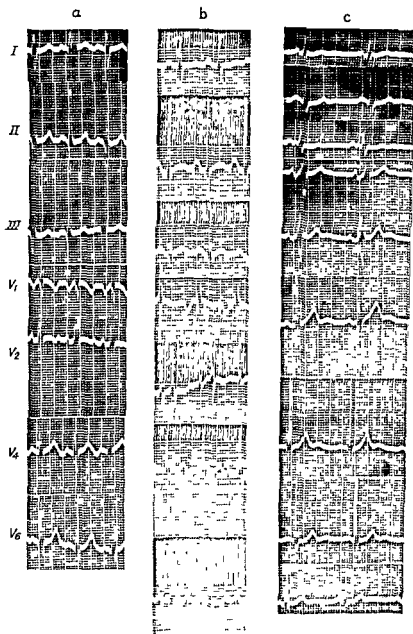
The theoretical expectation that the loop in combined hypertrophy is larger in all

dimensions than the loop of similar shape due to right ventricular hypertrophy alone cannot be verified easily by comparing tracings from different patients, for the size of the loop, even in normals, varies tremendously and the loops are at times very large in young adults. Therefore, some experience will be required for proper interpretation.

Combined hypertrophy may be seen in congenital heart disease (Fig. 205a) and is quite common in rheumatic mitral disease (Fig. 196).

PRECORDIAL LEADS. When both ventricles are hypertrophied the precordial leads will depend upon the extent of the hypertrophy of each ventricle. If there is much left ventricular hypertrophy and only little or moderate right ventricular hypertrophy the latter may not be discernible (see Fig. 196d). The reader is reminded that right ventricular hypertrophy of slight to moderate degree may not be discernible even in the absence of left ventricular hypertrophy (Fig. 187). If both ventricles are hypertrophied to the same extent the precordial leads may show, especially in V_1 , the effects of the right ventricular hypertrophy (a large R). In V_1 , V_4 , V_5 and sometimes in V_6 a deep or wide S resulting from the retreating waves of excitation in the bases of both ventricles is also common. At the same time a larger R wave than is seen in right ventricular hypertrophy alone will occur in V_2 , V_3 , and V_4 due to the proximity of the large waves of excitation in the hypertrophied left ventricle. Left ventricular effects are now so great as to exceed the negative effects of the wave of excitation in the hypertrophied right ventricle at V_6 , so that S in V_6 is not so large.

At times hypertrophy of both ventricles occurs and right bundle branch block is present. The recognition of left ventricular hypertrophy in the presence of right bundle branch block was discussed in Chapter 9. When right ventricular hypertrophy is also present there may be a very high and wide R' present in V_1 following a deep S due to left ventricular hypertrophy, while in other cases (Fig. 197)



the QRS complex of V_1 may be represented only by a very high R wave; V_1 shows no evidence of left ventricular hypertrophy. However, the great height of the R wave in V_5 and V_6 still shows the evidence of left ventricular hypertrophy in these cases.

Unfortunately the expected electrical effects

of right and left ventricular hypertrophy do not always occur. Figure 198 is an electrocardiogram from a patient with a very large heart due to an interatrial septal defect. The complexes are small in spite of the fact that great enlargement of the right ventricle and probably also of the left are present.

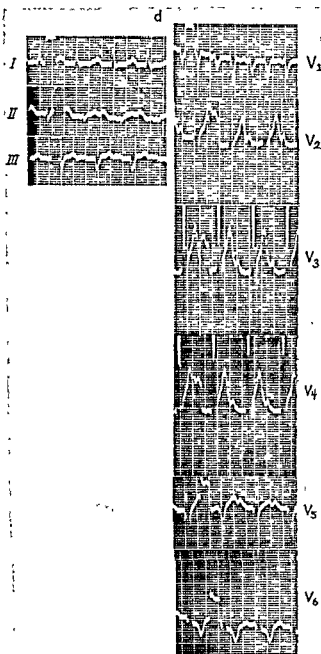


FIG. 196. Hypertrophy of both ventricles. Electrocardiograms of four patients who had rheumatic mitral stenosis and regurgitation. Note that the limb lead complexes in *a* correspond to those of the loop of Figs. 187 and 190*a*. The left precordial leads of tracings *a* and *b* show larger R's than are generally seen in right ventricular hypertrophy alone. On the other hand, the limb leads of these tracings are seldom seen in left ventricular hypertrophy alone.

V₁ of tracings *a* and *b* result from the balance between two large effects. It shows neither the large R of right nor the large S of left ventricular hypertrophy.

c, d, Tracings on patients with verified hypertrophy of both ventricles due to rheumatic heart disease with the loop in counterclockwise rotation. In neither case is the right ventricular hypertrophy discernible from the electrocardiogram.

Note the wide notched P waves due to left atrial enlargement. The largest P waves are seen in V₁ in these cases. In tracing *d* the P looks like a QRS complex.

one might employ the diagrams of Figures 187, 188, and 189 in reverse order to represent the evolution of changes which occurs in normal children's electrocardiograms from early infancy to childhood. It must be noted additionally (presumably because the infant's heart is large in relation to its body) that the complexes in the precordial leads of children's electrocardiograms may be rather large and may be more like those seen in hypertrophy of both ventricles. A prominent R in V₁ is constantly present in the infant and R in V₅ and V₆ may also be large.

The QRS complex is normally much narrower (0.04 second in the newborn and 0.06 in young infants) than in the adult, and right bundle branch delay may be present, even when the QRS is no longer than 0.07 second.

Thus, since infants' and young children's electrocardiograms *normally* are like those which occur in right or right and left ventricular hypertrophy it is necessary in most cases to watch for failure of the normal evolution of the electrocardiogram before conclusions regarding ventricular hypertrophy can be reached from the electrocardiogram alone.

The age at which the various characteristics of the electrocardiogram change varies considerably so that it is not possible to be pre-

Children's Electrocardiograms

Our approach to children's electrocardiograms begins with the anatomic facts that in the newborn the right ventricle is at least as thick or thicker than the left ventricle, and that in the succeeding few months unless some congenital malformation of the heart is present, the relative thickness of the two ventricles changes to that seen in the adult. It follows, then that

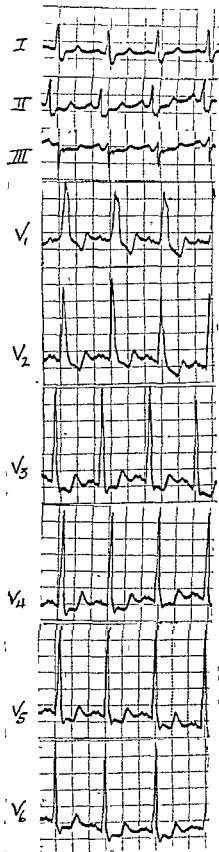


FIG. 197. Right and left ventricular hypertrophy in the presence of right bundle branch block. The patient, 90 years of age, had arteriosclerotic and hypertensive hypertrophy of the left ventricle and hypertrophy of the right ventricle due to long-standing asthma and emphysema. Note prominence of R in V₁ and in V₆ as well.

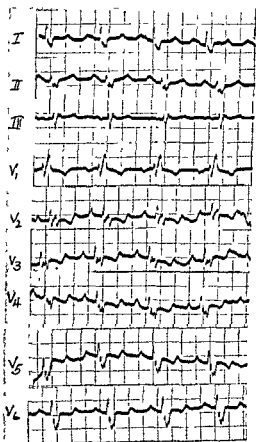


FIG. 198. Electrocardiogram from patient with great enlargement of the heart due to an interatrial septal defect. Note right bundle branch block but absence of the characteristics generally associated with ventricular hypertrophy.

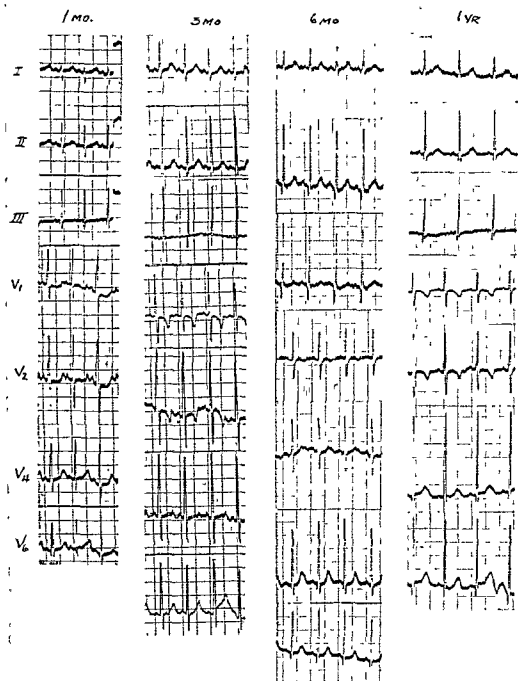


FIG. 199. Progression of changes in the electrocardiograms from one month to one year of age. Note changes of ratio of R_1 to S_1 and the change in V_1 from one month to one year. Some of the variation in the appearance of V_1 is due to difference in placement of the electrode.

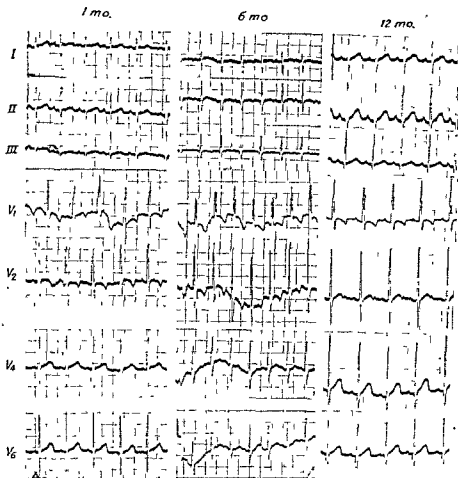


FIG. 200 Progression of changes in the electrocardiogram from one month to twelve months. Note changes in ratio of R_1 to S_1 . Compare with Fig. 199, in which S_1 has already disappeared at twelve months. Here the large R in V_1 persists to one year, but such broad notched R waves in V_1 are probably the result of right bundle branch delay.

cise in interpretation on this basis. For example, the infantile form of the complexes in V_1 (prominent R and little or no S wave) may persist well into the second year or longer in some individuals, while in others it may be replaced by a complex in which R and S are nearly equal before the age of one year (Figs. 199 and 200). It is important to note, too, that the same variation in the appearance of V_1 can often be recorded in the same child at the same sitting by raising and lowering the position of the electrode. However, generally, persistence of a large R in V_1 at

one year of age raises suspicions of right ventricular hypertrophy, often erroneously.

The same variation of changes with age seen in the precordial leads is also seen in the limb leads. Characteristically until about one month there is a marked right axis deviation (to the right of 90°), (Figs. 199, 200, and 201), a small R and deep S in Lead I, and a Q and large R in Lead III. Soon afterwards (Figs. 199 and 200) the R and S in Lead I are of about the same magnitude. On the other hand this latter pattern may be seen as early as one month (Fig. 202). It is

6-4-55

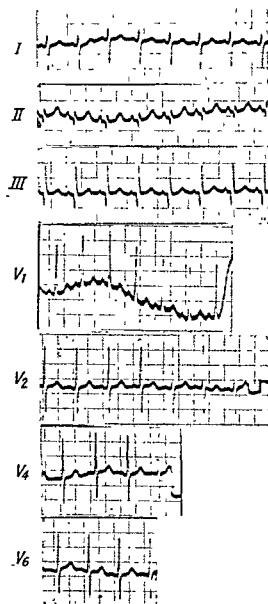


FIG. 201. Tracing commonly seen in first month of life. Note small R and deep S in Lead I, deep Q and large R in Lead III, and large R in V_1 with no S wave.

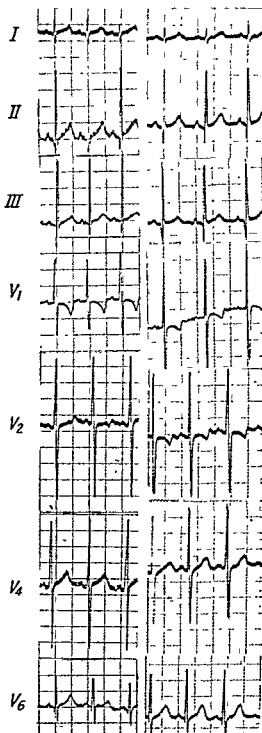


FIG. 202. Tracings at one month (*left*) and one year (*right*) on the same child. There is little difference between the two. In this child the tracing at one month has already reached a form which is not reached until one year in other children (Fig. 199).

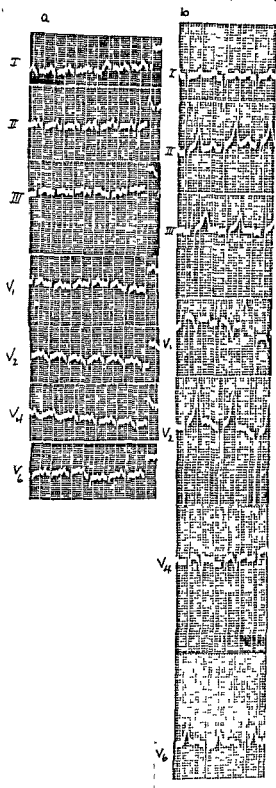


FIG. 203. *a*, Left axis deviation in a young infant (5 months). Autopsy verified clinical diagnosis of tricuspid atresia. Left axis deviation is due to the fact that right ventricle is rudimentary. *b*, Left axis deviation in a 5½-year-old child. Marked left ventricular hypertrophy was present due to a large interventricular septal defect.

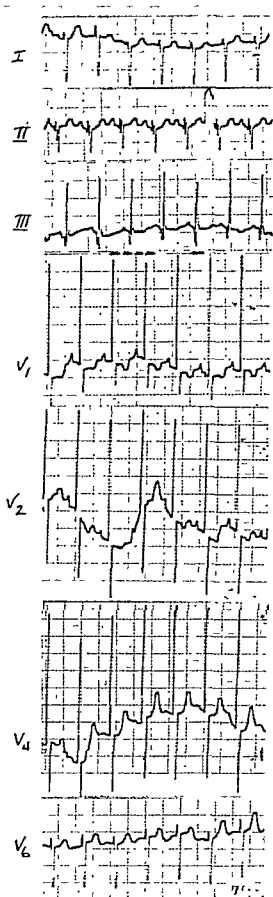


FIG. 204. Exaggerated right axis deviation and very large R in V_1 at 8 months of age. Note also small R and deep S in V_4 . These findings are indicative of right ventricular hypertrophy at any age. The patient had a completely anomalous pulmonary venous return and an interauricular septal defect.

a

b

c

I

II

III

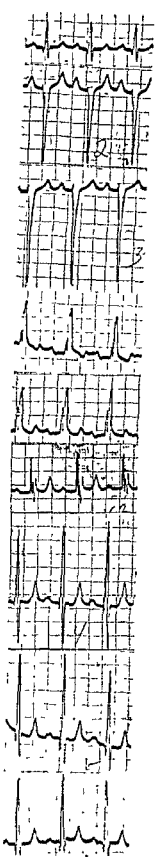
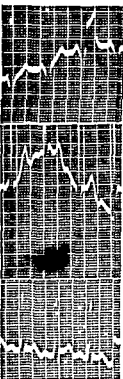
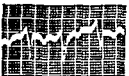
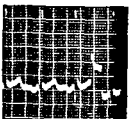
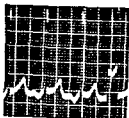
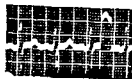
V₁V₂V₄V₆

FIG. 205. *a*, Hypertrophy of both ventricles in a child 2 years of age. The loop is constructed as Fig. 194c. The large R and S in the precordial leads (especially V_1 and V_2) are typical, as is the large rounded loop. V_1 shows neither the very large R typical of right ventricular hypertrophy nor the large S typical of left ventricular hypertrophy.

b, Hypertrophy of both ventricles in a child 5 years of age. Again the limb leads show those characteristics (right axis deviation with large R's in II and III) that are common in right ventricular hypertrophy (see loop of Fig. 190a). The small though broad R and the splintered relatively small S in V_1 are due to the effects of combined hypertrophy; in right hypertrophy alone the R is larger, in left hypertrophy alone the S would have been deeper and the R narrower. Truncus Arteriosus.

c, Right and left ventricular hypertrophy with right bundle branch block. The tracing is similar to that of Fig. 197. Autopsy showed Taussig-Bing syndrome.

important to note, also, that this change bears no close relationship to the change in V_1 from a large broad R and small S to the later RS form. The form of the electrocardiogram (limb and precordial leads) seen at 1 year is frequently the same as that seen at 9 or 10 years of age or even later.

Left axis deviation in a young infant is not rare but may suggest left ventricular hypertrophy or tricuspid atresia (Fig. 203).

Right ventricular hypertrophy, as outlined above, is difficult of recognition. The persistence of the very infantile tracing in the limb leads as late as one year, or an exaggeration of it earlier (Fig. 204) is highly suggestive. However, it must be emphasized that this refers only to tracings with large complexes, for even adults may normally have such clockwise rotations that R_I is very small and S_I is relatively deep while R_{II} and R_{III} are relatively large (see Fig. 46a, p. 66).

Actually the very deep S in I is the significant finding.

Commonly when both ventricles are hypertrophied at an early age (Fig. 205a) a huge loop like that of Fig. 188 results and is in clockwise rotation as in Fig. 194c. The precordial leads correspond also more or less to those depicted for Fig. 188b.

THE T WAVE IN CHILDREN'S ELECTROCARDIOGRAMS. The T wave of the child's electrocardiogram differs notably from that of the adult only in the precordial leads. Generally the T wave is inverted in V_1 , V_2 , and V_3 and it is frequently diphasic in V_4 . This might be regarded as a result of the greater relative thickness of the right ventricle in early childhood but the explanation is hardly acceptable because the finding persists long after the change to the adult ventricular architecture has been attained. As a matter of fact it is quite common in young adults and in females

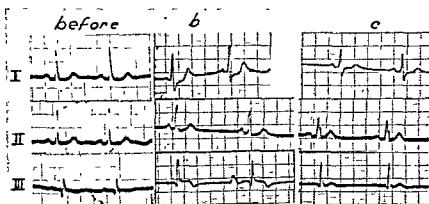
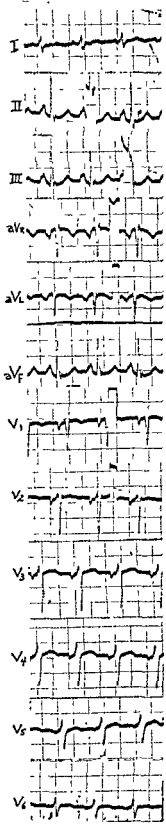


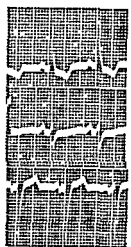
FIG. 206. Pulmonary embolism. *b*, Tracing taken within 15 minutes after occurrence of massive pulmonary embolism. Note S_T ; RS-T shifts here are probably in part due to myocardial anoxemia. *c*, Tracing made 15 minutes after *b*.



a



b



c

FIG. 207. *a*, Pulmonary disease. The patient had pulmonary emphysema. No enlargement or hypertrophy of the cardiac chambers was present. Note low T_1 and low R waves in precordial leads. The same findings are present regardless of the direction of the mean QRS. *b*, Pulmonary emphysema. Left axis deviation due to vertical, counterclockwise, apex-back position. *c*, Pulmonary emphysema. The tracing shows that even in the presence of left ventricular hypertrophy (note wide QRS and QRS-T relationship) the pulmonary disease reduces the height of the R waves in the precordial leads. Distinction from an old anterolateral infarct is impossible.

(especially colored) even into the forties. No adequate explanation of this "juvenile" phenomenon is presently available.

The Electrocardiogram in Pulmonary Embolism

With large pulmonary embolism a characteristic change occurs in the electrocardiogram (see Fig. 206). Generally the heart rotated clockwise causing an S wave to appear in Lead I if it was not already present and increasing the S if it was already present. The R wave in Lead III becomes larger as a rule. Frequently when the S which appears in Lead I is broad and the complex is slurred the tracing appears to show a depression of the RS-T junction. In other cases, as shown in Fig. 206, an RS-T shift is actually present probably due to anoxemia. In the case shown in Fig. 206 death ensued rapidly.

Electrocardiogram in Pleural and Pericardial Effusion

In pleural and pericardial effusion the com-

plexes in both the limb leads and the precordial leads become quite small presumably due to short circuiting of the current through the fluid which has a greater conductivity than the lungs.

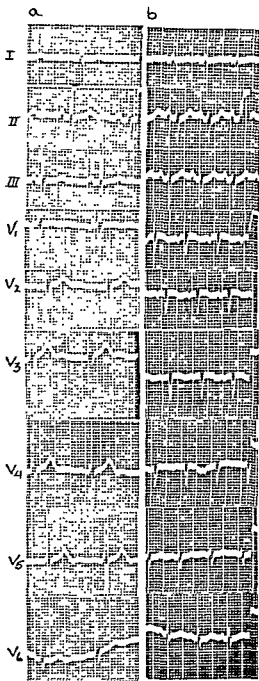


FIG. 208. Tracings before (*a*) and after (*b*) acute right ventricular dilatation. The patient collapsed in the operating room and was in deep shock when *b* was made. The change in the R waves (lowering) in all leads is to be noted. In some cases of acute pulmonary edema with rapid heart rate and in some cases of auricular flutter with rapid rate the R in Leads II and III may disappear and the QS's remaining may be mistaken for evidences of infarction. When the rate slows the R's reappear. Changes in rotation due to right ventricular dilatation may in part explain these changes.

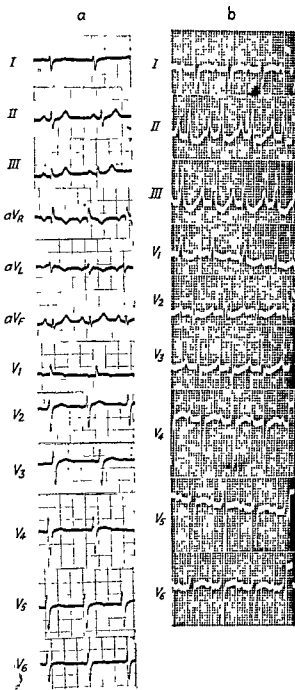


FIG. 209. *a*, Cor pulmonale. Note similarity (low T in I and low R's in precordial leads) to Fig 206, except in V_1 . V_1 shows a QR and no S. *b*, Cor pulmonale with extreme hypertrophy of the right ventricle which in this case was thicker and larger than the left. Note similarity to tracing of pure pulmonic stenosis.

In generalized anasarca there is also frequently a diminution of the complexes in all leads.

The Electrocardiogram in Pulmonary Disease and in Cor Pulmonale

It was first pointed out to us by Ashman that in persons with chronic pulmonary disease, (asthma, emphysema, tuberculosis) characteristic changes in the electrocardiogram may be seen. Figure 207*a* and *b* are examples. The important features are small complexes, especially the T wave, in Lead I even though the T wave in the left precordial leads is fairly normal (though it also is often small). Often the QRS complexes, like those of Fig. 41, 41*a* are those of an apex-back vertical heart with counterclockwise rotation.

In some of these cases the R waves are quite small in the precordial leads and are not unlike those seen in some healed anterior or apical infarctions, and in right ventricular hypertrophy or dilatation (Fig. 208). The R waves in the precordial leads may be small even in the presence of left ventricular hypertrophy (Fig 207*c*).

The physiologic explanation of the pulmonary disease electrocardiogram is not yet available. It may involve change in conductivity of the lungs.

The same characteristic occurs in the tracings of persons with air cysts in the lungs and in pneumothorax (especially on the left side).

In *cor pulmonale* the changes are those typical of right ventricular hypertrophy, exaggerated by the above described effect of the pulmonary disease. In some cases the tracing is actually that of marked right ventricular hypertrophy (Fig. 209).

13. Disturbances of the Cardiac Mechanism

by

Richard Ashman, Ph. D.*

Disturbances of the cardiac mechanism, involving a change in rate or irregularity of rhythm, may have either a physiologic or a pathologic basis.

Sinus bradycardia is a normal phenomenon, observable in nearly 40 per cent of normal adult males at rest. The heart beat originates in the usual place, the sinus node, and the wave of excitation is transmitted through the heart in normal sequence by the normal pathways. The slow rate, arbitrarily set at any rate below 60 beats per minute, is simply due to enhanced activity of the vagus nerve and to reduced sympathetic activity. Rates as low as 28 beats per minute have been reported, but rates below 40 are rare.

Sinus tachycardia, arbitrarily defined as a rate above 100 per minute when the mechanism is normal, is commonly, as during exercise, associated with reduced activity of the inhibitory fibers of the vagus, and increased activity of the cardiac sympathetic fibers. In fever or thyrotoxicosis other factors are present. In infants and young children it would seem well to abandon the term *sinus tachycardia* for rates slightly in excess of 100 per minute.

As the heart rate increases in sinus tachycardia, the P waves and QRS complexes tend to become narrower, and the P-R interval may be diminished from the average (in adult males) of 0.16 second to 0.13 or even 0.12 second. In contrast it may be noted that there is little tendency for the P-R interval to lengthen in sinus bradycardia. In sinus tachycardia, as a rule, the P waves become higher and more pointed. This may occur even during the periods of cardiac accelera-

tion in sinus arrhythmia. Frequently, perhaps especially after exercise, as the heart rate goes up, the amplitude of R waves goes down slightly.

It is noteworthy that in the tachycardia of thyrotoxicosis the P-R intervals are not shortened, nor are the P waves narrowed. This is probably due to the fact that here the augmented rate is not primarily of nervous origin.

Sinus arrhythmia is a more or less regular increase and decrease in the heart rate (Fig. 210), usually associated with respiratory movements. Acceleration occurs during inspiration and retardation during expiration. Though this has been attributed to a "spilling over" of nerve impulses from respiratory to cardio-inhibitory or acceleratory centers in the medulla, the primary cause of the respiratory arrhythmia is probably reflex. On inspiration the output of the left ventricle is reduced slightly and more blood is drawn into the thorax. The consequence is greater fullness of the right auricle and great veins and a slight fall in arterial blood pressure. The first effect augments the "Bainbridge" reflex; the second reduces the inhibitory action of the carotid sinus and aortic nerve (moderator) reflexes. Vagus action is reduced and the heart accelerates. In expiration the reverse effects occur. It is unlikely that the sympathetic nerves play any important role in sinus arrhythmia.

Even into old age slight arrhythmia may be present, but it is most marked in children and adolescents. On deep, slow breathing the longest cardiac cycles may be over twice the length of the shorter ones.

In general, the more rapid the heart rate the less the sinus arrhythmia. Hence it is in-

* Director, Heart Station of Charity Hospital, New Orleans.

conspicuous or practically absent when the heart rate is high. In defining high rate, age must be considered.

In normal children or adolescents no measurable variation in length of the P-R interval is associated with the arrhythmia. This fact tends to confirm the absence of variations in sympathetic activity as a cause of the arrhythmia. (Mild fluctuations in vagus tonus within ordinary heart rate ranges hardly affect A-V conduction time in the normal heart. One will occasionally observe a child with rheumatic carditis in whom a fairly marked sinus arrhythmia is present. In some of these cases, although the P-R interval is within the normal range, a measur-

The Refractory Period

A number of phenomena that appear in various disturbances of the cardiac mechanism cannot be explained without an understanding of the refractory period. During the time that heart muscle is depolarized, and almost until the time of its full repolarization, an applied physiologic stimulus, however strong, will evoke no response or beat. Hence in the period of full or partial depolarization the muscle is absolute refractory. If a strong stimulus be applied just as repolarization is being completed, a beat is evoked. In healthy cardiac muscle, for a short period after the end of the absolute refractory period, the



FIG. 210. Sinus arrhythmia.

able increase in that interval will occur (and should be confirmed in several different leads) at the ends of the *shorter* cycles. Since this is clearly not a vagus effect, it is attributable to a prolongation of the *relative refractory* period of the A-V junctional tissues. So far as we are aware, no systematic study of this indication of rheumatic carditis has been made by having suspected cases breathe deeply and slowly to augment the arrhythmia. This same phenomenon may appear after full or somewhat excessive digitalization in the absence of disease. Changes in P-wave amplitude commonly accompany the rate fluctuations in sinus arrhythmia. It is for this reason that several leads should be observed to determine whether apparent variations in P-R interval are real.

Occasionally in sinus arrhythmia, A-V nodal escaped beats may terminate some of the longer cycles. This is not evidence of disease.

stimulus must be strong to elicit a contraction; a little later the resting excitability is restored.

With respect to conduction of the wave of excitation, no wave, of course, can be conducted during the absolute refractory period. Very early during the relative refractory period, when a *stronger stimulus is needed*, the velocity of conduction is slow, becoming progressively faster and faster as the relative refractoriness approaches its end.

In the ventricular muscle it may readily be inferred that the absolute refractory period is as long as the interval from the beginning of QRS to about the apex of the T wave. In man, when the heart rate is 60/minute, this is about 0.30 second. In auricular muscle the absolute refractory period is less than half this, and the relative refractory period is here rather unimportant. Under the strong influence of the vagus nerve, the refractoriness of auricular muscle is shortened to a small fraction of its ordinary duration. The in-

hibitory fibers of the vagus do not innervate the ventricles, and the nerve, therefore, has no direct effect on the ventricular refractory period.

In connection with electrocardiography, certainly the most important of the factors influencing the duration of the refractory period is heart rate. We have already noted that the period in the ventricles and, probably, A-V node and bundle, is about as long as the interval from Q to the apex of T. The downstroke of the T wave lasts about 0.08 second. It follows, therefore, that Table B (Appendix II), relating the Q-T interval to the

emphasis, Fig. 211 was prepared. The monophasic curves are those which might be recorded by appropriate means from ventricular muscle. The duration of each curve is, roughly, the duration of the absolute refractory period of the muscle, were it uninjured.

For purposes of illustration in Fig. 211, we may assume a basic heart rate of 46.2 beats per minute, giving a cycle of 1.30 second. With each systole terminating cycles of this length the absolute refractory period is taken as 0.34 second, as shown by the horizontal bars just below the first monophasic curve of the upper group, and the first two

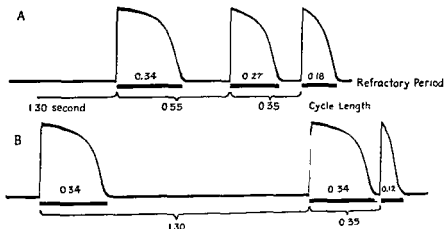


FIG. 211. Effect of rate on the refractory period.

heart rate, may also serve as a crude index of the ventricular absolute refractory period. At each rate, or cycle length, one simply subtracts about 0.08 second from the Q-T interval. Thus, in the male, at cycle 1.00 second, the period is 0.306 second; at cycle 0.50 second, the period is 0.203 second, etc.

If this estimate is correct, no ventricular premature beat can arise before the peak of the T wave, since to that point, all the muscle is refractory. The observed facts agree. Premature beats may start (since early slow conduction from focus of origin will not be shown) just after the peak of the T wave. Of course, they may, and usually do, arise later.

In order to give a graphic representation of the effect of rate (or cycle length changes) on the refractory period, and for purposes of

of the lower group in the figure. The monophasic curves are very slightly greater than this in duration. Following the cycle of 1.30 second (upper row of curves) a "premature beat" occurs after a cycle of 0.55 second (as shown). The refractory period of this beat is given as 0.27 second. Following this premature beat, another occurs after a cycle of 0.35 second, and the associated refractory period is 0.18 second. We may now turn to the lower group of curves. After the end of the regular cycle of 1.30 second, a premature beat occurs at the end of a cycle of 0.35 second, as does the second premature beat of the upper row. But, as shown, the associated refractory period is 0.12 second, not 0.18 second as in the upper series of curves. This is a most important fact, especially in rela-

tion to conduction of impulses, as will be shown below. The diagram demonstrates that it is not the mean heart rate, or average cycle length, that determines the duration of the refractory period associated with each systole, but rather the time between the end of one refractory period and the beginning of the next. In this example of Fig. 211, one cycle of 0.35 second is ended by a systole with a refractory period of 0.18 second, and another cycle of 0.35 second is ended by a systole whose refractory period is 0.12 second. Hence, if we are to analyze the effect of refractoriness on conduction, as in auricular premature beats, the duration of the "antecedent" cycle must be taken into account. In

beginning of the next, causes all the refractory periods to be short, so that the A-V node, bundle, and ventricles can respond to every impulse from the auricles, and all the impulses are conducted.

Figure 212 illustrates what happens when a paroxysm of supraventricular tachycardia begins, though here the rate chosen is 200 per minute. (The figure may, alternatively, be regarded as showing the conduction of three successive auricular premature beats). In this figure horizontal distance corresponds to time, as on the electrocardiogram. The upper horizontal line is the boundary between the sinus node and the auricular muscle, conduction through which is shown just below. The upper

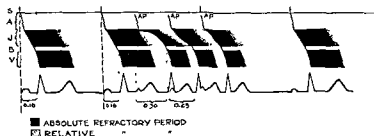


FIG. 212. P-R interval variations in auricular premature beats.

the upper part of Fig. 211 this antecedent cycle is 0.55 second, in the lower part, 1.30 second. The figure does not exaggerate the actually observed phenomena, though it is not very precise.

We may recall that the auricular absolute refractory period and systole are usually much shorter than those of junctional or ventricular muscle. For this reason, when the auricles are accelerated within the physiologic range, the degree of shortening of the auricular refractory period is much less than it is in junctional or ventricular muscle.

When the heart as a whole is greatly accelerated, as in auricular paroxysmal tachycardia, the great diminution in cycle length (to 0.25 second at a rate of 240 per minute), and the great decrease in the interval between the end of one refractory period and the

line of black areas marks the junctional tissues, conduction times through them, and duration of their refractoriness with successive beats. The lower dark areas do the same for the ventricles. Below is a diagram of the electrocardiogram, with P-R intervals indicated under it.

The diagram begins with the emergence of a regular impulse from the sinus. The oblique line (near A) shows the passage of the impulse through the auricular muscle to the A-V node (part of the junction). This takes 0.04 second. The slope of the line changes, corresponding to the lower velocity of conduction in the junctional tissues, which the impulse traverses in 0.12 second, giving a P-R interval of 0.16 second.

The duration of absolute refractoriness in J and V is here indicated as over 0.25 sec.

The stippling roughly approximates the intensity of *relative refractoriness*, and its duration as indicated, is short.

In 0.6 second after this first "beat," a second, regular beat appears. All the events are repeated, and the P-R, of course, is again 0.16 second. After another 0.3 second, an

other 0.3 second. Although its prematurity is the same as that of the first premature beat, it finds conductivity in the upper *J* nearly normal. Moving rapidly at first, it runs into relatively refractory muscle and is slowed down. This is shown by the curvature of the left margin of the black area. The most im-

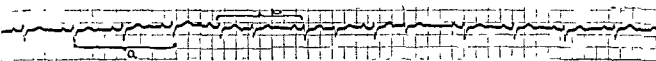


FIG. 213. Auricular premature beats. Note that the double cycle *b* containing the auricular premature beat is shorter than the double cycle *a* of two usual cycles' length.

auricular premature beat arises (not emerging from the sinus). Its impulse reaches the junction (*J*) while it is strongly relatively refractory. Hence, in the upper end of *J* it is conducted very slowly, as is indicated by the slope of the left hand margin of the black area. Because it at first moves so slowly, by the time it reaches the lower part of the

portant point to note is that, because the first premature beat had a very short refractory period, the P-R interval for this second premature beat is not 0.30 second, but (as assumed) 0.25 second. What happens with a third premature beat is sufficiently indicated by the diagram. Its P-R may or may not be slightly shorter than 0.25 second. If



FIG. 214. Auricular premature beats of varying degree of prematurity. A number of the premature P waves are labeled, *a*. The beats, *a*₁, *a*₂, *a*₃, and *a*₄, precede the peaks of the T waves on which they fall and the impulses are blocked. Other P waves, as for example *a*₅, fall on or just after the peak of a T wave, and the P-R intervals are much prolonged. In other instances, as *a*₆, the premature beats fall later, and prolongation of the P-R interval is less.

junction, relative refractoriness has nearly vanished, and the impulse moves with almost normal velocity. But the P-R has become 0.30 second, instead of 0.16 second. Note how very brief the absolute refractory period here is in the upper part of the *J*, and how it rapidly becomes longer as the interval between it and previous refractoriness increases. Note, too, how greatly the ventricular absolute refractory period is shortened.

A second premature beat arises after an-

this incipient paroxysm continued, conduction through *J* would soon become regular, but P-R would continue to be longer than the normal (for this case) 0.16 second. If a fall in blood pressure occurs as a result of the high heart rate (assuming the paroxysm to continue) "reflexly" augmented sympathetic and decreased vagus activity might operate to restore the P-R interval almost to its normal of 0.16 second.

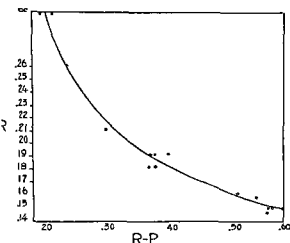


FIG. 215. To demonstrate that the effect of degree of prematurity of the auricular premature beats and the duration of the P-R interval is not a haphazard one, the P-R interval for a number of the premature and regular beats of Fig. 214 were plotted against the R-P intervals. Each point corresponds to an individual beat. Note that as the R-P (or rest) interval increases the P-R interval decreases, approximately along the course of the solid curve. Minor discrepancies are due to two (maybe three) factors: (1) Difficulty in measuring intervals with great accuracy; (2) Failure to attempt correction in accordance with the duration of the "antecedent" cycle (see Figs. 211 and 212); (3) Possible intervention of slight fluctuation in nervous or other influences. The curve of this figure is typical and is always observed if account be taken of possible interfering factors.

There will be occasion to return briefly to these principles later in this chapter.

Premature Beats (or Extrasystoles): Ectopic Beats

AURICULAR PREMATURE BEATS In theory these may arise from any part of the atrial muscle. In some instances premature beats may come from some part of the sinus node, as is indicated by the "sinus" form of the premature P waves, but this situation is not of clinical importance. A common site of origin appears to be near the upper margin of the A-V node, when the P wave will be inverted in Leads II and III, and these may be called A-V nodal, rather than auricular. But again, the distinction is neither certain nor important.

As the name indicates, a premature beat is one that arises earlier than the scheduled time of appearance of a regular beat. It may just anticipate the scheduled beat or it may arise as early as about 0.25 second after the beginning of a previous, regular P wave, or it may appear later.

If the premature beat arises in any part of the auricular muscle other than the sinus node, the associated wave of excitation spreads through the muscle in all possible directions to arrive at both the sinus and the A-V nodes. Usually, it enters both these nodes. The sinus node is, therefore, caused to respond prematurely and becomes depolarized. It then begins again to "build up" another sinus impulse, which may be "discharged" after a period of time corresponding to the regular cycle length. For this reason, there is no full compensatory pause (see below, *ventricular premature beats*). Consequently, when the times occupied by the two ventricular cycles (that terminated by the premature beat and that following it) are summed, the sum is less than the sum of the times of two regular cycles. This is illustrated in Fig. 213.

From the foregoing paragraph, one might expect the auricular cycle following the premature beat to have the same length as a regular cycle. But the fact is that this cycle is usually increased, partly by the added time required by the wave of excitation to travel from the focus in which the premature beat arose to the sinus node, and partly by unknown factors, which may well include a reflex vagus slowing induced by the premature beat, which has not let arterial pressure fall to its usual lowest diastolic level.

A very premature (early) auricular beat may be blocked at the A-V node, even in the normal heart. But if a beat which appears just before the peak of the T wave or later is blocked one is justified in suspecting a pathologic change in the junctional tissues.

The P-R interval associated with the auricular premature beat may be shorter, equal to, or longer than the P-R interval seen elsewhere on the tracing. If, as is frequent, the

premature beat arises near the A-V node (the P wave being inverted in Leads II and III), and if the beat is not very premature, the P-R may be shorter than the other regular intervals, because the wave does not have to traverse the auricular muscle from the sinus to the A-V node, which requires about 0.04 second. If the premature beat is more premature, the P-R interval is usually increased, and may even be doubled. Again, if the P-R is much prolonged when the premature P wave appears near or after the end of the T wave, one may suspect a pathologic change in the junctional tissues. Figures 214 and 215 demonstrate that the impulses of earlier auricular premature beats are conducted to the ventricles more slowly than the impulses of later ones.

Interpolated auricular premature beats may occur but are unusual. In such a case the wave of excitation, traveling from the ectopic focus to the sinus node, is blocked so that it does not enter and depolarize the node. The sinus node, therefore, releases its next impulse on schedule, the premature P wave, therefore, occurring between two regular, successive, sinus P waves.

Because of the almost continuous auricular activity in auricular flutter or fibrillation, auricular premature beats could hardly arise, nor could they be recognized as such in the latter condition. They may, of course, appear in A-V nodal rhythm.

Sometimes, though rarely, an auricular premature beat will appear when a patient takes a deep breath, though none appear elsewhere on the tracing.

Aberration in conduction in the ventricles is common in auricular premature beats, and in not less than 85 per cent of the instances it is due to "delay" in conduction or blockage in the right bundle branch. This definitely does not indicate disease. Other things being equal, the change in the QRS complex is greater the earlier (in one and the same person) the premature beat. Even complete right bundle branch block (for this one beat, of course) is by no means infrequent. When the

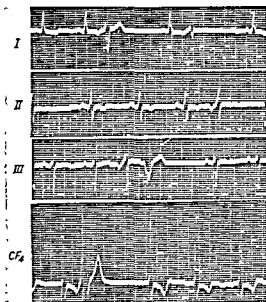


FIG. 216. Nodal premature beats. The inverted P waves in Leads II and III characterize the nodal premature beats in this tracing. Note that the P-R interval following the inverted P waves is shorter than the other intervals. Ventricular premature beats are also present.

aberration is due to "delay" or blockage in the left bundle branch, it is probable that left ventricular disease is present. The frequency of right bundle branch block in these instances poses an interesting problem. It would be unsafe to assume that the right branch actually has a longer absolute refractory period than other cardiac muscle. The more probable explanation is that, perhaps because of its small caliber, the right branch does not conduct the impulses freely even during the late relative refractory period.

JUNCTIONAL PREMATURE BEATS. Unless there is retrograde block between the A-V node or bundle, and the auricles, junctional premature beats will be associated with inverted (and prematurely occurring) P waves in Leads II and III (Fig. 216). As a practical, though not infallible, means of distinction, if the apparent P-R interval is 0.05 second or more shorter than the P-R interval on the rest of the record the premature beat may be called junctional. Sometimes the conduction time from the junctional focus back to the auricles approximately equals the con-

duction time to the ventricles, and the inverted P wave may therefore be quite lost in the QRS complex. If the retrograde conduction time is the longer, the P wave will appear at the end of the QRS complex or in the RS-T segment. The duration of the cycle following the premature beat may or may not equal a regular cycle. Aberration may occur, as with auricular premature beats. If the premature beat arising in the junctional tissues is blocked on its passage back toward the auricles and if aberration is also present, the beat will be indistinguishable from a ventricular premature beat.

VENTRICULAR PREMATURE BEATS. These are the most common form of premature beats, and those most likely to appear with a deep breath, when not seen elsewhere on the record.

Typically, the ventricular premature beat appears on the record as a single premature beat of right or left bundle branch block form, or the wide QRS complexes are typical of neither of these. If the form is like that seen in right bundle branch block, a left ventricular origin of the premature beat is indicated, and vice versa. The beat may appear just after the apex of the T wave of the previous beat or at any later time up to the moment of arrival in the ventricle of the next sinus impulse. Characteristically, the beat arises at a time that permits the associated wave of excitation to pass back from the ventricle by way of the A-V bundle branch into the A-V node, which is, therefore, refractory when the next sinus impulse reaches it from above. Consequently, this sinus impulse is blocked, and the ventricles must usually await the next following sinus impulse before beating again. As a consequence of this usual occurrence, the sum of the durations of the cycles preceding and following the premature beat is equal to the sum of the durations of two regular cycles. Hence, the pause or cycle following the ventricular premature beat is said to be compensatory, in contrast to the usual event in case of auricular premature beats. As stated, unless the beat arises in the

septum and reaches both ventricles simultaneously, the QRS complex is widened to 0.13 second or over, and, of course, secondary T wave changes also appear.

Not infrequently the wave of excitation passes from the ventricles back into the auricles (retrograde conduction) as indicated by the appearance of inverted P waves in Leads II and III. These P waves follow the beginning of the premature QRS complex by some 0.13-0.18 second, as a rule. The retrograde impulses rarely reach the sinus node early enough to disarrange its schedule appreciably.

Ventricular premature beats may often be seen whose associated impulses pass back into the A-V node, where they are blocked, not reaching the auricles. The next sinus impulse, when the heart rate is slow, may reach the A-V node after it has recovered from its refractoriness and therefore pass on to the ventricles, usually with some delay. Such ventricular premature beats are *interpolated*; that is, the beat is sandwiched in between two responses to successive sinus impulses. Typically, because of the slower conduction of the sinus impulse following the interpolated beat, the ventricular (double) cycle within which the premature beat is interpolated is longer, and the following ventricular cycle shorter, than a regular cycle (Fig. 217).

The retrograde impulse from a ventricular premature focus depolarizes the A-V node prematurely as a rule. This node may therefore not await the next impulse from the sinus, but may initiate a beat before the arrival of the next sinus impulse. This is an *escaped* beat. Sometimes a focus in the ventricles may escape, ending the "compensatory pause" prematurely.

If a ventricular premature beat arises so late that the regular sinus impulse is already entering the A-V node, the retrograde impulse does not reach the bundle or opposite ventricle before the impulse of sinus origin enters the opposite ventricle. Hence, although the initial portion of the QRS complex of the premature beat is like that portion of other, earlier premature beats on the tracing, it is

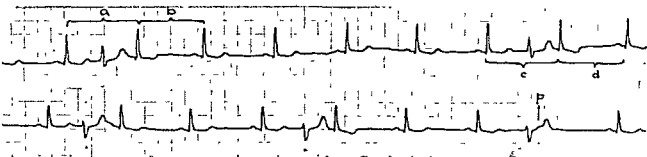


FIG. 217. Ventricular premature beats. Note that cycles *a* and *c*, containing interpolated ventricular premature beats, are longer than the following cycles *b* and *d* respectively. This is due to the fact that conduction of the sinus beats following the interpolated premature beats occurs during the relative refractory period of the junctional tissues and is, therefore, prolonged. Note, also, that when a ventricular premature beat (last in second row) occurs late the *P* wave of the scheduled sinus beat falls long before the peak of the *T* wave of the premature beat and is, therefore, not conducted.

cut short or narrowed. This QRS complex may be referred to as *combined*. The observed P-R interval is shortened slightly. In combination part of the ventricular muscle has responded to the ectopic focus, part to the supraventricular impulse. Sometimes the "combined" complex differs only slightly from the QRS complexes characteristic of the patient, and the shorter P-R interval typical in combination may not be apparent. These seemingly "aberrant" complexes may be puzzling unless this possibility is kept in mind.

When two or more ventricular premature beats occur in succession, we speak of *multiple* ventricular premature beats.

When a number of ventricular premature beats appear on a tracing, and differ in form in a single lead more than can be accounted for by respiratory movements, etc., the differently shaped complexes usually arise from different ventricular foci. We speak of *multifocal* ventricular premature beats. Caution is needed here. If one premature beat, for example, is very early, beginning within 0.05–0.07 second after the peak of the *T* wave, whereas another arises later, they may arise from the same focus but differ considerably in form because the conditions for conduction in the ventricles differ when they arise. But this factor will hardly cause very great differences in the forms of the QRS-T com-

plexes, such as appear when the foci are in different ventricles.

Bigeminy is spoken of when every other ventricular beat is premature whether of ventricular or auricular origin.

The term *trigeminy* is used when every third ventricular beat is premature or when a beat of sinus origin is regularly followed by two premature beats.

PARASYSTOLIC PHENOMENA. An adequate discussion of parasystolic phenomena would take several pages. Hence, the discussion here will be limited to the commonest and most readily demonstrable example. A focus, or group of cells (possibly a cell rest) is present within the ventricles, which is capable of automatic, independent "beating." In the typical instance, the regular impulses of supraventricular origin are prevented from entering the parasystolic focus by what Rothberger and Kaufman called "entrance blocks." Yet impulses originating within this focus may pass out to the surrounding muscle when it is not refractory; that is, "exit block" is absent.

In this simplest instance, the tracing is characterized by ventricular premature beats that follow the complexes of the regular beats at all possible time intervals, with "combination" complexes appearing on a long record. When the intervals from one premature beat

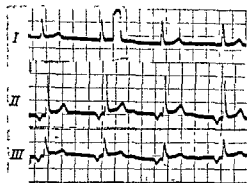


FIG. 218. A-V nodal rhythm. Note inverted P waves in Leads II and III and short P-R intervals.

to another are measured, it is found that each is a multiple of some least common divisor. An assumed example will make this clearer. Suppose the intervals mentioned above are 7.2, 4.9, 3.5, 8.3, 2.4, 9.6, etc. Each interval is divisible, not quite exactly, by 1.2 sec., which would be the cycle length of the parasystolic focus, which is not *absolutely* regular. This, and other possible physiologic factors, prevent the interval from being exact multiples of 1.2 sec. If, in the series of intervals between the premature beats, one also found 5.4, 2.9, 7.8, 3.2, etc., which are not nearly divisible by 1.2, either one is not dealing with a parasystolic focus or its rhythm is so disturbed that no proof of its existence is obtainable. Gouaux and Ashman observed the phenomenon in a 9-year-old boy, who had no heart disease.* Many hundreds of premature beats were observed, under a wide variety of conditions. Only one expected premature beat failed to appear when it was scheduled. The condition lasted at least two years. Other examples of the phenomenon, probably transitory, have been reported in damaged hearts.

Ectopic Rhythms

When some part of the heart muscle other than the sinus node becomes the pacemaker, we are dealing with an ectopic rhythm. The paroxysmal tachycardias are not included

under this heading because the actual mechanism is often not an ectopic rhythm, and, of course, the "circus" mechanism, auricular flutter, and fibrillation do not belong in this category.

AURICULAR RHYTHM. Electrocardiograms which suggest that the pacemaker is in the auricular muscle, not near a node, are rare. Such a mechanism may be assumed, for example, if the P waves in Lead I (assuming the technic is correct and dextrocardia absent) are all sharply inverted.

It is not uncommon to observe marked changes in P waves at different times in the same patient. In most such instances, the indications are that the site of the pacemaker within the sinus node has changed, rather than that a true ectopic pacemaker has been established.

A-V NODAL RHYTHM. When the pacemaker is located in the A-V node, the P waves are inverted in Leads II and III and usually very low in Lead I. As a rule, the P-R interval is short (Fig. 218). In most instances of A-V nodal rhythm the pacemaker appears to be located practically at the boundary between auricular and A-V nodal muscle, the P-R interval in the individual being about 0.04 second shorter than in "normal" sinus rhythm. If the pacemaker is located lower in the node, the P-R interval becomes still shorter, or the P waves may be lost within the QRS complexes, or even appear on the RS-T segments following the QRS complexes. In the last case the only safe conclusion to draw is that retrograde conduction (from pacemaker to auricles) takes much longer than "forward" conduction from pacemaker to ventricles; but a probable location of the pacemaker is then in the A-V bundle.

Although A-V nodal rhythm that persists for hours, days, or even permanently is seen, in most instances the phenomenon is transitory, even appearing and disappearing on one tracing. There are two circumstances that may cause a period of A-V nodal rhythm to appear: (1) The sinus node becomes slower and the inherent automaticity of the A-V

* Unpublished Report.

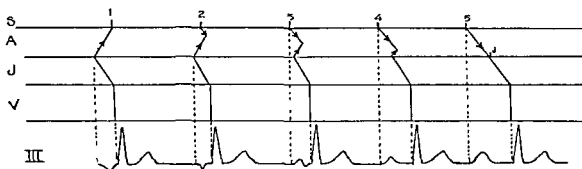


FIG. 219. To illustrate a phenomenon that has been called *shifting pacemaker*, the false assumption having been made that the pacemaker actually "migrates" from one node to the other. In beat 1 the pacemaker is in the A-V node and the impulse goes backward to the auricles, producing inverted P waves in Lead II and III. Ventricular response occurs also. With beat 2 (either because the A-V nodal pacemaker is slowing or the sinus increasing its rate) an impulse arises from the sinus node before the node is reached and depolarized by the impulse of A-V nodal origin. Since part of the auricular muscle is activated from the sinus node, the form of the P wave is changed. With beat 3, more of the auricular muscle is activated from the sinus node, and the P wave is mainly upright. Finally, with beat 5, the sinus has become pacemaker for the whole heart and the typical upright P wave is present.

node causes it to assume the pacemaker role.

(2) The automaticity of the A-V node increases, so that it usurps the role of pacemaker. No sharp line can be drawn between a period of A-V nodal rhythm due to this cause and a period of nodal or junctional tachycardia.

A-V nodal rhythm is likely to appear early in atropinization.

VENTRICULAR RHYTHM. It is theoretically possible for a pacemaker in the ventricular muscle to assume control of the heart's rhythm, the wide QRS complexes each being followed by a P wave. The P waves will be inverted in Leads II and III.

SHIFTING PACEMAKER. The phenomenon that has been called *shifting pacemaker* is described in the caption to Fig. 219.

DISSOCIATION DUE TO INTERFERENCE (INTERFERENCE DISSOCIATIONS). This is a phenomenon, rarely seen except after full digitalization, in which three conditions are simultaneously present: (1) The ventricles are responding to a pacemaker in the A-V node; (2) retrograde block is present, so that impulses do not pass back from the A-V node into the auricles; (3) the auricular rate is typically lower than the ventricular. Under these circumstances, at more

or less regular intervals, a sinus impulse will reach the A-V node after it has recovered from its refractoriness, and will enter and pass to the ventricles, usually with delay. The ventricles, therefore, beat prematurely, though the QRS-T complexes are usually of the same form as the others.

A-V Heart Block

BLOCK RESULTING SOLELY OR MAINLY FROM HIGH AURICULAR RATE. This is observed in auricular flutter, auricular fibrillation, and in rare instances of auricular (paroxysmal) tachycardia. Briefly, since the refractory period of auricular muscle is about half as long as that of A-V nodal or ventricular muscle, the auricles may respond at rates that the A-V node cannot follow, although it must be noted that when the auricular rate in flutter is not exceptionally high, 1:1 A-V conduction may be present for a time after the onset of the flutter, and 1:1 conduction may appear when the flutter is slowed by quinidine.

The problem of block resulting from high auricular rate, however, is complex and will be considered below in the appropriate places. The point to be stressed here is that a partial A-V block in the above-mentioned conditions,

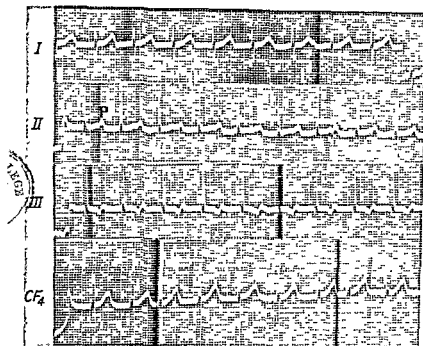


FIG. 220. A-V block. Prolonged P-R interval. Here the P-R is prolonged greatly so that the P waves are superimposed upon the T waves of the preceding beats. This is clearest in Lead II, but the notching of the T waves in the other leads in the absence of anything else which might be a P wave should suggest the possibility.

unless of high degree, is *not* evidence of pathologic change in the junctional tissues.

A-V BLOCK DUE TO CHANGES IN THE JUNCTIONAL TISSUES. Prolonged P-R Intervals. The name *first degree A-V heart block* has been applied to the phenomenon of prolonged P-R intervals, but that term is not employed in this book. The P-R interval will equal or exceed the upper limits of the normal, as given in Table I, in about one person in a hundred, but P-R intervals up to 0.24 second or even longer in adults are not necessarily evidence of heart disease (Fig. 220). Non-pathologic prolongation may appear during recumbency, disappearing when the patient sits or stands. Prolongation of the P-R interval may be permanent and unchanged in extent for years, or it may be transitory, as often after posterior infarction or in rheumatic fever. It may be induced by digitalis in some cases, but it is rare for therapeutic dos-

age to prolong the intervals above those of Table I.

Low-grade Partial A-V Block (Dropped Ventricular Beats). For purposes of discussion, reference may be made to the diagram of Fig. 221A. On the left and above, the auricles; on the right and below, the ventricles; between, the junctional tissues. The line between A and B is the level (plane) at which the blocked impulses (waves of excitation) are stopped. We shall begin with a 4.3 A-V block as in Fig. 221B. We assume the auricles are beating regularly in response to the sinus node; and we shall fix our attention upon a number of successive sinus impulses which may, chronologically, be called 1, 2, 3, 4, 5, 6, etc. We shall further suppose that one sinus impulse arises every 0.60 second (auricular rate being 100/minute). That part of the junction marked B (Fig. 221A) is most injured or depressed. An impulse, 1, ap-

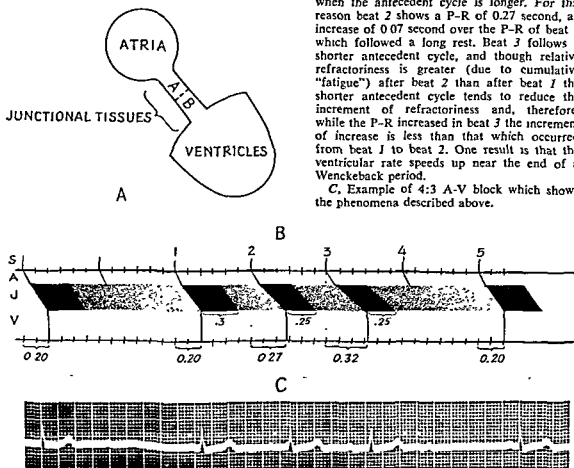
proaching the line between *A* and *B* arrives, causes *B* to respond (become depolarized), and moves on to the ventricles, the P-R interval being, for example, 0.20 second as shown in Fig. 211*B*. One cycle length later impulse 2 arrives at *B*. Now, *B* was depressed when impulse 1 arrived. Its response to impulse 1 left it more depressed (metabolic products not normally disposed of). By hypothesis, however, *B* responds to impulse 2, which, therefore, goes through *B* to the ventricles. The P-R interval may have increased to 0.27 second, since *B* was more depressed and less able to conduct when 2 arrived than when 1 arrived. A cycle length after 2, impulse 3 arrives at *B*. *B*, by hypothesis, can barely respond, yet 3 goes through, but the P-R interval has again increased to, say, 0.32 second. A cycle length later impulse 4 arrives, but now *B* is so depressed that it can-

not respond and 4 is blocked, not entering *B* at all. *B*, then, has time to "recuperate." When impulse 5 arrives, *B* has had two cycle lengths, not the usual one cycle length, for recovery, and impulse 5, like 1, goes through to the ventricles in 0.20 seconds, and the described sequence of events repeats itself.

One thing is not explained by this description. We observed that the P-R interval increased from 0.20 second to 0.27, then only to 0.32. The increase of the second P-R over the first is 0.07 second; of the third over the

FIG. 221. *A*, Simplified diagram of structures involved in problems of A-V block. *B*, Diagrammatic representation of 4:3 A-V block. The solid black rectangles represent the absolute refractory period of the junctional tissues. The prolongation of the relative refractory period (stippled) is due to disease. The relative refractoriness and the duration of the relative refractory period following any beat is greater when the antecedent cycle is longer. For this reason beat 2 shows a P-R of 0.27 second, an increase of 0.07 second over the P-R of beat 1 which followed a long rest. Beat 3 follows a shorter antecedent cycle, and though relative refractoriness is greater (due to cumulative "fatigue") after beat 2 than after beat 1 the shorter antecedent cycle tends to reduce the increment of refractoriness and, therefore, while the P-R increased in beat 3 the increment of increase is less than that which occurred from beat 1 to beat 2. One result is that the ventricular rate speeds up near the end of a Wenckebach period.

C, Example of 4:3 A-V block which shows the phenomena described above.



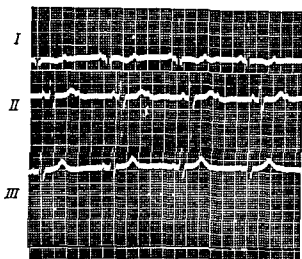


FIG. 222. 2:1 heart block with normal P-R interval in conducted beats. There are also QRS aberrations in some beats (note variability of S in Lead I).

second only 0.05 second. Why? There is really little doubt about the reason. When *B* responded to impulse 1 (and 5) it had had two cycle lengths rest instead of the usual one cycle length since the impulse preceding impulse 1 has been blocked. Now, the refractory period increases as rate slows or cycle length increases (see pp. 240-244). So after *B* responded to impulse 1, after a two cycle length rest, its absolute refractory period was longer than it was after its response to impulse 2, for example, when the rest period was only one cycle length. The consequence of this is that when impulse 3 reaches *B*, it arrives at a greater interval after the end of *B*'s absolute refractory period than did impulse 2. Consequently, in spite of cumulative fatigue or depression of *B*, it goes through in 0.32 second or less, not 0.34 second (as would be expected if the increment were again 0.07 second).

It will be observed that in this illustration the auricles beat four times to three for the ventricles. This is, therefore, called a 4:3 partial A-V block. The ventricular beats occur in groups of three, separated by longer ventricular cycles. These groups are sometimes referred to as *Wenckebach periods*.

In 2:1 A-V block, every other auricular impulse is blocked. This is the most stable form of partial A-V block because it may occur under a wide range of degree of depression of segment *B* (Fig. 221A). That is, when the conducted impulse arrives at *B*, *B* may be pretty well recovered or, on the other hand, it may just be able to respond. So we see 2:1 block with long P-R intervals (for the conducted beat) or normally short ones (Fig. 222). Degrees of block from 3:2 on up—4:3; 5:4; etc.—are likely to be unstable, since slight variations in sinus rate, rhythm, or facilitating or depressive nervous influences may shift one degree of block to another (Fig. 223).

Escaped beats in partial A-V block. It appears that the region of the junction called *B* in Fig. 221A is often part of the A-V node or even the upper margin of that node. But even when the node is depressed by drugs or by pathologic changes, it still has its automaticity, i.e., it may initiate its own impulses. In the 4:3 A-V block described, for example, *B* (or some lower segment of tissue) may not have waited for impulse 1 or 5 before beating spontaneously. Hence impulse 1 (or 5) may arrive at *B* just as (or some time after) *B* has sent its own impulse to the ventricles; and, if the P wave (of impulse 1 or 5) preceded the QRS complex for this beat, the P-R is not true conduction time, but shorter; or this P wave may fall within the QRS of the escaped beat or later. (An example of escape in partial A-V block is seen in Lead II of Fig. 223.) 3:1 and, particularly, 4:1 or 5:1 A-V block is rarely seen for the following reason: a lower "center" in the A-V node, bundle, or in the ventricles does not await the infrequent, occasional arrival past the block of an impulse from above. The block will then appear to be complete, though conduction is possible. Not infrequently block is seen in which most of the beats originate from lower "centers" though an occasional impulse from above gets by, usually with a much prolonged P-R interval. Since in complete block the ventricles are typically nearly

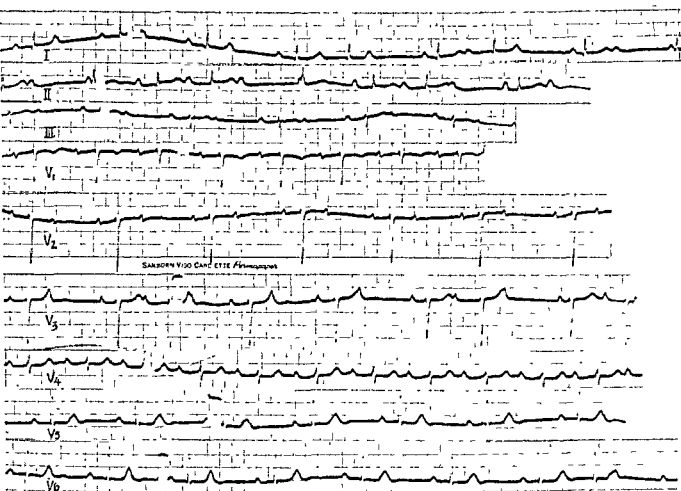


FIG. 223. Varying degree of A-V block. The degree of block varied greatly while this tracing was being made. In Lead I it changes from 2:1 to 3:2. In Lead II there are escaped beats following some of the blocked P waves of a 3:2 block. In Lead III there is a 2:1 block with an auricular rate of 85/min. When, as in V_1 , the auricular rate becomes sufficiently slow (62/min. in this instance) there is 1:1 response with prolonged P-R interval.

absolutely regular, slight irregularity in a block that is apparently complete usually means occasional conduction, and the somewhat constant location of the P waves before the QRS complexes terminating these shorter cycles will confirm a high-grade partial A-V block.

Partial Block with Constant P-R. Sometimes partial block is seen in which the progressive prolongation of the P-R interval, as described above, does not occur. It has been supposed that in these instances the depressed zone or segment of tissue, *B* (Fig. 221*a*), is very narrow, so that practically no time is spent by the impulse in going through it, and

in consequence, variations in that time hardly occur. In some such blocks no regular Wenckebach periods are seen, the block appearing irregularly, haphazardly.

Complete A-V Heart Block. When none of the auricular impulses are conducted from auricles to ventricles the disturbance is spoken of as complete A-V heart block (Fig. 224). Characteristically the ventricles are almost absolutely regular in this condition, although premature beats may occur in some instances. Particularly when the ventricular rate is low, a slight irregularity of the auricles is commonly present. Briefly, it may be said that the auricular cycles within which ventricular beats

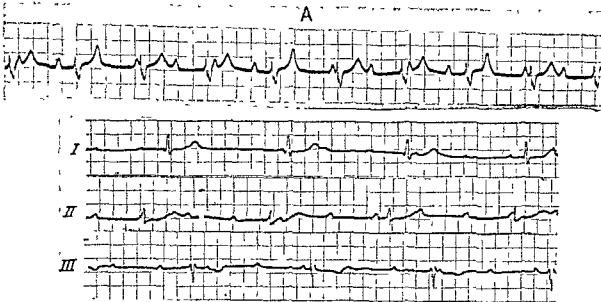


FIG. 224. Complete A-V block. The auricular and ventricular rhythms are both regular but at different rates and are, therefore, completely dissociated. In *A* (upper tracing), the ventricular rate is more rapid than usual. In the lower tracings the more common slower rate is seen.

happen to fall are slightly shorter than the other auricular cycles. This is a reflex vagus effect (Gouvaux and Ashman). In some cases, of course, premature auricular beats may occur, which do not effect the regular ventricular rhythm since they are not conducted.

The pacemaker for the independently beating ventricles may be in the A-V node or bundle, or in the ventricular muscle. If the QRS complexes are narrow, it may be assumed that the pacemaker is above the ventricular muscle. In this instance the ventricular rate is usually above 40 per minute. If the ventricular complexes are wide, the same damage that produced the A-V block may have blocked a bundle branch, though the pacemaker is still junctional, or the pacemaker may be in the ventricles. In the latter case, the ventricular rate is likely to be below 40 per minute. If in block which is apparently complete, occasional *slightly* shorter than average ventricular cycles appear, the beat terminating each such cycle being preceded by a P wave at about the same distance, a high-grade partial block may be assumed, as mentioned above.

When the ventricular beats originate in the ventricles, it does sometimes happen that they originate from different foci, as shown by variable form of the QRS complexes, and the rhythm may be somewhat irregular, or standstill, with syncope, may even occur. Perhaps a more common cause of the Stokes-Adams syndrome is abrupt change from 1:1 or 2:1 conduction to complete block, associated with a brief period of ventricular standstill.

Complete block is seen, though rarely, in patients with rheumatic carditis, especially if digitalized. Partial or complete block, usually transitory, is not infrequent in association with the acute to subacute stages of posterior myocardial infarction; but is not observed in association with anterior infarction, other lesions being absent.

In some badly damaged hearts, when the ventricles are very slow and often irregular, ventricular premature beats may precipitate short periods of ventricular "fibrillation," associated with syncope.

Occasionally "interference dissociation" will result when the A-V nodal pacemaker is

rapid. In these instances, the auricular rate being slower, no auricular impulse may reach the ventricles. Although a "complete A-V block" is present, its cause is physiologic rather than pathologic, and its significance is not the same.

Paroxysmal Tachycardias.

Although these are grouped together for convenience, the tachycardias, other than sinus, are not all due to a single intrinsic mechanism. In some instances the paroxysm appears to be due to the activity of an ectopic focus, which, for some reason not yet known, initiates impulses at a rate higher than the sinus rate. In other instances the paroxysm is probably due to a "circuit" mechanism, the circuits having various locations in different instances. If the auricles are involved in the rapidly repeated beats, the impulses from the ectopic pacemaker that produces the tachycardia enter the sinus node. The latter, therefore, is not given time to "build up" and send out impulses of its own.

SUPRAVENTRICULAR PAROXYSMAL TACHYCARDIA. *Auricular (paroxysmal) tachycardia.* This form (Fig. 97) is differentiated from sinus tachycardia by its abrupt onset and end, and sometimes by the excessive minute rate, which exceeds the approximate upper limit of 160 per minute for sinus tachycardia in adults, though in infants the latter may approach 200. The P waves, when identifiable (not being lost in T waves or QRS complexes) are often, but not always, of the sinus form, though typically slightly narrower than those observed before and after the paroxysm. The P-R interval may or may not be prolonged. Occasionally a 2:1 A-V heart block, or block of other degree, is present (Fig. 225*b*). Unless there is concomitant disease of the ventricles, the QRS complexes are normal, often, indeed, narrower than when a sinus mechanism exists; and the QRS complexes may be of somewhat lower amplitude. Both narrowness and lowness may be an indirect effect of increased sympathetic activity, which in turn results from the frequent moderate

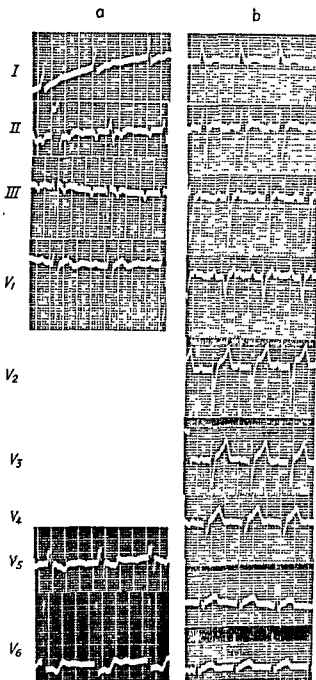


FIG. 225. *a*, Nodal tachycardia with 2:1 A-V block. *b*, Supraventricular tachycardia with 2:1 A-V block.

fall in arterial pressure. Minute rates rarely reach 300 in adults unless fever is present; but even higher rates may be observed in infants or young children.

When the onset of a paroxysm is recorded,

it appears to be introduced by an auricular premature beat. Near the end of a paroxysm, some slowing in rate may occur. Paroxysms may be very transitory, lasting for only a few beats. These could be called multiple auricular premature beats. Or they may persist for hours, days, or months. Before and after a paroxysm, it is common to observe auricular premature beats, for any such premature beat may initiate a paroxysm. Sometimes, in fact, paroxysm follows paroxysm, with longer or shorter periods of sinus rhythm between, with or without the presence of auricular premature beats.

If the ventricles are diseased, left bundle branch block may be present during the paroxysm. Right bundle block may also occur even in the absence of disease. In these instances, the differentiation from ventricular paroxysmal tachycardia may be difficult because the P waves may be lost in the QRS-T and not be identifiable, but the supraventricular origin of the paroxysm is practically proven if augmented vagus activity stops it. When the rate is high and regular, and the limb and precordial leads show QRS complexes characteristic of either right or left bundle branch block, and when no regular auricular activity at a slower rate can be demonstrated by the presence of P waves falling, hit or miss, in the record (i.e. not related to the ventricular rhythm), then the tachycardia is probably supraventricular, i.e., auricular, A-V nodal, or of a type seen in many persons with the Wolff-Parkinson-White syndrome.

In true auricular (paroxysmal) tachycardia the mechanism in most instances is probably circus. In the initiation, an impulse emerging from the sinus node at one end or side, but being blocked in its emergence elsewhere, "circles" through the auricular muscle near the node and re-enters the node at the other end or side. Having re-entered it can move to the original site of emergence and thus a circuit is established. Obviously most of the auricular muscle will respond to this rather narrowly localized circuit as if it was a "pace-maker" in a "focus," so that the reported

failure to discover a circus mechanism in the auricles as a whole in auricular tachycardia is based on a misunderstanding. No direct evidence of a circuit through the whole muscle can be expected. With rapid re-entry and the slight "fatigue," which increases susceptibility to the acetylcholine liberated by the vagus nerve, the action of the vagus in stopping many paroxysms is easy to understand. The action is to prevent re-entry by blocking. If the paroxysm is of A-V nodal origin, the vagus similarly may stop it.

Ventricular premature beats are unlikely to be observed in supraventricular paroxysmal tachycardias, especially when the minute rate of the ventricles is high. Auricular premature beats are yet more unlikely.

T wave and RS-T segment changes occur, as a result of the high rate, and are described elsewhere. The duration of the Q-T follows the rules shown in Table B (Appendix II).

A-V nodal (paroxysmal) tachycardia. What has been said of auricular paroxysmal tachycardia is also true of the A-V nodal form with few exceptions (Fig. 225a). The differences are:

The P waves are inverted in Leads II and III, and, as a rule, in V_4 to V_6 , and predominantly upright in V_1 and V_2 .

A partial, or even complete block, may be present between the auricles and the A-V node. If this is complete, or if high-grade partial block is present, the auricles will respond to sinus impulses as they usually do; and the ventricles are driven from the A-V node. If aberration (right or left branch block) is present, together with retrograde block from the A-V node to auricles, the appearance will be that of ventricular paroxysmal tachycardia, though the conclusion will be misleading.

Supraventricular paroxysmal tachycardia in the Wolff-Parkinson-White syndrome. The frequent association of the Wolff-Parkinson-White syndrome and paroxysmal tachycardia must mean a fundamental relationship between the two phenomena. Since an accessory pathway for conduction between auricle and

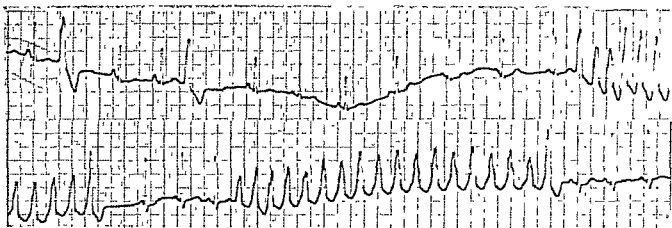


FIG. 226. Paroxysms of ventricular tachycardia and frequent ventricular premature beats.

ventricle exists in the W.-P.-W. syndrome in all likelihood, we may at once understand a possible basis for the tachycardias, on the basis of work first reported as early as 1913 by G. R. Mines in the *Journal of Physiology*, and later confirmed in various ways by A. G. Mayor, W. E. Garry, and Sir Thomas Lewis. It is easy to cause a wave of excitation or impulse to move in a "circle" in an excised turtle heart, split down the middle, but with a narrow bridge of muscle connecting the auricles at one end of the heart and the ventricular halves at the other end. Proper timing of an electric shock or two may set a wave in motion that descends on the right, for example, and ascends on the left, and that may thus continue for hours in a "circle" if the state of the muscle is good.

Similarly, one may suppose for example, a premature beat to arise in the auricle in a person with the W.-P.-W. syndrome. This may be blocked at the A-V node, but enter the ventricles by the accessory pathway. The impulse then "circles" back by way of a bundle branch and A-V bundle, enters the A-V node, and thence re-enters the auricles. It may then pass through the auricular muscle, re-enter the accessory pathway, again reach the ventricles, and so on. In this instance the paroxysm will look ventricular in the tracing. But if the blockage of the initiating premature beat is in the accessory pathway, and the impulse enters the ventricles by the usual

A-V pathway, then, if it can circle back by way of the accessory pathway into the auricles and thence re-enter the ventricles, the paroxysm will appear to be *supraventricular*. Since either appearance may, in fact, be observed in persons with the W.-P.-W. syndrome, the theory finds observational support. The vagus may stop such a paroxysm by blocking the normal A-V pathway, and there is some reason to expect, *a priori*, that left carotid sinus pressure should be more effective than right. If the patient is first digitalized, then carotid sinus pressure might stop a refractory paroxysm. Digitalis alone may also do this because of its effect on A-V conduction. But with carotid sinus pressure, *less* digitalis should be required. These are *a priori* expectations, not observations.

In some instances, supraventricular paroxysmal tachycardia may arise from a true ectopic focus. This whole question needs further expert study for clarification. In the experimental animal one may show that this or that happens, but there is evidence that such studies, pursued without adequate physiologic background, may deceive as often as they clarify, when applied to human mechanism disturbances.

VENTRICULAR PAROXYSMAL TACHYCARDIA. The minute rate of the ventricles is likely to be slower in this condition than it is in supraventricular tachycardia, say 130-200 per minute; and sometimes the rhythm may

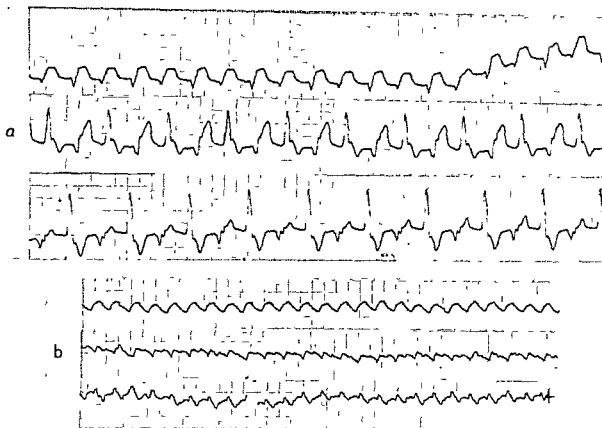


FIG 227. *a*, Unusual ventricular mechanism occurring in patient with unclassified myocarditis. Two separate and alternating foci appear to be involved. This is usually seen only in digitalis intoxication but this patient had received no digitalis. *b*, Later on same day. Ventricular tachycardia, approaching fibrillation. Large injury shifts are present in both tracings but no infarction was found at autopsy.

be slightly irregular (Fig. 226), even when the electrocardiographically similar condition of auricular fibrillation with bundle branch block (aberration) can be ruled out. The demonstration of a slower, independent auricular rhythm is not quite crucial, as was noted above under A-V nodal tachycardia.

The QRS complexes are wide and in limb and V leads they may or may not resemble those typical of right or left bundle branch block. As in left bundle branch block, secondary T wave changes will be present. Since the condition is rare when the myocardium is normal, primary T wave change is also likely to be present.

The nature of the paroxysm probably varies from case to case. The impulses may come

from one or more foci, with similar or variable (Fig. 227*a*) forms of successive QRS complexes. The more rapid rhythm may be essentially a ventricular flutter, a circus mechanism (Fig. 226 and 227*b*).

Unlike the auricles, the ventricles are *not* innervated by vagus cardioinhibitory nerve fibers. Hence, if vagus stimulation or analogous procedures stop a paroxysmal tachycardia which is apparently ventricular, it is *not* ventricular.

CIRCUS CONTRACTIONS: FLUTTER AND FIBRILLATION. *Auricular Flutter.* Apparently this mechanism disturbance is initiated in susceptible hearts by an early auricular premature beat, which encounters a barrier to conduction in one direction (due to refractori-

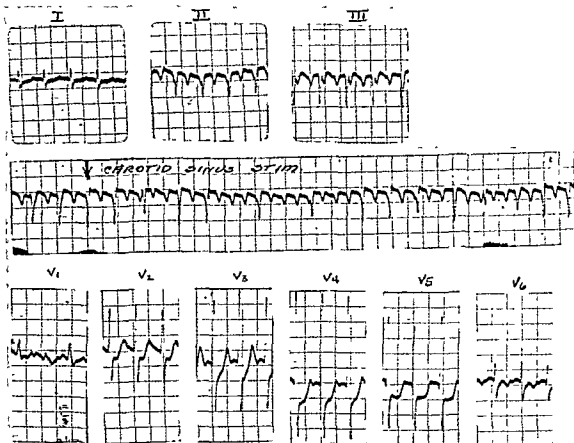


FIG. 228. Auricular flutter with 2:1 A-V block. The degree of block was increased by stimulation of the carotid sinus, thus exposing more clearly the flutter mechanism. Injury shifts are present in the precordial leads. Posterolateral infarction followed. Note that R_{II} has disappeared. It returned when mechanism was restored. This phenomenon is common with rapid heart rates and congestive heart failure. Caution should be exercised in interpreting QRS changes of this kind when the rate is very rapid.

ness) but which can travel in the other direction.* The wave of excitation con-

* We do not wish to enter into controversy, but may note (without discussion) some peculiarities of auricular flutter and fibrillation that accord with the circus movement theory, but which are not explained adequately by the view that these mechanisms are due to impulses arising from one or more foci: (1) The usual inconspicuousness of the P waves in Lead I. (2) The long period of time during which the conditions may persist. (3) The apparent roughly circular progress of the wave, as studied by Lewis. (4) The absence of effect on the auricular activity of increased vagus tonus, aside from a reported slight increase in rate, to be expected from the vagal shortening of auricular refractory period. (5) The difficulty of demonstrating that so-called flutter or fibrillation induced in the experimental mammal is really the same thing as the clinical condition. (6) The experimental work that does

subsequently "circles" around the auricles, and reaches the "barrier" from the opposite side, now being able to pass. Thus the wave, traveling in a "circle," can keep on going, as in the turtle heart of G. R. Mines. If the sweep of the wave of excitation with each "revolution" is uniform, we are dealing with *auricular flutter*. Were it not for the confusion in understanding introduced, we might say, in a manner of speaking, that the "circle" is established about the mouths of the great

support the circus movement thesis (7) The discreteness of the P waves in auricular tachycardia, where either a focus or a very local circuit is involved. (8) The easy demonstration with appropriate material that persistent circus movements are possible.

veins, but, of course, with each circuit there is an outward spread of the wave to involve all parts of the auricular muscle. Each circuit is completed in about 0.20 second, on the average, or 300 per minute; but the auricular

rate, or frequency of response, in flutter ranges from as low as about 130 (after heavy quinidine dosage in some few cases) to 370, or even 400 in children.

As each circuit is completed, the wave of excitation reaches the A-V node, but the node, because of its longer refractory period, can rarely respond to every wave, except in some instances early after the onset of flutter, or when the flutter rate is low. (Quinidine depresses the A-V node as well as the auricular muscle, but often, with the induction of quinidine therapy, the slowing of the auricles may permit the A-V node to respond more frequently, with an alarming increase in ventricular rate.) Typically, therefore, in auricular flutter, we observe 2:1, 3:1, or 4:1 A-V block, and often irregular rapid change from the one degree to another. Not rarely the ratio varies between 2:1 and 4:1 without the intermediate 3:1.

The P waves in auricular flutter are usually characteristic (see Fig. 228 and 229). Continuous auricular activity is indicated, so any division into P waves is arbitrary. In Leads II and III, the "P" wave shows a rather rapid ascent, a short, usually descending "plateau," and a more gradual descent, leading to the next ascent. The same form is repeated, usually with the utmost regularity. In Lead I, the amplitude of the P waves is so low that the flutter is often hard to detect. No P-R interval can be measured, since the time of arrival of the waves at the A-V node cannot be determined. In V_1 the waves often seem more separate, since the major potential changes are due to activation of the sub-jacent auricular muscle.

In most instances, pressure on the carotid sinus, or some other procedure that increases vagus activity, will produce a transitory complete block. On cessation of pressure, the ventricular rate rapidly returns to the rate observed before pressure.

Impure Flutter. When the flutter rhythm is slightly irregular, with slight variation in P wave form, it may be called "impure."

Auricular Fibrillation. This mechanism is

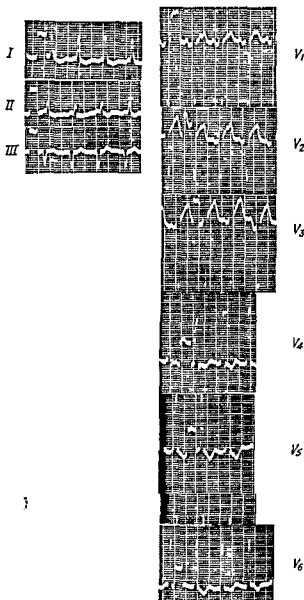


FIG 229 Auricular flutter with 2:1 block. Here the flutter mechanism is more difficult to discern than in Fig. 228 because of the inconspicuousness of the flutter waves in the limb leads. The nature of the mechanism is clearly revealed in Lead V_1 . The auricular rate is 288. Left ventricular hypertrophy is also present.

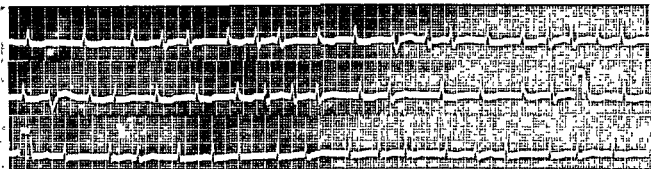


FIG. 230. Auricular fibrillation with aberration; also ventricular premature beats. Lead I and II (continuous) and Lead II. The first and second ventricular cycles of the upper row are relatively long (0.86 and 0.72 second, respectively). At an interval of 0.445 second after the second beat, an aberrant QRS complex appears. It is of the typical right bundle branch block form. This is followed, in 0.385 second, by another aberrant QRS. The next QRS, the sixth, follows the fifth in 0.61 second and is not aberrant; but the seventh QRS, ending a cycle of 0.415 second, is, as is the next.

The eleventh QRS complex is a ventricular ectopic beat, and the twelfth QRS complex, following in 0.48 second, is aberrant, despite the apparently relatively long "rest interval." This is due to the fact that the ectopic impulse passes backward to the junctional tissue, which was activated after, and not before, the QRS complex appeared. Thus the "rest period" in the junction was short before the twelfth QRS. Later, at the beginning of the second strip, another ventricular ectopic appears. The reason the second complex following it shows only slight right branch delay and not block is clearly due to the fact that the "antecedent cycle" (see text) is not so long as it looks, because of retrograde conduction of the ectopic beat.

The next to the last QRS complex of the upper strip is not aberrant, though it might have been expected. The *main* reason is the extreme shortness of the antecedent cycle, which is only 0.355 second.

fundamentally the same as flutter, and there is actually no sharp dividing line between the two, impure flutter being a transitional stage. In auricular fibrillation, the auricular rate is higher, as much as 400 per minute; the fibrillary waves of the tracing indicating the auricular activity, are often inconspicuous and variable in amplitude, duration, and form. The pathway of the circling wave is presumably shorter and the outgoing wave fronts, recurring so frequently, encounter islands or masses of refractory muscle, so that conduction is irregular and varies from revolution to revolution. In V_1 a greater appearance of regularity is often seen, with less variability in "fibrillary" wave form. This suggests that the central pathway for conduction in fibrillation is traversed by the wave with considerable regularity, and the irregular variable electrical deflection in the limb leads is mainly due to irregular conduction in outlying muscle regions in these cases, but that the muscle

subjacent to the V_1 electrode can respond fairly regularly, even at the high rate.

Because of the higher auricular rate, the consequent presence of temporarily refractory muscle masses, and the long refractory period of the A-V node, the response of the latter, and consequently of the ventricles, is typically very irregular. This is in contrast to flutter, where, if the ventricles are irregular, the irregularity is not absolute, there being two or three different cycle lengths, more or less irregularly repeated. Carotid sinus pressure will slow the ventricles in auricular fibrillation, but will not usually stop them as in flutter. This can be explained on sound physiologic principles, but would require space not here available. Fever, emotional disturbance, and exercise may increase the ventricular rate in auricular fibrillation.

The ventricular rate in untreated auricular fibrillation ranges around an average of about 130 per minute up to as high as 200. Rates

as low as 60 or lower probably indicate a slight defect in A-V conduction. Complete A-V block, with auricular fibrillation, is not very unusual, but is generally seen after treatment (digitalis). The ventricles are then regular, barring premature beats. Ventricular premature beats are not uncommon in auricular fibrillation, but need to be distinguished from aberration, which is more likely when the ventricular rate is fairly high.

Aberration in Auricular Fibrillation; Distinction from Ventricular Tachycardia. Aberration in intraventricular conduction in auricular fibrillation is a common phenomenon when the ventricular rate is fairly high and the rhythm very irregular and is important enough to demand special consideration (Fig. 230). In the discussion of auricular premature beats, the relationship between cycle length and absolute refractory period has been given. In principle, there is no distinction between aberration in fibrillation and in auricular premature beats. Because of the usual considerable variations in the duration of the ventricular (and therefore junctional) cycle lengths in auricular fibrillation, there are associated variations in the durations of the absolute refractory periods in the junctional tissues. For example, if a cycle is, say, 0.8 second, the refractory period of the beat terminating this relatively long cycle may be about 0.3 second. If an impulse from the fibrillating auricles reaches the A-V node just after the end of this period, it will enter, be conducted slowly to the ventricles, and be blocked in a bundle branch, usually the right. Thus aberration occurs. The ventricular cycle terminated by the widened QRS complex will not be of the same duration as the refractory period, but, because of the slow conduction, it may be, say, 0.4 second. This then, is a typical example of aberration in an assumed case when the "antecedent" cycle is 0.8 second. Let us suppose the antecedent cycle to have been near the average in this patient, say 0.6 second. Then the absolute refractory period of the junctional tissues would be shorter than 0.3 second, say 0.26

second. If an impulse reaches the A-V node at 0.3 second after the beginning of the absolute refractory period, no aberration will occur.

It follows, therefore, that to distinguish an aberrant complex from ventricular premature beats, four tests may be applied. (1) The "antecedent" cycle is a longer one. (2) The cycle ended by the wide (aberrant) QRS complex is at least nearly as short as any other cycles on the tracing, though slightly shorter ones without aberration may appear after short antecedent cycles. (3) No longer cycles will be followed by very short cycles which do not show aberration (a slight qualification is needed here, but would involve a lengthy, not very profitable, discussion of theory). (4) The "aberrant" QRS is typically of right bundle branch block form in all leads.

The foregoing description, while of some importance, is not so important as a further manifestation of aberration, which must be grasped if clinically significant disturbances are not to be misunderstood. Let us consider an example that was observed and carefully studied. A patient with auricular fibrillation (very impure flutter) had a ventricular rate of about 180 per minute. Digitalis was administered and the rate slightly reduced. Quinidine then reduced the auricular rate, with an associated speeding up of the ventricles to 200 per minute. The rhythm was irregular, though few ventricular cycles exceeded 0.4 second. At this time for short periods the rhythm was only slightly irregular, the rate about 200, and the QRS complexes narrow. On other parts of the tracing the rate and slight irregularity were the same, but the QRS complexes were all wide, of right bundle branch form. It was observed that these periods, (of apparent ventricular tachycardia) were each preceded by a longer cycle than the average (about 0.4 second) and that this "antecedent" cycle was terminated by a normal QRS complex. Following this complex the series of "aberrant" complexes began, at the 200 per minute rate.

If one refers to the diagram (Fig. 213,

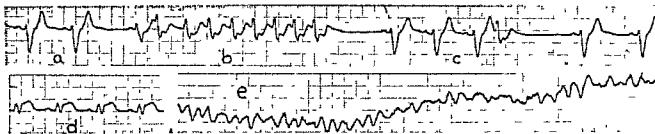


FIG. 231. Ventricular tachycardia and fibrillation in a patient with acute myocardial infarction. *a*, Sinus beats with intraventricular conduction defect. *b*, Paroxysm of ventricular tachycardia. *c*, Three sinus beats followed by a ventricular premature beat from the same focus which originated the paroxysm of ventricular tachycardia. *d*, Return to sinus mechanism (in another lead). *e*, Ventricular fibrillation.

The records were made in sequence on the same patient.

p. 243) in the section on auricular premature beats, the first "aberrant" complex is understandable. The question is, why did aberration persist when the shorter cycles must have been associated with shorter refractory periods. Consideration of theory supplies an obvious answer. When the first aberrant complex of the series appeared, the impulse was blocked in the right bundle branch. It, therefore, entered the ventricles by way of the left branch, passed through the septum (in about 0.06 second), and entered the lower part of the right branch. The impulse could not ascend the right branch because its proximal end was refractory from its recent activity (about the point of blocking). Now, when, 0.27–0.34 second after the earlier impulse had come from above, another impulse descends, it will find the right branch, below the blocking point, refractory, and right branch block again occurs. The right branch has "rested" for only 0.20–0.27 second and will not conduct. The block, with aberration, will persist, therefore, until a somewhat longer cycle occurs, say 0.35 second or longer. It was observed that the periods of aberration (which looked like ventricular tachycardia) did, in fact, all end with a slightly longer cycle. On the other part of the tracing, where the same average rate was reached *without* aberration, no "long" antecedent cycle had occurred to initiate a series of aberrant complexes. (Reference Gouaux and Ashman).

Auricular flutter or fibrillation may, of course, be associated with other disturbances or abnormalities, such as ventricular premature beats, left or right bundle branch block (not of the temporary, physiologic, type just described), and complete A–V block. The T waves in auricular fibrillation frequently vary in amplitude and form, especially when the ventricular rate is high, and the character of these changes may sometimes point to myocardial ischemia or to T wave changes due to changes in cycle length.

Ventricular Flutter. Ventricular flutter is probably the mechanism involved in some cases called ventricular tachycardia, as in Fig. 226.

Ventricular Fibrillation. Ventricular fibrillation is illustrated in Fig. 231*e*, which sufficiently presents the characteristic tracing in this condition. If auricular activity is present it is masked by the fibrillary waves, of varying amplitude of direction.

THE WOLFF-PARKINSON-WHITE SYNDROME. In this syndrome the P–R interval is shortened, the QRS complex is widened to the same absolute extent, as a rule, and about half the individuals are subject to paroxysms of tachycardia. The phenomena can all be logically related to the presence of one or more accessory pathways for conduction between auricles and ventricles, which, have, in fact, been proven to exist.

In some individuals, the typical electrocardiographic picture is constantly present; in

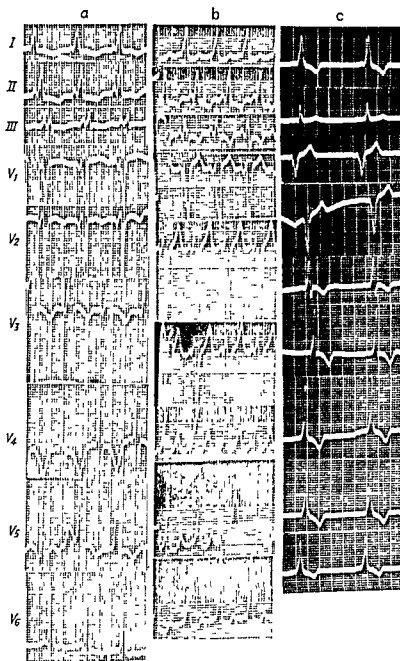


FIG. 232. Three cases of "W-P-W Syndrome"

others, various procedures may cause blockage in the accessory pathway with reversion of the electrocardiographic findings to normal. In a few cases, some of the impulses from above are conducted by the accessory

pathway and some are not on the same tracing.

When the phenomenon is present both the regular and accessory A-V pathways conduct, of course, but the wave of excitation

reaches the ventricles more promptly by way of the accessory pathway. Otherwise, the presence of a conducting accessory path could not be demonstrated, unless the normal P-R were prolonged in some manner.

Since the accessory pathway leads the impulse into ventricular muscle and not directly to Purkinje fibers, it is typical to find the upstrokes of the R waves slurred in several leads, and a pseudo-left bundle branch block

form is common. Since the net areas of the QRS complexes are increased, as a rule, the reciprocal effect on the T waves will necessarily occur (pp. 50-67).

If prolonged periods of tachycardia occur, primary T wave changes, even of apparent "ischemic" type, may follow the paroxysm and persist for hours or days. This may occur following a prolonged tachycardia (Figs. 232a and 97).

Suggested Reading

- Ashman, R., and Hull, E. *Essentials of Electrocardiography*. The Macmillan Co., New York, 2nd ed., 1941.
- Barker, P. S., Wilson, F. N., and Johnston, F. D. Mechanism of auricular paroxysmal tachycardia. *Am. Heart J.*, 26:435, 1943.
- Blair, H. A., Wedd, A. M., and Young, A. C. The relation of the Q-T interval to the refractory period, the diastolic interval, the duration of contraction and the rate of beating in heart muscle. *Am. J. Physiol.*, 132:157, 1941.
- Campbell, M., and Elliot, G. A. Paroxysmal tachycardia. Etiology and prognosis of 100 cases. *Brit. Heart J.*, 1:123, 1939.
- Garrey, W. The nature of fibrillatory contraction of the heart, its relation to tissue mass and form. *Am. J. Physiol.*, 68:128, 1914.
- Garrey, W. E. Auricular fibrillation. *Physiol. Rev.*, 4:215, 1924.
- Lewis, T., Feil, H., and Stroud, W. D. Observations upon flutter and fibrillation. Part II. The nature of auricular flutter. *Heart*, 7:191, 1920.
- Moe, G. K., Harris, A. S., and Wiggers, C. J. Analysis of the initiation of fibrillation by electrocardiographic studies. *Am. J. Physiol.*, 134:473, 1941.
- Rosenbaum, F. F., Hecht, H. H., Wilson, F. N., and Johnston, F. D. The potential variations of the thorax and the esophagus in anomalous atrioventricular excitation (Wolff-Parkinson-White Syndrome). *Am. Heart J.*, 29:281, 1945.
- Schwartz, S. P., Orloff, J., and Fox, C. Transient ventricular fibrillation. *Am. Heart J.*, 37:21, 1941.
- Wolff, L., Parkinson, J., and White, P. D. Bundle branch block with short P-R interval in healthy young people prone to paroxysmal tachycardia. *Am. Heart J.*, 5:685, 1930.

14. Drugs, Electrolyte and Metabolic Disturbances

by

Irving L. Rosen, M. D.*

The varied, and sometimes marked, changes produced in the electrocardiogram by drugs make it necessary that one be acquainted with these changes when interpreting electrocardiograms. This is especially true since some of the drugs used in the treatment of heart disease produce electrocardiographic changes, and these changes may mimic those due to organic heart disease.

Digitalis

The electrocardiographic changes due to digitalis result from the effects of the drug on repolarization of the ventricles, a depression of atrioventricular conduction, and increased myocardial irritability. In clinical doses therefore, the P wave and QRS complex are not affected, and the effects of digitalis are limited to the RS-T segments and T waves and to the cardiac mechanism.

As has been mentioned previously, digitalis diminishes the ventricular gradient and this effect has been summarized in Fig. 40 (p. 57). The first change is usually a slight shift of the first portion of the RS-T segment in a direction opposite to that of the main QRS deflection together with a slight decrease in the magnitude of the T wave (Fig. 233c). Commonly more marked effects are present and there is a greater RS-T segment shift with a progressive diminution of the T waves, so that the T wave becomes incorporated in the RS-T segment shift (Fig. 68A-b, p. 91). At the same time there is a further decrease in the Q-T interval. It should be noticed that the shape of the RS-T segment shift due to digitalis is frequently a straight line opposite to and directly propor-

tional in magnitude to the main QRS deflection (Fig. 68A-b). When present, this characteristic shape of the RS-T segment shift, its relationship in magnitude to the preceding QRS deflection, and the shortened Q-T interval may aid in the distinction of digitalis effects and ischemia. Since digitalis affects the ventricular gradient the most marked RS-T segment and T wave changes are to be expected in those leads upon which the projection of the ventricular gradient is greatest.

Occasionally the direction of the RS-T segment shift is not opposite to the main deflection of the QRS complex in the leads from the anterior chest. As can be noticed in Leads V_2 and V_4 of Fig. 234, the main deflection of the QRS is downward and the RS-T segment is also displaced downward. This paradox seems to be limited to the leads mentioned. As a rule the RS-T segment shifts due to digitalis are opposite in direction to the main QRS deflection. By using the principle that the RS-T segment and T waves effects of digitalis are due to a decrease in the ventricular gradient, an approach to tracings already abnormal when digitalis is administered can be made.

Since increase in heart rate also diminishes the gradient, a rapid rate will exaggerate the RS-T segment and T wave effects of digitalis. When the rate is slowed the RS-T segment and T waves effects diminish again. The similarity of the effects of rapid rate and of digitalis is shown in Fig. 235. Tracing A was made on a patient in congestive failure. An anterior and diaphragmatic infarction and right bundle branch block evidently had occurred sometime previously. Tracing B was made after the heart had slowed as a result of the administration of mercurhydrin. Note

* Instructor in Medicine, Louisiana State University School of Medicine, New Orleans.

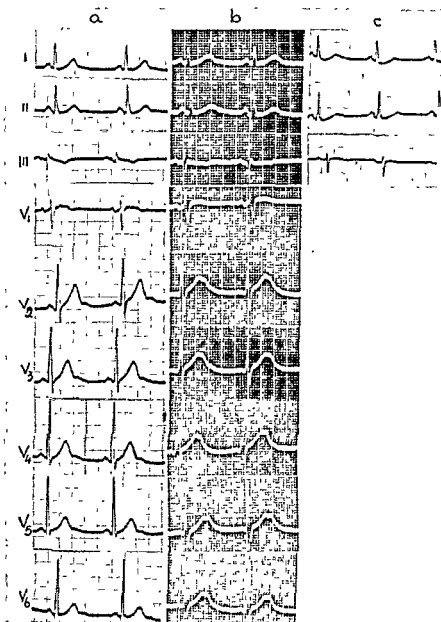
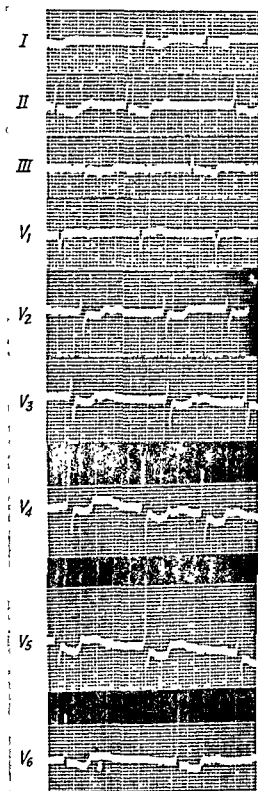


FIG. 233. Effects of quinidine and digitalis on the electrocardiogram. Three tracings from the same patient: *a*, prior to the administration of cardiac drugs; *b*, following the administration of quinidine; and *c*, after digitalization. Note the broad, flat, notched T waves following quinidine and the shortened QT interval with depression of the RS-T segments in Leads I and II following digitalization. The patient was not receiving quinidine when *c* was made.

that T_1 originally upright is now small and diphasic; T_{aV_1} , formerly upright, is now inverted. The RS-T segments in V_1 , V_2 , and V_3 , formerly displaced from the baseline, are now almost on the baseline. The T wave in V_1 is smaller while the T waves in V_2 , V_3 ,

V_4 , V_5 , and V_6 are definitely inverted. All these changes are attributable to the change in rate. If we had begun with tracing *B* and attempted to predict what might be expected from diminution of the gradient such as occurs with rapid rate it would have been nec-



essary to say that the RS-T segment and T waves would change in a direction opposite to that of the main deflection of the QRS complexes. This describes quite accurately the change between the two tracings. Of course they occurred in reverse order as a result of slowing the rate. Since digitalis also diminishes the gradient, it is seen in Fig. 235C that it tends to make all of the leads approach again the form which they had when the rate was rapid (compare *A* and *C*).

In Fig. 236, *A* was made before and *B* after digitalis. There is auricular fibrillation and left bundle branch block. It is impossible here to divorce rate changes from digitalis changes insofar as the QRS-T relationships are concerned. One can only say that apparently the very rapid rate alone is capable of diminishing the gradient to a greater extent than digitalis can at a slow rate. The slowing of the rate here is due to the effect of digitalis upon the conductivity of the A-V node and bundle of His. It was for this effect that the digitalis was administered.

When left ventricular hypertrophy is already present, the administration of digitalis diminishes the gradient and thus exaggerates the secondary T wave changes resulting from the increased QRS deflection. The effect of digitalis in Fig. 174 (p. 201) deserves some comment. Tracing *a* shows the result of an old myocardial infarction and left ventricular hypertrophy. The tracing *b* was made after digitalization had been carried to the point of nausea. The Q-T interval is markedly shortened and the RS-T segment displaced and curved in the manner which is more usual when the original tracing shows no secondary T wave change due to hypertrophy. It is possible that the T wave change in tracing *a* was more the result of ischemia than of hypertrophy.

FIG. 234. Tracing demonstrating the effects of digitalis on the RS-T segment and T wave. Digitalis characteristically displaces the RS-T segment in the direction opposite to the main QRS deflection. Leads V_1 and V_2 of this tracing show an exception to this rule.

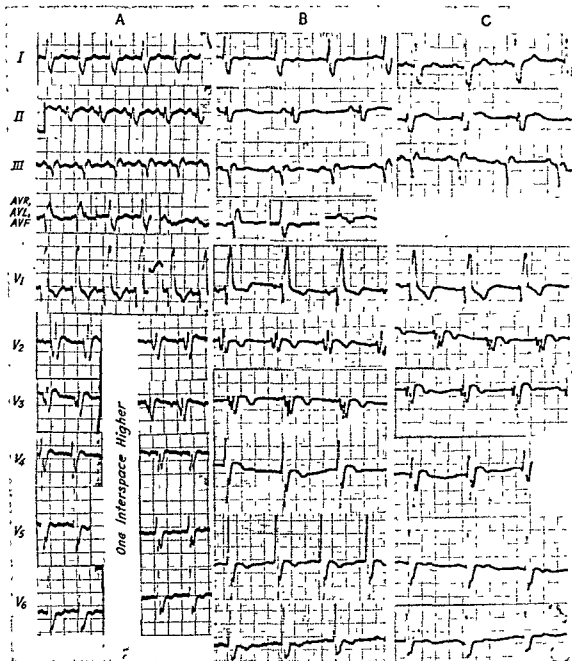


FIG. 235. Tracing showing the *similar* effects of rapid rate and digitalis in a patient with a healed anterior infarct and right bundle branch block. *A* was made when the rate was rapid due to congestive failure; *B* demonstrates a reduced heart rate due to therapy but with no digitalis; and *C* shows the changes due to digitalis.

From what has been stated above, seemingly the electrocardiogram would offer an excellent guide to the degree of digitalization of a patient. Unfortunately the effects on the electrocardiogram of a given dose of a digitalis preparation in different individuals

varies widely. Digitalization of one individual will produce none of the electrocardiographic effects discussed whereas the same dose will produce marked changes in another individual. As might be expected in individuals with an apex-back heart, the gradient points al-

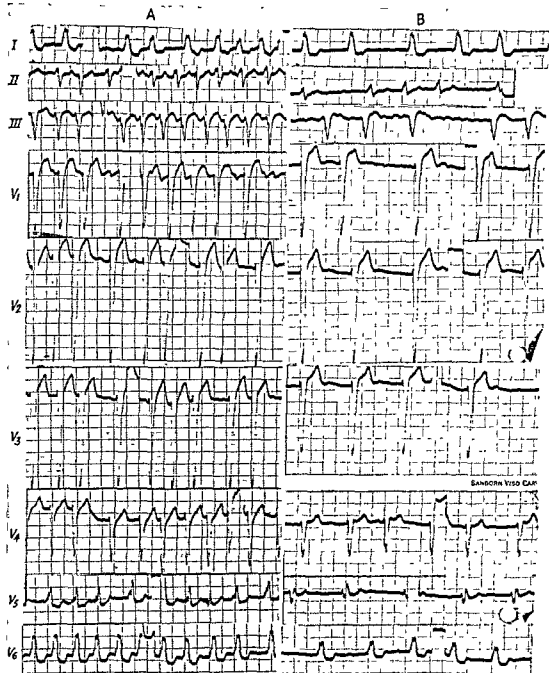


FIG. 236. Tracings of a patient with auricular fibrillation with rapid rate and left bundle branch block made (A) before and (B) after digitalization. A reduction in the rate followed digitalization. Since the RS-T segment shifts are more marked in A than in B, it would seem that a very rapid rate produced a greater diminution of the ventricular gradient than digitalization.

most straight back and shortening of the gradient does not produce significant changes on the extremity leads. This does not fully explain this phenomena, however, since occasionally tracings of digitalized patients who do not have an apex-back heart position are seen that demonstrate minimal or no electrocardiographic changes suggestive of digitalis. Also RS-T segment and T wave changes due to digitalis frequently seem to outlast the clinical effects of digitalis after the drug has been discontinued. The duration of these effects of digitalis varies according to the preparation used and when the more slowly acting preparations (such as digitalis leaf or digitoxin) are used, RS-T segment and T wave changes may remain for two to four weeks after the drug has been discontinued. Although the degree of electrocardiographic change produced by digitalization varies among individuals, the degree of change produced in the serial tracings of any single individual is proportional to the amount of digitalis administered.

Unlike the effects of digitalis upon the RS-T segments the development of a mechanism disturbance offers evidence of digitalis toxicity. The first effect on the cardiac mechanism due to digitalis is frequently a slowing of the heart rate, sometimes with a slight prolongation of the P-R interval.* This, at first, is predominantly due to a vagal action of the drug and can be partly or completely eliminated by atropine. Marked prolongation of the P-R interval or prolongation remaining after atropine is due to a direct action of the drug on the conducting system. Further digitalis administration may further depress A-V conduction resulting in a partial or even complete heart block. Most characteristic of digitalis (although it may be seen in the absence of the drug) is interference dissociation (see p. 249).

Digitalis also increases the myocardial irritability, and this, particularly in toxic doses,

* Rarely will digitalis in therapeutic doses cause the P-R interval to exceed the upper limits of normal shown in Table A (Appendix II) unless the conduction system is diseased.

may be responsible for the appearance of ventricular premature beats or even the precipitation of any of the paroxysmal tachycardias. Where frequent premature beats are present before digitalization, a diminution or even complete disappearance of these may occur after digitalization.

The development of premature beats following the administration of digitalis is usually indicative of toxicity. Bigeminy frequently occurs in such instances. Multifocal ventricular premature beats may also occur. Although auricular fibrillation may occur in patients with auricular flutter as a result of digitalization, the development of an auricular mechanism disturbance in a patient with a previous sinus rhythm is a rare result of digitalis toxicity. On the other hand, the further administration of digitalis in patients with toxicity not uncommonly results in ventricular tachycardia or fibrillation. At times the ventricular tachycardia due to digitalis has a peculiar form in which alternate complexes seem to arise from the opposite ventricles.

It should be mentioned that digitalis toxicity may result not only from a recent overdosage of the drug, but from sudden electrolyte changes. The hypokalemia resulting from a massive diuresis or from dialysis with the artificial kidney may precipitate electrocardiographic evidence of digitalis toxicity. On the other hand, potassium salts have been used with success in the treatment of severe digitalis toxicity.

Quinidine

Quinidine depresses myocardial irritability and conduction and is thus found useful in eliminating frequent premature beats and in the treatment of paroxysmal tachycardias. Like digitalis, the earliest electrocardiographic change due to quinidine, other than the possible establishment of a normal sinus rhythm in individuals with arrhythmias, is in the T wave, which usually becomes broad and develops a notch or umbilication near the peak. Unlike digitalis, however, there is a slowing

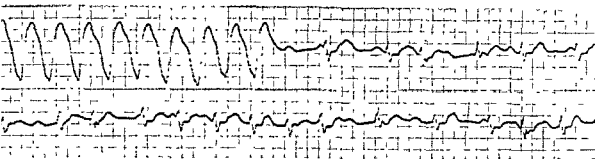


FIG. 237. Toxic effects of quinidine. Lead II of a patient with ventricular tachycardia which ceased after intravenous quinidine. Note the presence of a complete heart block, the wide P and QRS complexes, and the prolonged Q-T interval. These changes (except for the change in rhythm) are all manifestations of quinidine toxicity.

of repolarization with a prolongation of the Q-T interval (Fig. 233b).

Because of its effect on the conducting tissues a prolongation of the P-R interval may occur and even partial or complete heart block may be precipitated. Although heart block is usually seen only with toxic doses,

Figure 237 is a tracing of a patient with ventricular tachycardia who was receiving intravenous quinidine when the tracing was made. Following the cessation of the ventricular tachycardia the wide P waves become evident as well as wide QRS complexes and complete heart block. Marked widening of

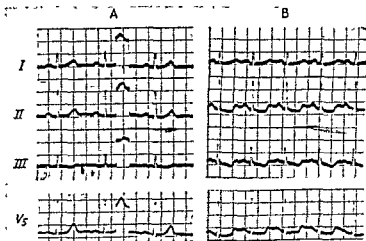


FIG. 238. The effects of amyl nitrite on the electrocardiogram. Tracing made on a normal young adult A before and B after the inhalation of amyl nitrite.

in the presence of myocardial disease affecting the conducting tissues even small doses of quinidine may precipitate heart block. In small doses quinidine has no effect on the P wave or QRS complex but large doses may cause widening of these complexes and a progressive increase in their duration may occur if the administration of quinidine is contin-

ued. Figure 237 is a tracing of a patient with ventricular tachycardia who was receiving intravenous quinidine when the tracing was made. Following the cessation of the ventricular tachycardia the wide P waves become evident as well as wide QRS complexes and complete heart block. Marked widening of the QRS complex is not uncommon when quinidine is administered intravenously. Patients with an initially wide QRS complex (bundle branch block or ventricular hypertrophy) do not show an increased sensitivity to the drug and initially wide QRS complexes do not serve as a contraindication to the use of quinidine. Further widening of the QRS

complexes however, is evidence of quinidine toxicity. Sometimes the gravity of the clinical condition (such as ventricular tachycardia) warrants continuing the drug in spite of this manifestation of its toxicity, but it must be remembered that quinidine can produce ventricular tachycardia, ventricular fibrillation, or ventricular asystole in toxic doses. It has been suggested that these arrhythmias occur more frequently when digitalis is also being administered.

Quinine, the optical isomer of quinidine, is capable of producing the same electrocardiogram effects as quinidine, but much larger doses are required.

Nitrites

The inhalation of amyl nitrite increases the heart rate and produces RS-T segment shifts (Fig. 238). Since these shifts may resemble injury shifts, tracings made on patients with chest pain shortly after the administration of amyl nitrite should be interpreted in this light. As can be seen in Fig. 238, the RS-T segment shifts are much more pronounced than would be expected if they were due solely to a decreased ventricular gradient because of the increased heart rate. Also the RS-T segment shifts in Leads II and III are proportionately greater than the shift in Lead I. This would not be expected from diminishing the gradient without changing its direction, and therefore the gradient must have changed markedly in direction. These RS-T segment shifts are seen in normal individuals inhaling the drug and usually last only a few minutes after inhalation is discontinued. Similar changes have not been seen with sublingual nitroglycerin nor with any of the nitrites used orally as coronary vasodilators.

Emetine

The drugs discussed above are used in the treatment of heart disease. Minor T wave changes have been attributed to a variety of drugs. Of these emetine is probably the most important. Emetine is a toxin to both skeletal

and cardiac muscle. Electrocardiographic changes due to emetine may follow the use of only a few grains in some persons, and yet other individuals fail to demonstrate any electrocardiographic change following the accidental use of large doses. The drug may

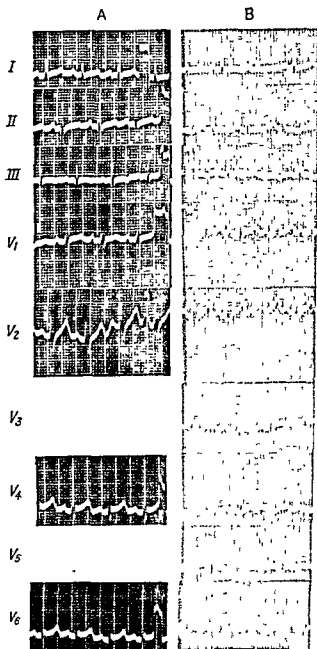


FIG. 239. The effects of emetine on the electrocardiogram of a 12-year-old female. Note the marked T wave changes in B as compared to the tracing A made prior to administering the drug.

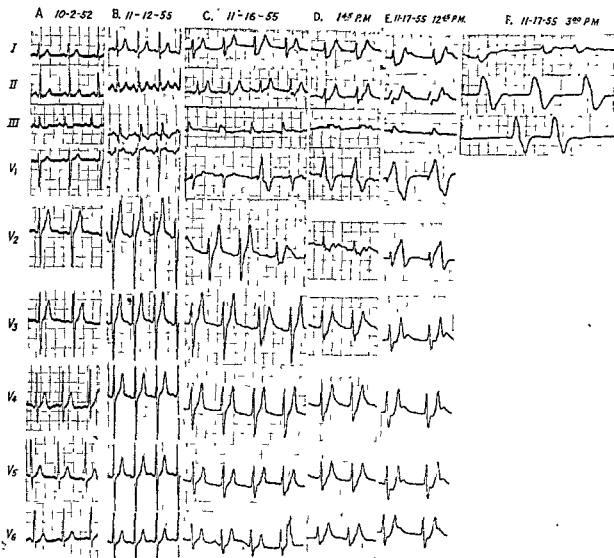


FIG. 240. Effects of a progressively rising serum potassium level on the electrocardiogram of a young adult with an "acute renal shutdown." *A*, Normal tracing made three years prior to the present illness. *B*, Tracing showing high peaked T waves and slight RS-T segment shifts. These T waves are the earliest manifestation of hyperkalemia and usually are best seen in V_4 , V_5 , and V_6 . *C*, Low P waves and wider QRS complexes with beginning right bundle branch block is now present. The serum potassium was 7.4 mEq/L. earlier this day. *D*, Auricular asystole and complete right bundle branch block are now present. The serum potassium level was 8.2 mEq/L. earlier this day. *E*, Extremely wide complexes are now present. The serum potassium level was 8.2 mEq/L. earlier this day. *F*, In this tracing the QRS complex has widened even further and periods of ventricular asystole are present. Complete asystole followed the last two complexes of Lead III. The serum potassium was 9.1 mEq/L. when death occurred.

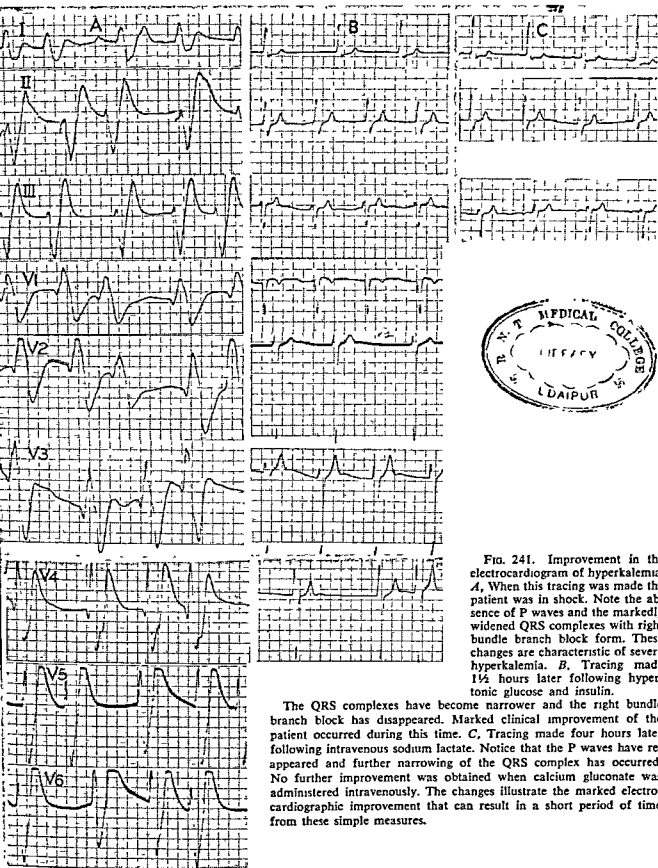


FIG. 241. Improvement in the electrocardiogram of hyperkalemia. *A*, When this tracing was made the patient was in shock. Note the absence of P waves and the markedly widened QRS complexes with right bundle branch block form. These changes are characteristic of severe hyperkalemia. *B*, Tracing made 1½ hours later following hypertonic glucose and insulin.

The QRS complexes have become narrower and the right bundle branch block has disappeared. Marked clinical improvement of the patient occurred during this time. *C*, Tracing made four hours later following intravenous sodium lactate. Notice that the P waves have reappeared and further narrowing of the QRS complex has occurred. No further improvement was obtained when calcium gluconate was administered intravenously. The changes illustrate the marked electrocardiographic improvement that can result in a short period of time from these simple measures.

produce prolongation of the P-R interval, but more commonly produces prolongation of the Q-T interval and lower or slightly inverted T waves. The latter may be seen in the tracing taken before and several days

after the use of the drug in a 12-year-old female (Fig. 239). Large inversions of T waves should not be attributed to emetine.

Electrolyte Disturbances

The electrocardiographic manifestations of changes in the body electrolytes are usually related to changes in the concentrations of the serum cations. Although changing levels of the serum potassium and calcium concentrations produce striking electrocardiographic changes, changes in the serum sodium level do not produce changes per se, but, as will be discussed below, the serum sodium level *does play an important role in determining the degree of electrocardiographic change produced by an abnormal potassium concentration.*

SERUM POTASSIUM. The first electrocardiographic evidence of *hyperkalemia* (an elevation of the serum potassium level) is an increased amplitude and peaking of the T waves. This is usually most easily noticed in the V leads from the anterior chest, but is also present to a lesser degree in other leads. In serial tracings caution should be exercised to place the chest leads in exactly the same anatomic position as previously, and even the QRS complexes should be compared to assure that this has been done before great significance is attached to T wave changes. Changes due to a progressively rising serum potassium can be seen in Fig. 240 and can be compared to the normal tracing taken three years earlier. Such changes begin with serum levels of approximately 6.5 mEq/L., but as will be described later, other factors influence the degree of electrocardiographic changes seen with any given serum potassium level. With further increase of the serum potassium level, there is depression of the RS-T segment (Fig. 240D) and then widening and flattening of the P waves followed by auricular asystole. Later intraventricular conduction delay with progressive widening of the QRS complex occurs (Fig. 240D). Finally, an idioventricular rhythm results and death may occur with ventricular fibrillation or ar-

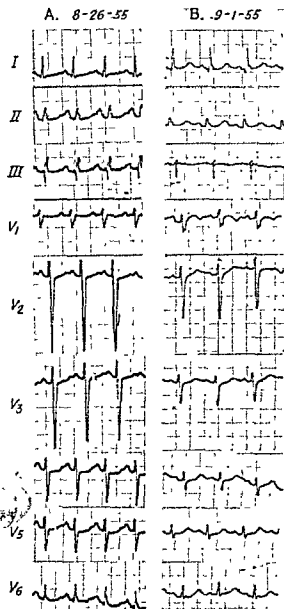


FIG 242 The electrocardiogram of hypokalemia: A, The serum potassium was 2.9 mEq/L at this time. Note the characteristic RS-T shifts and low T waves of hypokalemia. B, Return of tracing to a more normal appearance due to a fall in the serum sodium level without a change in the serum potassium level.

rest as in Fig. 240F. The last two complexes of Lead III in this figure were followed by cardiac arrest; the serum potassium level at that time was 9.1 mEq. L. Death commonly results at serum levels above 9 mEq./L.

Electrocardiographic changes are also to be expected in *hypokalemia*, but again the changes seen are not specific for any given level of serum potassium nor are they related quantitatively to the symptoms of hypokalemia. These symptoms seem to be related to the rapidity of change rather than to the absolute serum levels. Electrocardiographic changes are to be expected at levels of 3.0 mEq./L. or lower. Hypokalemia causes a prolongation of the Q-T interval together with flattening or even inversion of the T waves and depression of the RS-T segment. Prominence of the U wave may also occur, and this, if not recognized, may give a false impression of the degree of Q-T prolongation. Figure 242A shows the tracing of a patient with hypokalemia (serum potassium of 2.9 mEq./L.). As mentioned in relation to hyperkalemia, other factors influence the degree of change expected with any given serum potassium level. The change in Fig. 242B to the more normal tracing was not due to an elevation of the serum potassium, but rather to a fall in the serum sodium level to 112 mEq./L. Occasionally the RS-T segment and T wave changes of hypokalemia do not present the typical pattern and the T wave of some tracings mimic the T waves of ischemia. Figure 243 is the tracing of a 15-year-old female in diabetic acidosis and this tracing is similar to that of lateral ischemia.

When these changes were first recognized it was hoped that the electrocardiogram would offer a simple and accurate estimate of the serum potassium level. Unfortunately this has not proven to be true. Experiments and clinical observations have failed to reveal a close correlation between the potassium level and the electrocardiographic changes. Also the presence of organic heart disease, digitalis effects, and abnormal levels of other electrolytes (sodium and calcium)

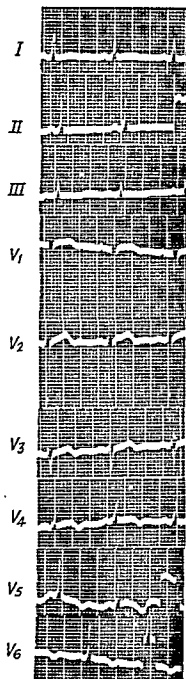
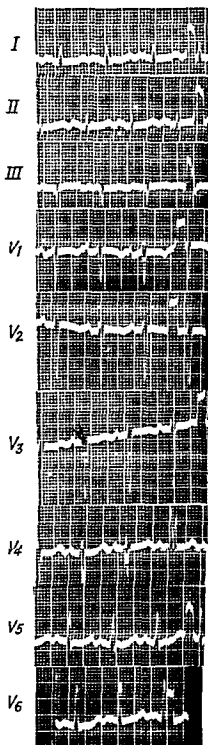


FIG. 243. Electrocardiogram of a 12-year-old colored female with hypokalemia. Note that in an older person this might easily be misinterpreted as lateral wall ischemia.



greatly influence the degree of change to be expected from a given elevation of the serum potassium level. Thus knowledge of the actual serum potassium level is of utmost importance in the diagnosis of either hyper- or hypokalemia. Once the diagnosis is established, the electrocardiogram serves as a guide to further changes in the serum potassium level and probably is a better index of the degree of myocardial toxicity due to hyperkalemia than the serum potassium concentration.

SERUM SODIUM. As mentioned above, the serum sodium level influences the degree of change resulting from a given serum potassium elevation. If the serum sodium level is low the electrocardiographic effects of hyperkalemia are exaggerated, and in the presence of hyperkalemia, increasing the serum sodium level causes partial retrogression of the changes in the tracing. Digitalization and increasing the serum calcium level cause a similar retrogression of the changes due to hyperkalemia. The knowledge that the electrocardiographic changes of hyperkalemia can be reduced by these measures is important clinically since it reflects a decrease in the myocardial toxicity due to hyperkalemia. The use of these substances, as well as the use of hypertonic glucose and insulin to promote the formation of liver glycogen thereby binding potassium and reducing the serum potassium concentration, often produces a marked decrease in the electrocardiographic manifestations of hyperkalemia. Such changes can be seen in the tracing in Fig. 241.

SERUM CALCIUM. Hypocalcemia is seen in a variety of clinical states. When the serum calcium level falls below 7-8 mg/100 cc. blood, electrocardiographic changes may result. The usual change due to hypocalcemia is a prolongation of the Q-T interval. Char-

FIG 244. Electrocardiogram in hypocalcemia. The Q-T interval is prolonged to 0.40 second (upper limit of normal for this rate is 0.33 second). Note the prolonged isoelectric RS-T segment and the T waves of normal form. Compare the RS-T segment shifts and low T waves due to hypokalemia in Fig. 242.

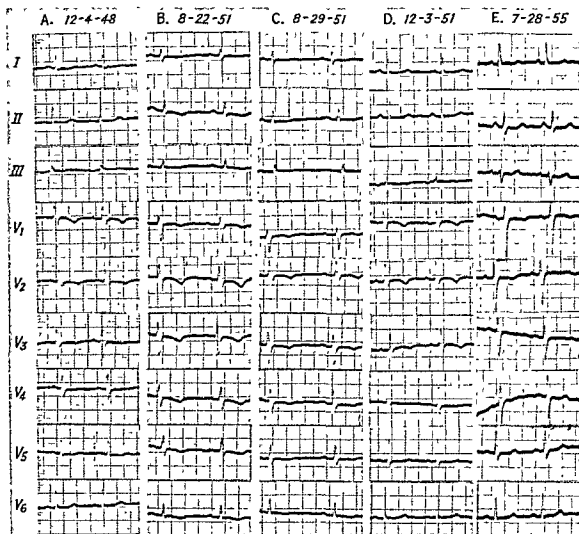


FIG. 245. Tracing made on a patient with hypothyroidism. *A*, During thyroid therapy. *B*, After discontinuing thyroid therapy. *C*, *D*, and *E*, Tracings made at intervals following the reinstitution of thyroid therapy. Note that even four years after the reinstitution of medication, the tracing is still not completely normal.

acteristically, this prolongation involves only the RS-T segment; the T wave is unchanged. With very low serum calcium levels the Q-T interval may become almost doubled. Figure 244 shows the tracing of a patient with hypocalcemia; the Q-T interval is 0.38 sec. whereas the normal Q-T interval for this rate (111/min.) is 0.33 second. Occasionally the typical pattern (a normal T wave following a prolonged isoelectric RS-T segment) is not present and the T waves are lowered or even changed in direction. In such instances one will have difficulty in differentiating be-

tween the electrocardiographic effects of hypocalcemia and ischemia.

Hypercalcemia is seen less commonly than hypocalcemia and manifests itself electrocardiographically by shortening the Q-T interval below the normal value. A prominent U wave may also occur.

Metabolic Diseases

Electrocardiographic changes are seen in a number of metabolic diseases. In many of these diseases, e.g., diabetic acidosis, Addison's disease, hypo- and hyperparathyroidism,

these changes result from electrolyte imbalances. The effects on the electrocardiogram in other diseases are not dependent on alterations in the serum electrolytes.

In *hyperthyroidism* there is usually an increased heart rate. Frequently the P-R interval is not shortened proportionally to the increased heart rate as is usual in sinus tachycardia and thus the P-R interval may be prolonged for the heart rate. The T waves are frequently increased in magnitude denoting an increased magnitude of the ventricular gradient.

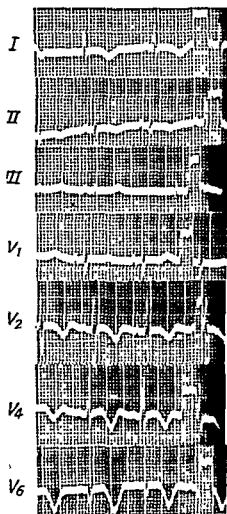


FIG. 246 The electrocardiogram of acute glomerulonephritis. This tracing from a 4-year-old demonstrates the marked T wave changes frequently seen in this disease.

In *hypothyroidism* the voltage of the QRS complex and the T wave may be low. Since this change is seen in the absence of myxedema, it is not due to a decreased skin conductivity. Also, T waves which are normally upright may become inverted. Following the administration of thyroid the T waves usually improve, but they may never completely return to normal. Figure 245 shows serial tracings on a female in her early forties with hypothyroidism. When the first tracing was made she was taking thyroid extract. This medication was discontinued prior to the second tracing and the T wave changes described above can be noted. Following this tracing, thyroid was reinstituted and the third and fourth tracings show progressive improvement. From the QRS complexes of the last tracings which was made four years after the resumption of her medication, it can be seen that a change in her cardiac position has occurred. However, even though the T waves are improved they have not returned completely to normal.

Electrocardiographic changes also occur in *acute glomerulonephritis*. In some patients with this disease the QRS complexes become smaller, but the most characteristic electrocardiographic changes in glomerulonephritis are found in the T waves. LaDue and Ashman, in a review of 101 cases of this disease, found that in approximately 40 per cent of cases the ventricular gradient was deviated markedly to the right resulting in a lowering or inversion of T_1 and an elevation of T_{III} . Lowering or inversion of the T waves in V_4 , V_5 , and V_6 may also occur (Fig. 246). In several of their patients in whom the gradient was deviated to the right there was also a prolongation of the Q-T interval. They called attention to the resemblance of this pattern to that of ischemia of the free wall of the left ventricle and suggested that the sudden and rapid onset of hypertension and cardiac dilatation were responsible for a myocardial metabolic change which was most marked in the free wall of the left ventricle.

Suggested Reading

- Barker, P. S., Johnston, F. D., and Wilson, F. N. The duration of systole in hypocalcemia. *Am. Heart J.*, 14:82, 1937.
- Berliner, K. The effect of calcium injections on the human heart. *Am. J. Med. Sci.*, 191:117, 1936.
- Ernstene, A. C., and Proudfit, W. L. Differentiation of changes in the Q-T interval in hypocalcemia and hypopotassemia. *Am. Heart J.*, 38:260, 1949.
- Kellog, F., and Kerr, W. J. Electrocardiographic changes in hyperparathyroidism. *Am. Heart J.*, 12:346, 1936.
- Sharpey-Shafer, E. P. Potassium effects on T wave inversion in myocardial infarction and preponderance of a ventricle. *Brit. Heart J.*, 5:80, 1943.
- Thomson, W. A. R. Potassium and the T wave of the electrocardiogram. *Lancet*, 1:808, 1939.

15. Heart Disease of Various Etiologic Types

Hypertension

Patients may have hypertension—even above 200 mm. Hg systolic—for many years without showing electrocardiographic changes. On the other hand electrocardiographic changes indicating the presence of left ventricular hypertrophy may develop rapidly or very slowly over a period of years. The same patient may have no cardiac symptoms and no discernible increase in the size of the cardiac silhouette. In others ischemic changes may be superimposed upon the electrocardiographic signs of hypertrophy although no pain or other cardiac symptoms have occurred. Frank angina and infarction are probably more common than in the nonhypertensive patient.

Acute pulmonary edema or more insidious cardiac failure may occur at any stage of the evolution of electrocardiographic changes. Left or right bundle branch block may and frequently does supervene.

The changes characteristic of left ventricular hypertrophy described in Chapter 8 are frequently referred to as evidences of left ventricular "strain." This concept seems to be a rather vague one. Its one justification seems to be the implication of reversibility, as after sympathectomy. Actually this implication should not be eliminated by employment of the designation *hypertrophy* as cardiac surgery has amply proven in congenital and rheumatic heart disease. Furthermore, there is frequently a notable absence of the empirical "strain" pattern in persons whose left ventricles have been "strained" to the point of failure.

Auricular pathology, with broad, notched P waves and prolongation of the P-R interval of various degrees, sometimes terminating in partial or complete atrioventricular block is not uncommon. Very frequently auricular premature beats occur more and more frequently until finally auricular flutter, or auricular fibrillation occurs, at first in paroxysms and, finally (in some) fibrillation becomes the fixed mechanism. Spontaneous ventricular tachycardia is less common.

Syphilitic Heart Disease.

In aortitis with involvement of the coronary vessels the electrocardiogram may show the changes described in Chapter 11.

With aortic regurgitation the electrocardiogram may show the changes which result from left ventricular hypertrophy.

Rheumatic Valvular Disease

The electrocardiographic changes in rheumatic myocarditis and in pericarditis are described under those headings.

In rheumatic *mitral stenosis* the chief changes are in the left atrium and in the right ventricle. The atrial changes produce broad notched P wave quite regularly and these may become very large even in the limb leads. In V_1 and V_2 the P wave may become diphasic and sharp at its peaks. In extreme cases the P waves may become so large that they resemble QRS complexes (see Fig. 196d). Evidence of right ventricular hypertrophy (q.v.) may or may not be clear.

When there is mitral regurgitation, an

aortic lesion, hypertension, or other complicating factors, left ventricular hypertrophy may also be present (see *hypertrophy of both ventricles*, pp. 224-226). Under these circumstances the evidence of the presence of right ventricular hypertrophy may be clear or may be masked by the left ventricular hypertrophy (Fig. 196, p. 227). While right bundle branch block is common, left bundle branch block may occur.

Cardiac mechanism disturbances of any type may occur. Auricular fibrillation is the most common.

Coronary disease may occur in rheumatic heart disease and any of the changes occurring in this condition may also occur. However, it is necessary to point out that at times when right or right and left ventricular hypertrophy occurs in rheumatic valvular disease a large Q wave and inverted T wave may occur in Leads II and III so that the tracing is difficult to distinguish from that of diaphragmatic infarction. In addition the large R in V_1 and V_2 due to right ventricular hypertrophy may be indistinguishable from the same deflection due to posterolateral infarction.

Congenital Heart Disease

In *patent ductus arteriosus* the tracing may be normal, or may show evidence of right or left ventricular hypertrophy or both.

In pure *pulmonary stenosis* the electrocardiogram shows evidence of right ventricular hypertrophy and, usually, high peaked P waves. In Eisenmenger's complex and the tetralogy of Fallot right ventricular hypertrophy is generally evident.

In *interatrial septal defect* the electrocardiogram may be normal, or may show evidence of right ventricular hypertrophy with or without right bundle branch block.

In *interventricular septal defect* the electrocardiogram may be normal or may show right or left ventricular hypertrophy or both.

In *tricuspid atresia*, as might be expected, the tracing shows largely left ventricular effects.

In *coarctation of the aorta and subaortic stenosis* the electrocardiogram may be normal or may show evidence of left ventricular hypertrophy.

In *transposition of the great vessels* there is evidence of hypertrophy of the right ventricle or of both ventricles.

Beri-Beri Heart Disease

When the heart shows changes in beri-beri the T waves are generally low. No other characteristic change is seen.

Anemia

No characteristic change in the electrocardiogram occurs in anemia. Tachycardia may occur. Occasionally middle-aged and older persons with anemia present symptoms and electrocardiographic changes typical of angina. These frequently disappear when the anemia is corrected. Such cases must be evaluated individually.

Pericarditis

In early acute pericarditis the electrocardiogram shows the evidence of diffuse epicardial injury described in Chapter 6. Figure 247 is a series of tracings from a patient with acute pericarditis due to rheumatic fever. The first tracings show the injury shifts referred to above. After a variable period of time the tracings show changes which suggest that repolarization in the epicardial fibers has been slowed. Inverted T waves appear. These may become quite deep. Finally after several weeks or months the tracing may return to normal.

Myocarditis

Acute degenerative disease in the myocardium occurs especially in acute rheumatic fever and diphtheritic myocarditis.

RHEUMATIC MYOCARDITIS. Here especially the earliest electrocardiographic sign may be a delay in atrioventricular conduction evidenced by prolongation of the P-R interval. Occasionally it is noted, when a sinus arrhythmia is present, that those complexes which follow

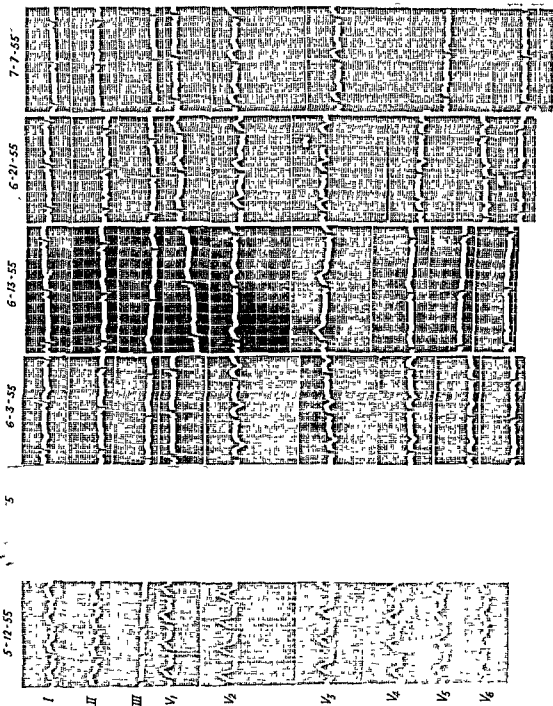


FIG. 247. Pericarditis. A series of tracings from a patient with rheumatic pericarditis beginning with the time of onset and followed for several weeks. Note transition from early injury effects (first records) to ischemic effects (later records).

the shortest cycle lengths have the longest P-R intervals.

The Q-T interval may be prolonged as a result of rheumatic myocarditis. T wave changes may occur.

DIPHTherITIC MYOCARDITIS. Changes in the electrocardiogram in diphtheritic myocarditis may be of any description. Early one may see simply a prolongation of the P-R interval, then a prolongation of the Q-T interval. Any type of T wave change, QRS change, or mechanism disturbance may occur. (Fig. 248).

FIEDLER'S MYOCARDITIS. In cases that are so classified, just as in diphtheritic myocarditis, any type of electrocardiographic change may occur. Figure 227 (p. 258) is a series of tracings made on such a patient. The striking feature in this case was that the patient neither appeared ill nor felt very ill when these tracings were made. The only evidence that death was imminent was contained in the electrocardiograms. Death occurred within 72 hours.

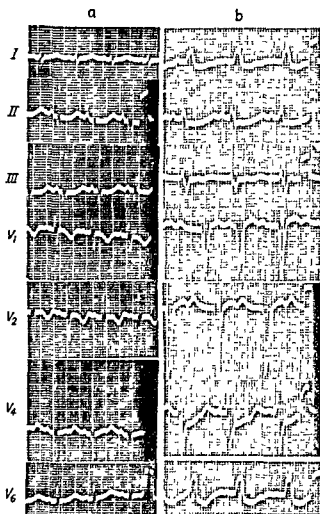


FIG. 248. Diphtheritic myocarditis in a 5-year-old child in early stage and a few days later. Death ensued.

16. Vectorcardiography and Spatial Vector Electrocardiography

Throughout this book, as far as possible, electrocardiographic phenomena have been presented in terms of the spatial QRS loop and the mean spatial QRS, T, and gradient vectors. The various spatial QRS loops and T wave vectors for the normal and abnormal conditions represented are not empirical; they are developed upon a physiologic basis which, although it is hypothetical, accords well with the greater portion of electrocardiographic data. Publication of a detailed presentation of the logical application of the basic hypothesis to a variety of abnormal conditions has been withheld for a period of 12 years because it was felt that only long-term observation of many patients and many autopsies could confirm or destroy the hypothetical basis.

The entire development depends for its spatial or three-dimensional construction upon inferences drawn from frontal plane observations. It cannot be denied that this method has its limitations. If one could actually record the spatial QRS loops and T loops or vectors by a satisfactory method some of these limitations would be removed. For instance, it might then be possible to detect that a T-wave vector such as that of Fig. 159 (p. 185) has a direction that lies out of the plane of the QRS loop to a greater extent than may be tolerated for the normal. For some years attempts have been made to record spatial loops and vectors by various methods. The principle involved is as follows: If, in addition to the loops or vectors recorded on the frontal plane one can also record or construct loops or vectors in a plane perpendicular to the frontal plane it would be possible to construct the spatial

loop and vectors much as one might construct a three-dimensional view of a box from the front and the side views.

It seems important at this time to discuss some of the methods that have been employed in attempts to record spatial loops directly and to construct spatial vectors from leads.

The recording of loops with the cathode ray oscilloscope has come to be known as vectorcardiography.

Vectorcardiography

The cathode ray oscillograph is simply a galvanometer of remarkable characteristics (when adjusted properly). Its frequency response (if not vitiated by characteristics of accessory amplifying equipment) is superior to that of any other electrocardiographic ap-

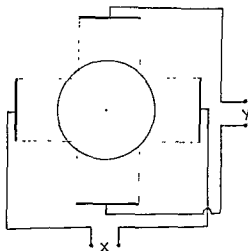


FIG. 249. Diagram of principles of oscillograph.

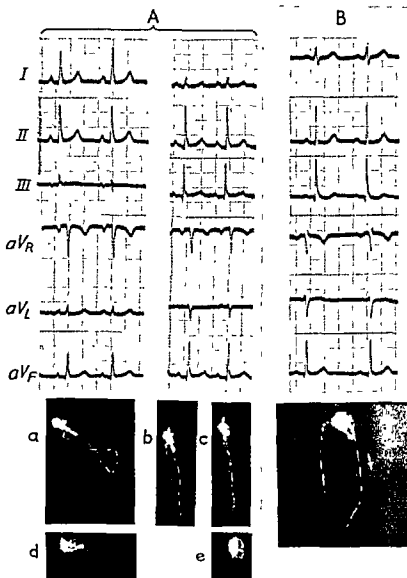


FIG. 250. In *A* the QRS loop has a figure-of-eight form. This can be determined quite easily from the leads above because the loop crosses the line of aV_R which is perpendicular to Lead III, producing an RSR' complex in the latter lead. However, in *A-b* the QRS loop crosses no lead line and it is not possible to know from the leads whether it is inscribed in a clockwise or counterclockwise manner. This can be determined with the oscilloscope. *a* and *b* of *A* are made before and after a deep breath.

paratus. Its recording is accomplished by the movement of a dot on the face of the tube. There are four terminals, two for the horizontal or X axis and two for the vertical or Y axis. Potential differences applied to the horizontal terminals move the dot horizontally and potential differences applied to the vertical terminals move the dot vertically (Fig. 249).

The X axis may be employed for the recording of time (sweep) and complexes can be recorded very accurately from any lead and on almost any desirable time base. Since the two axes of the conventional oscilloscope are perpendicular to one another it should be possible, theoretically, to plot the frontal plane loop automatically if we introduce Lead I

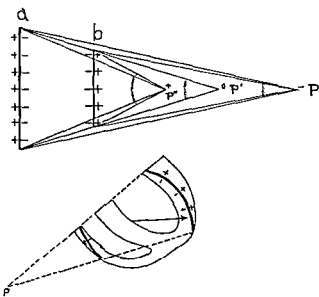


FIG. 251 Electrical effects of two oppositely directed waves of excitation. The upper diagram shows solid angles to both waves of excitation when the electrode is moved progressively nearer the heart from P to P'. When the electrode is at P the negative solid angle is larger and the potential at P is negative. When the electrode is at P' the solid angles are equal and the potential is zero. When the electrode is at P'' the positive solid angle is larger and the potential is positive. While the contour-eccentricity effects distort this representation the principle is undoubtedly qualitatively correct and evidence of its application is best seen in right ventricular hypertrophy.

into the horizontal axis and lead V_F into the vertical axis, for the lines of these two leads are horizontal and vertical respectively. In doing this V_F is usually increased (by amplification adjustment) by the factor $\sqrt{3}$. Such frontal plane loops do not correspond precisely to the loops that might be derived from the plotting of Lead I and Lead III on the Einthoven triangle but they are usually quite close. Only oscilloscopes whose axes are constructed at a 60° angle instead of a 90° angle can record precisely the loops that correspond to the limb leads.

Other opinions to the contrary notwithstanding it is easily possible in most cases to plot quite accurately the frontal plane QRS loops from ordinary electrocardiographic leads

as described on page 26. The accuracy of this method is enhanced by employing the unipolar limb leads in addition to the three standard limb leads after adjusting their magnitude by multiplying them by $\sqrt{3}$.^{*} It does not depend upon the accuracy of the simultaneity of the recorded leads since only the peaks of the deflections are used.

There are cases, however, in which the form of the complexes permit alternate forms for the QRS loop as plotted from ordinary electrocardiographic limb leads. Whether this will prove a clinically important fact has not yet been determined. Again, in left bundle branch block plotting the loop without an oscilloscope becomes difficult, tedious, and probably inaccurate because the peaks of the complexes are so broad and shattered. Finally, if a loop (QRS or T) does not cross one of the six limb lead lines it will be impossible to know whether it is inscribed in a clockwise or counterclockwise manner without an oscilloscopic record. This may in some conditions prove to be important (Fig. 250).

SPATIAL VECTORCARDIOGRAPHY. As stated above attempts have been made to construct the spatial QRS and T loops with the oscilloscope by recording loops in two planes perpendicular to one another. In the tetrahedron method of Wilson the frontal plane loop is recorded as described above and a horizontal loop is recorded by plotting Lead I against an anteroposterior lead obtained by connecting an electrode placed one inch to the left of the seventh thoracic spine to the central terminal. A sagittal view of the loop may be recorded by oscilloscopic plotting of the same anteroposterior lead against V_F .

In the "cube" method all of the electrodes are placed upon the chest and horizontal, vertical, and anteroposterior leads are arranged in different ways by the various investigators. Grishman, for example, employs a horizontal lead across electrodes which are placed in each posterior axillary line at a level somewhat below the inferior angles of the

* If the Goldberger leads are used for this purpose the correction is less.

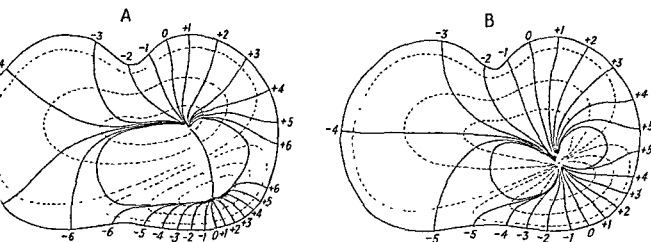


FIG. 252. *A*, The electrical field about a layer of dipoles. *B*, The electrical field about a single dipole of the same electrical moment. Note that with the dipole layer higher potentials would be expected to reach the surface of the anterior chest wall than appear in the same areas of the diagram for the single dipole. Other differences may be important.

scapulae. His vertical lead utilizes an electrode behind the right shoulder and the electrode of the right end of the horizontal lead described above. His anterior-posterior lead pairs this same electrode with an electrode placed on the anterior axillary line at the same level.

In attempts to preserve the theoretical concept of a single central dipole and equidistant electrodes the advocates of both frames of reference made calculations to determine the adjustment in amplification that would be required to correct for the different distances between the electrodes and heart.

Actually of course, even the limb lead electrodes are not equidistant from the heart (as was assumed in the early chapters) for the heart obviously occupies an eccentric position with respect to the apices of a triangle formed by the two shoulders and the symphysis pubis (or umbilicus). Furthermore, the body is not a sphere nor is it of unlimited extent and thus the effect of contour also tends to alter the validity of our earlier assumptions. Finally, the question as to whether the electrical phenomena accompanying the heart beat can be regarded as if they were derived from a single stationary dipole requires clarification. Nonhomogeneity seems to be a less important factor.

It is impossible to furnish here a complete

discussion of these subjects. However, some understanding of them is necessary to avoid confusion.

SINGLE DIPOLE REPRESENTATION. With regard to the matter of single stationary dipole

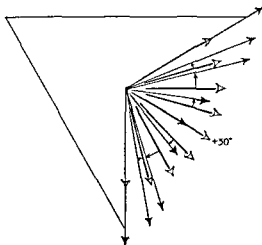


FIG. 253. The figure shows only the general order of the eccentricity effects as the axis of the dipole is changed from $+90$ degrees to -30 degrees as projected upon the frontal plane. The solid tipped vectors of eccentric point of origin represent the true spatial axis of the dipole. The black tipped vectors are the corresponding manifest vectors. Neither the extent of deviation of direction nor variation in magnitude of the manifest vectors is intended to be quantitative. (From Gardberg, M. *Circulation* 10:544, 1954. By permission of Grune & Stratton, publisher.)

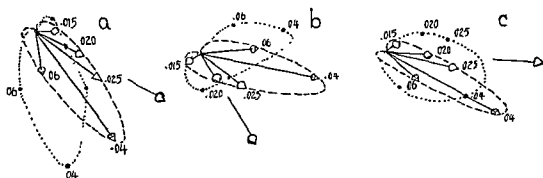


FIG. 254. This figure shows the effect of eccentricity, assuming the center of the heart is below and to the left of the center of the Einthoven triangle. *a* shows the projection of the actual spatial loop (in dashes) of a heart with anatomic axis at 30° and rotated slightly clockwise, the apex of the heart being viewed. The finely dotted loop is the manifest loop which results from the application of the approximated theoretic eccentricity effects. *b* depicts the effects of eccentricity when the anatomic axis of the heart is at 55° and the heart is rotated slightly counterclockwise. *c* depicts the effects of eccentricity when the anatomic axis is at 5° and the heart is rotated slightly clockwise.

Note that in *a* the manifest (dotted) loop is that of a more clockwise heart as a result of eccentricity while in *b* it is that of a more counterclockwise heart than that which the actual (dashed) loop represents. In *c* the loop is simply widened and shortened (From Gardberg, M. *Circulation* 10:544, 1954. By permission of Grune & Stratton, publisher.)

representation the reader will recall that throughout this book we have employed this concept (implicit in the vector method) in the analysis and synthesis of the limb leads, but that it was replaced by the solid angle method in the analysis and synthesis of the precordial leads. Theoretically, if two waves of excitation are present simultaneously the vector method may do well enough for a distant electrode but if the electrode is moved closer to the heart vector representation breaks down and may produce errors in polarity (Fig. 251).

Since in the normal heart the wave of excitation in the right ventricle is never very large at a time when its effect opposes that of the wave of excitation in the left ventricle, and since it also does not last very long it may be that single dipole representation will be found to be sufficiently accurate even for the chest leads. Frank has found it accurate within 10 per cent in a single human studied.* However, in the presence of bundle branch block and especially in right ventricular hypertrophy it is difficult to believe that either

*The writer is not prepared at this time to evaluate the significance of an error of ± 10 per cent in relation to this problem.

single dipole or stationary dipole representation can hold even approximately for the chest leads and probably it is occasionally erroneous even for the limb leads. The closer to the heart the electrode is placed the greater will be the evidence of the fallacy of single dipole representation of the potentials developed at that electrode and the greater will be the error in vector construction employing that electrode. The back electrode of the "tetrahedron" is such a close electrode. The anteroposterior lead of the cube employs two chest electrodes one of which (the anterior) is close to the heart. Figure 252 suggests another error that may occur as a result of the application of single dipole representation to chest potentials.

ECCENTRICITY OF THE HEART. The effects of eccentricity of the heart position with respect to the two shoulders and the third apex of the Einthoven triangle (wherever it may be anatomically) has been studied mathematically and experimentally. They may be represented in either of two ways: (1) by changing the shape of the triangle as was originally done by Burger; or (2) by a diagram showing

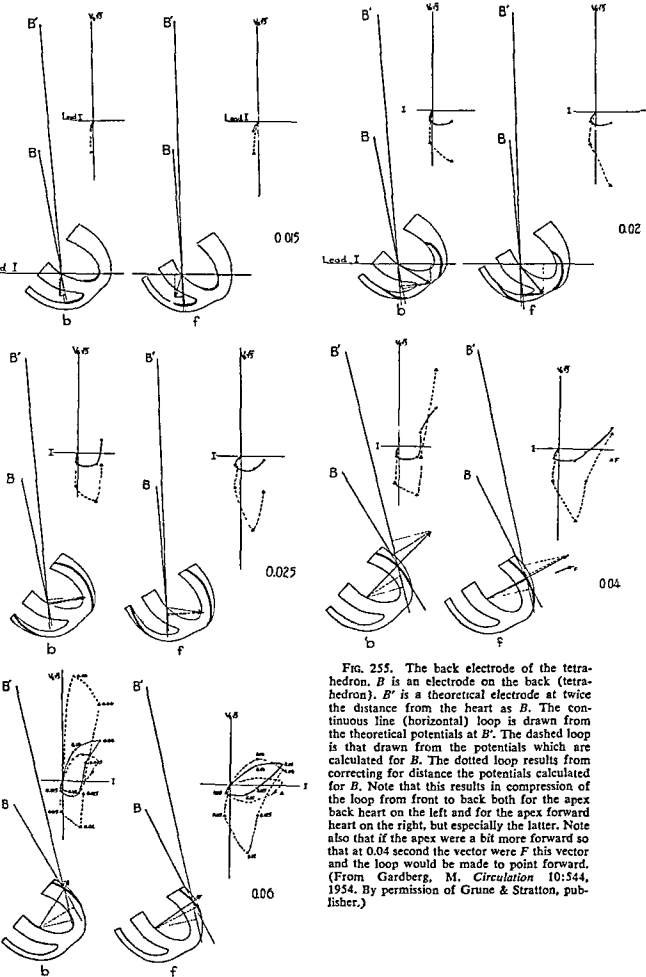


FIG. 255. The back electrode of the tetrahedron. B is an electrode on the back (tetrahedron). B' is a theoretical electrode at twice the distance from the heart as B . The continuous line (horizontal) loop is drawn from the theoretical potentials at B' . The dashed loop is that drawn from the potentials which are calculated for B . The dotted loop results from correcting for distance the potentials calculated for B . Note that this results in compression of the loop from front to back both for the apex back heart on the left and for the apex forward heart on the right, but especially the latter. Note also that if the apex were a bit more forward so that at 0.04 second the vector were F this vector and the loop would be made to point forward. (From Gardberg, M. *Circulation* 10:544, 1954. By permission of Grune & Stratton, publisher.)

change in vector direction and magnitude due to eccentricity (Fig. 253). Unfortunately, largely as a result of the limiting contour of the torso, the degree of eccentricity exerts a marked effect upon the degree of deviation of the manifest vectors and it is not at this time possible to know what degree of eccentricity effect is present in any given case. In general, however, the manifest vectors are rotated and changed in magnitude in a rather systematic fashion roughly as shown in Fig. 253. The general effect is an exaggeration of the effects of rotation of the heart. (Fig. 254).

The approach to the study of the effect of eccentricity upon the manifest QRS loops depends upon whether one adheres to stationary single dipole representation or to the idea that the dipole moves during depolarization of the ventricles. Despite the results of cancellation experiments it seems premature at this time to generalize. Stationary dipole representation will probably not hold for some cases. Certainly single dipole representation does not.

The effect of eccentricity of the heart upon the chest leads is greater than it is upon the limb leads for here the contour of the torso has an even greater effect. If a single electrode is employed on the back (as is done by oscillographers employing the tetrahedron) and it is assumed that single centric stationary dipole representation holds, serious errors even involving polarity will occur in the vectors constructed by the oscillograph (Fig. 255). No adjustment of amplification (to increase the theoretical distance) can be made to compensate for these errors. Since employing a single electrode anywhere behind the left ventricle produces the same errors the "tetrahedron" must be discarded.

For clinical purposes it is unnecessary for the method of recording spatial loops to be absolutely accurate. The manifest vectors derived from the limb leads are not absolutely accurate and yet as employed throughout this book they are very valuable for clinical purposes. However, any method employed must give fairly consistent results. The anteropos-

terior lead of the "cube" or "double cube" as employed by Grishman is more consistent than that of the tetrahedron and has made it possible for Grishman to find, in a general way, the changes in the QRS loop that result from infarctions in various locations which the writer had developed theoretically (in even more detail) on the basis of the hypothesis of the sequence of activation which was originally published by Gardberg and Ashman in 1943. (See Appendix III.) *Both the cube and the tetrahedron, however, produce loops which are compressed from front to back.*

Though the writer is inclined to view the anteroposterior lead of the cube with caution it is probable that in most conditions it will not cause the horizontal loop to be inscribed clockwise instead of counterclockwise or vice versa. One group of conditions constitutes a notable exception to this statement: right ventricular hypertrophy, right bundle branch block, and combined hypertrophies. The horizontal loop of the Grishman method at an early age is inscribed in a clockwise manner. At one month a change takes place and thereafter this loop is inscribed in a counterclockwise manner. It is doubtful (on theoretical grounds) that this early clockwise inscription of the horizontal loop is correct. One would expect this only if the right ventricle were thicker than the left. Carefully controlled studies may prove that the exaggeration of right ventricular effects by Grishman's method will prove an advantage rather than a disadvantage, but his statement that in normal children the horizontal loop is not inscribed clockwise is not true in early infancy. On the other hand the back electrode of the tetrahedron frequently, but not always, exaggerates the left ventricular effects (Fig. 256).

In left bundle branch block Grishman's method causes the horizontal loop to start backward and to the left and finally forward and to the left. This clockwise inscription of the horizontal loop is not to be expected in ordinary left ventricular hypertrophy (see Fig. 65). However, in some left bundle branch

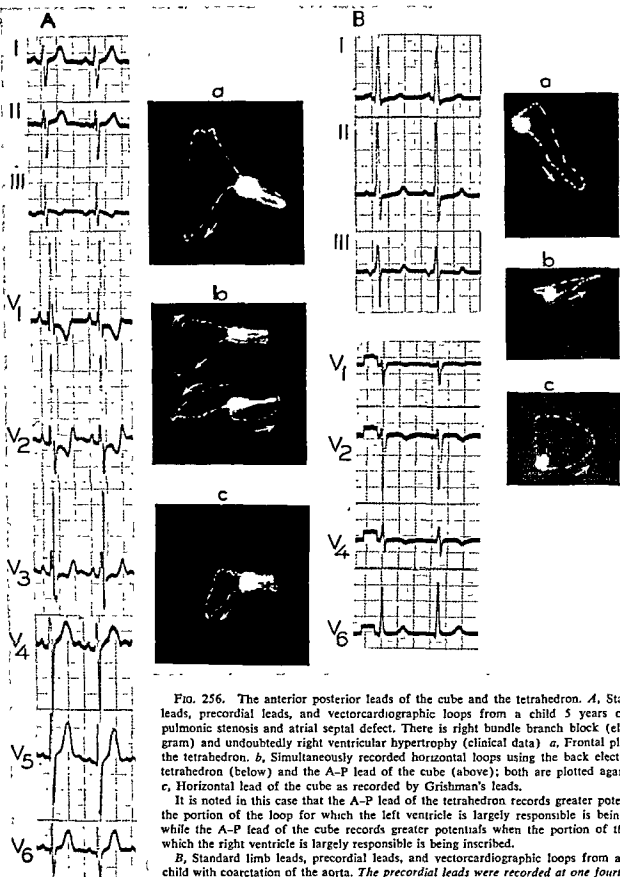


FIG. 256. The anterior posterior leads of the cube and the tetrahedron. *A*, Standard limb leads, precordial leads, and vectorcardiographic loops from a child 5 years of age with pulmonic stenosis and atrial septal defect. There is right bundle branch block (electrocardiogram) and undoubtedly right ventricular hypertrophy (clinical data). *a*, Frontal plane loop of the tetrahedron. *b*, Simultaneously recorded horizontal loops using the back electrode of the tetrahedron (below) and the A-P lead of the cube (above); both are plotted against Lead I. *c*, Horizontal lead of the cube as recorded by Grishman's leads.

It is noted in this case that the A-P lead of the tetrahedron records greater potentials when the portion of the loop for which the left ventricle is largely responsible is being inscribed, while the A-P lead of the cube records greater potentials when the portion of the loop for which the right ventricle is largely responsible is being inscribed.

B, Standard limb leads, precordial leads, and vectorcardiographic loops from a 6-year-old child with coarctation of the aorta. The precordial leads were recorded at one fourth the usual standardization and the vector loops at one half the standardization employed in recording other loops seen in this book. *a*, Frontal plane loop (tetrahedron). *b*, Horizontal loop made with the anterior posterior lead of the cube. *c*, Horizontal loop made with the anterior posterior lead of the tetrahedron. Note that in this case in which left ventricular effects predominate the anterior posterior lead of the tetrahedron gives the vectors much larger anterior posterior components than does the cube.

blocks the horizontal loop is not inscribed in a clockwise manner but is more like the loop of Fig. 81. The most characteristic feature of the left bundle branch block loop is the relatively great amount of time that the dot spends in one relatively small portion of the loop—usually near the part most remote from the origin. The absence or small size of an early rightward-directed portion is notable. The inscription of a loop in the clockwise manner is to be expected of large anterior infarctions and if the septum is also widely involved the early rightward portion of the loop is absent even when left bundle branch block is absent. If there is also hypertrophy of the left ventricle the QRS may be wide and the loop may be as long in duration as in some left bundle branch blocks. One cannot help but feel that the so-called distinction between left bundle branch block and left ventricular hypertrophy by means of horizontal loops is accomplished by establishing arbitrary criteria. If the distinction between left bundle branch block, left ventricular hypertrophy, and anteroseptal infarction cannot be made from examination of all of the limb and precordial leads it seems unlikely that it can be made from using two electrodes on the chest, one of which is significantly closer to the heart than the other.

It seems that employment of the limb electrodes for recording the frontal plane loop is superior to the method which Grishman uses for that purpose, and it is difficult to see why Grishman should sacrifice the advantages of the Einthoven method. The former's anteroposterior lead is superior to that of the tetrahedron. This lead may make it possible to make studies of the spatial gradient that will result in satisfactory correlations. However, again it must be established that consistent results can be obtained in serial observation on the same patient before clinical conclusion can be drawn from changes which may be noted. This will be discussed further.

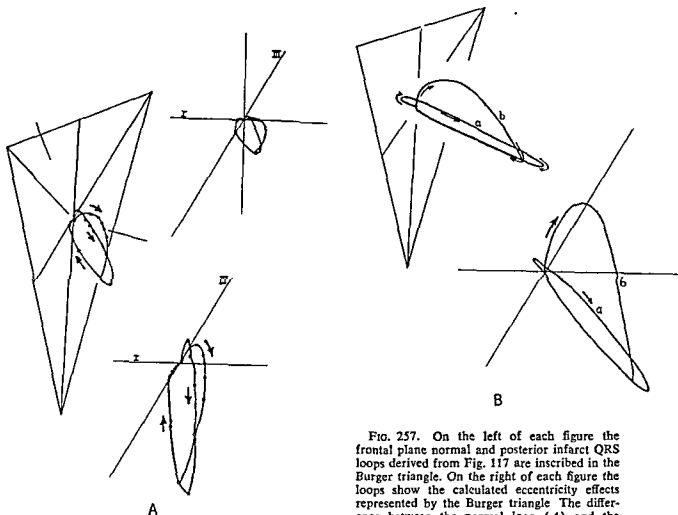
Other more complicated methods are not available to most and require closer examination before they can be recommended. A

method devised by and presently under investigation by Ernest Frank may prove sufficiently accurate and practical but no conclusion can yet be drawn. There is the ever-present danger of too early generalization. A method which may be proven to hold for one subject may be extremely inaccurate for another.

For these reasons it seems, at the present time, that the inferences drawn from the frontal plane observations and the precordial leads are more accurate for construction of the spatial QRS loop than any oscillographic method which has, thus far, been devised. The reader may have noted the extent to which they prove useful in the analysis of a great part of the observed electrocardiographic phenomena in health and disease. One can think in terms of the spatial loop without recording it directly. When a satisfactory method of recording is found it is believed that the spatial loops recorded in each condition will correspond reasonably well to those presented in this book. Grishman's loops do this fairly well though one need not agree with every conclusion he has drawn from them.

Due to the sensitivity of the body surface potentials to the dipole location which has been described above, even records made with a very accurate "orthogonal" system (Frank, Schmitt) must show variations from beat to beat due to varying eccentricity effects. Furthermore, if the patient takes a deep breath the accuracy of the record must be affected tremendously. Finally, abdominal distension and changes in posture must also have some of the same effects.

It is not to be inferred that the writer believes that recording with the oscilloscope is valueless. Certain details of both the frontal plane QRS and T loops mentioned above require attention and there is the possibility that some problems will yield to the method. If a method is evolved that eliminates much of the eccentricity-contour effect more satisfactory correlations may be found in studying a variety of electrocardiographic phenomena.



but this is by no means certain. (Fig. 257). The eccentricity contour effects may serve to "bring out" abnormalities as often as they conceal them.

Many signs that are being "discovered" in "spatial" loops were already known to those who have been thinking of leads as projections of the spatial loop. This was originated by Mann and was taught by Bayley in 1942 and earlier. The writer, with the aid of Ashman expanded Lewis' theory of the formation of the QRS complex into three dimensions, assigned to the normal spatial QRS loop an idealized form, and gave its various portions hypothetical anatomic physiologic significance. The extent to which the hypothesis correlates with electrocardiographic observations in health and disease the reader may judge for himself. In the writer's opinion

FIG. 257. On the left of each figure the frontal plane normal and posterior infarct QRS loops derived from Fig. 117 are inscribed in the Burger triangle. On the right of each figure the loops show the calculated eccentricity effects represented by the Burger triangle. The difference between the normal loop (A) and the abnormal loop is as clear in the one figure as in the other. In B eccentricity seems to exaggerate the effects of posterior infarction. The apparent exaggeration of the clockwise rotation of the heart in the lower figure is similar to that developed by the author by another method.

there is little reason to continue to regard the QRS loop as an empirical phenomenon.

Most of the confusion that characterizes electrocardiographic thinking today results from treatment of the QRS loop as an empirical phenomenon and from preoccupation with attempts to record the potentials more accurately to the exclusion of attempts at analysis. Attempts to devise more accurate methods of recording can never be criticized but the notion that the solution to the problem of empiricism in electrocardiography resides in the method of recording is false. Presumably, it is thought that if we can just find

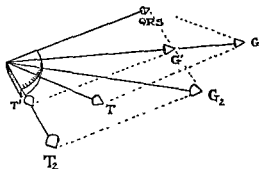


FIG. 258. The angle between the spatial QRS and T vectors. As depicted in Fig. 40, if the gradient diminishes from G to G' the spatial T vector becomes T' (this commonly results from rapid rate, exercise, food, and digitalis). The angle between the mean QRS and mean T axis widens considerably.

On the other hand, if the gradient changes direction from G to G_2 , the mean T axis becomes T_2 . This involves precisely the same change in the angle between the mean T axis and the mean QRS as was produced by the change from T to T' .

Furthermore, if the mean QRS increases without changing direction the same widening of the angle between T and QRS could be accomplished.

Thus, the spatial angle between the mean QRS and the mean T axes has little meaning except when evaluated in terms of the gradient

the "right" method of recording everything will fall into place. Actually we will still have loops though of somewhat different shape; they will be no less empirical than the loops recorded by present methods. The notion that more accurate recording will substitute for analytic thinking on a physiologic basis is illogical.

Measurement of Mean Spatial Vectors by Three-Dimensional Methods

The physiologic basis of the spatial relationship of the mean spatial QRS axis, the spatial mean T axis, the spatial gradient, and the anatomic axis was elucidated in Chapter 5. The effects of abnormal conditions have been presented throughout this volume. The principle originated with Wilson, was developed by Bayley and the spatial relationship of the mean spatial vectors was determined by Ashman, Gardberg, and Byer. Some years

later there appeared a number of attempts to determine the direction of the mean QRS vectors and T vectors in two perpendicular planes and to measure the angle between them in space. Obviously such attempts can be made by recording the potentials of the tetrahedron or of the cube as leads instead of loops, making the proper area measurements on these leads, and plotting them upon the tetrahedron or cube respectively. It is doubtful whether such methods (or any of the more naive methods which have been employed) yield as reliable results as can be inferred from the frontal plane measurements.

Attention must be drawn, too, to the fact that many of the methods for determining the direction of the "spatial" mean QRS and T vectors neglect the gradient entirely. They are entirely preoccupied with the spatial angle between the mean QRS and T axes and all sorts of attempts are made to establish, on purely empirical basis, criteria of normalcy for this angle. A review of Chapter 5 (Fig. 40) will serve to remind the reader that the angle between the spatial mean QRS and spatial T vectors varies from individual to individual and, more important, varies considerably in the same individual under non-pathological as well as pathologic conditions. Furthermore, it has also been demonstrated that the angle between the mean QRS and mean T vectors may remain the same though the electrocardiogram has changed from normal to abnormal. In Fig. 258 QRS , T , and G represent the resting normal spatial QRS, T, and gradient vectors. When the gradient is diminished to G' , as by a combination of food and physical activity, the T vector becomes T' . The spatial angle between QRS and T increases. This is represented in Fig. 40, (p. 57) for a variety of cardiac positions and rotations. On the other hand, with the development of lateral wall ischemia of the proper degree and location the gradient becomes G_2 and the T vector becomes T_2 . The spatial angle between QRS and T' is precisely the same as the spatial angle between QRS and T_2 , yet the former (T') is normal and

the latter (T_2) is abnormal. Thus the spatial angle between the mean QRS and the mean T wave is meaningless unless interpreted according to the principle of the gradient. The fact that no narrow limits can be established for the direction (or the magnitude) of the gradient is no excuse for ignoring a fundamental principle which is still the only instrument available for the evaluation of T wave potentials.

But even if the gradient is employed it is necessary to ask whether the addition of the anterior posterior lead adds much to the analysis of spatial vectors by inference from frontal plane components. The principle difficulty of the simple methods of spatial vectorcardiography resides in their anteroposterior leads. Both the tetrahedron and the cube produce spatial loops that are compressed from front to back and frequently the main axis of the loop points forward instead of backward. It must be apparent that from our point of view the loop in the normal may not point forward. Regardless of point of view it must be admitted that the compression of the anteroposterior components of the vectors into the narrow range that is apparent in most (but not all) normal sagittal and horizontal loops recorded with the cube, or the tetrahedron makes it impossible (in most cases) to feel that their anteroposterior leads can add much to the measurement of the mean manifest (frontal plane) QRS, T, and gradient vectors.

It has been emphasized here and previously by Ashman and also by Bayley that it is the direction and magnitude of the spatial gradient as related to the direction and magnitude of the spatial mean QRS that is important. However, it is important to realize that the theoretical approach and all calculations based upon it are made here and in Bayley's discussions without taking into consideration the effect of eccentricity. If the problem is approached with this in mind it must be remembered, when calculations are made from body surface potentials, that it is the QRS and T potentials that are recorded directly;

the gradient potentials are derived from these. We have then to consider the possibility of eccentricity effects upon the QRS and upon the T and the effects upon the gradient may then be derived.

It seems to the writer that eccentricity effects probably commonly cause the manifest mean QRS and the manifest mean T vector to be affected in the same manner, and this probably accounts for the preservation of the order of relationship derived in theoretic discussions. On the other hand it also seems probable that the effects of eccentricity upon the directions of the manifest vectors, the QRS and T, are not infrequently *different* either in direction or of degree of deviation and this may account for examples of apparent lack of correlation with the theoretical predictions. It is to be noted that it is not possible to assume, even if we grant that single stationary dipole representation holds for the QRS, and for the T, that the location of the dipole is the same for the QRS as for the T potentials. It is quite possible that it is not. Finally, even if we grant that the same dipole location holds for both, the eccentricity effects differ for different dipole axes.

Furthermore, these difficulties are probably much more important in the calculation of gradient directions and magnitudes in the horizontal (or sagittal) plane than in the frontal plane (if these are measured with the cube or tetrahedron).

Theoretically, a three-dimensional study of the spatial QRS loop, mean QRS, gradient, and T vectors may be attempted if we retain a fixed point of view and cause the heart to rotate about the anatomic axis. This occurs when the patient takes a deep breath; the electrocardiogram most often behaves as if the heart becomes more vertical and rotates clockwise. The apparent if not real clockwise rotation of the heart (about the anatomic axis) was demonstrated in normals, in left ventricular hypertrophy, and in many patients with diaphragmatic infarcts. At the same time the heart becomes more vertical. The impos-

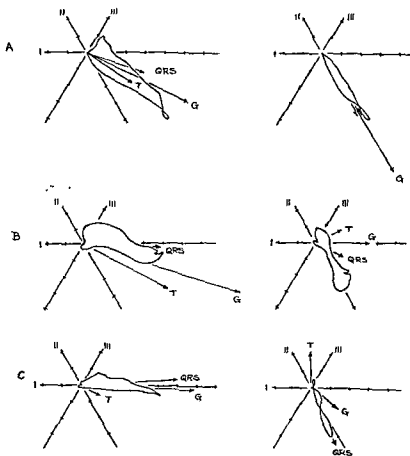


FIG. 259. Effect of a deep breath upon the electrocardiogram in three originally counterclockwise hearts. The triaxial system of Bayley is employed. The diagrams show the frontal plane QRS loop, and the frontal plane vectors for the mean QRS, gradient and T wave; on the left at rest, on the right with a deep breath.

Note that with a deep breath the loop of all three subjects (A, B, and C) is viewed more on edge than when at rest presumably due to clockwise rotation. All three also become more vertical. In A the vectors, as expected in an apex-forward heart, are almost superimposed when the loop is on edge. In B, the vectors are made to diverge more, which is not unexpected when an apex-back loop is viewed on edge. Again the sharp diminution of the magnitude of the vectors may be presumed to result in part from the assumption of a more apex-back position. Eccentricity, however, undoubtedly plays a large part. However, it is noted that it is the T vector which points upward, having behaved as if it were above the plane of the loop as shown in Fig. 159. Both A and B are normal subjects. In C also, the T vector moves in the opposite direction to that seen in A and becomes larger. This, however, is not an apex-back heart, and furthermore, closer examination shows that in this projection the magnitude of the ventricular gradient is much diminished in relation to the magnitude of the mean QRS, causing the T vector to assume the direction and magnitude shown. The exposure of the relationship (not evident without the deep breath) may prove of value. It is not normal for the loop in the position shown, for the frontal

sibility of measuring the degree of rotation is a distinct disadvantage, but the methods of "spatial" vectorcardiography also have disadvantages.

The *rotation* method presently under detailed investigation occasionally yields important results (Fig. 259). However, interpretation requires great caution at this time. Some normal persons have gradient axes and

therefore T axes which lie out of the plane of the QRS loop (Fig. 259B). A detailed investigation of these normals must be completed before the method can be evaluated further. It is here that the effects of eccentricity upon the T potentials and QRS potentials must be considered separately. It is yet too early to evaluate these studies.

plane gradient may be smaller than the frontal plane *QRS* only when the heart is in an *extremely* apex-back position or when food and vigorous exercise, postural changes, smoking, or digitalis has diminished the gradient. In contrast, *B*, which shows a marked diminution of the magnitude of all the vectors, retains the more normal relationship between the magnitude of *G* and of *QRS*.

The deep breath maneuver, if it is of value, may prove to be an instance of employment of eccentricity effects (which are different with full inspiration).

Further investigation of the phenomena presented in *B* and *C* is required before proper evaluation can be made. For example, it is necessary to know whether a sustained deep breath diminishes the magnitude of the gradient.

Subject *C* was subsequently proven to have heart disease by "unearthing" two tracings made elsewhere two years before which were definitely abnormal, and which, somehow, were misinterpreted.

Appendix

Appendix I

The Quantitative Relationship between the Standard and Unipolar Limb Leads

A simple derivation of the quantitative relationship between the standard limb leads can only be made for a special example. In Fig. A1 the vector E' represents the electromotive force produced by a dipole whose direction lies on the axis 0° . The potentials produced at L and R (V_L and V_R respectively) are obtained by projecting this vector E' upon the lines of those leads (see dashed projections at center of figure). Conversely, given these potentials at V_R and V_L the magnitude and direction of the vector E' can be deduced.

Passing on to the bipolar or standard limb leads, it may be seen that the direction of E' has been chosen so that its projection upon Lead I will equal the magnitude of the vector which will be constructed from the standard limb leads, for E' is parallel to Lead I.

$$1) \text{ Lead I} = V_L - V_R$$

$$2) \quad V_L = (E' \cos 30^\circ), \text{ and}$$

$$V_R = (-E' \cos 30^\circ)$$

substituting these values in (1) we have

$$3) \text{ Lead I} = E' \cos 30^\circ - (-E' \cos 30^\circ)$$

$$= E' \cos 30^\circ + E' \cos 30^\circ$$

$$= E' 2 \cos 30^\circ$$

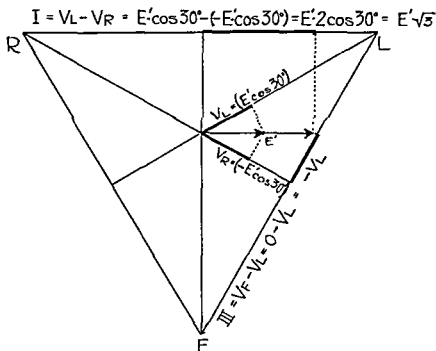
$$\text{since } \cos 30^\circ = 1/2 \sqrt{3}$$

$$4) \text{ Lead I} = E' \sqrt{3}$$

Thus for this special case it is shown that the vector E' as reflected on the standard limb leads is larger by $\sqrt{3}$ than E' which is constructed from the unipolar limb leads.

Those interested in the derivation of this relationship for the general case should consult the paper by Hill (*Am. Heart J.*, 32:72: 1946).

Goldberger produced the augmented uni-



polar limb leads (aV leads), in an attempt to bring the unipolar limb leads in closer correspondence to the standard limb leads. His technique as shown in Chapter 1, p. 9, involved disconnecting each electrode in turn from the central terminal (see Fig. 7). It may be shown that

$$1. (a) \quad aV_L = V_L - \frac{V_R + V_F}{2}$$

$$(b) \text{ While } V_L = V_L - \frac{V_L + V_R + V_F}{3}$$

2. Multiplying 1 (a) by 2 and 1 (b) by 3

$$(a) \quad 2 aV_L = 2 V_L - V_R - V_F$$

$$(b) \quad 3 V_L = 3 V_L - V_L - V_R - V_F$$

$$(c) \quad 3 V_L = 2 V_L - V_R - V_F$$

$$(d) \quad 2 aV_L = 3 V_L$$

$$(e) \quad aV_L = 3/2 V_L$$

$$\text{Thus } aV_L = 1.5 V_L$$

Since $\sqrt{3} = 1.732$ it may be seen that the Goldberger leads must be recorrected to be brought into proper relationship with the standard limb leads.

Appendix II

Tables A and B are reproduced from Ashman, R., and Hull, E. "The Essentials of Electrocardiography." The MacMillan Co.,

New York with the kind permission of the authors and publisher.

TABLE A. UPPER LIMITS OF THE NORMAL P-R INTERVALS

Rate	Below				Above 130
	70	71-90	91-110	111-130	
Large Adults	0.21	0.20	0.19	0.18	0.17
Small Adults	0.20	0.19	0.18	0.17	0.16
Children, ages 14 to 17 ..	0.19	0.18	0.17	0.16	0.15
Children, ages 7 to 13...	0.18	0.17	0.16	0.15	0.14
Children, ages 1½ to 6..	0.17	0.165	0.155	0.145	0.135
Children, ages 0 to 1½ ..	0.16	0.15	0.145	0.135	0.125

TABLE B. NORMAL Q-T INTERVALS AND THE UPPER LIMITS OF THE NORMAL

CYCLE LENGTHS SEC.	HEART RATE PER MIN.	MEN AND CHILDREN SEC.	WOMEN SEC.	UPPER LIMITS OF THE NORMAL	
				MEN AND CHILDREN SEC.	WOMEN SEC.
1.50	40	0.449	0.461	0.491	0.503
1.40	43	0.438	0.450	0.479	0.491
1.30	46	0.426	0.438	0.466	0.478
1.25	48	0.420	0.432	0.460	0.471
1.20	50	0.414	0.425	0.453	0.464
1.15	52	0.407	0.418	0.445	0.456
1.10	54.5	0.400	0.411	0.438	0.449
1.05	57	0.393	0.404	0.430	0.441
1.00	60	0.386	0.396	0.422	0.432
0.95	63	0.378	0.388	0.413	0.423
0.90	66.5	0.370	0.380	0.404	0.414
0.85	70.5	0.361	0.371	0.395	0.405
0.80	75	0.352	0.362	0.384	0.394
0.75	80	0.342	0.352	0.374	0.384
0.70	86	0.332	0.341	0.363	0.372
0.65	92.5	0.321	0.330	0.351	0.360
0.60	100	0.310	0.318	0.338	0.347
0.55	109	0.297	0.305	0.325	0.333
0.50	120	0.283	0.291	0.310	0.317
0.45	133	0.268	0.276	0.294	0.301
0.40	150	0.252	0.258	0.275	0.282
0.35	172	0.234	0.240	0.255	0.262

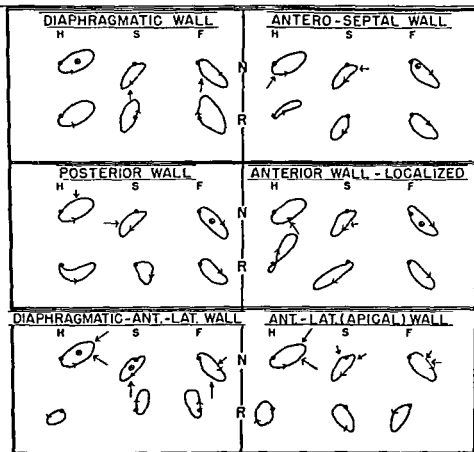
Appendix III

Summary of Grishman's analysis of the effects of infarcts in various locations upon the spatial QRS loop as recorded with the double cube frame of reference.

Reproduced from Grishman, Arthur: *Spatial Vectorcardiography*, W. B. Saunders Co., Philadelphia, with the kind permission of the author and the publisher.

MYOCARDIAL INFARCTION - VENTRICULAR COMPLEX

RESULTANT (R) OF NORMAL VECTORS (N) AND OF ABNORMAL VECTORIAL FORCES (→) DUE TO MYOCARDIAL INFARCTION



N: NORMAL VECTORS F: FRONTAL PROJECTION →: INFARCTION VECTOR
 R: RESULTANT VECTORS S: SAGITTAL PROJECTION •: SAME, PERPENDICULAR
 H: HORIZONTAL PROJECTION IN DIRECTION TO PLANE OF PROJECTION

Index

- Aberration of QRS complex, in auricular premature beats, 245
 - in auricular fibrillation, 261
 - in paroxysmal tachycardias, 256
- Addison's disease, 279
- Amyl nitrite, 273
- Angina pectoris, 71, 79, 112-136, 192-204
- Arrhythmia, sinus, 239-240
- Auricular fibrillation, 258, 260-263
 - aberrations of QRS in, 261
 - distinction from ventricular paroxysmal tachycardia, 262
 - A-V block in, 258-259, 261
 - carotid sinus stimulation in, 261
 - mechanism in, 260-261
 - T waves in, 263
- Auricular flutter, 258-260
 - carotid sinus stimulation on, 260
 - impure, 260
- Auricular paroxysmal tachycardia, 240
 - See also* Paroxysmal tachycardias
- Auricular premature beats, 240-244, 244-246
 - in supraventricular tachycardia, 256
- A-V block. *See* Heart block
- A-V nodal paroxysmal tachycardia, 256
- A-V nodal rhythm, 248-249
- Axis, anatomic, of the heart, 23
 - anterior-posterior, 23
 - vertical, 23
 - deviation, 27
 - electrical, 27
 - mean, definition and determination of, 27*
- Beri-beri, 283
- Bipolar lead, definition of, 4
- Bradycardia, sinus, 239
- Burger triangle, 295
- Cardiac mechanism disturbances, 79
- Cathode-ray oscilloscope, 286-288
- Central terminal, definition of, 4, 7
- Chest leads. *See* Precordial leads
- Children's electrocardiograms, 227-237
 - evolution of changes from birth to childhood, 77, 78
 - T waves in, 235
 - variations in, 227-237
- Conduction, refractory period and, 240-244
- Congenital heart disease, 283
- Congestive heart failure, effect on ventricular gradient, RS-T shifts and T waves, 199
 - effect on QRS complexes, 204
- Coronary disease, 112-211
 - angina pectoris, induced and spontaneous, 112-136
 - exercise tests in diagnosis of, 115-122
 - normal vs. pathologic exercise effects and, 115-124
 - RS-T shifts following exercise, 118
 - RS-T shifts due to digitalis vs. coronary disease, 125, 192-204
 - following exercise, 118
 - due to large gradient vs. coronary disease, 123
 - due to rapid rate vs. coronary disease, 122
 - serial T wave changes in diagnosis of, 124-128
 - serial EKG changes in diagnosis of, when initial tracing is normal, 192-211
 - significance of nonpathologic factors in evaluation of EKG's in, 128-135
 - T wave changes following premature beats in, 135
 - following exercise and, 119-122
- See* Myocardial infarction
- Cor pulmonale, 238
- Depolarization, definition of, 10
 - of interventricular septum, 17-20
 - in left bundle branch block, 104-111
 - in right bundle branch block, 92-103
 - of left ventricular wall, 17-20
 - of a mass of muscle, electrical effect of, 12-16
 - of right ventricular wall, 17-20
 - of syncytium, 10
 - of ventricles, normal, 17-20
 - in left bundle branch block, 104-111
 - in right bundle branch block, 92-103
- See* Injury
- See* QRS complex
- Digitalis, 266-271
 - combined effect of rapid rate and digitalis, 199, 267-268
 - dosage and effect of, 269

- Digitalis (contd.)**
 effects on cardiac mechanism, 271
 on P wave, 266
 on P-R interval, 271
 on Q-T interval, 90
 on RS-T segments, 123, 175, 192-204, 266
 on ventricular gradient, 60
 in left ventricular hypertrophy 90, 192-204
 serum potassium and, 271
 toxic rhythms due to, 271
 A-V block, 271
 bigeminy, 271
 ventricular premature beats, 271
 ventricular tachycardia, 258, 271
- Dipole field of potential of, in volume conductor, 4-6**
 effects of eccentricity of, 288, 290-292
 single dipole representation, discussion of, 289-292
- Drugs, 92**
- Ectopic rhythms, 248-249**
 auricular, 248
 A-V nodal, 248-249
 interference dissociation, 249, 254
 shifting pacemaker, 249
 ventricular, 249
- Einthoven's law, 9**
- Einthoven triangle, 7**
- Electrical axis, 27**
- Electrolyte disturbances, 276-279**
- Emetine, 273**
- Escaped beats, 252**
- Excitation, definition of, 10**
 solid angle representation of electrical effects of, 30
 spread of in heart muscle, 10
 vector representation of electrical effects of, 10-16
- Frontal plane, 8**
- Frontal plane loop, construction of, from limb leads, 26**
 definition of, 21
- Glomerulonephritis, 280**
- Goldberger unipolar limb leads, 8-9**
- Heart block, 249-254**
 in auricular tachycardias, 249-250
 due to change in junctional tissues, 250
 complete A-V block, 253
 auricular rhythm in, 253-254
 A-V nodal rhythm in, 254
 in myocardial infarction, 254
 in rheumatic carditis, 254, 283
 Stokes-Adams syndrome in, 254
 Heart block, due to change in junctional tissues, complete A-V block (*contd.*)
 ventricular rhythm in, 254
 partial A-V block, 250-253
 dropped beats in, 250
 escaped beats in, 250
 P-R interval in, 252, 253
- Hypercalcemia, 279**
- Hyperkalemia, 276-278**
 digitalis in, 277, 278
 glucose and insulin in, 275
 increase of serum calcium in, 277, 278
- Hypertension, 283**
- Hyperthyroidism, 280**
- Hypertrophy of both ventricles, 224-226**
 precordial leads in, 275
 QRS loops and limb leads in, 224-225
 and right bundle branch block, 225
- Hypertrophy of the left ventricle. See Left ventricular hypertrophy**
- Hypertrophy of the right ventricle. See Right ventricular hypertrophy**
- Hypocalcemia, 278-279**
- Hypokalemia, 276-278**
 serum calcium and, 277, 278
 digitalis and, 277
 serum sodium and, 277, 278
- Hyponatremia, 278**
 and hypokalemia, 277
- Hypothyroidism, 280**
- Injury, current of, 69**
 endocardial injury, 72, 75-79, 166-175, 189, 199
 epicardial injury, 71-79, 166-175, 189
 effect of on QRS complexes, 74
 on RS-T segments in precordial leads, 73, 76
 in limb leads, 72-73
 RS-T segment shifts in, 69-79
 in angina pectoris, 71, 79, 112-115
 in patients with initially abnormal EKG, 192-204
 in presence of left bundle branch block, 192-204
 in presence of left ventricular hypertrophy, 192-204
 in relation to myocardial infarction, 69-79, 136, 166-175, 192-204
- Interventricular septum, infarction of, 148-154, 191**
 depolarization of, normal, 17-20
 in left bundle branch block, 104-111
 in right bundle branch block, 92-103
- Interference dissociation, 249, 254**
- Ischemia, 71-79, 80-87**
 in angina, 80, 82

Ischemia (*contd.*)

- apical ischemia, 81, 82
- diaphragmatic ischemia, 81
- lateral ischemia, 80
- limb leads in, 80-82
- in myocardial infarction, 72-79, 166-175
- precordial leads in, 82-86
- Q-T interval in, 71, 83, 127
- repolarization in, 71-72
- ventricular gradient in, 54-57, 63, 81-82

Junctional premature beats, 245-246

Left bundle branch block, 104-111

- incomplete, 106
 - difficulty in distinguishing from left ventricular hypertrophy and septal infarction, 109
- limb leads in, 104
- in myocardial infarction, 189, 190-204
- in paroxysmal tachycardias, 256
- precordial leads in, 104
- QRS loops and complexes in, 104-109
- variations, 111
- T waves in, 109, 111

Left ventricular hypertrophy, 87-91

- effect of congestive heart failure in, 90
 - of digitalis in, 90, 195-200
- myocardial infarction and. *See* Myocardial infarction
- precordial QRS complexes in, 87
 - absence of R in V leads on the right in, 88
- QRS complexes and loops in, 87-90
- T waves in, 89
- ventricular gradient in, 89-90

Left ventricular "strain," 282

Long axis of the heart, 23

Monophasic action potential curve, 38

- effect of cooling upon, 38-48
- heart rate and, 43, 48
- ventricular gradient expressed in terms of, 50

Myocardial infarction, 136-211

- added infarction, 166
- left bundle branch block and, 189, 190-204
- right bundle branch block and, 190
- endocardial infarction, 171
- injury phenomena and, 69-79, 136, 166-175, 192-211
 - reversibility of injured state in, 166-175, 185
- in patients with initially abnormal tracings, 192-211
 - due to left bundle branch block, 192-204
 - due to left ventricular hypertrophy, 192-204

Myocardial infarction, in patients with initially abnormal tracings (*contd.*)*due to previous infarction, 204-211*

- QRS loop and complexes in apical infarction, 155
 - silent apical infarcts, 158-159
 - apical infarcts without Q waves in precordial leads, 159
- QRS loops and complexes in high anterior infarctions, 159-161
- QRS loops and complexes in infarcts in combined locations, 161
- QRS loops and complexes in diaphragmatic infarction, 143
 - difficulty in distinguishing from normal, 146-147
 - difficulty in distinguishing from left ventricular hypertrophy, 147, 283
 - evaluation of V_r in, 146-147
 - evaluation of esophageal lead in, 147
- late QRS changes following (in the absence of additional coronary events), 183
 - due to changes in intraventricular conduction, 183, 189, 195
 - due to left ventricular hypertrophy, 185, 195
 - due to changes in cardiac rotation, 183, 195
- QRS loop and complexes in lateral (posterolateral) infarction, 137-143
- QRS loop and complexes in septal infarction, 148-154
 - anteroseptal infarction, difficulty in distinguishing from chronic pulmonary disease, and right ventricular dilatation, 151, 159
 - difficulty in distinguishing from left ventricular hypertrophy and incomplete left bundle branch block, 109, 143, 151
 - transmural septal infarction, 149, 191
- RS-T and T wave changes in, 69-79, 136, 166-175
 - persistent RS-T shifts in, 174
- T wave changes following, acute, 60-79, 136, 166-175
 - disappearance of, due to left ventricular hypertrophy, 189
 - due to left bundle branch block, 189
- Spatial T vector in, 177-181

Myocarditis, 284

- diphtheritic, 285
- Fiedler's, 285
- rheumatic, 284

P wave in atrial enlargement, left, 227

- right, 223
- in auricular flutter, 260

- P wave in atrial enlargement (*contd.*)**
 definition, 1
 in ectopic rhythms, 248-249
 in hyperkalemia, 276
 in paroxysmal tachycardias, 255
 quinidine and, 272
 in rheumatic carditis, 284
- Parasystolic phenomena, 247**
- Parathyroid disease, 279**
- Paroxysmal tachycardias, 255**
 aberration of QRS complexes in, 256
 auricular, 255, 256
 nodal, 256
 supraventricular, 255
 in Wolff-Parkinson-White Syndrome, 256-257
 ventricular, 257-258
- Pericarditis, 73, 237, 283**
- Polarized membrane theory, 9**
- Potassium. *See* Hyperkalemia and hypokalemia**
- Potential, definition, 3**
 development of in heart muscle, 9-33
 distribution of in volume conductor, 4-6
 limb lead potentials, vector representation of, 7, 21-29
 precordial potentials, solid angle representation of, 31-33
 single dipole representation of cardiac potentials, 4-9, 289-290
 vector representation of, 4-9
 vectorcardiographic representation of, 286-303
- Precordial leads, 30**
 electrode placement for recording of, 31, 36
 effect of non-pathologic factors on T waves in, 40
 solid angle representation of potentials in, 31-33
- Pregnancy, position of heart in, 59**
- Premature beats, 244-248**
 auricular, 240-244, 244-246
 blocked, 244
 timing of in relation to disease, 244
 interpolated, 245
 P-R interval of, 244
 as a sign of disease of junctional tissues, 245
 ventricular conduction aberrations in, 245
 junctional, 245-246
 P waves in, 245-246
 P-R interval in, 245-246
 ventricular, 246
 bigeminy, 247
 escaped beats following, 246
 combined forms, 247
 compensatory pause following, 246
- Premature beats, ventricular (*contd.*)**
 interpolated, 246
 multifocal, 247
 QRS complexes in, 246
 retrograde conduction in, 246
 T wave changes following, 135-137
 trigeminy, 247
- P-R interval, definition, 1**
 in auricular premature beats, 242-244, 244-246
 in A-V block (partial), 252, 253
 in A-V nodal rhythm, 248
 digitalis effects upon, 271
 electrolyte disturbances and, 276
 maximum normal values for, 305
 quinidine effects upon, 272
 in sinus arrhythmia, 239-240
 effect of rheumatic carditis in, 240
 in thyrotoxicosis, 239
- P-Q segment, definition, 1**
- Pulmonary disease, 238**
 difficulty in distinguishing from healed anterior infarction, 238
- Pulmonary embolism, 237**
- Q wave, definition, 1**
 in myocardial infarction. *See* Myocardial infarction
 normal, 21-26
- QRS axis, definition of, 27**
- QRS complex, definition, 1**
 aberrations of, in auricular fibrillation, 261
 in auricular premature beats, 245
 in paroxysmal tachycardias, 256
 in congestive heart failure, 204
 in cor pulmonale, 238
 in hyperkalemia, 276-278
 in hypertrophy of both ventricles, 224-226
 in left bundle branch block, 104-109
 in left ventricular hypertrophy, 87-90
 in myocardial infarction. *See* Myocardial infarction
 normal, formation of in limb leads, 17-29
 changes in due to cardiac rotations, 21-29, 45
 in precordial leads, 30-37
 in pulmonary disease, 238
 quinidine effects upon, 272
 effects of rapid rate, 239
 in right bundle branch block, 92-103
 with left ventricular hypertrophy, 102
 in right ventricular hypertrophy, 215-224
 with left ventricular hypertrophy, 224-226
 secondary changes in, due to current of injury, 43
 vector analysis of, in limb leads, 21-29

- QRS complex (contd.)**
 vector loop representation of, 21-29
 frontal plane, 21-29
 spatial, 21-29
- QRS loop, application of idealized model of to EKG analysis, 26-29, 64**
 definition of, 21
 and frontal plane loop, 21-29
 spatial QRS loop, 21-29, 288
 in children, 227
 in hypertrophy of both ventricles, 224-226
 in left bundle branch block, 104-109
 in left ventricular hypertrophy, 87-90
 in myocardial infarction. *See* Myocardial infarction
 in right bundle branch block, 91-103
 in right ventricular hypertrophy, 215-224
 with right bundle branch delay, 218-221
 techniques of direct recording of, 289-299
- QRS vector, mean spatial, 29**
 spatial relationship of, to spatial gradient vector and to long axis of heart, 52
 relationship to mean spatial T wave axis, 44-67, 296-299
- QRS-T relationship, 44-67**
 in left bundle branch block, 109-111
 in left ventricular hypertrophy, 89-90
 normal variations, 44-67
 effect of changes in anatomic axis, 44-46, 58
 effect of rotation about anatomic axis, 45-58
 effect of rotation about vertical axis, 59
 effect of non-pathological factors on, 45, 48, 57-67
 in right bundle branch block, 100-101
 ventricular gradient as an instrument for evaluation of, 53-63
- Q-T interval, definition, 1**
 average and maximum normal values for, 306
 digitalis effects upon, 90
 emetine and, 276
 in glomerulonephritis, 280
 in hypocalcemia, 279
 in ischemia, 71, 83, 127
 quinidine effects upon, 72
- Quinidine, effects on mechanism disturbances, 273**
 on myocardial physiology, 271
 on P waves, 272
 on P-R interval, 272
 on QRS complexes, 272
 on Q-T interval, 272
 on T waves, 271
- Quinine, 273**
- R wave, definition, 1**
R' wave, definition, 1
- Refractory period, 240-244**
 absolute and relative, 240
 effects of cycle length upon, 241
 effects of refractoriness upon conduction, 241-244
 at onset of auricular tachycardia, 242
 in partial A-V block, 250-251
- Repolarization, 31**
 in cooled muscle, 42
 effect of cycle length upon rate of, 46-47
 in injured muscle, 69
 in ischemic muscle, 70, 71, 80-86, 166-175
 in normal muscle, 38
 ventricular gradient as measure of net effect of local differences in rate of, 50-53
- Rheumatic myocarditis, 283**
Rheumatic valvular disease, 283
- Right bundle branch block, 92-103**
 difficulty in distinguishing from right ventricular hypertrophy, 218-221
 formation of QRS loop and complexes in, 92-103
 incomplete, 101-102
 simulating left bundle branch block in limb leads, 94
 with left ventricular hypertrophy, 102
 in paroxysmal tachycardia, 256
 with right ventricular hypertrophy, 218-221
 T wave in, 100
- Right ventricular hypertrophy, 215-224**
 difficulty in distinguishing from right bundle branch block, 221
 formation of QRS loop and complexes in, 215-221
 lead V_1 in, 223
 lead V_{3R} in, 224
- Rotations of the heart, 23**
 about anatomic axis, 23, 58
 about anteroposterior axis, 23, 58
 about vertical axis, 23, 59
 effects of change in posture on, 26
 effects of respiration on, 58, 59, 177-181
 effects upon T waves and RS-T relationship, 58, 59, 177-181, 195
 exaggeration of effects of, by eccentricity of the heart, 26, 288, 290-292
- RS-T segment, definition, 2**
 shifts of, due to angina pectoris, 71, 79, 112-136
 due to digitalis, 123, 175, 192-204
 due to exercise, 118
 in hypocalcemia, 279
 in hyperkalemia, 276
 in hypokalemia, 277

RS-T segment, shifts of (*contd.*)

- in injury, 69-79, 156, 166-175, 192-204
- in left bundle branch block, 111, 175, 192-204
- in left ventricular hypertrophy, 89, 175, 192-204
- in myocardial infarction, 69-79, 136, 166-175, 192-211
- in myocarditis, 258
- in normal tracings, 51, 115-119
- normal vs. abnormal RS-T shifts, 115-124
- in pericarditis, 73, 283
- due to rapid rate, 51, 115-119, 122, 192-204

S wave, definition, 1

- formation of in limb leads, 21-26
- in precordial leads, 34-37

S' wave, definition, 1

Shifting pacemaker, 249

Single dipole representation, 289-290

Sinus arrhythmia, 239-240

- A-V nodal escaped beats in, 240
- P-R interval in, normal, 239-240
- in rheumatic carditis, 240

Sinus bradycardia, 239

Sinus tachycardia, 239

Solid angle, 31

Spatial vector electrocardiography, 296-299

- spatial angle between spatial mean T vector and spatial mean QRS vector, 296-297

- spatial mean vectors and analysis, 296-299

Standard limb leads, definition, 7

- quantitative relationship to unipolar limb leads, 8, 303

Syphilitic heart disease, 98

T wave, analysis of, employing monophasic action potential curves, 31, 32

definition of, 1

- in angina pectoris, 112-136
- in auricular fibrillation, 263
- in left bundle branch block, 109, 111
- in children's electrocardiograms, 235
- digitalis effects upon, 49, 60, 123
- exercise effects upon, 60, 119
- food effects upon, 49, 60, 128-135
- formation of, introduction to, 38-50
- in glomerulonephritis, 280
- in hyperkalemia, 276, 278
- in hypokalemia, 276, 278
- in hypothyroidism, 280
- in injury, 69-79
- in ischemia, 71-79, 80-87

T wave (*contd.*)

- in myocardial infarction. *See* Myocardial infarction

- in pericarditis, 73, 237

- postural changes in, 45, 66, 131

- in precordial leads, normal, 36

- in pulmonary disease, 238

- quinidine effects on, 271

- rate change effects, 43, 48, 60

- regression, 51

- relation to QRS, the ventricular gradient.

See QRS-T relationship

- representation as mean vector, 43

- in right bundle branch block, 100

- ventricular gradient only method of finding orders in, 54, 61

- in left ventricular hypertrophy, 89

- following ventricular premature beats, 135-137

T wave loop, 43

- in left bundle branch block, 109

- in right bundle branch block, 100

Tetrahedron, as a frame of reference for spatial vectorcardiography, 101

U wave, definition, 1

- exercise effects upon, 120

- in hypokalemia, 277

- inverted, significance of, 128

Unipolar leads, definition of, 4

- unipolar limb leads, 7, 21

- vector analysis, 7

- unipolar precordial leads, 30

Vector, definition of, 4

- analysis, introduction to, 4-6

- of standard limb leads, 7

- of unipolar limb leads, 7

- frontal plane, definition of, 8

- frontal plane gradient, 50

- mean frontal plane QRS, 28

- spatial gradient*, 296

- spatial QRS, 29, 296

- spatial angle between mean spatial QRS and mean spatial T, 296

- spatial relationship of spatial mean QRS,

- spatial gradient and anatomic axis, 50, 296

Vectorcardiography, 286, 299

- spatial, 286, 288

- method, 289-299

Ventricles, depolarization of, 17-20

Ventricular fibrillation, 254

Ventricular flutter, 254, 258

Ventricular gradient, 50-67

- definition, 50

- frontal plane, measurement of, 50

- in left bundle branch block, 63

Ventricular gradient (*contd.*)

in left ventricular hypertrophy, 63
normal variations in magnitude and direction of, 54, 58

in right bundle branch block, 63

significance of, 53, 54, 61

in evaluation of T wave changes in ischemia, 54-57, 63, 81-82

Ventricular paroxysmal tachycardia, 257-258, 271

Ventricular paroxysmal tachycardia (*contd.*)

distinction from auricular fibrillation with QRS aberrations, 262

distinction from supraventricular tachycardia with QRS aberration, 256

QRS complexes in, 257-258

Wolff-Parkinson-White Syndrome, 256-257, 263